

Development of a Class of Cyclopropenimine Based Compounds for Applications in Catalysis

Peter Stoyanov

B.Sc. (Honours), Biochemistry, 2014

Brock University Chemistry Department

A thesis submitted in partial fulfillment of the requirements for the degree of
Masters of Science

Faculty of Mathematics and Science, Brock University

St. Catharines, Ontario

© August 2016

Abstract:

The present thesis outlines our latest findings in the pursuit of novel bis(diisopropylamino)cyclopropenimine (DAC) compounds. Particular focus was placed on the synthesis and investigation of DAC-substituted proton sponges, as well as their application in organo-catalysis. Herein, we report the synthesis of a non-symmetric DAC-functionalized proton sponge coined “Janus” sponge. Theoretical and experimental investigation of this sponge provided a monoprotonated salt, without a N-HN intramolecular hydrogen bond and a relatively low freebase strain. Instead, DFT calculations and X-ray crystallography revealed the presence of a hydrogen bond to the Cl⁻ counter ion, leading to the unprecedented *in-out* geometry of the molecule. Furthermore, the salt of the Janus sponge was found to be highly fluorescent both in the solid state and solution. Its experimentally measured p*K*_a of 23.8 was found to be in good agreement with the calculated value of 23.9. The use of Janus, as well as the previously synthesized DACN (a naphthalene DAC derivative) sponge in phase transfer catalysis was also explored. The DACN proton sponge was found to be a highly efficient bifunctional phase-transfer catalyst, facilitating the movement of charged intermediates from the interface to the organic layer via favourable partitioning of hydrophilic/hydrophobic surface areas.

Acknowledgements:

First and foremost, I would like to thank my supervisor, Dr. Travis Dudding, for giving me the opportunity, equipment and facilities to pursue my research interests. The continuous guidance and encouragement he provided me with was essential to my progress. I would also like to thank my committee members, Dr. Metallinos and Dr. Pilkington for their advice and guidance. The completion of the project would not have been possible without your help, thank you both.

I would like to thank my fellow members of the Dudding group, it has been a real pleasure working with you all. I am especially grateful for the patience and knowledge shared with me by Lee Belding, Roya Mirabdolbaghi, and David Hurem in the laboratory research, and Nazanine Maryamdokht for the guidance on the computational side. What I have learned will stay with me for the rest of my life, both in laboratory and beyond. Also I would like to thank Razvan Simionescu and Dr. Metallinos for sharing their knowledge of NMR with me.

This page of acknowledgements would not be complete without recognizing the vast impact and encouragement my parents had on my studies. I would like to thank my mother Elena Bondarenko for inspiring me to reach my highest potential, teaching me the value of hard work and the importance of independence. She brought me to this wonderful country where I have the opportunity to make my dreams a reality. I would also like to thank my stepfather, Yuriy Bondarenko and grandfather, Gabdulhak Timirgaleev for their help, patience, and trust. They provided me with a roof over my head, and transportation to work, which allowed me to avoid debt and obtain my post-secondary education. Most importantly, I would like to thank my late grandmother Zoya Timirgaleeva, who was a devoted organic chemist for her inspiration to become an educated, honest, and good person. I wish she could see me graduate.

Table of Contents:

Abstract.....	ii
Acknowledgements.....	iii
Table of Contents.....	iv
List of Tables.....	vii
List of Figures.....	viii
List of Schemes.....	xi
Abbreviations.....	xiv
1. Introduction:.....	1
<i>1.1 General Background on Cyclopropenylum ions.....</i>	<i>1</i>
1.1.1 Historical	1
1.1.2 Predicted Nature of Aromatic Systems	4
1.1.3 Synthesis and Investigation of Cyclopropenylum Ions	6
1.1.4 Preparation of Halogenated Cyclopropenylum Precursors	13
1.1.5 Investigation of Substituent Effects on Cyclopropenylum Ions	14
1.1.6 Application of Cyclopropenylum Compounds in Synthesis and Catalysis	23
1.1.7 Computational Studies of Cyclopropenylum Compounds	31
<i>1.2 Superbases and Proton Sponges in Organic Chemistry.....</i>	<i>36</i>
1.2.1 Review of Basicity in Organic Chemistry	36
1.2.2 Amines, Amides and Guanidines	38
1.2.3 Phosphazenes and Phosphorous Containing Compounds	41
1.2.4 Recent Development of Superbases and Proton Sponges	42
1.2.5 Discovery and Synthesis of the Proton Sponge	45
1.2.6 Applications of the DMAN Proton Sponge in Organic Synthesis	46
1.2.7 Investigation of Proton Sponge Properties via Computational Methods	48
1.2.8 Defined Properties and Major Findings on Proton Sponges	53
<i>1.3 Summary of Planned Syntheses and Investigation.....</i>	<i>54</i>
2. Results and Discussion:.....	55
<i>2.1 Janus Proton Sponge.....</i>	<i>55</i>
2.1.1 Strategic Approach to the Synthesis of Janus (45)	55
2.1.2 Strategies for Mono-protection of 1,8-diaminonaphthalene (46)	60

2.1.3	Strategies for <i>N</i> -methylation to Obtain Compound (47)	64
2.1.4	Strategies for Deprotection to Obtain Compound (48)	66
2.1.5	Synthesis of Janus Proton Sponge (45) and Protonated Salt (49)	67
2.1.6	Investigation of Janus Properties (45)	70
2.1.7	Computational Analysis of Janus (45)	74
2.1.8	Comparison of Janus (45) and DACN (50)	79
2.2	<i>DACN Proton Sponge Phase Transfer Catalysis</i>	82
2.2.1	General Background on Cyclopropenimines in Phase-Transfer Catalysis	82
2.2.2	Experimental Screen for Catalyst Alkylation and Decomposition	84
2.2.3	Optimization of DACN Phase Transfer Reaction Conditions	85
2.2.4	Application of DACN in Phase-Transfer Catalysis via Electrophile Screen	86
2.2.5	Mechanistic Determination of DACN Phase-Transfer Catalysis	88
3.	Conclusion:	94
4.	Experimental Procedures:	95
4.1	<i>Synthesis of Janus Proton Sponge</i>	96
4.1.1	Synthesis of tert-butyl (8-aminonaphthalen-1-yl)carbamate (46)	96
4.1.2	Synthesis of tert-butyl (8-(dimethylamino)naphthalen-1-yl)carbamate (47)	96
4.1.3	Synthesis of N ¹ ,N ¹ -dimethylnaphthalene-1,8-diamine (48)	97
4.1.4	Synthesis of N-(2,3-bis(diisopropylamino)cycloprop-2-en-1-ylidene)-8-(dimethylamino)naphthalen-1-aminium chloride (Janus•HCl) (49)	98
4.1.5	Synthesis of N ¹ -(2,3-bis(diisopropylamino)cycloprop-2-en-1-ylidene)-N ⁸ ,N ⁸ -dimethylnaphthalene-1,8-diamine (Free base of Janus) (45)	99
4.1.6	Reference Information	100
4.2	<i>Synthesis of Compounds and Derivatives for PTC DACN Proton Sponge Catalysis</i> ..	100
4.2.1	General procedure for phase transfer catalysis	100
4.2.2	Synthesis of tert-butyl-2-(diphenylmethyleamino)-3-(phenyl)propanoate (43a)	100
4.2.3	Synthesis of tert-butyl-2-(diphenylmethyleamino)-3-(naphthalen-2-yl)propanoate (43b)	101
4.2.4	Synthesis of tert-butyl-2-(diphenylmethyleamino)-3-(phenyl)butanoate (43c)	101
4.2.5	Synthesis of tert-butyl-2-(diphenylmethyleamino)-3-(phenyl)propanoate (43d)	102
4.2.6	Synthesis of tert-butyl-2-(diphenylmethyleamino)-3-(4-methylphenyl)propanoate (43e)	102
4.2.7	Synthesis of tert-butyl-2-(diphenylmethyleamino)-3-(4-chlorophenyl)propanoate (43f)	103

4.2.8	Synthesis of tert-butyl-2-(diphenylmethyleamino)-3-(4-nitrophenyl)-propanoate (43g)	103
4.2.9	Synthesis of tert-butyl-2-(diphenylmethyleamino)-3-(4-methoxyphenyl)-propanoate (43h)	103
4.2.10	Synthesis of tert-butyl-2-(diphenylmethyleamino)-5-(phenyl)-pentanoate (43i)	104
4.2.11	Synthesis of tert-butyl-2-(diphenylmethyleamino)-pent-4-enoate (43j = 43k)	104
4.2.12	Synthesis of tert-butyl-2-(diphenylmethyleamino)-hex-4-enoate (43l)	105
4.2.13	Synthesis of (E)-tert-butyl-2-(diphenylmethyleamino)-pent-4-enoate (43m)	105
5.	Supporting Information:.....	105
5.1	<i>Appendix A: Janus Proton Sponge.....</i>	<i>105</i>
5.1.1	X-ray Experimental Data	105
5.1.2	Quantum Yield Calculation	106
5.1.3	Relative p <i>K</i> _a Calculations	107
5.1.4	Experimental p <i>K</i> _a Determination	108
5.1.5	QTAIM Structures	108
5.1.6	B3LYP/6-31G(d,p) Computed LUMO+1 of 45 _{opt} and 49 _{xray}	109
5.1.7	Spectral Data of Janus Related Compounds	110
5.1.1	DFT Calculated Geometries and Thermo-chemical Data	124
5.2	<i>Appendix B: DACN Proton Sponge Phase Transfer Catalysis.....</i>	<i>134</i>
5.2.1	Results for the extraction-type phase transfer reactions	134
5.2.2	Proton and Carbon NMR Spectra	135
5.2.3	Coordinate and thermochemical data of all computed structures	147

List of Tables:

Table 1: IR band comparison of cyclopropene and cyclopropenylium compounds.....	9
Table 2: Calculated stability based on pK_R 's of a series of phenyl cyclopropenylium compounds.....	15
Table 3: Determined stability based on pK_R 's of a series of <i>p</i> -anisyl cyclopropenylium cations.....	16
Table 4: Vibrational frequencies of normal deformation modes of $C_3X_3^+$ systems.....	17
Table 5: Experimental pK_a values of conjugated acids of naphthalene type proton sponges.....	52
Table 6: Optimization screen for production of 46 by varying the rate of Boc_2O addition.....	62
Table 7: Solvent systems used in the attempts to crystallize compound 49	68
Table 8: Computed NICS (-1, 0, 1) values for compounds 49 _{opt} , 45 _{opt} , 49 _{xray}	77
Table 9: Comparison of basicity enhancing factors between Janus (45) and DACN (50)	80
Table 10: Optimized reaction conditions using di-protonated DACN sponge 51	85

List of Figures:

Figure 1: Contrast of σ - and π -orbital symmetry.....	2
Figure 2: Relationship between geometrical construction and equation for energy.....	3
Figure 3: Calculated delocalization energies (DE) of various cyclic hydrocarbons, where: T = triplet ground state, +R = cation, \cdot R = radical, -R = anion.....	5
Figure 4: Chemical shift of aromatic proton, related to benzene, as a function of ρ_{π} per C-atom.....	10
Figure 5: Hybridization of cyclopropenyl cation, consistent with ^{13}C -H coupling constant.....	12
Figure 6: Linear relationship between relative stability (pK_R) of various cyclopropenyl ions and IR active vibrational mode (E') for ring deformation.....	18
Figure 7: Linear relationship between relative stability (pK_R) of various cyclopropenyl ions and Raman active vibrational mode (A'') for ring deformation.....	20
Figure 8: 2, 3-bis(dialkylamino)cyclopropenimine, pK_a in acetonitrile.....	25
Figure 9: Resonance structures of aromatic protonated cyclopropenimine giving rise to exceptionally high basicity.....	31
Figure 10: One example of a computationally examined, branched cyclopropenimine...34	
Figure 11: Structures of amine derivatives and their examples (pK_a of the conjugate acids in H_2O): DBU = 1,5-diazabicyclo[5.4.0]undec-5-ene; TMG = 1,1,3,3- tetramethylguanidine.....	39
Figure 12: Resonance forms of amidinium and guanidinium ions.....	39
Figure 13: Vinylogous conjugation system of amidine and guanidine derivatives.....	40
Figure 14: Hydrogen bonding stabilization effect.....	40

Figure 15: P ₁ and P ₄ phosphazene base examples (P ₁ with resonance).....	41
Figure 16: General structure of Verkade's base and the trans-annular P-N bond formation that is responsible for the basicity (shows the flattening of the 7-membered ring upon protonation).....	42
Figure 17: Proton sponge (DMAN), and structurally related derivatives; TMGN, HPMN, DACN (50).....	43
Figure 18: Synthesis of 1, 8-bis (dimethylamino) naphthalene (DMAN), pK _a 's also listed.....	45
Figure 19: N-alkylation of pyrrolidine derivative using proton sponge DMAN.....	46
Figure 20: O-alkylation of optically active alcohols using DMAN Proton sponge.....	47
Figure 21: Efficient synthesis of azide isocyanate from aliphatic azide amine.....	47
Figure 22: Structure of the Janus proton sponge (45).....	55
Figure 23: Synthesis of Janus proton sponge (45) – Steps One to Three.....	56
Figure 24: Synthesis of Janus proton sponge (45) – Steps Four to Five.....	58
Figure 25: Synthesis of Janus proton sponge (45) – Steps Six to Seven.....	58
Figure 26: (a) Two-dimensional representation and corresponding numbering scheme for compound 49 and selected B3LYP/6-31G(d,p) computed MOs for 49 _{xray} . (b) ORTEP3-generated X-ray structure of compound 49 (purple = nitrogen, blue = carbon, green = chlorine). Thermal ellipsoids are displayed at 50 % probability.....	70
Figure 27: Depiction of the <i>in-out</i> and <i>in-in</i> lone pair configuration in proton sponges..	71
Figure 28: Computed structure and charge density map of the Janus salt (49).....	72
Figure 29: (Left) UV/vis absorption spectra of 45 and 49 as 1×10 ⁻⁵ M solutions in DCM. (Right) UV/vis emission spectra of 45 and 49 as 1×10 ⁻⁵ M solutions in DCM.....	73

Figure 30: Visual portrayal of the luminescent character of compound 49 as a solid (left vial) and as a solution in dichloromethane (right vial).....	73
Figure 31: B3LYP/6-31G(d,p) optimized geometries and selected MOs for compounds 45 _{opt} , 49 _{opt}	75
Figure 32: Homodesmotic Reaction Scheme for the Determination of H-Bonding Strength and Ground State Destabilization.....	79
Figure 33: Janus article on the front cover of <i>J. Org. Chem.</i> Jan. 1 st , 2016.....	81
Figure 34: Reported cyclopropenimine compounds by Dudding <i>et al.</i>	83
Figure 35: Alternative compounds screened for PTC activity.....	86
Figure 36: Proposed hydroxide-initiated interfacial PTC mechanism for alkylation of imine 41 to afford product 43	90
Figure 37: Hydrophobic (orange)/hydrophilic (blue) surfaces of 51 (left) and the 51 · 57 ⁻ complex (right) generated using Macromodel.....	91
Figure 38: (a) Computed complex 51 · 57 ⁻ (right). Two-dimensional rendering of favorable binding interaction in 51 · 57 ⁻ (left). (b) Computed benzylation transition state, TS1 (right). Two-dimensional rendering of TS1 (left). Computations performed at the wb97xd/6-31g(d)/def2sv (scrf = dichloromethane) level.....	93

List of Schemes:

Scheme 1: Resonance integrals of direct and indirect bonded atoms.....	2
Scheme 2: All overlap integrals, when $i = j$, atomic orbitals are assumed normalized.....	2
Scheme 3: Benzene 6 x 6 secular determinant with eigen-values $E = \alpha \pm 2\beta, \alpha \pm \beta, \alpha \pm \beta$	3
Scheme 4: Calculated delocalization energy of benzene.....	4
Scheme 5: Synthesis of <i>s</i> -triphenylcyclopropenyl cations (3, 4, 5).....	7
Scheme 6: Synthesis of unsubstituted cyclopropenyl cation 7	10
Scheme 7: Calculation of thermodynamic quantity pK_{R+}	11
Scheme 8: Equilibrium established upon reaction of 3-ethoxycyclopropene with strong acid.....	11
Scheme 9: Comparison of appearance potentials of cyclopropenyl related ions.....	12
Scheme 10: Synthesis of pentachlorocyclopropane and tetrachlorocyclopropene (13, 14).....	13
Scheme 11: Synthesis of trisdimethylamino cyclopropenyl cation.....	17
Scheme 12: Synthesis of tris-anilino cyclopropenyl cation.....	19
Scheme 13: Synthesis of cyclopropenyl compounds using precursor 20 as a reagent.....	21
Scheme 14: Synthesis of tetraiodocyclopropenyl cation.....	22
Scheme 15: Photochemical rearrangement of triphenylcyclopropenyl bromide salt.....	23
Scheme 16: Sensitized photolysis of bicyclopropenyl compounds.....	24
Scheme 17: Michael addition catalyzed by cyclopropenimine derivative under mild conditions.....	26

Scheme 18: Synthesis of N^I -centered catalyst and applications under phase transfer conditions.....	27
Scheme 19: Fluorination of benzyl bromide with cesium fluoride and N^I -catalyst 40	27
Scheme 20: Synthesis of dual-charged salt, $40 \cdot H^{2+}$ and catalyzed hydroamination.....	28
Scheme 21: Proposed $40 \cdot H^{2+}$ and Au(I)-Catalyzed Cycle for Alkyne Hydroamination..	29
Scheme 22: Synthesis of homoleptic gold(I) complex 40b	30
Scheme 23: Equations used for the calculation of the absolute proton affinity	32
Scheme 24: Acid dissociation equilibrium, derived equation for acidity constant, and pK_a	36
Scheme 25: Henderson-Hasselbalch derived equation for the measure of acidity (pH) in chemical and biological systems, and the self-ionization constant of water.....	37
Scheme 26: Equilibrium of base association, derived equation for the basicity, and pK_b	37
Scheme 27: Equilibrium in water, derived equation for the basicity relative to the K_a	37
Scheme 28: Equation for the proposed superbases definition.....	43
Scheme 29: Nucleophilic aliphatic substitution catalyzed by quaternary phosphonium salt.....	60
Scheme 30: Optimized conditions for mono-protection used in synthesis of Janus (45).....	64
Scheme 31: Optimized conditions for <i>N</i> -methylation used in the synthesis of Janus (45).....	66
Scheme 32: Optimized conditions for the deprotection in the synthesis of Janus (45).....	66

Scheme 33: Optimized conditions for production of Janus (45) and its salt protonated (49).....	68
Scheme 34: Comparison of DACN and Janus salts in PTC benzylation of a Schiff's base.....	80
Scheme 35: Electrophile screen for PTC of di-protonated DACN (51).....	87
Scheme 36: Extraction type PTC reactions with di-protonated DACN (51).....	89

Abbreviations

AB ₂	Peak pattern in nuclear magnetic resonance spectra
APA	Absolute proton affinity
β	Beta
Bn	Benzyl
BF ₄	Tetrafluoroborate
Boc ₂ O	Di- <i>tert</i> -butyl dicarbonate
Br	Bromo- or Bromine
Bu	Butyl
B3LYP	Becke 3-parameter (exchange), Lee, Yang, Parr
CN	Nitrile
Cy	Cyclohexyl
DAC	Bis(dialkylamino)cyclopropenimine
DACN	1,8-bis(bis(diisopropylamino)cyclopropenimine) naphthalene
DBU	1,8-Diazabicycloundec-7-ene
DCA	9, 10-dicyanoanthracene
DCM	Dichloromethane
DE	Delocalization energy
DFT	Density functional theory
DMAN	1,8-(bis)Dimethylaminonaphthalene (Archetypal proton sponge)
DMF	Dimethylformamide
DMS	Dimethyl sulfate
DMSO	Dimethyl sulfoxide
E	Energy
ee	Enantiomeric excess
Et ₃ N	Triethylamine
equiv.	Equivalents
eV	Electron volt (unit)
GB	Gas-phase basicity
h	hour(s)
H ⁺	Proton
HCl	Hydrochloric acid
HOMO	Highest occupied molecular orbital
<i>i</i>	Iso
IEFPCM	Integral equation formalism polarizable continuum model
IMHB	Intramolecular hydrogen bond
IR	Infrared
kcal	Kilocalorie (unit)
KHMDS	Potassium bis(trimethylsilyl)amide
KOH	Potassium hydroxide
LCAO MO	Linear combination of atomic orbital molecular orbital
LED	Light emitting diode(s)
LiClO ₄	Lithium perchlorate
LiCl	Lithium chloride
LUMO	Lowest unoccupied molecular orbital

<i>m</i>	Meta
M	Molarity (mol/L)
Me	Methyl
MeOH	Methanol
MeCN	Acetonitrile
MO	Molecular orbital
<i>n</i>	Normal
NBO	Natural bond order
<i>n</i> BuLi	Butyllithium
NICS	Nucleus-independent chemical shift
NMR	Nuclear magnetic resonance
<i>o</i>	Ortho
OCH ₃	Methoxy
<i>p</i>	Para
PA	Proton Affinity
Ph	Phenyl
p <i>K</i> _a	Acid dissociation constant (logarithmic scale)
p <i>K</i> _{R+}	Thermodynamic quantity
ppm	Parts per million (chemical shift)
PTC	Phase-transfer catalysis
PTCs	Phase-transfer catalyst(s)
π	Pie (orbitals)
rf	Retardation factor
rt	Room temperature (~25 °C)
<i>s</i>	Secondary
σ	Sigma (orbitals)
<i>t</i>	Tert
TFA	Trifluoroacetic acid
THF	Tetrahydrofuran
TLC	Thin layer chromatography
TMG	Tetramethylguanidine
UV	Ultra-violet
V	Volt (unit)

1. Introduction

1.1 General Background on Cyclopropenium ions

1.1.1 Historical

Since its introductory mention in 1856 by August Wilhelm Hofmann, aromaticity has intrigued chemists all over the world.¹ August Kekulé was the first to propose the cyclohexatriene structure for benzene in 1865,² while Erich Hückel, a German born physical chemist was the first to model the inherent stability associated with these compounds, tracing the origins to quantum mechanics.³ Hückel pioneered the consideration of the bonding arrangement in terms of separate sigma (σ) and pi (π) electrons. His contribution led to the acceptance of the four major characteristics defining aromatic compounds today.⁴ First, a molecule was required to have a structure with alternating single and double bonds, resulting in the delocalized conjugated π -system. Secondly, it was necessary for the contributing atoms to be joined in one or more ring systems, which were coplanar with respect to the structure. The last and perhaps the most important rule, would define a molecule aromatic if it had an even number of π -delocalized electrons, which was not a multiple of four. Hence, the molecule was aromatic only if it met all four of the attributes, and anti-aromatic if the number of delocalized π -electrons was a multiple of four. In short, this last rule led to the simple $4n+2$ and $4n$ equations commonly used today, where n refers to the number of electron pairs and could be any positive integer or zero. This theory was a result of Hückel's 1930 proposition, in which he determined the energies of π -electron molecular orbitals using a simple linear combination of atomic orbital molecular orbital (LCAO MO) method.⁴ The method was revolutionary because of the assumptions Hückel integrated in it, allowing for simplification of the mathematical work. The first assumption was that there is an anti-symmetric character in the atomic orbitals contributing to π -bonding with respect to the molecular plane reflection. This meant that there was a varying symmetry

compared to the atomic orbitals contributing to the σ -bonding, thus the two could be considered independently, (**Figure 1**).

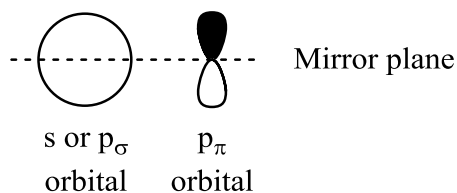


Figure 1: Contrast of σ - and π -orbital symmetry.⁴

It was also stipulated that the Coulomb integrals (α -values) for all carbon atoms were identical, neglecting the small differences that arise from variable chemical environment. Directly bonded atoms were assumed to have the same resonance integrals, while the integrals of atoms not bonded directly were ignored, (**Scheme 1**).

$$\begin{aligned} \int \phi_i \hat{H} \phi_j. d\tau &= \beta : \text{if } i \text{ and } j \text{ atoms bonded directly} \\ &= 0 : \text{if } i \text{ and } j \text{ atoms not bonded directly} \end{aligned}$$

Scheme 1: Resonance integrals of direct and indirect bonded atoms.⁴

Finally, it was proposed that the overlap of atomic orbitals situated on different atoms results in negligible overlap integrals, (**Scheme 2**).

$$\begin{aligned} \int \phi_i \phi_j. d\tau &= 0 : \text{if } i \neq j \\ \int \phi_i \phi_j. d\tau &= 1 : \text{if } i = j \end{aligned}$$

Scheme 2: All overlap integrals, when $i = j$, atomic orbitals are assumed normalized.⁴

These assumptions allowed Hückel to form secular determinants which account for bonding from the overlap of two orbitals. The secular determinant was initially solved by Hückel

for ethylene; however, he went on to solve it for butadiene, benzene and cyclobutadiene. The method is used to this day due to its accuracy, and the relation to frontier orbitals, that facilitate spectroscopic transitions. The solution to a benzene secular determinant (**Scheme 3**) can be expressed with a polyhedron (hexagon), illustrating the three main rules for cyclic conjugated systems (**Figure 2**).⁵

$$\begin{vmatrix} \alpha - E & \beta & 0 & 0 & 0 & \beta \\ \beta & \alpha - E & \beta & 0 & 0 & 0 \\ 0 & \beta & \alpha - E & \beta & 0 & 0 \\ 0 & 0 & \beta & \alpha - E & \beta & 0 \\ 0 & 0 & 0 & \beta & \alpha - E & \beta \\ \beta & 0 & 0 & 0 & \beta & \alpha - E \end{vmatrix} = 0$$

Scheme 3: Benzene 6 x 6 secular determinant with eigen-values $E = \alpha \pm 2\beta, \alpha \pm \beta, \alpha \pm \beta$.⁴

They are as follows; the highest energy molecular orbital (MO) may be degenerate (if n is odd) or non-degenerate (if n is even), the lowest energy MO is always non-degenerate, while all the remaining possibilities result in pairs of degenerate MO's. The consequence of this molecular orbital arrangement is that stable molecules are made only when a specific number of electrons are accommodated.

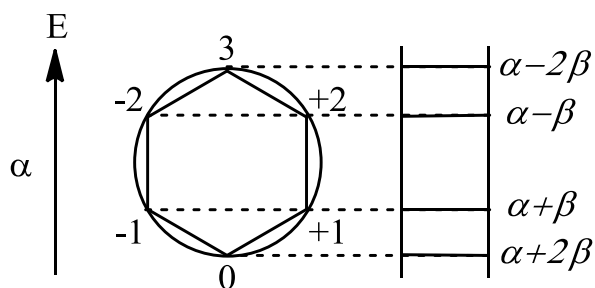


Figure 2: Relationship between geometrical construction and equation for energy.⁵

The energy of three C=C bonds in ethene is then subtracted from the total π -electron energy of benzene, resulting in delocalization energy that is responsible for the additional stability in aromatic compounds, (**Scheme 4**).⁵

$$\text{Total } \pi\text{-electron E of benzene:} \quad 2(\alpha + 2\beta) + 4(\alpha + \beta) = 6\alpha + 8\beta$$

$$\text{E of three C=C bonds in ethane:} \quad 3(2\alpha + 2\beta) = 6\alpha + 6\beta$$

$$\text{Calculated Delocalization E:} \quad 2\beta = -460 \text{ kJ/mol}$$

Scheme 4: Calculated delocalization energy of benzene.⁵

Hückel's work has been further integrated into modern computational chemistry, including semi-empirical, *ab initio*, and density functional theory methods. The early computational chemistry methods relied on Hückel's LCAO MO in order to make predictions about properties of compounds that had not been synthesized yet. The aromatic stability brought forth by the delocalization of electrons was the main interest of chemists, and continues to gather attention to this day.

1.1.2 Predicted Nature of Aromatic Systems

The development of the LCAO MO method had inspired theoretical chemists all over the world to begin work on predicting stability of various aromatic compounds. This, in essence, was the starting point in the search for new cyclic conjugated systems. The cyclic systems under investigation were not limited to neutral compounds and included anions, cations and radicals. The assumption that Hückel's rule of aromaticity was applicable to polycyclic as well as monocyclic conjugated polyolefins was also put to the test under the pretext of these studies. The first broad and cumulative study using the linear combination of atomic orbital molecular orbital method was done by John D. Roberts and co-workers in 1952.⁶ They used Hückel's method to

calculate electron delocalization energies, bond orders and free-valence indexes for various small-ring hydrocarbons (**Figure 3**),⁶ thus exploring the nature of these aromatic compounds.

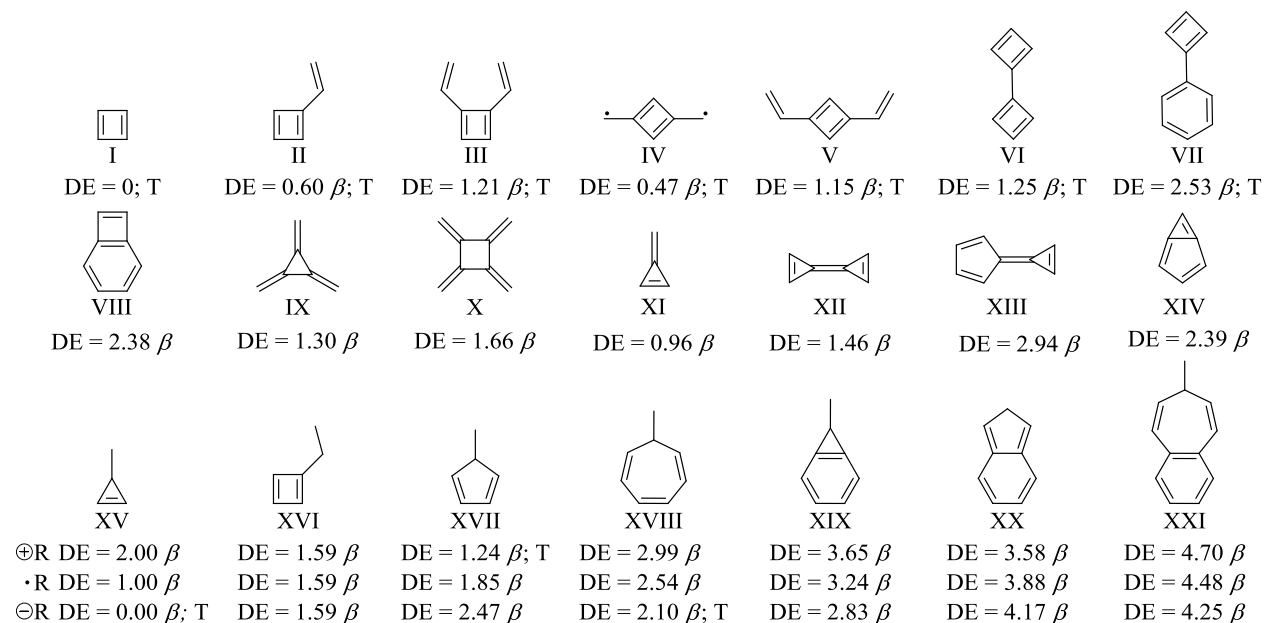


Figure 3: Calculated delocalization energies (DE) of various cyclic hydrocarbons, where: T = triplet ground state, +R = cation, \cdot R = radical, -R = anion.⁶

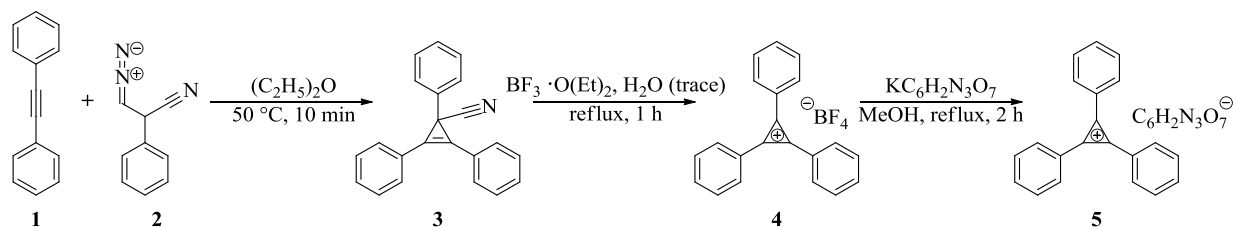
There were a number of interesting observations from these calculations. In terms of stability it was predicted that cyclobutadiene (**I**) will have a zero delocalization energy, and a triplet ground state. Given that the cyclopropene should have greater yet comparable angular strain, the apparent instability of (**I**) was attributed to the triplet ground state. The authors suggested that there is a lack of theoretical justification for the $4n+2$ π -electron rule when applied to polycyclic systems, and that compound (**VIII**) violates the rule although predicted to have singlet ground-state. It was assumed that the cyclobutadiene ring has a destabilizing effect and that the compound is aromatic, regardless of failing to pass the $4n+2$ rule. Cross-conjugated polymethylene substituted systems such as compounds (**IX-X**) were predicted to have singlet ground-states irrespective of the symmetry and the number of π -electrons. The free-valence

indexes for these compounds were quite high at the terminal CH₂ positions, suggesting that these molecules should readily polymerize, similar to *p*-quinodimethane.⁶ The fulvene-like substances (XI-XIV) were all predicted to have quite stable π -electron systems and singlet ground-states, the most interesting of which was (XIII). The authors proposed that the unsaturated five- and three- membered rings could allow for charge separation thus simultaneously harboring negative and positive charges respectively. Compound (XIV) was of additional interest, both for its predicted high resonance energy, and the possibility of it being a non-pseudoaromatic analog of pentalene and azulene.⁷ Low delocalization energy was predicted for (IV), while the molecular orbital theory agreed with the classical valence theory on diradical structure. Structures (XV-XXI) exemplify a series of conjugated cyclic anions, free radicals, and cations. The first four of the series, in particular (XV-XVIII), demonstrated that the DE can vary greatly depending on the ring size. The latter three structures (XIX-XXI) showed that a benzene substitution did not alter the relative ionic stability sequence, the differences in the DE were small and that none of these species were predicted to have a lowest triplet state.⁶ Although the conclusion of this study was that Hückel's $4n+2$ rule was only applicable to monocyclic conjugated compounds, this was the first mention of the smallest π -aromatic system. Not only was the cyclopropenium cation (XV) introduced, but its relative stability was predicted, along with the ability to exhibit dual properties of stability and ionic charge.

1.1.3 Synthesis and Investigation of Cyclopropenylum Ions

Since the prediction of cyclopropenium ions and their stability, there has been a race among chemists to provide experimental proof of this aromatic system. Synthesis of such compounds would also allow for the investigation of their physical properties, while opening a whole new class of molecules with an undiscovered potential. In 1957, Ronald Breslow was the

first to verify the prediction of a stable cyclopropenium ion. This was achieved via reaction of diphenylacetylene (**1**) with phenyldiazoacetonitrile (**2**), which yielded 1,2,3-triphenyl-2-cyclopropene carboxylic acid nitrile (**3**) (**Scheme 5**).⁸



Scheme 5: Synthesis of *s*-triphenylcyclopropenyl cations (**3**, **4**, **5**).^{8,9}

Breslow managed to obtain a melting point, 145-146 °C, IR-spectrum, and combustion analysis, all supporting the claim for **3**. It was observed that (**3**) did not precipitate out of ethanolic silver nitrate solution, and was soluble in non-polar solvents such as benzene. Thus a conclusion was made that the compound was covalent. Upon treatment with boron trifluoride etherate containing trace amounts of water (**3**) was converted to a white crystalline solid. This novel substance (**4**) was no longer soluble in benzene, chloroform or ether. It was found to dissolve in methanol, and upon recovery and reconversion to (**3**) was determined to be 1,2,3-triphenylcyclopropenyl fluoroborate. This result established that the aromatic cyclopropenyl cations were only soluble in solvents of high polarity such as alcohols, acetonitrile, aqueous acids and DMF. Compound (**4**) was then subsequently converted to a picrate (**5**), with M.P. of 195-196 °C, a bright yellow powder, insoluble in benzene or ether. Just as (**4**), the picrate was soluble in methanol, it was also noted that ethanol was a good solvent, and recovery of (**5**) from these solutions was possible. However, prolonged standing in either methanol or ethanol would result in partial decomposition. The observed slow decomposition in alcohols, which was attributed to the strain of three trigonal carbons constituting a ring, led to the

conclusion that the *s*-triphenylcyclopropenylium cation (**5**) was moderately reactive.

Additionally, it was established that this cation is relatively stable due to the conjugation of the three phenyl rings with the positively charged cyclopropenylium ring system.^{8,9}

The first analysis of the X-ray crystal structure of triphenylcyclopropenylium was performed a few years later, and confirmed the structure. It was also revealed that the C-C distance in the three membered ring was 1.40 Å, very close to that of benzene (1.39 Å), and that the semi-cyclic C-C bonds were 1.45 Å, which was shorter than the typical distance (1.54 Å). This length was closely related to the previously measured central bond of butadiene and biphenyl (1.48 Å).¹⁰ Unlike the cyclopropene, and aryl cyclopropenylium cations, the alkyl substituted salt does not absorb ultraviolet light in regions above 185 nm, which is in agreement with the predicted 3β excitation energy for the π to π^* transition. This is greater than the calculated 2β , π to π^* transition in ethylene, which explains why the cyclopropenylium transition occurs at very short wavelengths.¹⁰

Besides Breslow, the groups of Farnum and Kende contributed to the synthesis of cyclopropenyl cations. In particular, their synthesis of various tri- and diaryl cyclopropenylium salts occurred via direct addition of arylchlorocarbenes to mono- and diaryl acetylenes or decarboxylation of 1,2-disubstituted cyclopropene-carboxylic acids using strong acids in acetic anhydride.^{11, 12, 13} The desire for these salts was fueled by the fact that attempts to synthesize the unsubstituted cyclopropenylium salt via hydride abstraction from cyclopropene were unsuccessful. Once that was finally achieved, attempts to determine its heat of formation using mass spectrometry also failed to distinguish if the observed $C_3H_3^+$ ion had the structure of (**7**) or that of propargyl cation.^{14, 15} In contrast to the $C_3H_3^+$ results, Tobey and West observed that the tribromo- and trichlorocyclopropenylium cations could be obtained upon treatment of

tetrahalocyclopropene with aluminium trihalides. Careful hydrolysis of these salts also resulted in the reverse reaction, producing back the tetrahalocyclopropene in upward of 60% yield.¹⁶ Trihalocyclopropenyl cation salts served as excellent models for investigation of electronic properties, and confirmation of the $C_3H_3^+$ ion structure. A comparison of the IR-spectra for the various salts and their parent compounds provided evidence for the highly symmetrical nature of the of the trigonal planar cyclopropenyl cation structure (**Table 1**).

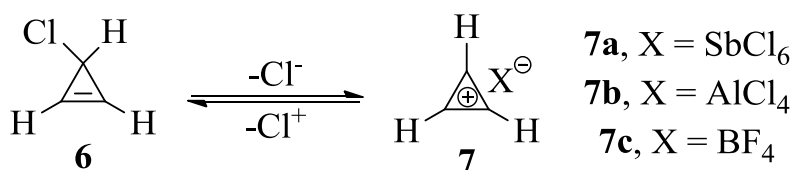
Table 1: IR band comparison of cyclopropene and cyclopropenylum compounds

Compounds	Number of bands	Vibrations in cm^{-1} (Intensity, Type)	Type of Symmetry
$C_3Cl_3^+AlCl_4^-$	4	1350 (m,s), 1315 (vs,b), 731 (m,s), 482 (vs,b)	D_{3h}
$C_3Cl_3^+SbCl_6^-$	3	1348 (s,s), 1313 (vs,b), 735 (m,s)	D_{3h}
C_3Cl_4	3	1810 (vw,s), 1155 (vs,s), 1053 (vs,s), 617 (s,s)	C_{2v}
C_3Br_4	6	1757 (m,s), 1135 (s,s), 1121 (vs,s), 1075 (m,s), 1002 (vs,b), 664 (vs,b)	C_{2v}
C_3Br_6	4	862 (s,s), 719 (vs,s), 677 (s,s), 651 (m,s)	D_{3h}

Simple and related IR-spectra for the products of tetrachlorocyclopropene reaction with $AlCl_3$ and $SbCl_5$ make the formation of molecular adducts or π -complexes a highly unlikely result. Furthermore, trichlorocyclopropenylum ion readily dissolves in sulfur dioxide without decomposition, and is able to redeposit in large refined crystals upon cooling to $-78\text{ }^\circ\text{C}$. Therefore, these factors affirm the preserved integrity of the three-membered ring.¹⁶

Since the initial proof, Breslow and his co-workers continued to make cyclopropenylum cation derivatives, however, the focus of his group was the development of new methods to synthesize such compounds. In 1969, his group demonstrated that 3-chlorocyclopropene (**6**) readily reacts with various halogenated metals such as aluminium trichloride, silver fluoroborate

and antimony pentachloride to produce the corresponding unsubstituted cyclopropenyl cations (**Scheme 6**).¹⁷ Near quantitative yields of products (**7a**, **7b**, **7c**) were obtained from the reactions. Detailed characterization of the cations was undertaken, involving NMR, molecular orbital calculations and potentiometric titrations in order to confirm the extra stabilization and their structural assignment.



Scheme 6: Synthesis of unsubstituted cyclopropenyl cation **7**.¹⁷

A rule established for “classical” aromatic systems has been frequently used to test the aromatic character of novel compounds such as cyclopropenyl cation (**7**). This relates the chemical shift of aromatic protons from benzene’s value (ppm) to the π -electron density (ρ_{π}) of the aromatic system per carbon atom, as show in (**Figure 4**).^{10, 17, 18}

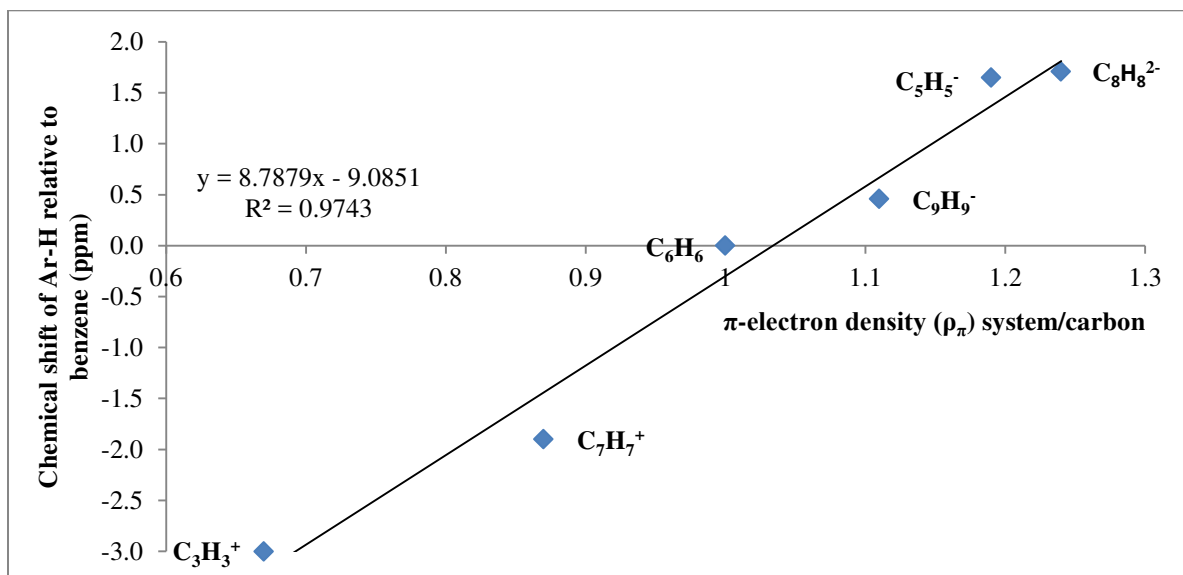
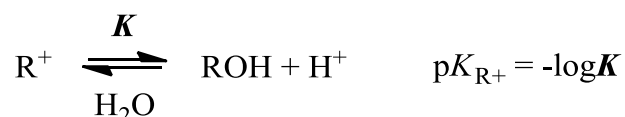


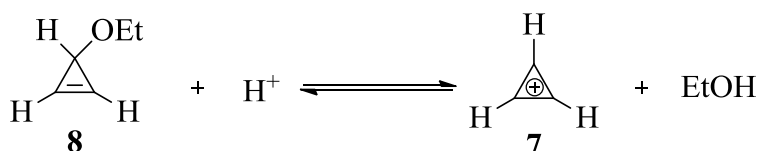
Figure 4: Chemical shift of aromatic proton, related to benzene, as a function of ρ_{π} per C-atom.¹⁸

It was observed that the -3.0 ppm value for the cyclopropenyl ion was in good relation to the expected value from this rule. A change in the hybridization of the three-membered ring was balanced out by the effects of ring current, noted at the position of the ^1H -resonance absorption, confirming the agreement of the observed and expected values. Thus only the influence of π -electron density for each carbon atom is important.¹⁷ The stability of the carbonium ion was further studied by determining the thermodynamic quantity $\text{p}K_{\text{R}^+}$, which is the negative logarithm of the H^+ ion activity required to establish a 1:1 equilibrium in water with the derived alcohol (**Scheme 7**).



Scheme 7: Calculation of thermodynamic quantity $\text{p}K_{\text{R}^+}$.¹⁷

The $\text{p}K_{\text{R}^+}$ partially corrects for the various strain factors which contribute to the total free-energy of the carbonium ion. Cyclopropenyl cations typically have UV-transitions below 200 nm, and the expected $\text{p}K_{\text{R}^+}$ value for (**7**) is well below zero. This rendered both the UV and potentiometric titration techniques useless, thus NMR analysis was employed on the system (**Scheme 8**).



Scheme 8: Equilibrium established upon reaction of 3-ethoxycyclopropene with strong acid.¹⁷

It was found that in the presence of an acid, compound (**8**) had a singlet at 6.58 ppm instead of AB_2 ring system pattern. It was presumed that the ether equilibrated rapidly through

cation (7). When the acidity was raised a singlet at 11.08 ppm was observed as equilibrium shifted right. Thus a signal at 8.85 ppm would correspond to a 1:1 mixture of ether and carbonium ion. A pK_{R^+} value of -7.4 ± 0.1 was obtained for cation (7), confirming extra stabilization in this compound. Molecular orbital calculations together with the NMR data resulted in the proposed hybridization scheme shown below (**Figure 5**).

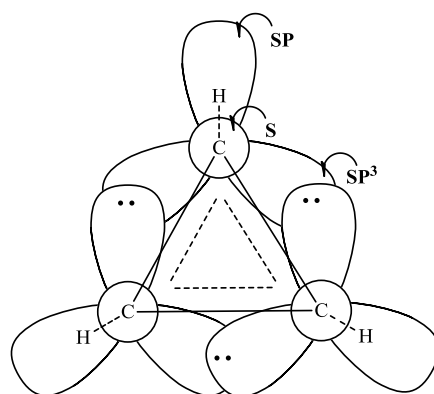
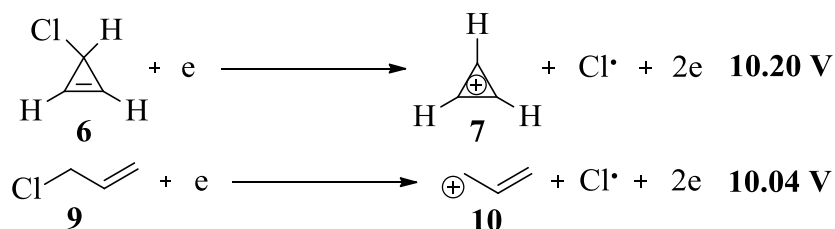


Figure 5: Hybridization of cyclopropenyl cation, consistent with ^{13}C -H coupling constant.¹⁷

The allyl cation, an open chain analog of the cyclopropenyl cation, was compared to the benzyl cation via solvolysis data. It was observed that it forms about ten times slower than the benzyl cation estimating the pK_{R^+} of the allyl of -20, thus corresponding to an 18 kcal/mol difference in stabilization from the cyclopropenyl cation. Lossing's gas-phase determination of appearance potentials for the 3-chlorocyclopropene and allyl chloride followed a similar trend with a difference of 0.84 eV, which amounts to 19.3 kcal/mol difference in stabilization energy.

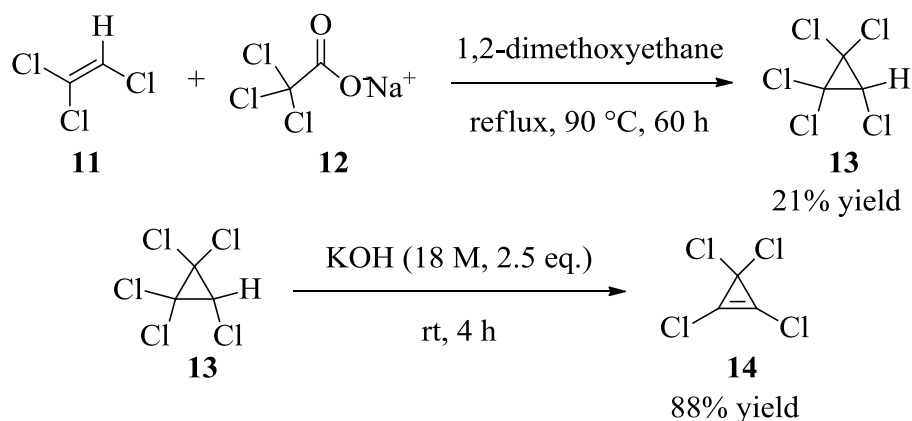


Scheme 9: Comparison of appearance potentials of cyclopropenyl related ions.¹⁷

All experiments confirmed the presence of additional stabilization energy in cyclopropenyl cations. They also demonstrated that the energy differences in gas-phase and solution were in agreement, thus suggesting that the solvation energies of ions such as allyl and cyclopropenyl were similar.¹⁷

1.1.4 Preparation of Halogenated Cyclopropenium Precursors

In 1963, Stephen Tobey and Robert West published truly ground-breaking work for this field. They reported the first synthesis of a pentachlorocyclopropane (**13**), which was achieved by the addition of a carbon dichloride carbene to chlorinated olefin (**Scheme 10**).¹⁹ Their work also included the conversion of (**13**) to tetrachlorocyclopropene (**14**), via β -hydride elimination under very basic conditions (18 M KOH). The authors found that tetrachlorocyclopropene was highly reactive, and readily underwent ring opening reactions in the presence of water, and ammonium hydroxide.



Scheme 10: Synthesis of pentachlorocyclopropane and tetrachlorocyclopropene (**13**, **14**).^{19, 20}

Tobey and West went on to expand their novel method, by describing the synthesis of various other halogenated cyclopropenes, and the subsequent reactivity of such compounds, including the use of light to convert them to cyclopropanes.^{20, 21} Their procedure for generating

tetrachlorocyclopropene as a precursor to the cyclopropenylium cation provided many chemists with the ability to study and expand this class of compounds. It is still being used today, as demonstrated by the likes of Dudding and Lambert. In an effort to prepare mono- and diiodo-perfluorocycloalkenes Soulen and Sepiol modified the original procedure for the synthesis of tetrachlorocyclopropene in 1975. In particular, they employed half the quantity of glyme previously suggested by Tobey and West, which resulted in a two-fold increase of the yield for pentachlorocyclopropane, and thus the final product (**14**) tetrachlorocyclopropene. This was rationalized by a slower decomposition of the sodium trichloroacetate and reduction of by-products from the reaction of the generated dichlorocarbene with glyme. The reaction time was subsequently increased from 3 to 5 days to maximize the consumption of starting materials.²²

1.1.5 Investigation of Substituent Effects on Cyclopropenylium Ions

With the cyclopropenylium cation isolated, and its structure and stability proven, the interest in this compound did not end there. The work that followed was focused on the synthesis of new derivatives in order to determine what effects substituents had on the stability of the cation. The ease with which the cyclopropenylium cation was formed from a cyclopropene derivative was also put into question. In particular, what influence do the ring substituents and anions have on the formation of the cation? Both factors were found to play a role in cation formation. In terms of the counter ion, a series of cyclopropene derivatives defined the relationship between the nature of the anion and the type of bonding found in the compound. This series where X is the anion, was as follows: X= H, OCH₃, CN, 2,4,5-(NO₂)₃C₆H₂O⁻, Br⁻, BF₄⁻, where the first three were covalently bonded to the cyclopropene carbon, while in the remaining three the bond was ionic.²³ As per the previous series it was clear that the amount of positive charge on the carbons of the three-membered ring system depended on the number and

nature of substituents present. The first study was conducted on the phenyl series of cyclopropenium cations by Manatt and Roberts. They determined that substitution of phenyls for hydrogen in the cyclopropenyl cation led to an increase in both the total and excess delocalization energies of the ion (**Table 2**). The calculation of DE for the mono-, di- and tri-phenylcyclopropenyl cations was carried out using Hückel's MO method. The excess delocalization energy was calculated by subtracting the DE_{Cp} of unsubstituted cyclopropenyl cation and the sum of phenyl DE_{Ph} from the total DE of the compound. In general, cation stability was found to increase with each substitution.²⁴

Table 2: Calculated stability based on pK_R 's of a series of phenyl cyclopropenylium compounds

Cyclopropenylium Bromides	DE (β)	Δ DE (β)
Unsubstituted	2.00	-
Mono-phenyl	4.39	0.39
Di-phenyl	6.70	0.70
Tri-phenyl	9.16	1.19

* Calculated: Δ DE = DE - DE_{Cp} - ΣDE_{Ph} .

Breslow and co-workers were also heavily involved in the determination of substituent effects on the stability of the cyclopropenyl aromatic system. Their work showed that the more delocalized the charge was on to the substituents the greater was the stability of the cyclopropenyl cation, which reduced the compound's electrophilicity. A study was conducted on the *p*-anisyl series of the cyclopropenium cations. It was observed that for the cyclopropenylium bromides the stability of the cations is also increased with each additional *p*-anisyl substitution when compared to that of the tri-phenyl cation (**Table 3**).^{23, 25, 26}

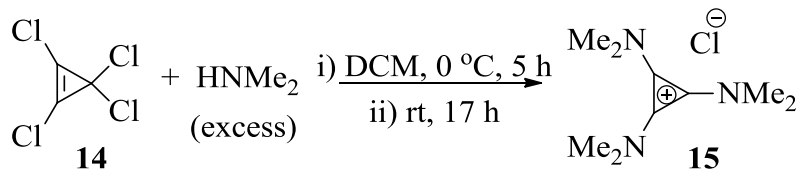
Table 3: Determined stability based on pK_R 's of a series of *p*-anisyl cyclopropenylium cations

Cyclopropenylium Bromides	$pK_R \pm 0.05$	DE (β)
Tri-phenyl	2.80	2.31
Di-phenyl- <i>p</i> -anisyl	4.00	2.34
Di- <i>p</i> -anisylphenyl	5.22	2.37
Tri- <i>p</i> -anisyl	6.42	2.40

* pK_R 's determined in 23% ethanol solution due to insolubility of related carbinols.

Further work by this group found that dialkoxy-cyclopropenyl cations were more stable than diaryloxy-cyclopropenyl analogues. Thus given the same degree of substitution electron donating substituents had a more stabilizing effect on the cation than electron withdrawing. An analysis of the NMR spectra for the di- and tri-propylcyclopropenyl cations showed equivalence of all propyl groups. Therefore, confirming that all cyclopropenylium salts, regardless of the nature of substituents, gave similar charge distribution, and rarely spread it to the outer aromatic systems such as phenyl groups. Additionally, Breslow and co-workers proved that the electron-donating σ -inductive effect from substituents (*n*-propyl) is greater than the electron-donating π -conjugative effect (phenyl) on the stabilization of the cyclopropenylium cations.^{10, 12, 26}

In light of Breslow's work, Yoshida and his group set out to find a substituent that would provide a greater π -conjugative donation. They succeeded when they managed to synthesize and isolate various amino substituted cyclopropenyl systems. Initially, trisdimethylamino-cyclopropenyl cation was synthesized by treating tetrachlorocyclopropene with excess dimethylamine at 0 °C and then room temperature over the course of 22 hours, followed by addition of 70 % perchloric acid (**Scheme 10**).^{27a} Other tri-amino cyclopropenyl cations were also obtained in near quantitative yields using the same procedure with *N*-ethylaniline, *N*-methylaniline, piperidine, morpholine, and diphenylamine.



Scheme 11: Synthesis of trisdimethylamino cyclopropenyl cation.^{27a}

In the case of diisopropylamino, and diethylamino, only the 1,2-bisdialkylamino derivatives were obtained. Analysis of the NMR spectra showed two kinds of magnetic alkyl environments, explained by the increased double bond character of the C-N linkage that arose from the enhanced rotational barrier about the bond. Initial observation of reactivity determined that the aminocyclopropenyl cations were very stable in the presence of water (even at high temperatures), compared to the trichloro- and triphenyl- cyclopropenyl analogues.^{27a} Yoshida and his group went on to find a relationship between the pK_R values of various cyclopropenyl cations and the frequencies of their skeletal deformation modes. They recalled that the x-ray structural analysis of tri-substituted cyclopropenyl cations determined the molecular symmetry to be D_{3h} and that the three skeletal deformation modes of the ring can be classified into two normal vibrations; the Raman active (A_1), and both Raman and IR active (E_1) species. This allowed for the calculation of the totally symmetric deformation modes (A'') and degenerate deformation (E'') modes in order to estimate the stability of the cyclopropenyl systems. When compared the A'' and E'' frequencies for the trisdimethylamino cyclopropenyl cation were greater than compounds tri-substituted with methyl, phenyl and chloride (**Table 4**).^{27b}

Table 4: Vibrational frequencies of normal deformation modes of $C_3X_3^+$ systems

Substituent X	A'' (cm^{-1})	E'' (cm^{-1})
NMe ₂	1985	1553
CH ₃	1880	1490
C ₆ H ₅	1845	1411
Cl	1791	1312

The large shifts of both ring deformations were presumed to occur due to the mass and electronic effects of the substituent. If the mass effect was predominant then the shift to shorter frequencies would follow the order; $H < CH_3 < N(CH_3)_2 < Cl$. However, the E' mode for $C_3H_3^+$ is one of the lowest reported, at 1276 cm^{-1} , thus the vibrations are more sensitive to the electronic effects of substituents. The empirical relationship between pK_R and E' values, given its linear nature, was able to estimate the pK_R value of 15 for trisdimethylamino cyclopropenyl cation. In comparison to the pK_R of trichloro cyclopropenyl cation which is -5, this is a large amount of stability, and additional proof for the donating π -conjugative effect of amino substituted ring systems (**Figure 6**).^{27b}

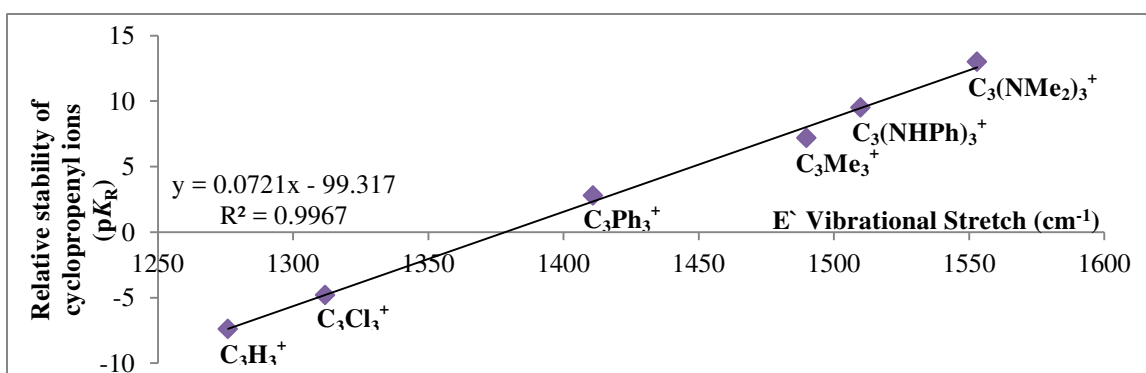
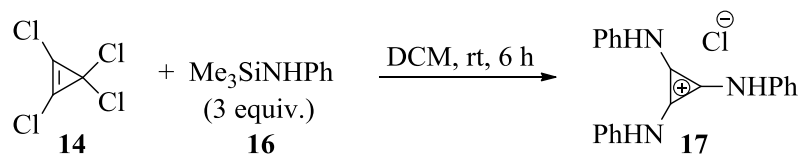


Figure 6: Linear relationship between relative stability (pK_R) of various cyclopropenyl ions and IR active vibrational mode (E') for ring deformation.^{27a, 27b}

Weiss and co-workers also contributed significantly to this area through their synthesis and investigation of various substituted derivatives of cyclopropenyls. In particular, Weiss was the first to synthesize the tris-anilino derivative of cyclopropenyl cation (**17**). A reaction of tetrachlorocyclopropene with three equivalents of trimethylsilylaniline (**16**) at room temperature in DCM, provided a 72 % yield of product (**17**) after a low temperature work-up (**Scheme 12**).²⁸



Scheme 12: Synthesis of tris-anilino cyclopropenyl cation.²⁸

However, this derivative was found to be thermally unstable, resulting in complete decomposition over several days at ambient temperature. It was possible to store the compound at $-30\text{ }^{\circ}\text{C}$, under an atmosphere of nitrogen for several weeks. Although a characteristic ring vibration was reported by Weiss at 1510 cm^{-1} (E^{\prime}) as a broad vibrational stretch, the relative instability of this system was blamed on the delocalization of amine electrons by the aromatic phenyls.²⁸ Additionally, it must be noted that the lack of Raman related data on cyclopropenyl cations forced Yoshida to use the empirical relationship between pK_R and E^{\prime} (IR active) to estimate stability. Initial models of $C_3(C_6H_5)_3^+$ cation based on potential energy distributions determined that the Raman active line (A^{\prime}) was caused 80 % due to ring deformation with a weakly coupled $C_3-C_6H_5^+$ stretching vibration responsible for the remaining 20 %, while the dual Raman and IR active vibration (E^{\prime}) was 41 % and 51 % of the respective contributing factors. Thus, an accurate relation of substituent effects to stability of the cation must involve the A^{\prime} parameter due to its higher contribution of the C_3^+ ring deformation modes, a linear correlation between the pK_R and the Raman active vibrational mode was established in (**Figure 7**).^{27b}

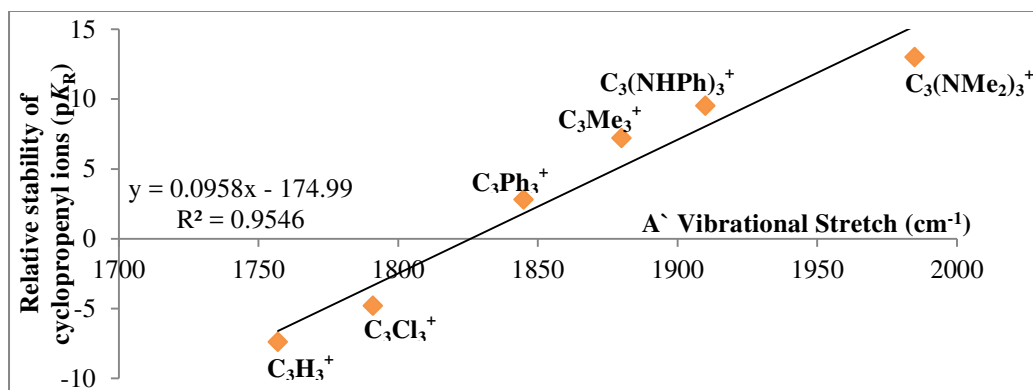


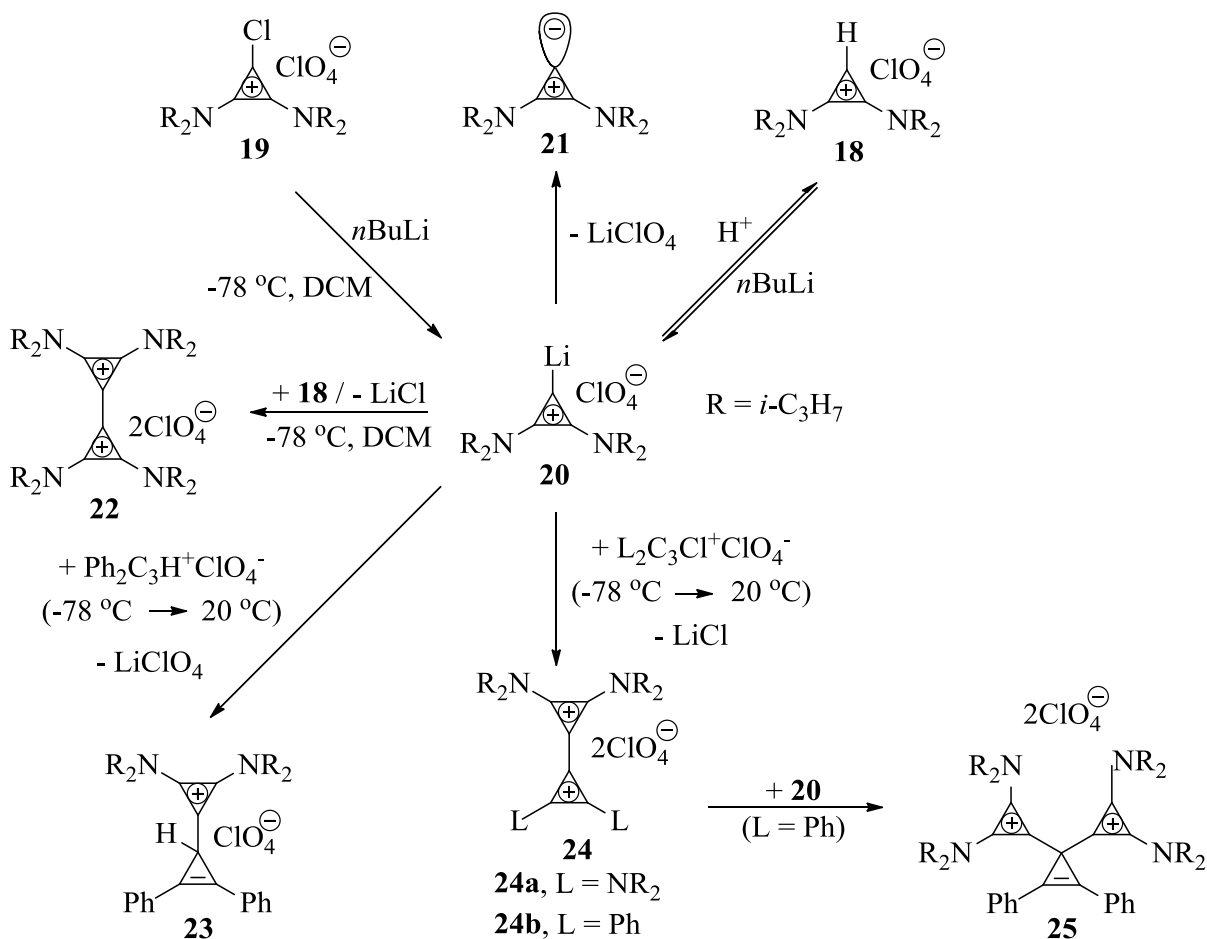
Figure 7: Linear relationship between relative stability (pK_R) of various cyclopropenyl ions and Raman active vibrational mode (A') for ring deformation.^{27a, 27b}

Weiss reported the A' vibration at 1910 cm^{-1} which is significantly lower than the observed 1985 cm^{-1} for (**15**).²⁸ The thermal instability of the compound is evidence that substitution of cyclopropenyl cations with aryl amino derivatives is a deficient strategy for enhancing the delocalization energy, and thus the stability of these compounds. In contrast alkyl amino analogues of cyclopropenyl systems with greater electron donating π -conjugative and σ -inductive effects should be explored.

The group of Weiss is famous for many other developments in the area of cyclopropenylium cation substitution. They were the first to demonstrate that the aromatic ring of the cyclopropenyl salts can undergo electrophilic aromatic substitution, since all previous methods of substitution were nucleophilic aromatic substitution and exchange reactions. Utilization of strong electrophiles and harsh conditions was necessary for these S_E reactions to proceed.²⁹ Nevertheless, the most interesting contributions of this group involved the employment of cyclopropenylium cations as electrophilic components. This was made possible by their procedure for the halogen/lithium exchange on the aromatic ring, converting the aromatic proton of compound (**18**) to a metallocyclopropenylium system (**20**). The more

electrofugic group allowed S_E reactivity, activating the σ -skeleton of the aromatic system.

Various novel derivatives (**21-25**) of the cyclopropenyl cation systems were synthesized thanks to (**20**), the precursor compound (Scheme 13).³⁰

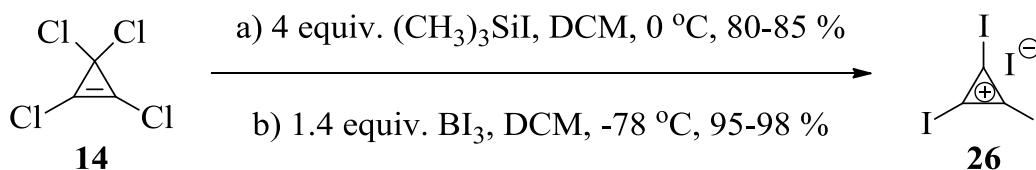


Scheme 13: Synthesis of cyclopropenyl compounds using precursor **20** as a reagent.³⁰

The reaction to convert the halogenated cyclopropenyl cation (**19**) to the lithium precursor (**20**), then to dehalogenated product (**18**) quantitatively from treatment with water shows that the halogen-metal exchange is possible for (**19**) as for haloacetylenes. Weiss proposed that the lithium precursor (**20**) is a reactive intermediate, the generation of which would be promoted by two factors. First, the C-X bond of the halo-cation (**19**) is vulnerable to S_N attack at

the halogen due to the sp hybridization. Secondly, it is possible that the intermediate forms due to the hindrance of nucleophilic attack at the 3 position of the cyclopropenyl ring owing to the cyanine character of the compound. In all the use of cyclopropenylium cations as weak electrophiles under harsh to moderate conditions was demonstrated by Weiss and his colleagues.³⁰

The group of Dr. Weiss did not stop there, their greatest achievement in regards to cyclopropenylium cations was the isolation of the ever elusive tetra-iodocyclopropenylium cation. The work of Yoshida and West was used in order to synthesize the C_3I_4 (**26**), from tetrachlorocyclopropene. Two procedures were presented, both halogen exchange reactions, with the first method employing four equivalents of iodotrimethylsilane in DCM at $0\text{ }^\circ\text{C}$, with 85 % yield. The second method used boron triiodide in 3-4 equivalents in DCM at $-78\text{ }^\circ\text{C}$, to provide **26** in near quantitative yield (**Scheme 14**).



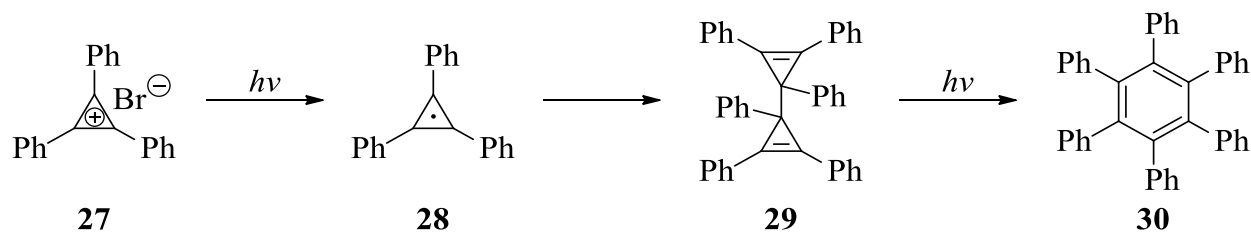
Scheme 14: Synthesis of tetraiodocyclopropenylium salt.³¹

Although the yields are impressive, the amounts produced are actually deceptive. The reason for this is that the product (**26**) is highly reactive and can explode when handled both in the dry state and when dissolved in polar solvents. It is thus highly recommended that no more than 1 mmol of the product is made in a single experiment, and equally important that no operation, manipulation or work-up is done with anything other than moist DCM. The halocyclopropenyl (**26**) is easy to isolate as it is an insoluble crystalline powder easily separating

from DCM. The insolubility suggests the ionic structure, while the IR-spectrum, which is dominated by a large absorption at 1200 cm^{-1} , confirms a high degree of symmetry. This spectrum peak also fits into the series of E`-ring deformation vibrations of cyclopropenylium ions; $\text{SCH}_3 = 1241\text{ cm}^{-1}$, $\text{SeCH}_3 = 1220\text{ cm}^{-1}$, $\text{TeCH}_3 = 1169\text{ cm}^{-1}$, $\text{Cl} = 1313\text{ cm}^{-1}$, $\text{Br} = 1276\text{ cm}^{-1}$. The position of the band is expected given the change of going from lighter to heavier substituent that brings a red shift. Covalent cyclopropene and isomeric allene structures are ruled out on account of missing bands in the range $1600\text{-}2000\text{ cm}^{-1}$. Thus, twenty years after the initial discovery of the bromo- and chloro- derivatives by Tobey and West, Weiss synthesized and isolated the iodo derivative of cyclopropenylium cation salt.³¹

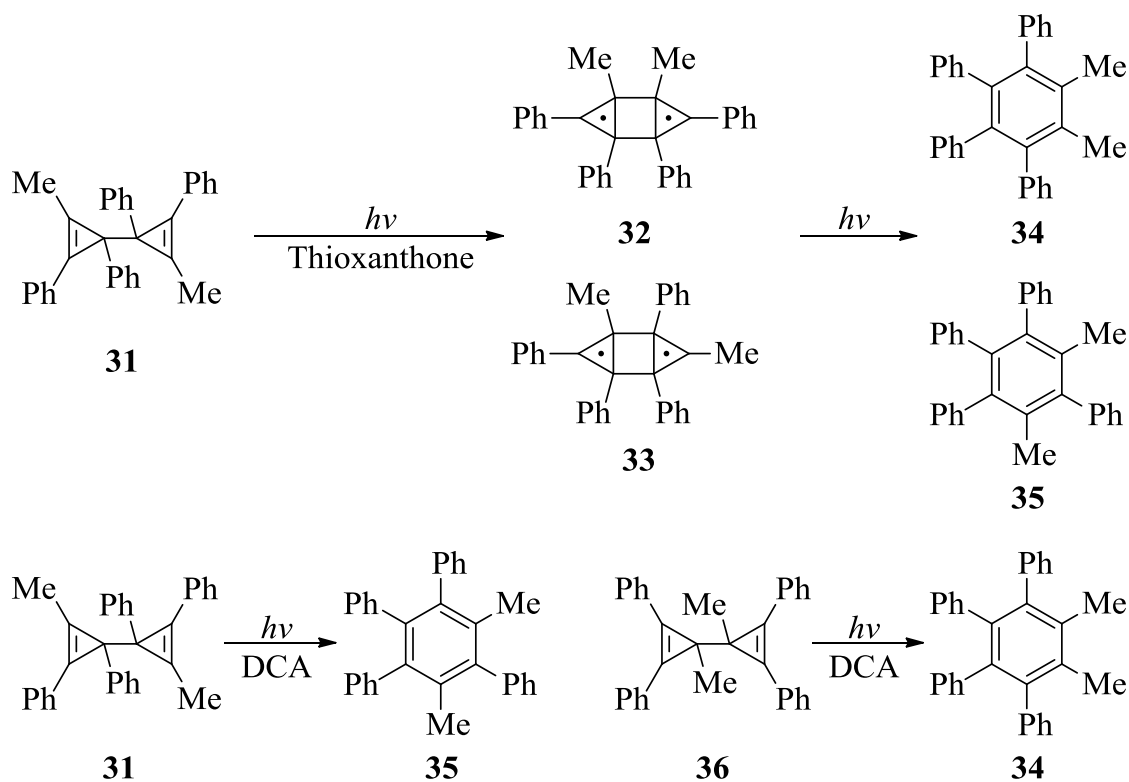
1.1.6 Application of Cyclopropenylium Compounds in Synthesis and Catalysis

Among the first applications for cyclopropenylium compounds was the photo-rearrangement to various functionalized derivatives. The first mention of such rearrangement was published in 1968, by Van Tamelen and coworkers, they observed that irradiation of triphenyl cyclopropenylium cation with 300 nm UV-light and 10 % aqueous sulfuric acid produces hexaphenylbenzene (**Scheme 15**).³² The mechanism was proposed to involve charge transfer that produced the cyclopropenyl radical that coupled to form bicyclopropenyl precursor **29**, which then gave the benzene derivative.³²



Scheme 15: Photochemical rearrangement of triphenylcyclopropenyl bromide salt.³²

The groups of Weiss and Padwa also studied this phenomenon, reporting on the photolysis of bicyclopropenyls (**31**, **36**) as shown below. In particular it was found that thioxanthone sensitized photolysis of (**31**) produced a 4:1 mixture of ortho to meta isomers, while 9, 10-dicyanoanthracene (DCA) sensitized photolysis would produce the meta isomer exclusively (**Scheme 16**).³²

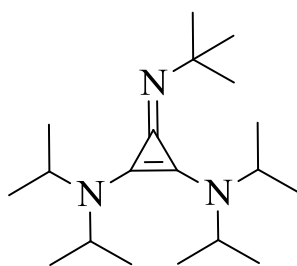


Scheme 16: Sensitized photolysis of bicyclopropenyl compounds.³²

This photo-rearrangement is an excellent example of quick functionalization of benzene derivatives, however, it requires additional study to determine all possible products and expand its potential.

The use of cyclopropenyl cations is not limited to synthesis of functionalized aromatics, today these compounds are involved in catalysis given their inherent basicity and

remarkable reactivity. It is well known that stabilization of conjugate acids leads to an increase in the pK_a of a chemical species, thus the discovery of many stable cyclopropenyl cation salts has ultimately transferred over to catalysis involving highly basic molecules or their protonated analogues. This approach provided the scientific community with many test subjects, such as the 2, 3-bis(dialkylamino)cyclopropenimine which was experimentally determined to have a pK_a of 26.9 in acetonitrile. This means that the pK_a of cyclopropenimine compound (**Figure 8**) is greater than that of most amidines and guanidines, and is comparable to P_1 -*t*Bu phosphazene base ($pK_a = 26.98$).³³ Such high basicity is a remarkable development, as it is rarely observed in small molecules, leading to more research and development of cyclopropenimine systems as catalysts.

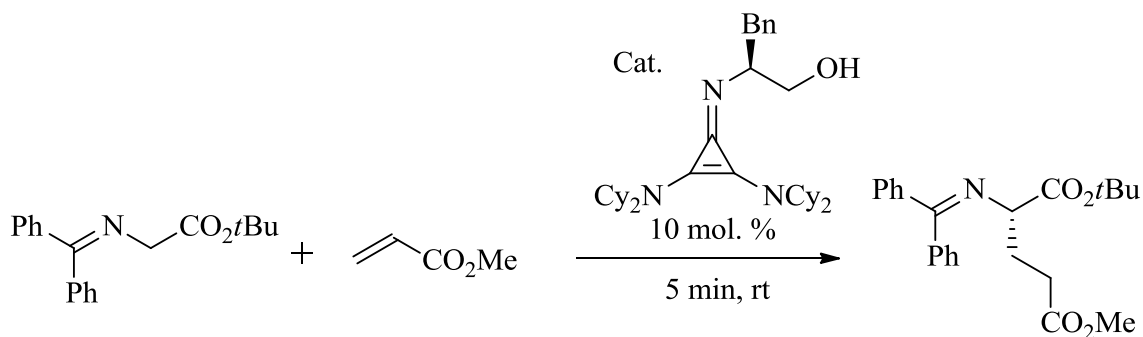


$$pK_a = 26.9$$

Figure 8: 2, 3-bis(dialkylamino)cyclopropenimine, pK_a in acetonitrile.³³

The use of Brønsted bases by chemists as indispensable tools for organic synthesis has resulted from the importance of proton transfer as a key mechanistic event in many chemical reactions.³⁴ Given the ability of superbasic molecules such as Lambert's cyclopropenimine to facilitate this proton transfer, they have become a centre of attention in catalysis. An advantage of 2,3-bis(dialkylamino)cyclopropenimines is the extreme ease of synthesis from which a highly basic molecule is obtained. Lambert explored the potential of this cyclopropenimine compound via several screens. The Michael addition was chosen as the target reaction for catalysis, while

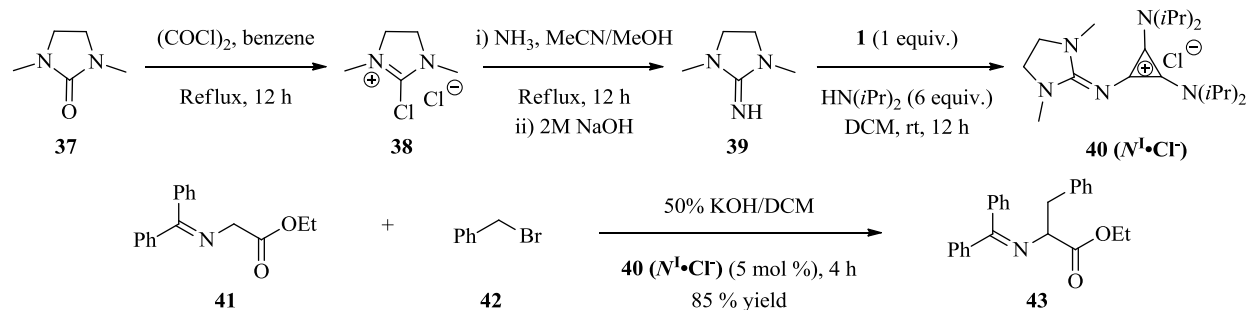
the optimization of the reaction conditions to yield the best enantioselectivity was carried out by varying solvents, concentrations and reaction time. These experiments produced some interesting results. Catalytic use of cyclopropenimine derivatives for Michael additions of glycine imine with methyl acrylate obtained a near quantitative yield of 90 %, with 91 % enantiomeric excess (*ee*). The most remarkable result of these experiments was the rapid rate of reaction (5 min.), under neat (solvent free) conditions (**Scheme 17**).³³



Scheme 17: Michael addition catalyzed by cyclopropenimine derivative under mild conditions.³³

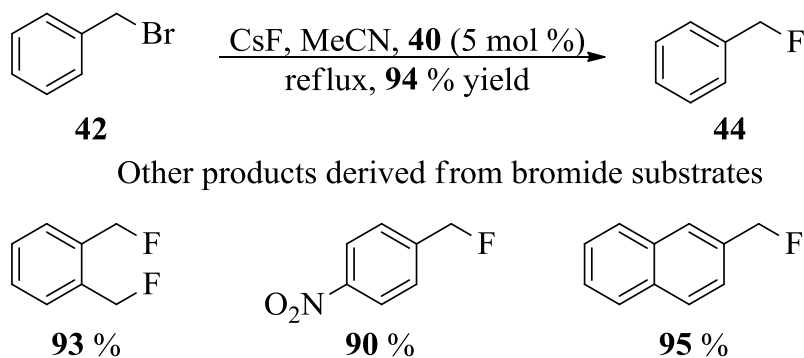
The use of multiple screens revealed that acetonitrile accelerated the reaction, but provided the poorest *ee* (28 %). The propensity of acetonitrile to participate in hydrogen-bonding is known to interfere with the organization of the transition state. Ester solvents on the other hand, slowed down the reaction considerably from one to twenty-four hours. Longer reaction time led to an increase in the enantiomeric excess. It was suggested that the catalytic cycle closed via rapid proton transfer from the cyclopropenium ion to the resulting enolate.³³

Apart from nucleophilic catalysis, cyclopropenylium functionalized compounds have been used to enhance rates of phase transfer reactions. A three step synthesis developed by the Dudding group produced an interesting *N*¹-centered cation, **40** that was able to catalyze benzylation of a Schiff base under KOH aqueous phase transfer conditions (**Scheme 18**).³⁵



Scheme 18: Synthesis of N^1 -centered catalyst and applications under phase transfer conditions.³⁵

This notably represented the first instance of a PTC reaction employing a mixed N^1 -centered catalyst, with both imidazoliumyl and N^1 -cyclopropenylum functionalities. This compound was also successfully applied to fluorination of benzyl bromides (**Scheme 19**).³⁵

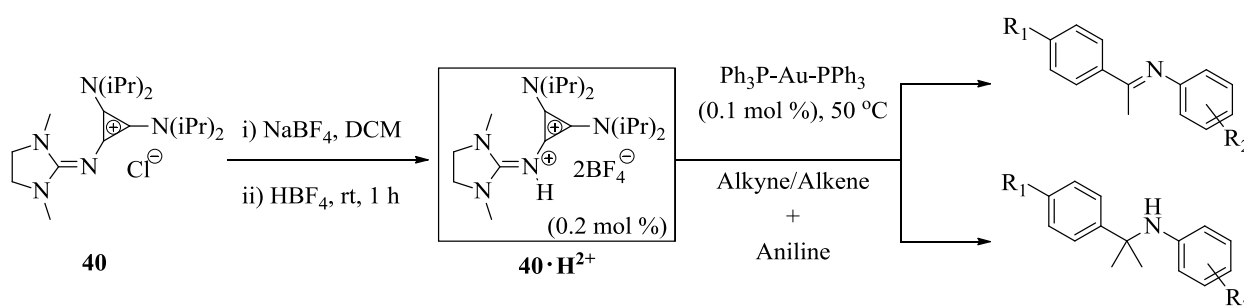


Scheme 19: Fluorination of benzyl bromide with cesium fluoride and N^1 -catalyst **40**.³⁵

Of note, in the absence of catalyst **40**, only trace amounts of fluorinated products were obtained. Furthermore, the reaction proceeds for various bromide substrates, thus demonstrating its versatility as an approach to fluorination. An additional strength of this methodology included column free purification of products, as well as facile recovery of the catalyst via crystallization from hexanes. What is more, no loss of catalytic activity was observed upon repeated use of recovered catalyst (**40**) even after five cycles. In comparison to the widespread stoichiometric use of tetrabutylammonium fluoride for fluorination, the use of **40** does not require harsh

conditions, and affords products in higher yields. Moreover, this method does not require functionalized reagents which take time to prepare.³⁶ This was an impressive feat given the current demand for fluorination methodologies, particularly metal-free procedures.

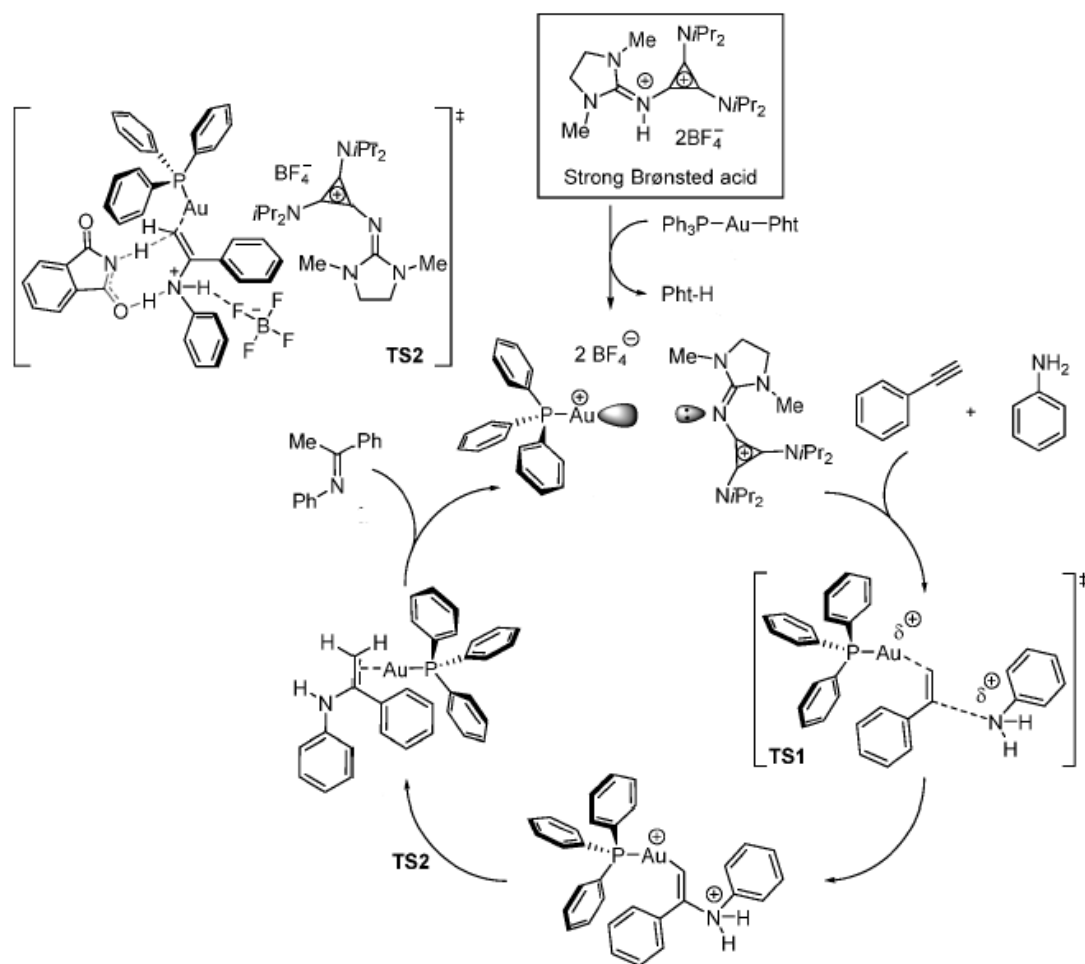
Additionally, protonation of compound **40**, followed by an anion exchange to obtain a dual charged tetrafluoroborate salt **40·H²⁺**, produced a strong Brønsted acid (**Scheme 20**). This species was utilized in gold catalyzed alkyne, and alkene hydroamination. Strong Brønsted acidity of **40·H²⁺** was a key factor in the activation of the Au(I)-olefin complex.^{37a}



Scheme 20: Synthesis of dual-charged salt, **40·H²⁺** and catalyzed hydroamination.^{37a}

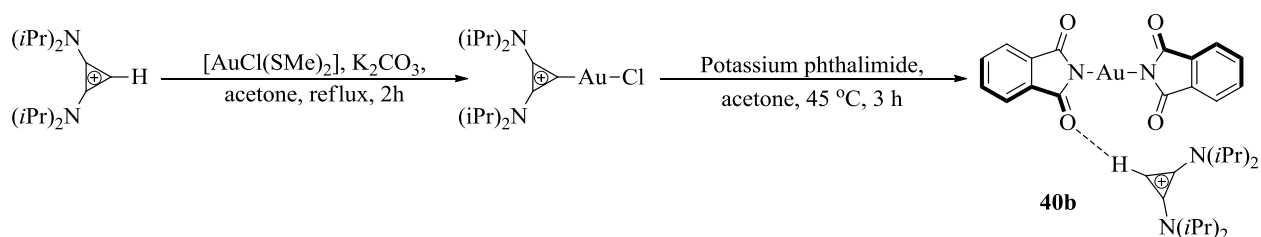
A probe of this catalyzed hydroamination demonstrated a wide scope of alkyne and alkene substrates, including bicyclic compounds. Meanwhile, the nucleophile screen included anilines of different ortho- and para- substitutions. In comparison to the majority of the reported gold-catalyzed procedures, the use of **40·H²⁺** eliminated the need for silver mediated activation of gold(I) precatalyst. The activation is typically done via halogen abstraction, however, silver salts and their by-products can form various Au, and Ag catalytically inactive adducts. The high cost, difficult preparation and sensitivity to light of silver salts make them an unfavourable choice for catalysis. Another advantage of **40·H²⁺** is that it can be used in very small quantities (0.2 mol %) to catalyze the reaction. A catalytic cycle for the hydroamination of alkynes with anilines was proposed to occur via several steps (**Scheme 21**).^{37a} Strong Brønsted acid, **40·H²⁺** is

thought to initiate the cycle via protonolysis of Au-N bond of the precatalyst complex. This generates the phthalimide and gold(I)-triphenylphosphine species. The addition occurs through **TS1**, with the Au(I)---alkyne π -complex activated by the aniline. Proton transfer from either water, phthalimide by-product, or $\mathbf{40} \cdot \mathbf{H}^{2+}$ catalyst then yields the coordinated enamine following photodeauration. The cycle is completed by a tautomerization, which yields the product and releases the Au(I)-catalyst. Other than precatalyst activation, $\mathbf{40} \cdot \mathbf{H}^{2+}$ also has a secondary role, the diffuse cyclopropenyl cation of the ion pair $\mathbf{40}^+ \cdot \mathbf{BF}_4^-$ prevents Au(I) counterion association by sequestering the \mathbf{BF}_4^- away from the metal center. The innate reactivity of the electron deficient gold(I) catalyst is therefore enhanced, allowing binding to the alkyne.^{37a}



Scheme 21: Proposed $\mathbf{40} \cdot \mathbf{H}^{2+}$ and Au(I)-Catalyzed Cycle for Alkyne Hydroamination.^{37a}

Building on the success of the strong Brønsted acid-Au(I) catalytic system above, application of bis(diisopropylamino)cyclopropenylidene with gold as a precatalyst was achieved. The precatalyst complex was synthesized by a short and efficient route, reacting bis(diisopropylamino)cyclopropenium chloride with chloro(dimethylsulfide)gold(I) in the presence of potassium carbonate. The homoleptic Au(I) complex **40b** was obtained in 87 % yield when potassium phthalimide in acetone was added at 45 °C (Scheme 22).^{37b}



Scheme 22: Synthesis of homoleptic gold(I) complex **40b**.^{37b}

Apart from balancing the overall charge of the complex, the cyclopropenium was engaged in a stabilizing hydrogen bonding interaction with the phthalimido oxygen. This solid bench-stable, gold precatalyst was able to catalyze hydroamination of alkynes in the presence of catalyst **40·H²⁺**. It should be noted that the catalytic loadings of the catalyst (**40·H²⁺**) and precatalyst (**40b**) complex required for the reaction to proceed and provide products in fair to excellent yield, were as low as 0.16 mol % and 0.08 mol % respectively. The catalytic cycle was similar to the hydroamination by the strong Brønsted acid **40·H²⁺**. However, in this case the proton of the dual charged catalyst was exchanged for a gold atom during the cycle, with this complex participating directly in catalysis by binding the alkyne.

Cyclopropenimine based compounds have shown various applications in catalysis, primarily due to their charged aromatic character. Their ability to act as Brønsted acids and bases has expanded their use, particularly in PTC. Furthermore, the use of this functionality will

expand synthetic possibilities and enhance catalysis in organic chemistry. Overall, this is a unique structural class that should be further explored in order to determine its properties to the full extent. A deeper insight into the nature of cyclopropenimine compounds can be obtained by using computational methods and is presented in the following section.

1.1.7 Computational Studies of Cyclopropenylum Compounds

Proton affinity (PA) is one of the most useful characteristics of the electronic structure in molecules. It can provide valuable information such as: the distribution of electron density, hydrogen bonding, susceptibility of aromatic compounds to electrophilic substitution, the propensity for the transmission of substituent effects, and more. Lambert calculated a 10 kcal mol⁻¹ higher proton affinity for 2, 3-diaminiiminocyclopropene than the DMAN archetypal proton sponge, which is truly interesting considering the cyclopropenimine system is half the size.³⁹ Several computational studies have been conducted on cyclopropenimines by Z. Maksic and B. Kovacevic,^{38, 39} in order to estimate the proton affinity at the imino group of cyclopropene moieties. The imino centre was found to have a high proton affinity because protonation at that site resulted in significant aromatization (**Figure 9**).

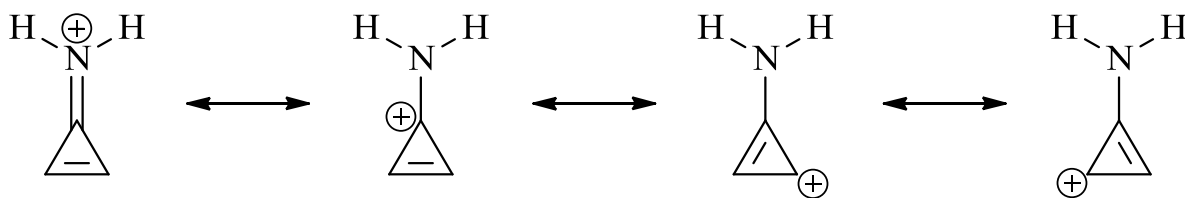


Figure 9: Resonance structures of aromatic protonated cyclopropenimine giving rise to exceptionally high basicity.³⁸

This PA was further increased through NH₂ substitutions at the carbon-carbon endo-double bond, because amino groups enhance aromatization of the cyclopropene fragment by resonance donation. There is an additional effect due to the partial release of lone pair density, therefore contributing to the distribution of the positive charge uniformly not only in the ring, but throughout the entire molecule. The lone pair density is released when a protonation occurs at the imine nitrogen. The close proximity of the adjacent nitrogen atoms results in further stabilization of the molecule through the formation of a hydrogen bond between them. The observed effect was shown to be much more pronounced in the diaminoiminocyclopropene systems that are substituted by bulkier alkyl groups. Given these observations, it was concluded that alkyl groups serve as reservoirs of electron density.³⁸ These reservoirs allow an extremely energetically favorable reorganization of charge to occur.³⁹ Furthermore, two important observations were made during this study that deserved attention. First, the resonance directly assists the strength of the hydrogen bond. The second observation noted that the hydrogen atom that is directly attached to nitrogen on the bridgehead partially protonates the adjacent nitrogen atom of the bridgehead as shown in (**Figure 10**). A reliable model at the MP2 level of theory was used (MP2(fc)/6-311+G**+ZPVE), as well as, a (DFT/B3LYP/6-311+G**) model, in order to calculate the absolute proton affinities of 2, 3-diaminiiminocyclopropene and its derivatives in the gas phase, along with the following equations (**Scheme 23**).

$$APA(B_{\alpha}) = (\Delta E_{el})_{\alpha} + (\Delta ZPVE)_{\alpha} + \left(\frac{5}{2}\right)RT.$$

Where: $(\Delta E_{el})_{\alpha} = E(B) - E(BH^{+})$ and $(\Delta ZPVE)_{\alpha} = ZPVE(B) - ZPVE(BH^{+})$

Scheme 23: Equations used for the calculation of the absolute proton affinity.³⁹

Moller-Plesset perturbation theory (MP2), one of several post-Hartree-Fock ab initio methods, approximately on the same level as DFT, was used. It improves on Hartree-Fock theory by adding electron correlation effects using the Rayleigh-Schrodinger perturbation theory generally to the second (MP2), third (MP3), or fourth order (MP4). In the latter two equations, B and BH⁺ denoted the base under investigation and its conjugate acid respectively, while the site of proton attachment was signified by α . The term $(\Delta E_{el})_{\alpha}$ is the difference in the electronic energy contributions to the proton affinity between the protonated and neutral base forms. The contribution of the pressure-volume work term $\Delta(pV)$ and the translational energy of the proton was accounted for by the additive temperature dependent term $(5/2)RT$. The difference in zero point vibrational energy contributions to proton affinity is also considered by the $\Delta ZPVE$ term. It is important to note that all calculations were performed using the Gaussian 98 suite of programs, and that the authors also used diffused basis sets for their functions, doubling the number of orbitals (**6-311+G****) in order to obtain the most accurate results.

Structurally understandable and intuitively appealing factors arise from the deconvolution of the energetics in the protonation process when calculating the intrinsic gas-phase basicity. However, it must be noted that true chemistry takes place in solution where structural factors and energetics can vary. This simply means that the calculation for the protonation in the gas-phase helps better understand the structural properties and the amount of influence each of the effects (sterics, electronics, IMHB, etc.) have on the process, while not entirely reflecting the exact chemical process that takes place in a flask with a solvent. It is for this reason that the basicity calculation was also carried out in acetonitrile. Additionally, consideration was given to multi-substituted diaminocyclopropenimines in order to fully characterize the contributions of multiple IMHBs to the proton affinity.³⁸ The approach for the determination of the IMHB strength was

done via estimation, through the unfolding of the *N*-dimethylaminopropyl chain, followed by obtaining the difference of these energies. Subsequent determination of the proton affinity for a 2, 3-diaminocyclopropenimine, that contained long branches with a terminal tertiary amine, and *N,N',N''*-tris(3-aminopropyl)guanidine (which has a triple IMHB effect, stabilizing the base) was done. The results revealed that these bases had considerably higher PA than the archetypal proton sponge (DMAN = 245 kcal mol⁻¹). The PA's were calculated to be in the range of 286.8 kcal mol⁻¹ to 260.3 kcal mol⁻¹.³⁸ This experiment concluded that additional IMHB (there were multiple intramolecular hydrogen bonds for each molecule and each had variations in the looping of the chain involved in the bridge formation (**Figure 10**), can enhance the proton affinity.

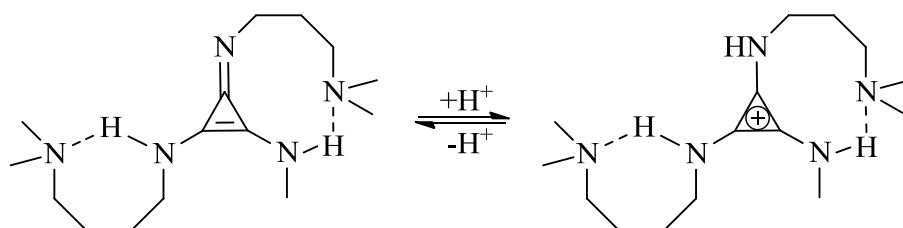


Figure 10: One example of a computationally examined, branched cyclopropenimine.³⁸

Many other species of multi-branched cyclopropenimine molecules along with their respective derivatives representing branch length variations were examined. Aromatization of the cyclopropenyl cation assisted by the resonance effect with directly bonded amino groups in the conjugate acids was observed. In light of the results aromatization of the ring was concluded to be the greatest factor for the increase in proton affinity when comparing these species to the original proton sponge DMAN. A small increase (2.5-4 kcal mol⁻¹) in the proton affinity due to the IMHB contributions was observed.³⁸ Continued computational analysis of cyclopropenimine systems revealed a striking feature: there is a clear tendency to equalize the carbon-carbon bond distances within a ring, again due to the aromatization. An important structural factor, the change

upon re-hybridization at the protonated NH center was also brought to light. Assuming there are $[\text{H-N-H}]^+$ angles of $117\text{-}118^\circ$ in all conjugate acids, the protonated $[\text{NH}_2^+]$ group is planar, corroborated by the natural bond orbital analysis of the hybrid s-character. Results showed that the N-H s-character was increased from 23 % in the neutral base to 31 % upon protonation, this fits the transition to sp^2 canonical states from the sp^3 classical (Pauling's).

The significance of this result was underlined because hybridization parameters are one of the most important covalent bonding indices, and can influence many bond properties at the local level, especially the PA assuming that the lone-pair s-content decreases.³⁹ Therefore it is inferred that during the amplification of PA in tri-amino substituted cyclopropene ring all groups help establish high stability of the resulting cation through a planar arrangement which allows for π -delocalization. There were a few important conclusions to the properties of cyclopropenimines and potent organic bases in general; given the existence and proper arrangement of planar cyclic π -electron networks, aromaticity as a mechanism can lead to potent organic bases. The authors also extracted a few more important conjectures; when considering first row elements the imino group is undeniably the most basic one; exocyclic double bond of the cyclopropene moiety will greatly enhance the imino basicity; and that given the proper orientation (planar) and substitution of strong electron releasing NH_2 groups, additional PA amplification can be obtained.

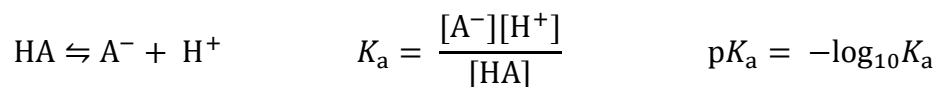
Additionally, the increased electron relaxation effect in the resulting conjugate acids is simultaneously provided by bulky alkyl groups along with π -electron system protection; and approximately 10 kcal mol^{-1} enhancement of the PA can be gained upon the formation of a proper aminoalkane 'crown' that is attached to the imino group during protonation.³⁹ All factors both explain and emphasize the high proton affinity of cyclopropenimines which should be applied in synthesis of a new compounds including proton sponges. Additional investigation

would be required in terms of catalytic applications for these compounds. However, more must first be understood about basicity, superbases and proton sponges as per the following section.

1.2 Superbases and Proton Sponges in Organic Chemistry

1.2.1 Review of Basicity in Organic Chemistry

The concept of acids and bases is paramount to the field of organic chemistry. In this light there are two commonly used definitions, namely, Brønsted acids and bases, and Lewis acids and bases. Brønsted acids and bases are compounds that donate and accept protons respectively. A Lewis base is a chemical species with an available lone pair of electrons, while a Lewis acid is a chemical species that has the ability to accept a lone pair of electrons.^{40, 41} In terms of basicity, the measure of the strength of a particular base is related to the stability of its conjugate acid. This can be quantitatively determined by the acid dissociation constant (K_a , **Scheme 24**) of the compound in a specific medium (most often water). Given the range of possible K_a values a logarithmic scale, known as the pK_a scale, is commonly used.^{40, 41} This is represented by the equations given below (**Scheme 24**).



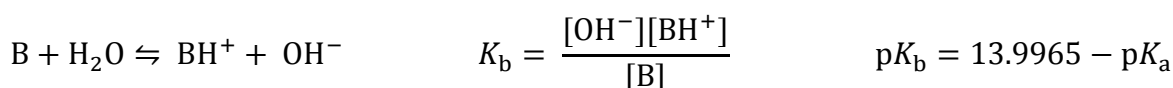
Scheme 24: Acid dissociation equilibrium, derived equation for acidity constant, and pK_a .^{40, 41}

Generally, a larger pK_a value, means a weaker acid due to a smaller extent of dissociation at any given pH.^{40, 41} The pH is derived using the Henderson-Hasselbalch equation (**Scheme 25**).

$$\text{pH} = \text{p}K_a + -\log_{10} \frac{[\text{A}^-]}{[\text{HA}]} \quad K_w = [\text{H}_3\text{O}^+][\text{HO}^-]$$

Scheme 25: Henderson-Hasselbalch derived equation for the measure of acidity (pH) in chemical and biological systems, and the self-ionization constant of water.^{40, 41}

Using the same concept, the association constant for the protonation of a base to form its conjugate acid, K_b can be determined with the help of the self-ionization constant of water (K_w), (**Scheme 24**). The determination of K_a , K_b , and K_w under identical conditions of ionic strength and temperature give the equation ($\text{p}K_b = \text{p}K_w - \text{p}K_a$), where the $\text{p}K_w$ in aqueous solution at 25 °C is equal to 13.9965.⁴¹ Therefore, K_b is defined by the following set of equations (**Scheme 26**).



Scheme 26: Equilibrium of base association, derived equation for the basicity, and $\text{p}K_b$.^{40, 41}

The association constant is related to K_a for the conjugate acid in water by the concentration of the hydroxide ion relative to the proton (**Scheme 27**).

$$[\text{OH}^-] = \frac{K_w}{[\text{H}^+]} \quad K_b = \frac{[\text{BH}^+]K_w}{[\text{B}][\text{H}^+]} = \frac{K_w}{K_a}$$

Scheme 27: Equilibrium in water, derived equation for the basicity relative to the K_a .^{40, 41}

There is an important effect related to the acidity and basicity of chemical species in non-aqueous solvents. Protic solvents that are able to form hydrogen bonds, and solvents that are strong Lewis bases, or are excellent solvents for ionic species that have a high dielectric constant are promoters of ionization of a given acid dissolved in solution. A higher extent of hydrogen bond formation can be observed in water, which has a dielectric constant of 78 compared to 35.5 for acetonitrile both at 25 °C.⁴² Aprotic solvents such as acetonitrile and dimethyl sulfoxide

(DMSO) are common in the measurements of pK_a of organic compounds, because they are able to stretch the limited range of pK_a in water to 1-30 in DMSO. Apart from the lower dielectric constant, there is another advantage that dimethyl sulfoxide offers in that it is less polar and is able to dissolve hydrophobic substances. There is a slight difference between acetonitrile and dimethyl sulfoxide in that DMSO is more basic than acetonitrile, this results in a different pK_a as bases are stronger and acids are weaker in acetonitrile.^{42, 43}

1.2.2 *Amines, Amidines, and Guanidines*

At an elementary level organobases can be, but are not limited to amines that are classified as weak bases. Greater basicity is achieved through the introduction of imine functional groups ($=NH$) at the α -carbon of amines, giving rise to corresponding amine species, structurally equivalent to carboxylic acid imidates (carboxylic esters) called amidines. The strongest Brønsted basicity of amine derivatives is observed in guanidines that are amine equivalents of carbonimidic diamidines (ortho esters) and are defined by the presence of three nitrogen groups, one imine and two amines. In terms of basicity, guanidines are similar to hydroxyl ions (OH^-) with high pK_a values, greater than 13.6.⁴⁴ The pK_a values of guanidines can be explained by the added stability of the conjugate acid allowing for the spread of the positive charge across all available nitrogen centers. Thus, each addition of a nitrogen functional group to the α -carbon of an amine subsequently increases the basicity (**Figure 11**).

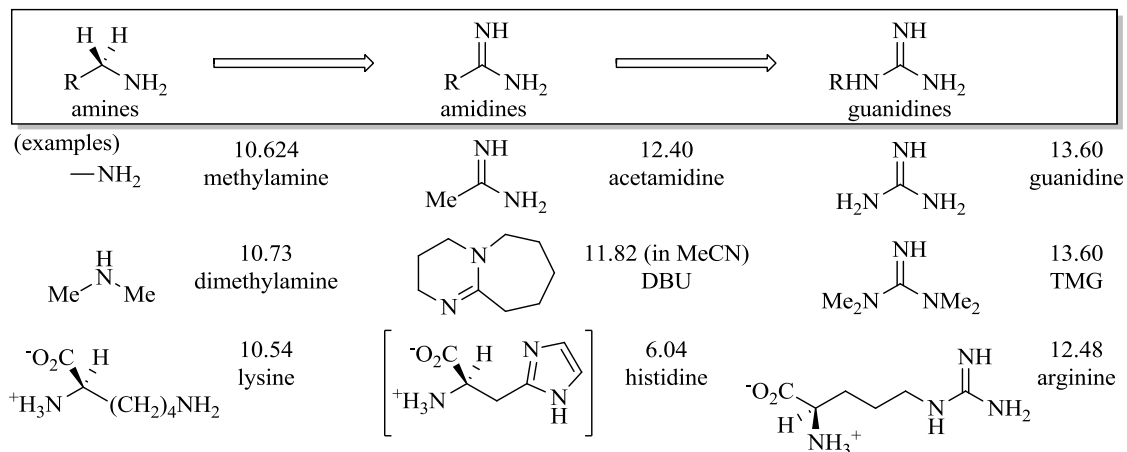


Figure 11: Structures of amine derivatives and their examples (pK_a of the conjugate acids in H₂O): DBU = 1,5-diazabicyclo[5.4.0]undec-5-ene; TMG = 1,1,3,3-tetramethylguanidine.⁴⁵

The basic properties of these amine derivatives are primarily due to the increase in the number of isoelectric forms (canonical forms) in the resonance system. This results in a highly efficient system of conjugation following protonation under reversible conditions. Guanidines are stronger bases than amidines because of that particular factor.⁴⁶ A good example of this phenomenon is shown in **(Figure 12)**. A more direct example of the strong basicity⁴⁹ is **(Figure 13)** in pentacyclic amidine (vinamidine)⁴⁷ and biguanide⁴⁸ due to the vinylogous conjugation.

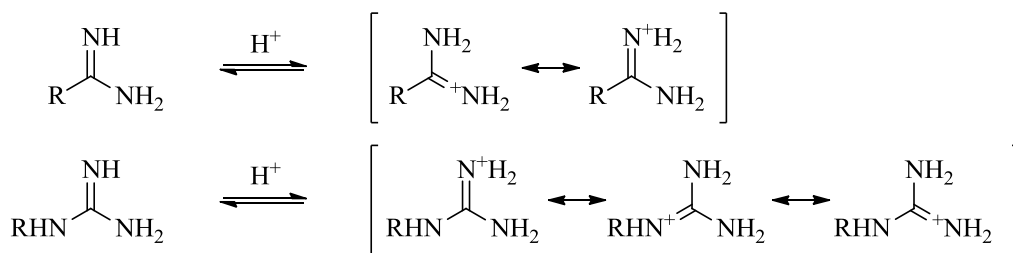


Figure 12: Resonance forms of amidinium and guanidinium ions.^{45, 46}

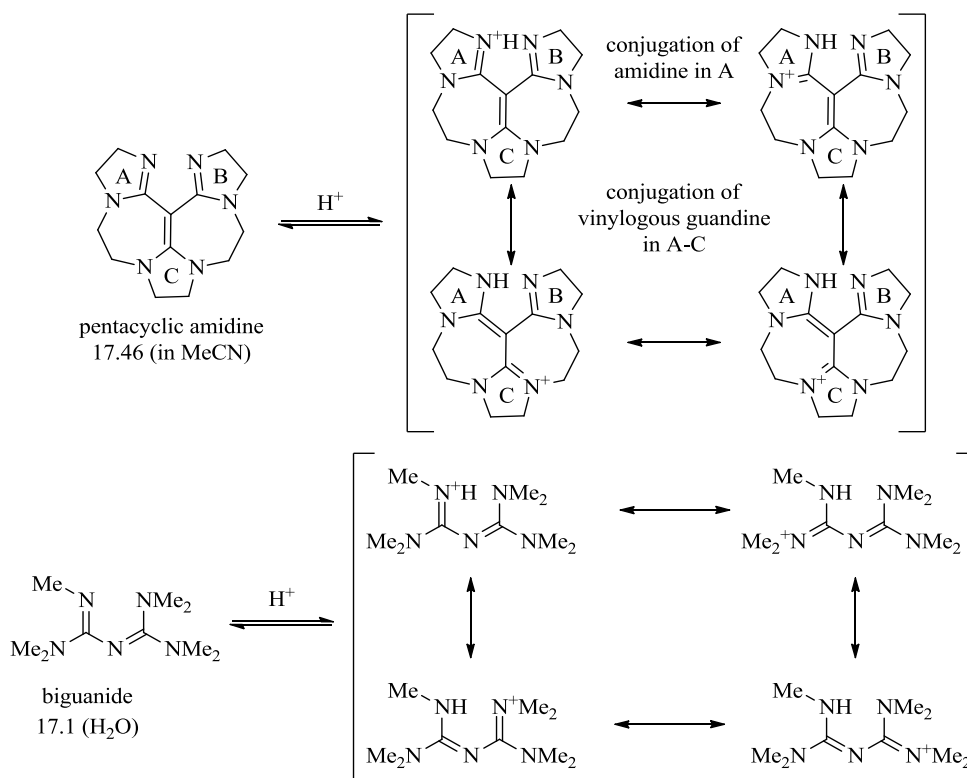


Figure 13: Vinylogous conjugation system of amidine and guanidine derivatives.^{45, 47, 48, 49}

Another way to denote the stabilization effect on protonated bases in (**Figure 13**) is shown by the resonance states in (**Figure 14**), where the high basicity is achieved via bidentate hydrogen bonding. The molecular strain is relieved by occupying the lone pair at one nitrogen centre with a proton, which allows the adjacent nitrogen to form a hydrogen bond using its lone pair of electrons. This subsequently changes the distance between the nitrogen centres and no longer pins the electron pairs against each other, reducing the strain caused by their repulsion.⁵⁰

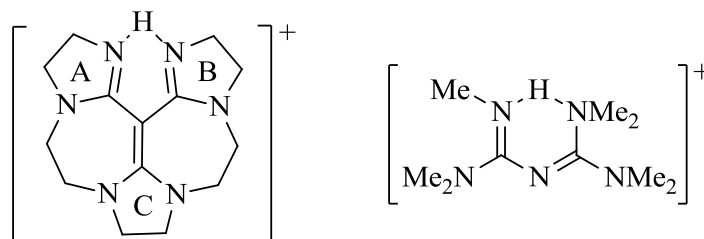


Figure 14: Hydrogen bonding stabilization effect.^{45, 50}

1.2.3 Phosphazenes and Phosphorus Containing Compounds

Phosphazenes (triaminoiminophosphorane skeletons) that contain a [P(V)] phosphorus atom bonded to one imine and three amine groups are another type of organobase, which were introduced by Schwesinger in 1985.⁵¹ Their classification is given by P_n, where (n) is the number of phosphorus atoms in the molecule.⁵² The phosphazene branch of organobases is important because it includes the strongest phosphazene P₄ bases, that were observed to have basicity close to organolithium compounds. Again, the increased basicity was caused by the efficient distribution of positive charge in the conjugated system of the molecules.⁵³ The advantage of these bases is in their steric bulk, which gives them stability to hydrolysis and prevents an attack on electrophiles. They are also quite soluble in common organic solvents.⁵⁴ Examples of P₁ and P₄ phosphazene bases are given in (Figure 15).

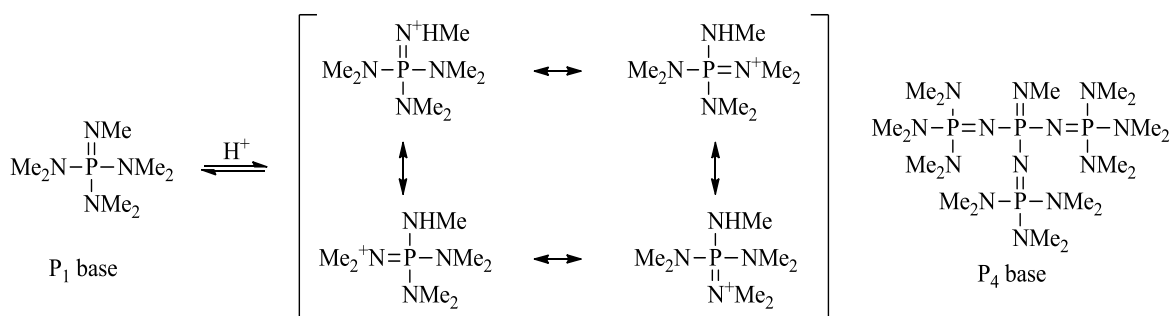


Figure 15: P₁ and P₄ phosphazene base examples (P₁ with resonance).^{45, 52, 54}

An alternative class of phosphorus organobases which contain a P(III) atom at a bridgehead of a bicyclic system, that is bonded to amino groups was discovered by Verkade.⁵⁵ These were named proazaphosphatranes or cycloazaphosphines. Stability of the phosphonium salt of this base following protonation at the phosphorus atom was generated through an effective formation of a *trans*-annular N-P bond, using the fourth nitrogen at the adjacent bridge head

position. This bond yielded propellane like compounds containing tricyclo[3.3.3]dodecane skeletons (**Figure 16**).

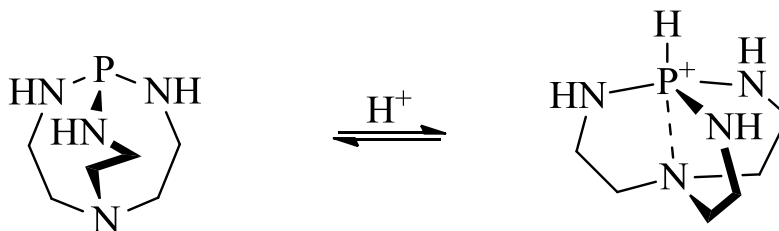


Figure 16: General structure of Verkade's base and the trans-annular P-N bond formation that is responsible for the basicity (shows the flattening of the 7-membered ring upon protonation).^{45, 55}

1.2.4 Recent development of Superbases and Proton Sponges

Unusually high basicity of organic diamines was first simply described in proton sponge, which was initially discovered by Alder in 1968. It was produced via *N*-methylation of 1,8-diaminonaphthalene that yielded 1,8-bis(dimethylamino)naphthalene (DMAN).⁵⁶ The observed bidentate coordination between two dimethylamino groups at the *peri* position of the naphthalene ring system resulted in the exceptional proton affinity. The discovery of this compound provided the backbone for further derivatives such as: 1,8-bis(tetramethylguanidino) naphthalene (TMGN)⁵⁷, 1,8-bis(hexamethyltriaminophosphazanyl) naphthalene (HPMN)¹⁹, and 1,8-bis(bis(diisopropylamino)cyclopropenimine) naphthalene (DACN).⁶⁶ Greater basicity of the proton sponge was the main goal for the synthesis of these compounds. This new generation of compounds utilized previously discussed concepts of guanidine function, phosphazene skeleton, as well as a recently discovered and employed cyclopropenimine (**Figure 17**).

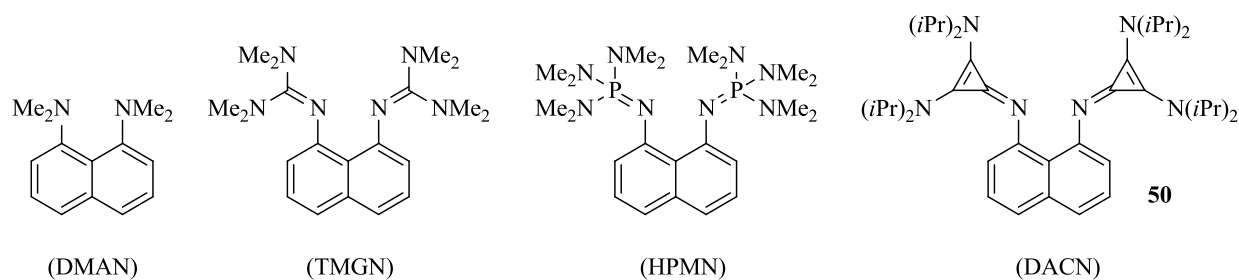


Figure 17: Proton sponge (DMAN), and structurally related derivatives; TMGN, HPMN, DACN (**50**).^{45, 57, 58, 66}

The hypothesis of increased proton affinity in this new generation of proton sponges was confirmed by computational calculations.^{53, 59} Ambiguous criteria and extensive use of the words “strong” and “super” for the description of basic properties in molecules led to some confusion among organic chemists. This led to the initial argument for the proposed definition of a superbases by Caubère: *The term ‘superbases’ should only be applied to bases resulting from a mixing of two (or more) bases leading to new basic species possessing inherent new properties. The term ‘superbase’ does not mean a base is thermodynamically and/or kinetically stronger than another, instead it means that a basic reagent is created by combining the characteristics of several different bases.*⁶⁰ The general equation for Caubère’s proposed definition is illustrated below (**Scheme 28**).^{60, 61}



Scheme 28: Equation for the proposed superbases definition.^{60, 61}

The initially proposed definition of a superbases by Caubère was not broad or detailed enough and would later be redefined, by specific thermodynamic properties that could be calculated using computational methods. One of the reasons for the pursuit of new, stronger superbases is their broad employment in catalysis, specifically in reversible proton transfer

between the substrate (acidic counterpart) and base. This is due to their relatively weak nucleophilicity and high basicity, given by the high kinetic activity in proton exchange reactions. Therefore, there is an extreme benefit from an environmental perspective as superbases can be re-used. The ability to recycle superbases attracts considerable attention for various organic syntheses that require base catalyst for the reactions. Prior to obtaining and applying superbases in organic synthesis it is important to determine their pK_a in order to appropriately match for reactions. Various physical methods such as titrations, condensed media experiments, and mass spectrometry (for values in the gas phase) can be applied to measure and determine the basicity of organic molecules. The determination of pK_a 's via condensed media studies of strong bases typically uses solvents such as dimethyl sulfoxide (DMSO), tetrahydrofuran (THF) and especially acetonitrile (MeCN). An important point is raised by the variety of results that were obtained using different methods. It is paramount to carry out as many measurements as possible, using a variety of solvents in order to obtain accurate results.⁴⁵ Quantum chemical calculations are also a valuable tool to obtain the proton affinity and relative pK_a .

The emergence of more superbases led to the more specific and now commonly accepted definition of this term requiring it to be a stronger base than the original 'proton sponge' (DMAN). This meant that a superbase must have an absolute proton affinity (APA) greater than $245.4 \text{ kcal mol}^{-1}$ and it must also have a gas phase basicity (GB) of over $239 \text{ kcal mol}^{-1}$.⁶⁴ As this thesis is focused on the synthesis of a novel cyclopropenimine compounds combined with properties of proton sponges, further discussion will pertain to that topic explicitly, only mentioning guanidine and phosphazenes briefly where related. The broad applications of such compounds will be touched upon as well, in particular the possibilities that proton sponges provide in catalysis.

1.2.5 Discovery and Synthesis of the Proton Sponge

As previously mentioned, the first proton sponge was synthesized and reported in 1968, by R. W. Alder and co-workers at the University of Bristol in the United Kingdom.⁵⁶ The authors defined proton sponges as organic diamines with unusually high basicity, specifically, high thermodynamic basicity (proton affinity). Generally this is also accompanied by kinetic inactivity to deprotonation, which is the origin of the name “proton sponge”, since such molecules retain the proton they abstract like a sponge retains water.⁵⁶ Their synthesis was a simple N-methylation of a 1,8-diaminonaphthalene by dimethyl sulfate (DMS) in acetonitrile (MeCN) at room temperature. The products were isolated using various types of column and alumina chromatography. Initially, the basic properties of the product were not entirely apparent. This was because the pK_a of the conjugate acid in water following each of the four individual methylations would increase slightly. However, upon the fourth and final N-methylation the pK_a almost doubled (**Figure 18**), pK_a 's of the intermediates and product were measured in water:

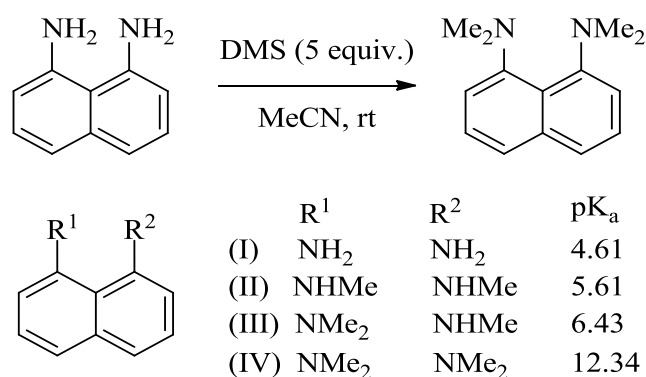


Figure 18: Synthesis of 1, 8-bis (dimethylamino) naphthalene (DMAN), pK_a 's also listed.⁵⁶

The last pK_a is significant as it is stronger than that of a normal aliphatic amine, meaning that the basicity of the new compound is 10 million times higher than similar organic amines.⁵⁶

1.2.6 Applications of the DMAN Proton Sponge in Organic Synthesis

The original proton sponge (DMAN) has been used in a variety of reactions as a base, including hetero-Michael addition, alkylation, and amide formation reactions.^{73, 74, 75} Its applications as a hindered, weakly nucleophilic and nonionic strong base have been utilized alone and in combination with other superbases.⁴⁵ Proton abstraction and shuttling, without nucleophilic attack was the general purpose of the DMAN proton sponge in the following reactions. An *N*-alkylation produced a tertiary amine in a 75 % yield from a reaction of 3-butenyl triflate with a pyrrolidine derivative at room temperature, in dichloromethane, (**Figure 19**).⁷³

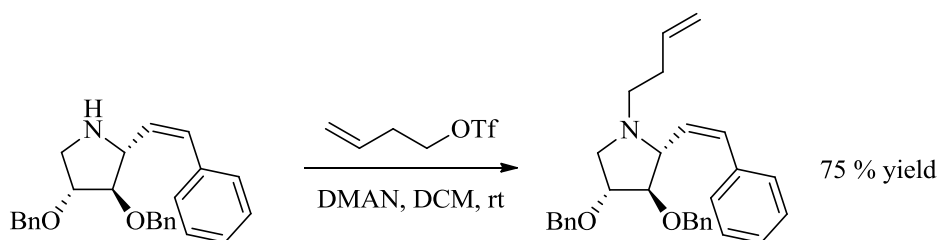


Figure 19: *N*-alkylation of pyrrolidine derivative using proton sponge DMAN.⁷³

The Williamson reaction, utilizing silver oxide and alkyl halide together with an alkyl triflate and 2,6-di-*tert*-butyl-1,4-methylpyridine is a good example of an efficient and fairly mild alcohol alkylation. However, it often results in ethers that are racemized, and may also prove to be ineffective when dealing with sterically hindered alcohols. Therefore, optically labile and sterically hindered alcohols require an alternative method that is both mild and efficient.

Trialkyloxonium tetrafluoroborate (Meerwein's salt) has been used to synthesize ethers that retain the chirality of the alcohol. The major concern here is that the tetrafluoroboric acid produced can promote structural isomerization, racemization and possibly polymerization in systems prone to carbenium ion formation. The rationale for the use of DMAN proton sponge

was that it would remove the acid as it forms avoiding the formation of carbenium ions. The low nucleophilicity and steric hindrance of this base avoided any unwanted reactivity, thus proving it to be an excellent choice. Experimentally achieved 69 % yield of the optically active methyl ether corresponding to the (R)-(+)-1-phenylethyl alcohol that reacted with a Meerwein's salt (2.1 equiv.) and DMAN (2.1 equiv.) was obtained. This was a great example of utility of the proton sponge as a catalyst under mild conditions (**Figure 20**).⁷⁴

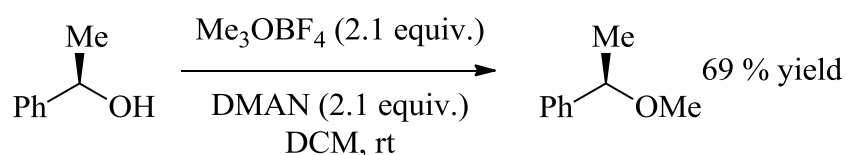


Figure 20: O-alkylation of optically active alcohols using DMAN Proton sponge.⁷⁴

Additionally, remarkable yields of over 90 % were achieved for the *O*-methylation of sterically hindered molecules at room temperature and in dichloromethane at very rapid rates. Proton sponge (DMAN) was used with Meerwein's salt as well as 4 Å molecular sieves to vastly improve the methylation.⁷⁵ Another application of proton sponge is the synthesis of isocyanates at room temperature. This was done using two equivalents of DMAN, as well as, one equivalent of trichloromethyl chloroformate and, (S)-1-azidobut-3-en-2-amine each, to produce the (S)-4-azido-3-isocyanatobut-1-ene, in 88 % yield.⁷⁶ (**Figure 21**).

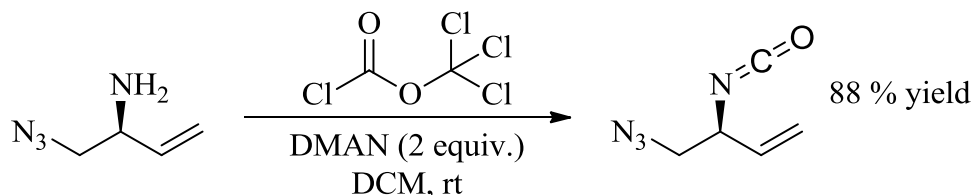


Figure 21: Efficient synthesis of azide isocyanate from aliphatic azide amine.⁷⁶

1.2.7 Investigation of Proton Sponge Properties via Computational Methods

The first experimentally measured proton affinity (PA) of DMAN in the gas phase was determined to be $246.3 \text{ kcal mol}^{-1}$ ⁶² while the computationally calculated value was 246.5 and $258.7 \text{ kcal mol}^{-1}$, using 6-31G**/6-31G+ZPE and 6-31G basis sets of the DFT/B3LYP method and function.⁶³ In computational chemistry density functional theory is commonly used as it allows for accurate calculation of structural and electronic properties for the chemical species at hand. Calculations involving DFT consider the charge density of a molecule, meaning that it is independent of the wave function. The modern, hybrid DFT method calculates the energy of a system as a sum of 6 components: nuclear-nuclear repulsion, nuclear-electron attraction, electron-electron Coulomb repulsion, kinetic energy of electrons, correlated movement of electrons of different spin and electron-electron exchange. When comparing DFT to the Hartree-Fock theory the first four energy components are calculated in a similar manner. The increased accuracy of DFT calculations arise from the addition of the last two components which are only estimated by the Hartree-Fock theory. The treatment of the attractive and repulsive Coulomb interactions by self-consistent mean potential in the Hartree-Fock method allows the data to be collectively calculated and stored, this would otherwise be impossible. As one of the most common levels of theory for computation, DFT is almost always accompanied by Beck, 3-parameter, Lee-Yang-Parr additional functional (B3LYP), which considers the hybrid electron coordination, further improving the accuracy of the calculation. Basis sets such as 6-31G are also commonly employed. These are a set of functions that are combined in linear combinations for quantum chemical calculations, in order to create molecular or atomic orbitals. The selection of a specific basis set generally depends on the functionalities present in the molecule and is based primarily on electrostatics.

There are three general classes of basis sets; split valence (3-21G), polarized (6-31G-d or 6-31G*), and diffused (6-31++G-d). The split valence separates the core electrons (3-21G) from the valence electrons (3-21G) during the calculation for accuracy, since the two contaminate each other via interaction. Valence is further classified by denoting the **2** as the inner and **1** as the outer electrons, G simply stand for ground state. Overall the split valence basis set is only able to change the size of the orbitals on which the calculations are performed. A polarized basis set adds both d and p orbitals to the molecule further increasing the accuracy of calculations especially for molecules with a variety of atoms. This changes the size and shape of the orbitals when atoms of various electro-negativities are present. Addition of the d-orbital is usually to the heavy atoms and *p*-orbital to the hydrogens. The diffused basis set allows orbitals to occupy a larger space, and is important for systems which have atoms with electrons far from the nucleus, also when radicals, anions, and excited states are present.

The authors of the computational studies above selected polarized basis sets at the DFT level of theory. They could have also improved on their calculations by using 6-311G* which simply doubles the number of orbitals (both s and p) for a more accurate calculation. The +ZPE in one of the authors' calculation methods simply means that they used a diffused basis set, and corrected for the zero-point energies (lowest energy that a quantum mechanical physical system can have, *i.e.* true ground state energy). The basis set of 6-31G(d,p) will be used to calculate the proton affinity of the novel cyclopropenimine proton sponge reported in this thesis.

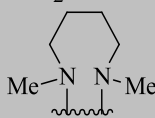
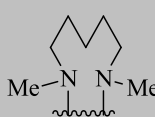
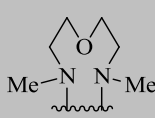
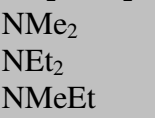
The orientation of the two basic nitrogen centers in proton sponges usually allows for the uptake of only one proton, which yields a stabilized intramolecular hydrogen bond (IMHB). The remarkable increase in basicity in the aromatic proton sponge was explained by the ground state destabilization of the neutral species due to the strong repulsion of unpaired electrons at the

nitrogens. These are pinned almost directly towards each other due to the steric bulk of the methyl groups restricting rotation. The other factor enhancing the basicity was the formation of an intramolecular hydrogen bond (IMHB) upon protonation, which relieved the steric strain of the molecule via loss of the destabilizing lone pair-lone pair repulsion. The destabilization arises from the slight bend in the aromatic backbone of the proton sponge due to the lone pair repulsion. An additional factor is the difference in solvation energies of the neutral and protonated species in solution, this effect is minimal when compared to the previous two.⁶⁵ It is important to note that there is currently a debate over the basicity, specifically if it is caused solely by the steric strain of the molecule or the nature of the hydrogen bond in the monoprotonated species.

Over the last twenty years, great interest has been placed on the proton sponge and its derivatives by chemists, which gave rise to over 100 spectroscopic and 70 structural papers, a few of which are shown in (**Table 5**).^{67,68} This generated interest led to the analysis of IMHB, lone pair repulsion and solvation energy effects on the pK_a of the proton sponge. Understanding of these contributions was necessary in order to better define these parameters and allow for the design of future compounds with specific pK_a 's. The extensive experimental and theoretical studies were able to point out that the solvation energies along with the IMHB could each increase the basicity by 2-4 pK_a units, while the lone pair repulsion could increase the pK_a by as much as 6 units. A formation of virtually linear and thus strong IMHB between the nitrogen atoms upon protonation was also shown to be favored ($N - H^+ \dots N$ around 175° most stabilized). Linear IMHB was determined to be strongest because the lone pair on the nitrogen participating in the hydrogen bonding is able to donate its electron density directly into the anti-bonding orbital of the hydrogen. This donor-acceptor interaction results in more electron density being

shared between the nitrogen centres and thus better stabilization of the positive charge. An investigation of the IMHB in twenty proton sponges obtained an average N...N distance of 2.717-2.792 Å in the neutral species. While in the protonated form the N...N, N – H⁺, and N...H⁺ distances were found to be 2.541-2.881, 0.86-0.92 and 1.376-1.580 Å respectively.⁶⁹ The angles of the IMHB between nitrogens varied between 150 and 180⁰. Using this data and additional experiments, the strength of the IMHB was calculated to be in the range of 16-21.5 kcal mol⁻¹.⁷⁰

Table 5: Experimental pK_a values of conjugated acids of naphthalene type proton sponges.^{67, 68}

Compound	R ³	R ⁴	R ⁵	R ⁶	pK_a (solvent)
1					12.00; 12.03; 12.34 (H ₂ O); 12.10 (30% DMSO/H ₂ O); 18.28; 18.18 (MeCN); 7.47 (DMSO); 16.8 (THF); 11.5 (20% dioxane)
2	NEt ₂ NMe ₂	NEt ₂ NMe ₂	H OMe	H OMe	18.95 (MeCN); 12.7 (20% dioxane) 16.1 (35% DMSO/H ₂ O); 16.3 (H ₂ O); 11.5 (DMSO)
	NEt ₂ 	NEt ₂	OMe	OMe	16.6 (H ₂ O)
		Between R ³ – R ⁴	H	H	13.6 (30% DMSO)
		Between R ³ – R ⁴	H	H	13.0 (30% DMSO)
		Between R ³ – R ⁴	H	H	12.9 (30% DMSO)
	CH ₂ NMe ₂	CH ₂ NMe ₂	H	H	18.26 (MeCN)
	NMe ₂	NMeEt	H	H	18.5 (MeCN)
	NEt ₂	NMe ₂	H	H	18.7 (MeCN)
	NMeEt	NMeEt	H	H	18.7 (MeCN)
	NEt ₂	NMeEt	H	H	18.9 (MeCN)
	NMe ₂	NMe ₂	NH ₂	H	10.3 (MeCN)
	NMe ₂	NMe ₂	NMe ₂	H	9.0 (MeCN)
	NMe ₂	NMe ₂	NMe ₂	NMe ₂	11.2 (MeCN); 15.8 (DMSO)
	NMe ₂	NMe ₂	Me	Me	9.8 (DMSO)
	NMe ₂	NMe ₂	SMe	SMe	8.1 (DMSO)
	NMe ₂	NMe ₂	Pyrr ^a	Pyrr ^a	15.5 (DMSO)
3					8.0 (DMSO)
4					9.8 (H ₂ O); 14.4 (DMSO)
5					7.7 (DMSO); 18.3 (MeCN)

^a Pyrrolidinyl.

1.2.8 Defined properties and major findings on Proton Sponges

Two main concepts can be used to increase the thermodynamic basicity of a proton sponge. First is the variation of the backbone skeleton from naphthalene to other aromatic spacers, which will vary the non-bonding distances of the N- -N proton acceptor lone pairs (Buttressing effect). The second concept is the variation of basic nitrogen centers or their adjacent environment.⁴⁵ This latter concept is the primary focus, since a highly basic cyclopropenimine functionality at the nitrogen center is used in the synthesis of the new proton sponge (**45**) reported in this thesis. A detailed analysis of the ‘buttressing effect’ found that it is defined by a complex combination of interactions of the dimethylamino groups with the *ortho* substituents within the corresponding neutral and protonated bases, in a detailed study by Pozharskii.⁷¹

The interplay of several factors determined the basicity in a proton sponge. One of these factors was the polar effect of *ortho* substituents, where the electron-donating substituents were observed to increase basicity. The reduction of conjugation between *peri*-N(CH₃)₂ groups and the naphthalene system could also yield a maximum enhancement of 1.2 to the p*K*_a. An increase in the *p*-character of the nitrogen lone pairs was found to contribute to the increase in basicity as well. Additionally, an increase of the IMHB strength, and a decrease of the steric strain in the cation and electrostatic repulsion between lone pairs of the dimethylamino (N(CH₃)₂) groups, were found to increase the p*K*_a. One of the few factors decreasing basicity was determined to be the *p*, *d*-interaction of the N(CH₃)₂ groups with *d*-elements of such *ortho*-substituents as SCH₃, Si(CH₃)₃ and bromine (slight decrease). The substituent driven changes in solvation also lowered the p*K*_a because hydrophobic groups inhibit solvation thus decrease the basicity, in contrast, hydrophilic groups can provide an increase.⁷¹ The *p*-character of the lone electron pair at the

nitrogen and the distortion of the n, π -conjugation has been confirmed to be of great importance by several other authors.⁷² Mutual repulsion is increased due to the flattening of the nearby NR_2 groups (planarization caused by sp^3 to sp^2 re-hybridization). This also is supplemented by the Coulomb repulsion due to high charge density on the nitrogen atoms, resulting in the structural destabilization of the neutral proton sponge. Loss of conjugation between NR_2 and naphthalene π -system is the consequence of substantial twisting of the $\text{N}(\text{CH}_3)_2$ groups out of the ring plane, which is initially reduced by greater sp^2 character of the nitrogen atom. The basicity is consequently increased by both the repulsion and loss of conjugation with the naphthalene backbone.⁷²

1.3 Summary of Planned Synthesis and Investigation

Since the goal of this thesis is the synthesis and investigation of cyclopropenimine based compounds it is natural to start with the DACN proton sponge and its applications. The initial investigation of DACN revealed that aromaticity was a fourth and deciding factor in the enhancement of basicity of this proton sponge. The computed $\text{p}K_{\text{a}}$ of this compound was found to be 27.0 in acetonitrile, however, experimental confirmation of this value was impossible. The reason for this was that DACN could not be isolated in its mono-protonated form. Regardless, the diprotonated salt of DACN, was presumed to be catalytically active, and thus was put to the test. Alkylation of Schiff's base under hydroxide initiated phase transfer conditions would be selected as a probe based on the success of Roya's N^{I} -centered cyclopropenimine cation (**40**). Alternatively, focus was also placed on the synthesis of a mono-cyclopropenimine substituted proton sponge (Janus) in order to investigate its properties and applications in catalysis. More importantly, this work would allow for the confirmation of the computed $\text{p}K_{\text{a}}$ for this compound since it was presumed that only the mono-protonated salt of this compound would be isolated.

Detailed investigation would also allow for a direct comparison of properties between Janus and DACN, as well as their potential in catalysis. Additional work is currently underway in the Dudding laboratory to synthesize and investigate a derivative of Royá's N^1 -centered cyclopropenimine cation (**40**), particularly one with an aromatic backbone. However, this work will be included only if the synthesis and analysis of this new compound will be completed.

2. Results and Discussion

2.1 Janus Proton Sponge

2.1.1 Strategic Approach to the Synthesis of Janus (**45**)

Synthesis and investigation of a new proton sponge derivative: N^1 -(2,3-bis(diisopropylamino)cycloprop-2-en-1-ylidene)- N^8, N^8 -dimethylnaphthalene-1,8-diamine, or Janus (**45**) will be discussed in the following section (**Figure 22**),

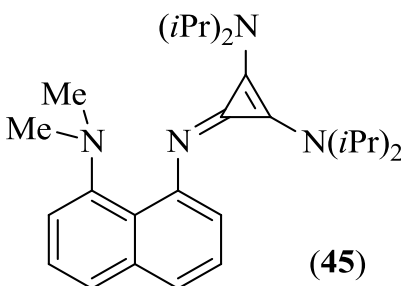


Figure 22: Structure of the Janus proton sponge (**45**).⁷⁷

The primary focus will be the work pertaining to the preparation of (**45**) including purification of all products and intermediates, as well as the optimization of the synthetic path. Determination of the proton affinity (PA) and pK_a of this species along with further insight and investigation of the hydrogen bonding (both experimentally and computationally) will be the secondary focus of the project. Finally, a search for potential applications, such as the alkylation

of Schiff's base will be done in order to compare Janus with DACN. This synthesis may lay a path for future development of derivatives, particularly optically active compounds. Chiral proton sponges are especially interesting for the future of asymmetric synthesis and catalysis. Reaction schemes (**Figures 23-25**), illustrate the planned synthetic pathway for the preparation of Janus (**45**), however this route will be subjected to change upon trial and error in the laboratory.^{38, 77, 78}

Based on the initial literature examination the key step in this synthesis will be the selective mono-protection of the amino groups present. Optimization of this reaction will provide a valuable methodology for future production of similar compounds that possess different functional groups at the *peri*-nitrogen centers. Each step in the synthesis will introduce the necessary bonds in order to reach the product requisite functionality. Assembly of the structure and introduction of functionality will occur through single synthetic manipulations.

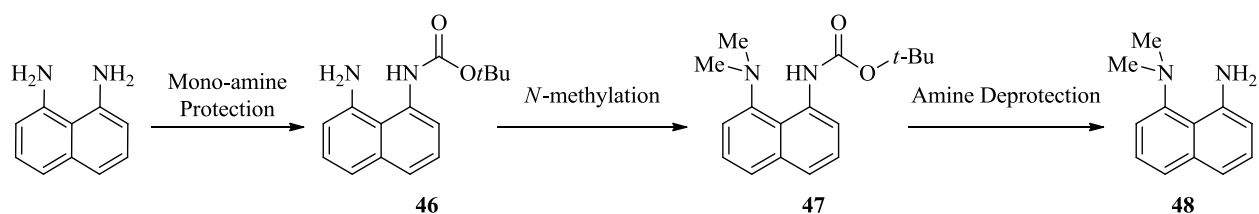


Figure 23: Synthesis of Janus proton sponge (**45**) – Steps One to Three.^{38, 77, 78}

The first step involved protection of a single nitrogen centre on the 1,8-diaminonaphthalene backbone, which will be achieved by introducing a carbamate functionality. It was suspected that the di-substitution of the amines would be unlikely due to the bulk of one carbamate. A nucleophilic attack by the lone pair of amine on the electrophilic carbonyl of a di-carbonate type species should result in the formation of the carbamate functionality, which serves as a protecting group during the synthesis. The best candidate for the reaction with the

diaminonaphthalene backbone will be di-*tert*-butyl dicarbonate, since it is inexpensive and commonly used for the protection of amines.^{38, 78} Generated stability of the carbamate group on **46**, towards base catalyzed hydrolysis is ideal since the subsequent methylation of the unprotected amine required basic conditions.

In the second step addition of the dimethylamino functionality to the free nitrogen is essential in creating the steric bulk in order to prevent rotation and pin the lone pair of the nitrogen towards the *peri*-position. Intermediate **47** will be generated through an S_N2 type reaction, where a base catalyzed nucleophilic attack of the free amine on an electrophilic methyl species occurs.^{79, 80} Strong methylating agents such as methyl iodide (MeI) and dimethyl sulfate (DMS) are necessary to avoid the difficulties associated with increased of steric bulk at the reaction site once secondary amine is formed. Along with the steric bulk that prevents favourable approach for the nucleophile, S_N2 type mechanisms require stronger nucleophiles. The strength of the nucleophilic nitrogen is reduced with each alkylation due to the introduction of F-strain.⁸⁰ The strength of the methylating agent is based on its leaving group. Dimethyl sulfate and methyl iodide are good examples of strong methylating agents because their leaving groups, methyl sulfate and iodide, can efficiently stabilize negative charge.

The following step in the synthetic route will be a deprotection; the carbamate group of **47** is removed to give intermediate **48**. This transformation is achieved by acid catalyzed hydrolysis, and strong acids such as trifluoroacetic acid (TFA) are required to hydrolyse the N-C bond, resulting in decarboxylation.⁸¹

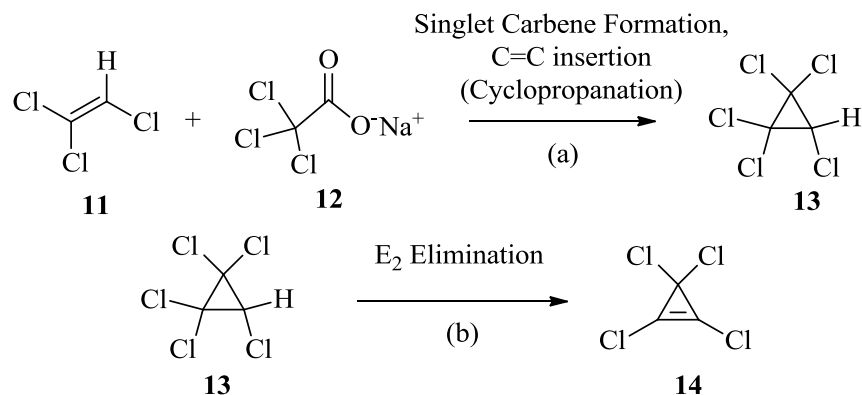


Figure 24: Synthesis of Janus proton sponge (**45**) – Steps Four to Five.^{19, 20, 77}

A well known and previously discussed procedure for the formation of pentachlorocyclopropane **13** from trichloroethylene and trichloroacetate will be used in step four (a) of the synthesis.¹⁹ Singlet carbene formation occurs via α -elimination of a chloride caused by the decarboxylation. Then, the ring formation occurs through carbon-carbon double bond insertion. Step five will utilize a high concentration of a strong base in order to promote E₂ elimination of chloride, producing the highly strained tetrachlorocyclopropene **14**.²⁰

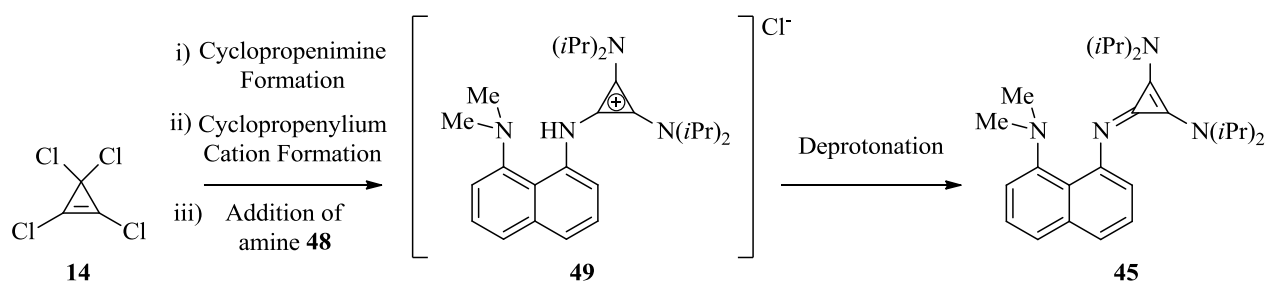


Figure 25: Synthesis of Janus proton sponge (**45**) – Steps Six to Seven.^{66, 77}

The following step needs an excess of diisopropylamine in order to form the cyclopropenimine via nucleophilic addition of amine **48** to intermediate **14** and chloride elimination in the form of HCl. The excess diisopropylamine neutralized any protons remaining in solution. This step will be immediately followed by the addition of intermediate **48** to yield

the protonated intermediate **49** by a similar mechanism. The final step involves the use of potassium bis(trimethylsilyl)amide (KHMDs) to deprotonate **49** and yield the final product, Janus proton sponge (**45**). This base is chosen for deprotonation as it is very strong, ($pK_a = 26$), and non-nucleophilic, avoiding by-products and degradation of Janus.^{43, 45, 66, 77}

An important part of this project is the purification and characterization of each intermediate in the multi-step synthesis. Proton and carbon NMR spectra will be obtained, followed by mass-spectrometry data, and IR data. A variety of acid-base titrations with colour indicators and traditional titration curves exist for the measurement of the pK_a , and may be employed in addition to the computational analysis using DFT methods on the Gaussian 98 suite of programs. However, the main experiment for the investigation of the hydrogen bond and pK_a involves a combination of a known base with Janus, observing ^1H NMR shifts on a 600 MHz NMR instrument. Utilizing the computational tools, IMHB bond distances and angles will be determined. A calculation of the energy range in kcal mol^{-1} for this hydrogen bond will be used as a parameter to help understand the structural properties of the molecule. Additionally, insight into the catalytic applications of proton sponge (**45**) or its salt (**49**) will be conducted. Initial preference will be given to phase-transfer reactions as similar compounds have seen fair success as catalysts in such procedures.⁹⁵

Phase-transfer catalysts generally facilitate the migration of a reactant between two immiscible phases. Thus, the reaction can occur between reagents that are otherwise insoluble in one phase. These catalysts generally target ionic substrates that are insoluble in organic layers but highly soluble in aqueous, functioning similar to a detergent for solubilizing salts into the organic phase. A general example is provided below (**Scheme 29**).



Scheme 29: Nucleophilic aliphatic substitution catalyzed by quaternary phosphonium salt.⁸²

Under normal conditions and in the absence of the phase transfer catalyst, the above reaction would not occur, as the sodium cyanide does not dissolve in ether. Similarly the 1-bromooctane has a very poor solubility in the aqueous phase, thus the reagents never meet and are unable to react. Yet in the presence of a small (catalytic) quantity of hexadecyltributyl-phosphonium bromide, this reaction progresses to completion rapidly to yield nonyl nitrile. The cyanide ions are transferred from the aqueous layer to the organic by the quaternary phosphonium cation. The formation of NaBr ionic species and its departure to the aqueous layer drives the reaction, but only in the presence of the catalyst.⁸² Some advantages of PTC are faster reaction times, higher conversion or yield, fewer by-products, and simple conditions. In current synthetic applications simple and mild reaction conditions that minimize waste and reduce the need for expensive starting materials are highly regarded and extensively sought after. This approach may diminish the need for expensive and dangerous solvents from the synthesis, which are usually required to dissolve all reactants in one phase. Phase-transfer catalysis pushes the frontiers of green chemistry, allowing for the development of more environmentally responsible methods, this is essential in our present, pollution plagued world.

2.1.2 Strategies for Mono-protection of 1,8-diaminonaphthalene (46)

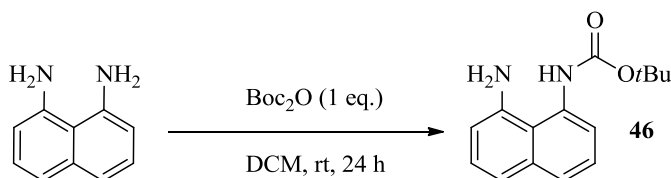
The synthetic plan predominantly involved reactions utilizing basic conditions, because of this a protecting group resistant to base hydrolysis (*N*-Boc) was selected and formed using di-*tert*-butyl dicarbonate reagent (Boc₂O). An exact procedure for the Boc-protection of a single amine on the 1,8-diaminonaphthalene was reported in 2006.³⁹ Commercially available 1,8-

diaminonaphthalene was reacted with Boc₂O, in tetrahydrofuran (THF), at room temperature over twelve hours. The method provided a good yield (81 %) ³⁹ of the required mono-*N*-Boc protected product **46**, with little formation of di-*N*-Boc species. As a result, the key step in the synthesis became more practical, as well as a great alternative to procedures involving *N*-protection of molecules containing only one amine group. These cannot entirely reflect the possible outcome of reaction in systems that have multiple amines. However, variations applied to these procedures will be explored for their potential optimization of synthesis.

Over the course of the study nineteen reactions to produce intermediate **46** were conducted. In the first attempt, *p*-toluenesulfonyl chloride was combined with the diaminonaphthalene backbone and refluxed in pyridine at 115 °C. However, the sulfonyl reagent proved to be too reactive resulting in over 80 % yield of the di-protected sulfonyl by-product. The procedure was abandoned, and cheaper more common di-*tert*-butyl dicarbonate reagent was selected instead. Initially procedures using water as solvent were considered, however, both the 1,8-diaminonaphthalene and subsequent product were poorly soluble and the reaction did not proceed. A TLC plate spotted with a standard of the starting material and the contents of the reaction flask after 30 minutes, 1 hour, 6 hours, and 24 hours showed a significant amount of leftover 1,8-diaminonaphthalene. A solvent system of 1:1 DCM-H₂O was utilized in an attempt to solve the solubility problem. The subsequent micro-scale reaction proceeded to completion, however, there was a high ratio of di-Boc product to almost insignificant amounts of requisite intermediate **46** (8:1). Lowering the equivalents of di-*tert*-butyl dicarbonate to 0.9 and 0.8 yielded slight improvements in the ratio of mono to di-protected amine products, (1:7) and (1:6) respectively. In an effort to improve this step, it was decided that a complete elimination of water from the reaction, replaced with DCM would yield better results. This solvent system was tested

over extended reaction times and it yielded some improvements. The most significant result was obtained when the reaction was run in DCM at room temperature, over 24 hours, and yielded 30 % of intermediate **46**. The ratio of mono to di-Boc products was accounted for by NMR as they ran up the TLC plate together (one thick band) across virtually all the solvent systems attempted. The most important optimization made during the screening of this reaction system was the variation of time that one took to perform the Boc₂O addition, illustrated in (Table 6):

Table 6: Optimization screen for production of **46** by varying the rate of Boc₂O addition.



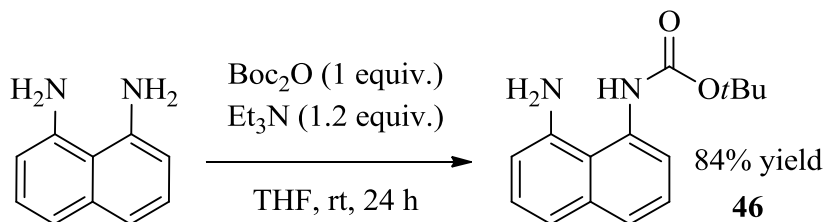
Time of di- <i>tert</i> -butyl dicarbonate addition (min.)	Obtained yield of intermediate 46
3	12%
5	21%
10	28%
15	45%
20	64%
30	74%

Other screens, such as temperature, and concentration of Boc₂O added (dissolved in solvent prior to the addition) gave little improvement on the yield of **46**. The final optimization of this synthetic step was achieved using a reported procedure for the synthesis of **46**. This method used THF as solvent, triethylamine, nitrogen atmosphere, at room temperature with an extended reaction time (18- 24 hours).³⁹ These experimental conditions were combined with the slow addition of Boc₂O reagent and yielded 84 % of intermediate **46**. Originally, column chromatography with a solvent system of 4:1 hexane-ethyl acetate was used for the isolation of product **46** but di-Boc by-product eluted together with **46**. This mix eluted first with an R_f value

of 0.35, while the starting material eluted last with an Rf of 0.05. In the interest of efficiency the product mix of intermediate **46** and the di-protected contaminant was pushed further through the synthesis since the by-product was unreactive toward methylation. A new strategy was employed for the purification which involved the addition of triethylamine (2 %) to the solvent system of 8:1 hexane-ethyl acetate, and was found to provide good separation. The di-Boc contaminant eluted first, Rf value of 0.48, product **46** second, Rf of 0.25, while the starting material was left on the baseline (Rf = 0.01). Hydrogen bonding interactions of the free amine on **46** were suspected to be the cause of slowing down the elution of this intermediate. This was a significant development for the optimization of the synthesis. Further work determined that the product of this reaction crystallized out of hexane if the contaminated mixture is heated and allowed to cool, thus an additional purification method was discovered.

The introduction of carbamate functionality at one nitrogen of diaminonaphthalene was determined to be an ideal route as it prevented N-methylation at that site. This therefore allowed the conversion of the adjacent amino group to the NMe₂ functionality. An explanation for this is that carbamates are able to delocalize their lone pair of electrons into the orbitals of the adjacent carbonyl group giving rise to resonance stability. The strong electron withdrawing nature of two near-by oxygen atoms is the cause of stability. This effect has two advantages: the nucleophilic nature of carbamates is substantially lower than that of amines, and their electrophilic nature is weaker than esters. Subsequently this makes them more tolerant to hydrolysis, and therefore requires strong bases or acids for them to make them susceptible to nucleophilic attack that cleaves the carbon-nitrogen bond. Their weaker nucleophilic nature due to the conjugate stabilization also reduces their potential for N-alkylation thus rationalizing their application in

the synthesis of **45**.⁸⁰ Past this initial step there are many known procedures available for the remaining reactions.^{66, 77, 78}



Scheme 30: Optimized conditions for mono-protection used in synthesis of Janus (**45**).^{39, 77}

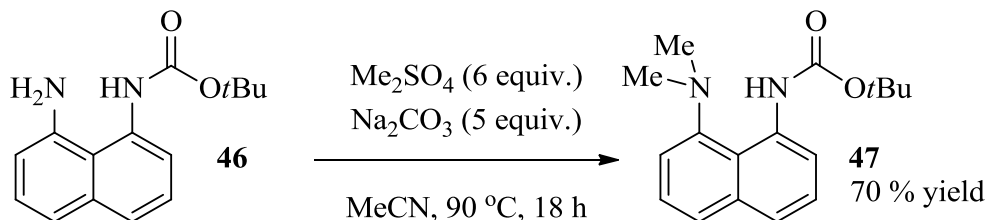
2.1.3 Strategies for *N*-methylation to Obtain Compound (**47**)

Addition of methyl groups to the free amine by a powerful methylating agent, dimethyl sulfate, was used for the *N*-alkylation, to produce compound **47**. Excess base was added to the reaction in order to increase the nucleophilic character of the secondary amine following the first methylation. The reaction occurred under an inert atmosphere of N₂ gas, and product **47** could be isolated by column chromatography.

There were twelve attempts of this reaction step in total; however, the highest yield achieved was 70 %. In the first attempt methyl iodide and sodium carbonate were selected as reagents, and DMF as the solvent, for the reflux reaction (60 °C). Analysis of TLC plates and ¹H NMR showed no product formation, and the reflux time was extended from 4 to 24 hours in an attempt to push the reaction to completion. However, this did not yield significant improvement and dimethyl sulfate was chosen as the next candidate for the reaction. The next attempt was carried out using the same base (Na₂CO₃) in water, at room temperature over 24 hours. Formation of product **47** was observed by TLC and confirmed by ¹H NMR (15 % yield). Excess base was used to encourage the second methylation (2.5-3 equiv. of sodium carbonate). It was

observed that water was a poor solvent for the reaction and it was suspected formed H_2SO_4 may interfere with the reaction. Before the use of the improved column chromatography and crystallization to isolate pure **46**, di-Boc by-product was partly responsible for the poor yield of intermediate **47** (15 %). After several reactions in which dimethyl sulfate (Me_2SO_4) was used, it was noted that the septum of the bottle was broken. The reagent was dark yellow and ^1H NMR confirmed its impurity, therefore it was distilled prior to any further use. This in combination with a switch to acetonitrile as the solvent resulted in a slight improvement of the yield to 18 %. A yield of 21 % of compound **47** was found when excess dimethyl sulfate was used (6 equiv.). The reaction was set up at room temperature, in acetonitrile with excess dimethyl sulfate (5 eq.), a slight excess of sodium carbonate (2.5 eq.), and left to run for 18 hours. It was concluded that use of less than five equivalents of Me_2SO_4 resulted in poorer yields of 6-15 %. An increase in the temperature to 90 °C (reflux) along with a slower addition of methylating agent (DMS), particularly 10 minute drop-wise addition under dry conditions, along with excess sodium carbonate (5 equiv.) provided an improved yield of 70 %. Attempts to optimize the reaction further failed and improvement of purification of product was undertaken instead. One problem encountered in the purification of **47** was that a small amount would always elute on the back end with the contaminants, resulting in additional chromatography. This problem was solved via application of a smaller amount of crude product, employment of wider columns and slower rate of elution. Isolation of pure **47** was then confirmed by both proton and carbon NMR. Column chromatography required a solvent system of 6:1 hexane-ethyl acetate, with the product eluting first ($R_f = 0.60$), by-products second ($R_f = 0.55, 0.50, 0.40$), and starting material could be recovered last ($R_f = 0.1$). An interesting discovery was that one of the contaminants ($R_f = 0.55$) was the mono-methylated by-product. It was recovered for possible use in the synthesis of chiral

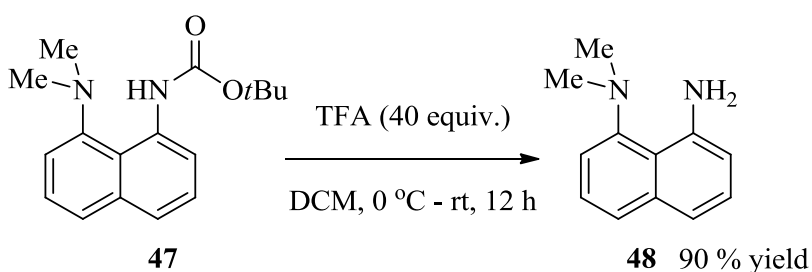
proton sponge derivatives of Janus (**45**). The optimized reaction conditions are given below (Scheme 31).



Scheme 31: Optimized conditions for *N*-methylation used in the synthesis of Janus (**45**).^{77, 79}

2.1.4 Strategies for Deprotection to Obtain Compound (**48**)

Once compound **47** was obtained, the carbamate protecting group was removed using TFA (40 equiv.) in dichloromethane under a nitrogen atmosphere to provide **48** (89-90 %). It is noted that slow addition of TFA (10 min.) at 0°C (ice bath) is essential during this procedure. Column chromatography, with a 12:1 hexane-ethyl acetate mixture was used to isolate intermediate **48**, which eluted last ($R_f = 0.2$) and appeared on the TLC as a distinctly dark spot. Starting material **47** eluted first and could be recovered from the column ($R_f = 0.39$). A ninhydrin stain of the TLC plate confirmed the presence of a free amine prior to structure confirmation by proton and carbon NMR. No further optimization of this step was pursued given that the product was obtained in 90 % yield.



Scheme 32: Optimized conditions for the deprotection in the synthesis of Janus (**45**).^{77, 81}

2.1.5 *Synthesis of Janus Proton Sponge (45) and Protonated Salt (49)*

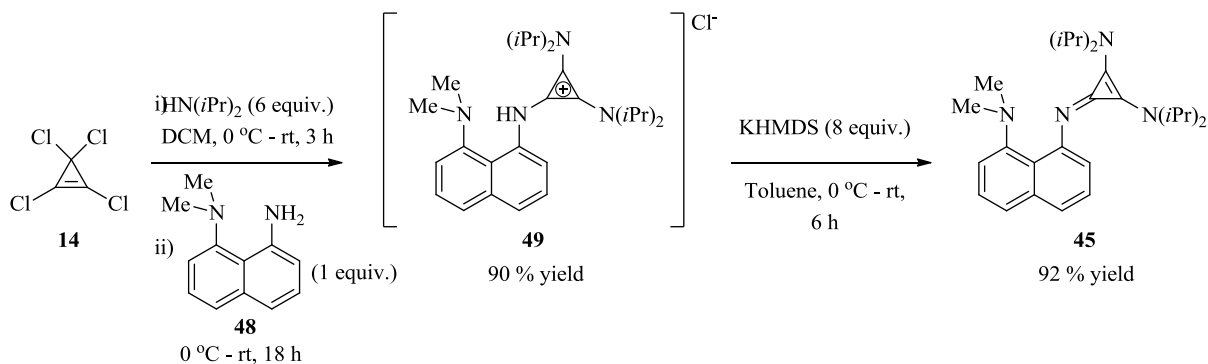
During the course of the project five reactions to produce the protonated base, intermediate **49**, were conducted. The first reaction attempt yielded product **49** in a 76 % yield, which was approximately 100 mg. However, the second attempt failed due to impure tetrachlorocyclopropene, some of the starting material **48** was recovered by column chromatography. Optimization of this reaction was complete upon the third attempt, the following reactions provided over a gram of nearly pure product once a crystallization procedure was developed. The optimization was realized once the equivalents of diisopropylamine were doubled from three to six. Slower reaction time for the cyclopropenimine to form was also a factor. The success of the optimization (90 % yield) was overshadowed by the difficulty in the crystallization of the product, which was required to prove the atomic structure of **49** using X-ray crystallography. The obtained cyclopropenimine salt (**49**) was observed to be opaque, brown oil, and was difficult to crystallize. The isolation of **49** was done using column chromatography, 9:1 DCM-MeOH, where the starting material **48** eluted first and product **49** eluted last, R_f values of 0.8 and 0.3 respectively. There was also a small fraction of contaminants eluting in between, R_f value of 0.48. Initial solvent systems tested for crystallization of **49** were unsuccessful and are listed in (**Table 7**). In these attempts the first 100 mg sample of **49** was split into 4 fractions (25 mg) and placed in small vials (5 ml). Upon the addition of the solvents the vials were placed into a beaker that contained sand submerged by the less polar solvent (2nd solvent listed in **Table 7**), and covered with aluminum foil to slow the evaporation and crystallization. Variations of this technique have been around for years, it was suggested as an option by Lee Belding. Poor crystallization was observed in DCM-ether and ethyl acetate-ether systems. The breakthrough

came when this same technique was applied using a mixture of benzene-ethyl acetate, the product (**49**) crystallized to yield an off-white solid after 72 hours at 5 °C.

Table 7: Solvent systems used in the attempts to crystallize compound **49**, (all values in ml).

Vial	MeCN- Benzene	MeCN- Hexane	MeCN- Ether	DCM- Hexane	DCM- Ether	EtOAc- Hexane	EtOAc- Ether	EtOAc- DCM
A	0.20/0.25	0.10/0.25	0.20/0.40	0.10/0.25	0.20/0.40	0.10/0.25	0.20/0.40	0.20/0.25
B	0.25/0.25	0.20/0.25	0.30/0.40	0.20/0.25	0.30/0.40	0.20/0.25	0.30/0.40	0.25/0.25
C	0.30/0.25	0.30/0.25	0.40/0.40	0.30/0.25	0.40/0.40	0.30/0.25	0.40/0.40	0.30/0.25
D	0.50/0.25	0.50/0.25	0.60/0.40	0.50/0.25	0.60/0.40	0.50/0.25	0.60/0.40	0.50/0.25

The final reaction was a deprotonation and required a very strong base. As a result of the proton abstraction and steric hindrance, the nitrogen lone pairs were directed towards each other. This subsequently destabilized the ground state electronics of proton sponge **45**, and enhanced the basicity.



Scheme 33: Optimized conditions for production of Janus (**45**) and its salt protonated (**49**).^{66, 77}

Potassium bis(trimethylsilyl)amide (KHMDS) was chosen as base for it is non-nucleophilic properties due to bulk, and for its pK_a , approximately 26. The base is also soluble in organic solvents, thus making it a perfect candidate for the final reaction.⁴³ The last step of the synthesis was conducted three times, where the flask with intermediate **49**, partially dissolved in

toluene had to be cooled in an ice bath (0 °C) since the reaction was exothermic. It is important to note that upon the addition of KHMDS the reactant **49** instantly become more soluble and a colour change from yellow/brown to yellow/green was observed. Based on previous work (Lee Belding)⁸⁴ in the synthesis of the DACN proton sponge it was rationalized that only half of the KHMDS equivalents would be required to deprotonate intermediate **49**. The reaction reached completion rapidly, finishing two hours earlier than the equivalent in DACN synthesis.⁸⁴ Isolation of proton sponge **45** proved to be highly challenging as column chromatography was out of the question, due to fear of protonating the product and thus obtaining back intermediate **49**. Following the completion of reaction, the solvent was removed using rotary evaporation and hexane was used to extract the first fraction of product, followed by diethyl ether. The fractions were passed through a fine frit to remove any solid impurities, TLC and NMR analysis showed that they both contained significant amount of product. Crystallization using hot hexane provided yellow crystals, pure Janus proton sponge in a 92 % yield. An attempt to purify the product by column chromatography using DCM-MeOH (9:1) failed, which was unsurprising considering the basicity of the product. Proton NMR showed evidence of this protonation (a distinct proton peak at 14 ppm), with the spectrum of the isolated fraction being identical to that of intermediate **49**. Alternatively, the Janus proton sponge could be obtained by deprotonating its salt (**49**) in THF using sodium hydride with nearly identical yield.⁷⁷

2.1.6 Investigation of Janus Proton Sponge Properties

Given that the goal of this project was not only the synthesis, but the investigation of this cyclopropenimine substituted sponge, a variety of experiments were conducted to unveil the true

nature of this compound (**45**). Janus salt (**49**) was investigated as well, as it presented a number of interesting findings. X-ray quality crystals of the hydrochloride salt (**49**) were obtained by the vapour diffusion crystallization from benzene-ethyl acetate. Using single crystal X-ray diffraction analysis the molecular structure was determined, but the results were somewhat unexpected.

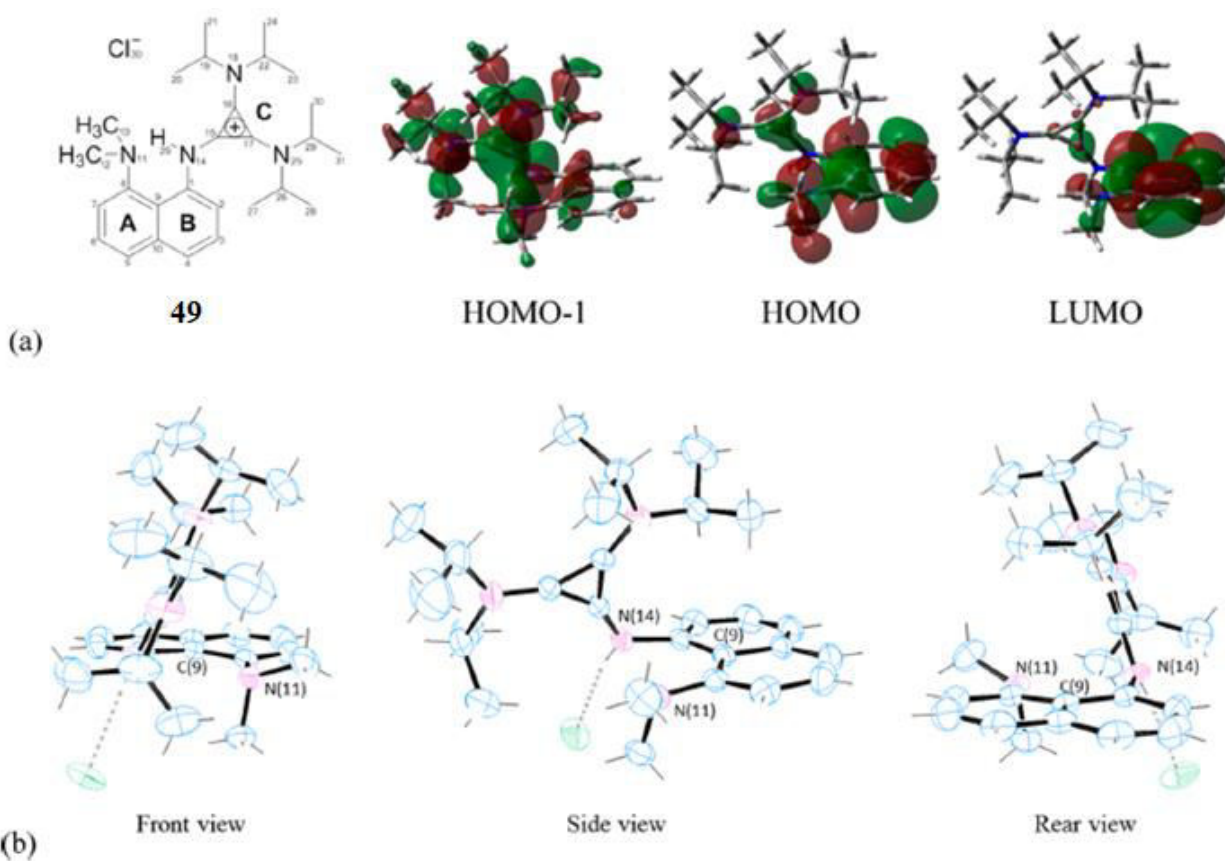


Figure 26: (a) Two-dimensional representation and corresponding numbering scheme for compound **49** and selected B3LYP/6-31G(d,p) computed MOs for **49**_{xray}. (b) ORTEP3-generated X-ray structure of compound **49** (purple = nitrogen, blue = carbon, green = chlorine). Thermal ellipsoids are displayed at 50 % probability.

The typical N(11)···H(29)N(14) IMHB observed on most proton sponges was absent, instead it was superseded by a N(14)H(29)···Cl(30) hydrogen-halogen bond to the chloride counterion (2.29 Å). The noticeable distortion of the naphthalene backbone ($\Theta_{5-10-9-1} = 175.4^\circ$)

and the relatively long N(11)···N(14) interatomic distance of 2.81 Å were more consistent with that of a neutral proton sponge (**Figure 26**).⁸³

Another distinguishing feature was the hybridization of N(14), which according to natural bond order (NBO) analysis, displayed a significant sp^3 character and the presence of a lone pair. This was intriguing since the orientation of the lone pair implied that the two amino groups had adopted an *in-out* geometry. This configuration has the lone pair of one amino group pointing in towards the other nitrogen, while the lone pair of the adjacent amino group is pointed out, away from the naphthalene (**Figure 27**).

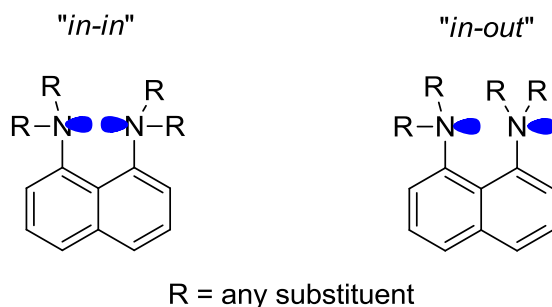


Figure 27: Depiction of the *in-out* and *in-in* lone pair configuration in proton sponges.⁷⁷

Although this type of geometry has been previously reported,⁸⁴ to the best of our knowledge it represents the first reported isolation of a proton sponge with an *in-out* configuration lacking an *ortho*-substituent. This also is the first instance of this type of configuration in a protonated proton sponge. In addition to this surprising *in-out* configuration, the cyclopropenimine ring (ring C) was oriented overtop of the naphthalene backbone (ring A/B), opposite to what has been observed in previously reported proton sponges having basic sp^2 nitrogens, including DAC substituted sponge **50** (**Figure 28**).⁸⁵

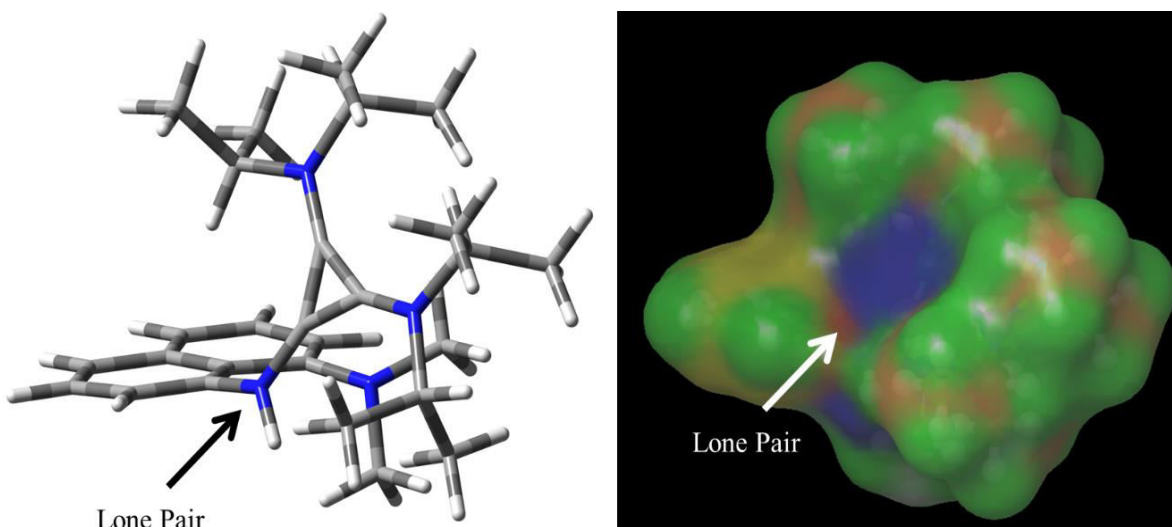


Figure 28: Computed structure and charge density map of the Janus salt (**49**).⁷⁷

By far, one of the most intriguing features of the Janus sponge **45** was its luminescent properties. Upon absorption of UV light ($\lambda_{\text{max}} = \lambda_{\text{ex}} = 283$ nm) in a DCM solution at room temperature, **45** emits UV light at a longer wavelength ($\lambda_{\text{em}} = 341$ nm), corresponding to a Stokes shift of 58 nm (**Figure 29**). Conversely, a DCM solution of its protonated salt, **49**, absorbs light in the long-range UV region ($\lambda_{\text{max}} = \lambda_{\text{ex}} = 333$ nm) and emits light in the visible wavelength ($\lambda_{\text{em}} = 472$ nm), corresponding to a Stokes shift of 139 nm (**Figure 29**). Interestingly, this trend is opposite to that reported with DMAN proton sponge in acetonitrile, wherein the neutral species absorbs at a higher wavelength ($\lambda_{\text{max}} = 340$ nm) than the protonated species ($\lambda_{\text{max}} = 286$ nm).⁸⁶

The change in Stokes shift and fluorescence intensity between **45** and **49** is substantial, though not all too surprising considering the generation of aromaticity upon protonation, which constitutes a considerable geometric and electronic transformation. Notably, under persistent illumination, **49** fluoresces indefinitely as a solid and in solution (**Figure 30**), having a quantum yield of 0.37 in ethanol (**Appendix A**). There has been extensive study into the photophysical properties of DMAN, which may shed light on the possible fluorescent origins of Janus (**45**).^{83, 86} According to these reports, the electronic excitation of DMAN originates from its 1L_a state, with

considerable contribution from the NMe₂ groups, and after internal conversion leads to the emissive, naphthalene based, 1 π * internal charge transfer state. Twisting of the methyl groups on N(11) (i.e., geometry reorganization) plays a major role in the large Stokes shift. Considering this role of NMe₂ in the fluorescence of DMAN, the NMe₂ group of the Janus sponge is likely important for its luminescent characteristics.

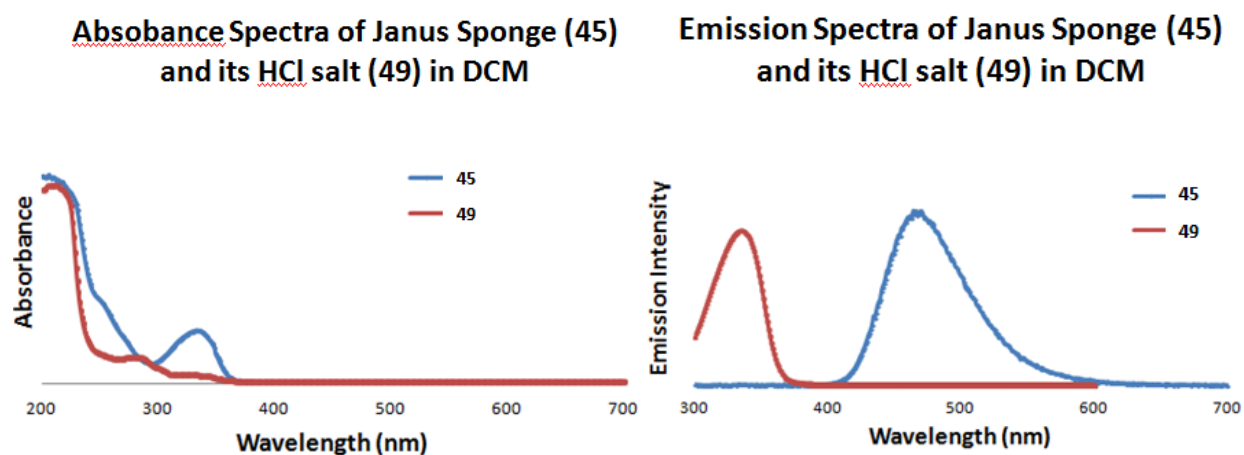


Figure 29: (Left) UV/vis absorption spectra of **45** and **49** as 1×10^{-5} M solutions in DCM. (Right) UV/vis emission spectra of **45** and **49** as 1×10^{-5} M solutions in DCM.

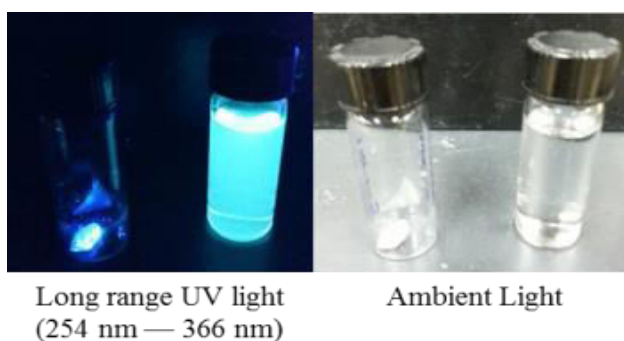


Figure 30: Visual portrayal of the luminescent character of compound **49** as a solid (left vial) and as a solution in dichloromethane (right vial).⁷⁷

Furthermore, there is little doubt that the aromatic cyclopropenium ion also plays a key role in the electronic transition(s) leading to fluorescence, considering that it is the only structural difference from DMAN. From these two conjectures (that the NMe₂ group and

cyclopropenium ion are key factors in Janus's luminescent characteristic) and given that the computed LUMO of **49**-xray (or the LUMO+1 for that matter; **Appendix A**) does not possess significant contribution from either the NMe₂ group or the cyclopropenium ion, excitation likely originates from a MO involving both the cyclopropenyl cation and the NMe₂ group (i.e., the HOMO or HOMO-1), while emitting from a MO involving the naphthalene system. Though the exact electronic transitions leading to **49**'s fluorescent properties remain uncertain, the drastic effect observed upon adding a single cyclopropenimine unit is evidence that cyclopropenimine-based fluorescent probes, LEDs, and dyes may be worth studying. This robust fluorescent nature of **49** expands the potential applications of cyclopropenimines, especially considering that it represents a fluorescent compound derived from the protonation of a neutral, organic superbase, with the potential to be a bidentate metal chelating ligand. The pK_a of the Janus proton sponge was experimentally determined to be 23.8 (**Appendix A**).⁷⁷

2.1.7 Computational Analysis of Janus (45)

While all of the factors responsible for this unprecedented geometry are uncertain, one contributing element leading to this unusual geometry is a stabilizing donor-acceptor interaction between the N(11) lone pair and the cyclopropenyl π -system (N(11)···C(15) = 2.84 Å), as revealed by NBO analysis (N(11)LP \rightarrow C(15) _{σ^*} , E_{NBO} = 3.1 kcal mol⁻¹), and the computed MOs of **49**_{xray} (**Figure 26**, HOMO-1). In contrast to the x-ray crystal structure, the DFT B3LYP/6-31G(d,p) optimized geometry of **49** (**49**_{opt}), lacking a chloride ion, did possess a N(11)···H(29)-N(14) intramolecular hydrogen bond (1.77 Å), though the geometry obtained when optimized in the presence of the Cl⁻ counterion matched the crystal structure quite closely,

leading us to believe that the observed molecular geometry of **49**_{xray} is not simply an effect of crystal packing forces.

A detailed inspection of computed **49**_{opt} proved instructive as the aromatic naphthalene backbone ($\Theta_{5-10-9-1} = 178.3^\circ$) was found to be less distorted and the N(11)⋯N(14) interatomic distance of 2.68 Å was significantly shorter than that in **49**_{xray}, due to the presence of a highly non-symmetric IHB having a N(14)–H(29) bond distance of 1.05 Å and N(11)⋯H(29) H-bond measuring 1.77 Å. Furthermore, the *in-in* electron pair configuration in **49**_{opt} (**Figure 27**) allowed for the effective delocalization of the N(14) lone pair into the naphthalene ring system, resulting in ring C being tilted away from the naphthalene backbone and providing a geometry that was more in line with that of conventional proton sponges. Interestingly, the computed geometry of freebase **45** (**45**_{opt}), (**Figure 31**) closely resembled that of **49**_{xray}, more so than **49**_{opt}.

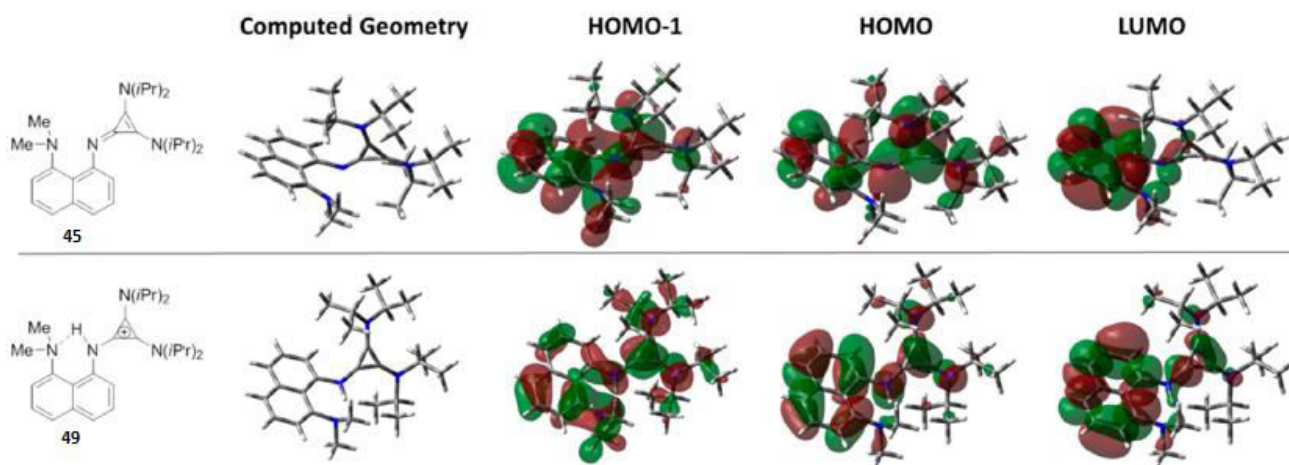


Figure 31: B3LYP/6-31G(d,p) optimized geometries and selected MOs for compounds **45**_{opt}, **49**_{opt}.⁷⁷

Manifesting from the N(11), N(14) lone pair-lone pair repulsion in **45**_{opt} was a substantial distortion of the naphthalene backbone from ideal planarity ($\Theta_{5-10-9-1} = 171.4^\circ$) concomitant with elongation of the N(11)⋯N(14) interatomic distance to 2.91 Å. Meanwhile, the calculated

N(14)–C(1) bond distance of 1.40 Å was slightly shorter than the N(11)–C(8) bond distance (1.42 Å) yet longer than the N(14)–C(15) bond distance (1.32 Å). Like **49**_{xray}, **45**_{opt} displayed an *in-out* type geometry with ring C tilted toward the A/B ring system, and as such, it would appear that the Janus sponge, regardless whether or not it is protonated, favors an *in-out* lone pair-lone pair geometry with the cyclopropenyl ring geared inward toward the naphthalene ring. Thus, it would clearly seem that the observed molecular structure of **49** was not simply a result of a strong N(14)H(29)···Cl(30) hydrogen bond to the chloride ion but instead originates from the aforementioned stabilizing donor-acceptor interaction between the N(11) lone pair and the cyclopropenyl π -system.

Shown in **Figure 31** are the corresponding HOMO–1, HOMO, and LUMO of **45**_{opt} and **49**_{opt}. In both cases, the HOMO possesses significant orbital density on the cyclopropenyl ring, which is consistent with previous reports detailing the electron-rich nature of the cyclopropenyl cation,⁸⁵ as well as those reports of further oxidizing the cyclopropenyl cation to the radical dication.⁸⁶ In this respect, there was minimal contribution from the N(11) lone pair in the HOMO of **49**_{opt} or **45**_{opt}, as evidenced by the lack of orbital density. In terms of the HOMO–1, **45**_{opt} displays substantial orbital contribution from the N(11) lone pair and the cyclopropenyl ring system, which is perhaps not surprising considering the similar geometry to **49**_{xray}. Nevertheless, even though **49**_{opt} also displayed significant contribution from the N(11) lone pair and cyclopropenyl ring system in the HOMO–1, the lobes are not oriented toward one another nor are they of the same sign, in contrast to **45**_{opt}. Lastly, both LUMOs are primarily centered on the naphthalene backbone, with only a small contribution from the cyclopropenyl ring system in **49**_{opt}. At that stage, to ascertain the respective aromaticity of the A, B, and C ring systems,

nucleus-independent chemical shift (NICS) calculations⁸⁷ were performed on **45**_{opt}, **49**_{opt}, and **49**_{xray} at the center of each ring system (NICS(0)), as well as 1 Å above (NICS(1)) and 1 Å below (NICS(-1)) the center of each ring to circumvent σ -contamination from the carbon framework of the ring, which is particularly prominent within the small cyclopropenyl ring systems.

Table 8: Computed NICS(-1, 0, 1) values for compounds **49**_{opt}, **45**_{opt}, and **49**_{xray}.⁷⁷

Aromatic region	Type	Freebase Janus (45) _{opt}	Protonated Janus (49) _{opt}	Protonated Janus (49) _{opt}
Ring A	NICS (-1)	9.22	10.80	10.46
	NICS (0)	8.11	9.39	8.76
	NICS (1)	9.43	10.31	10.01
Ring B	NICS (-1)	9.28	10.15	9.97
	NICS (0)	8.34	8.76	8.97
	NICS (1)	10.13	9.57	10.56
Ring C	NICS (-1)	8.72	8.78	9.22
	NICS (0)	29.84	31.08	32.30
	NICS (1)	8.46	8.96	9.08

* B3LYP/6-311++G(d,p)//B3LYP/6-31G(d,p) computational method and basis set used.

As observed (**Table 8**), there is an increase in the NICS values for all three ring systems upon protonation of N(14), regardless of the geometry. For **49**_{opt}, the increase in NICS values for rings A and B is consistent with the formation of an IHB, wherein the N(11) lone pair is oriented orthogonal to the naphthalene ring, substantially diminishing perturbation of the aromatic backbone. However, in the case of **49**_{xray}, there is no IMHB, and the increase in aromaticity of the A/B ring system is likely a consequence of N(11) lone pair donation into ring C rather than into ring A. Not surprisingly, an increase in the C ring NICS values occurred for both **49**_{xray} and **49**_{opt}, presumably as a direct result of generating the cyclopropenyl cation upon protonation.

The noticeably larger NICS value of ring C in **49**_{xray} relative to that in **49**_{opt} conceivably originates from the N(11) lone pair donation into the cyclopropenyl cation, thus suggesting that the geometry of **49**_{xray} is more conducive to cyclopropenyl cation stabilization. Subsequently, to

determine the likelihood of **45** being a strong organic base, presumably a superbases, the PA was computed at the B3LYP/6-311G++(d,p)//B3LYP/6-31G(d) level, taking into account thermal corrections estimated at the B3LYP/6-31G(d) level resulting in a computed gas phase basicity of 266.8 kcal mol⁻¹, which for reference was substantially less than DACN (282.3 kcal mol⁻¹) computed at the same level of theory. A relative p*K*_a (MeCN) calculation at the IEFPCM/B3LYP/6-311G++(d,p)//B3LYP/6-31G(d,p) level, using 1,8-bis(tetramethylguanidino)-naphthalene as a reference base, estimated the p*K*_a value at 23.9 in MeCN. For comparison, the p*K*_a of DACN computed at the same level of theory was 27. To substantiate these computational results, the p*K*_a of **45** was experimentally measured in MeCN using a previously reported NMR titration approach.⁸⁸ Gratifyingly, using 1,1,3,3-tetramethylguanidine as a reference base, the measured p*K*_a value of 23.8 was very close to the computed value. It is interesting to note the lower p*K*_a of **45**, relative to *t*-Bu-(bisdiisopropylamino)-cyclopropenimine, as it would appear the withdrawing effect of the naphthalene ring decreases the basicity more than it is increased by the presence of an IMHB and ground state destabilization. With respect to the effects of geometric constraints on basicity, homodesmotic reactions were applied to discern between the effect of ground state stabilization (eq.1) and IMHB strength (eq.2) on the basicity of **45** (**Figure 32**).⁷⁷ According to equation 1, ground state stabilization contributes 7.7 kcal/mol, while the stabilization associated with the IMHB was found to be only 0.6 kcal/mol. Within the context of QTAIM analysis, the presence of a (3,-1) bond critical point indicative of a maximum of electron density (i.e., a bonding interaction) between the N(11) and H(29) supported the presence of an intramolecular hydrogen bond, and NBO analysis revealed a 23.5 kcal/mol donation of the N(11)_{LP} into the N(14)–H(29) bond. Given the lower ground state destabilization and relatively

weak IMHB, it is perhaps not surprising that **49** possesses a hydrogen bond to the chloride ion rather than an IMHB.⁷⁷

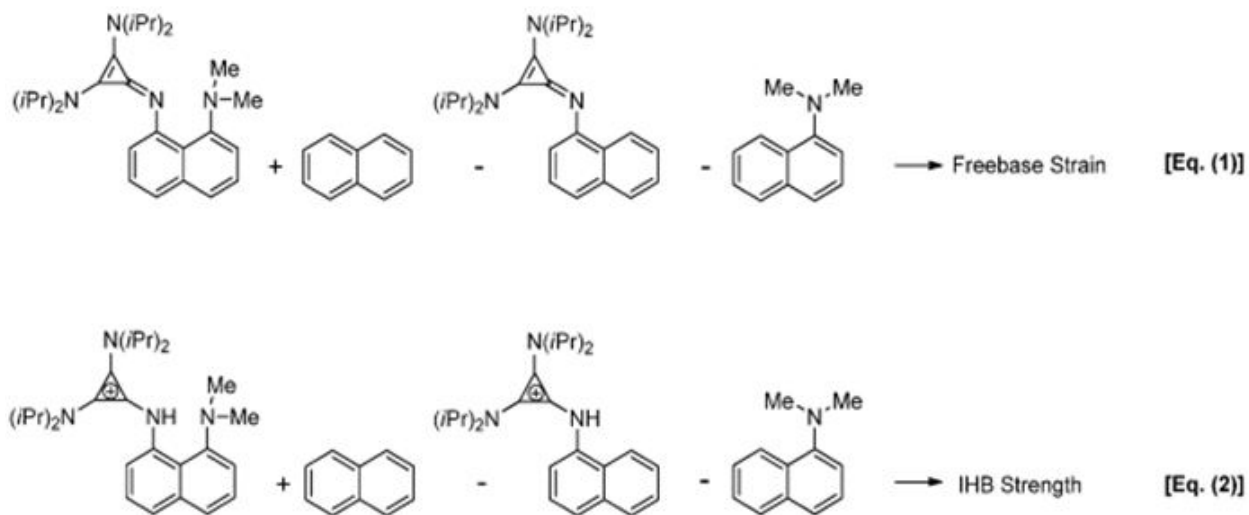


Figure 32: Homodesmotic Reaction Scheme for the Determination of Hydrogen-Bonding Strength and Ground State Destabilization.⁷⁷

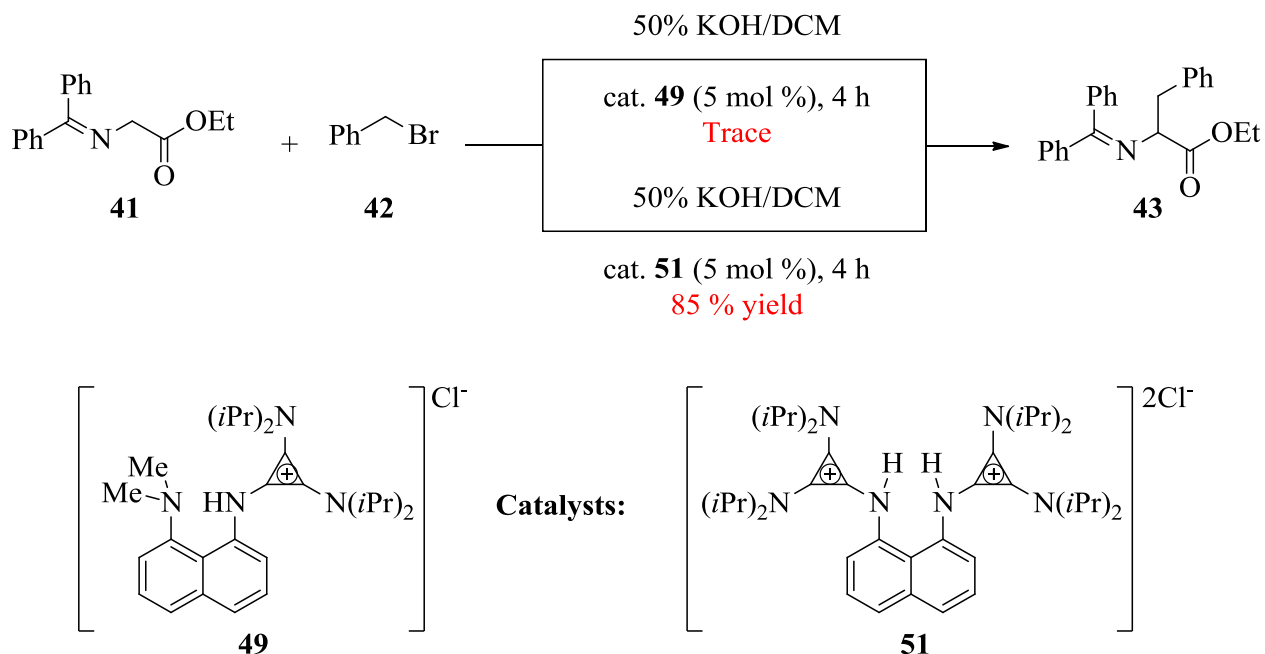
2.1.8 Comparison of Janus (**45**) and DACN (**50**)

When comparing the DACN proton sponge to Janus, it was first noticed that unlike DACN, the nonsymmetrical sponge (**45**) was not prone to the second protonation in the presence of moderately strong acids such as acetic acid or concentrated HCl. This is likely due to the increase in strain that would accompany an introduction of a second proton. However, this did allow for the confirmation of the pK_a of Janus, consequently proving our computational method accurate within a $pK_a \pm 0.1$ unit margin of error. A useful comparison between **45** and **50** clearly shows that the roughly 1000 times difference in K_a originates predominantly from a drastic decrease in the freebase strain. Though the hydrogen bond energy in **45** was only one-half that observed in **50**, its effect on the pK_a is likely not as significant.

Table 9: Comparison of basicity enhancing factors between Janus (**45**) and DACN (**50**).⁷⁷

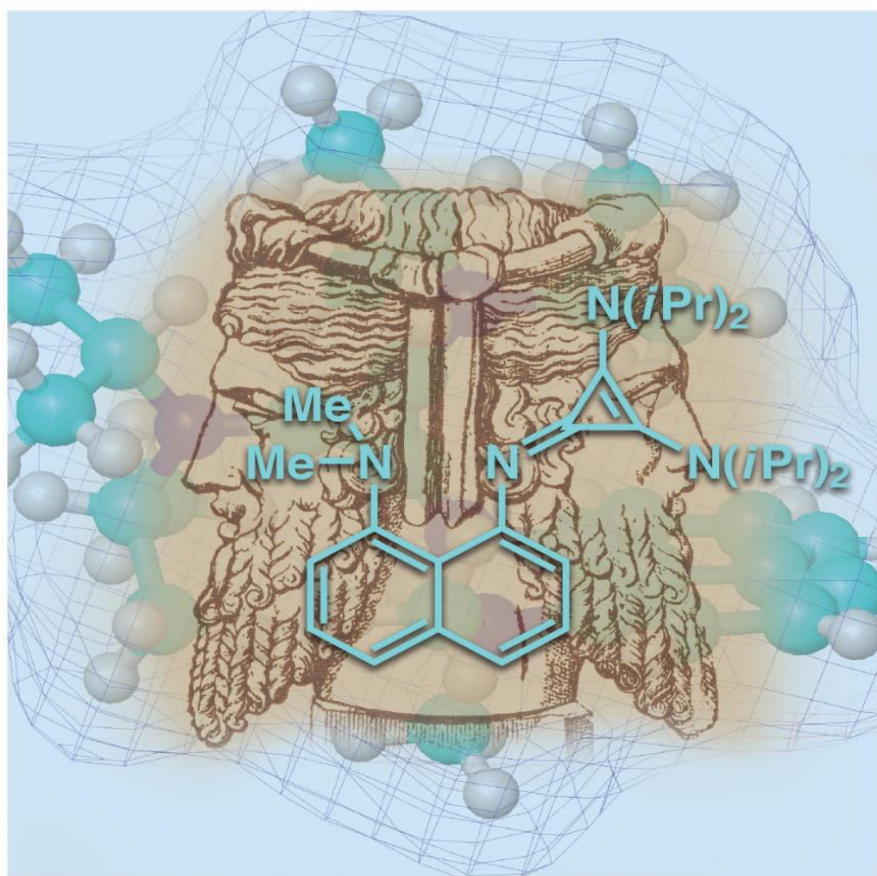
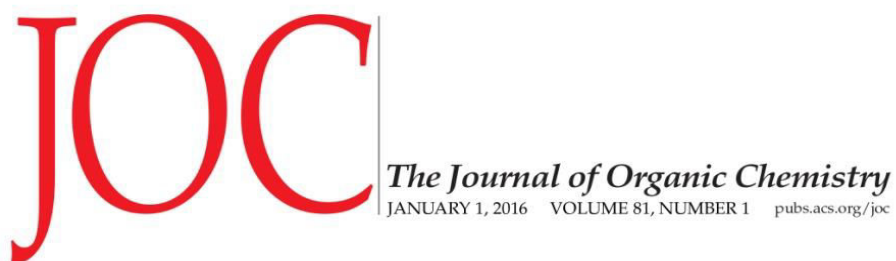
Compound	IMHB E_{NBO}	IMHB Strength	Freebase Strain	Computed PA	Calculated pK_a	Measured pK_a
Janus (45)	26.0 kcal/mol	0.6 kcal/mol	7.7 kcal/mol	266.8 kcal/mol	23.9	23.8
DACN (50)	27.3 kcal/mol	1.2 kcal/mol	21.1 kcal/mol	282.3 kcal/mol	27	--

Additionally the salts of the two proton sponges (**49**, **51**) were also compared in their ability to catalyze a phase transfer benzylation of Schiff's base (**Scheme 34**). Remarkably the di-protonated DACN (**51**) was an excellent catalyst (85 % yield), while the Janus salt (**49**) yielded only a trace of the desired product. The reasons for the success of the DACN salt as a phase transfer catalyst will be discussed in detail in the following section.

**Scheme 34:** Comparison of DACN and Janus salts in PTC benzylation of a Schiff's base.⁷⁷

The inefficiency of Janus at catalyzing this PTC benzylation as well as the fascinating structural and fluorescent properties ultimately led to the publication of this work without

applications. However, the fluorescent properties show promise and a potential use, which is currently under investigation in our laboratory. The novelty of our group's collaborative work has also landed us on the front page of the *Journal of Organic Chemistry* (**Figure 33**).⁷⁷



 ACS Publications
Most Trusted. Most Cited. Most Read.

www.acs.org

Figure 33: Janus article on the front cover of *J. Org. Chem.* Jan. 1st, 2016.⁷⁷

2.2 *DACN Proton Sponge Phase Transfer Catalysis*

2.2.1 *General Background on Cyclopropenimines in Phase-Transfer Catalysis*

Bis(dialkylamino)cyclopropenimine (DAC) motifs have markedly attracted attention in recent years, due in large part to their emerging use in organocatalysis⁸⁸ and phase-transfer catalysis,⁹⁰ in addition to applications as ionic liquids⁹⁰ and nitrogen-based ligands.⁹¹ Avid curiosity in the practical uses of DACs has arisen among physical organic chemists and theoreticians alike, particularly for the strong Brønsted-Lowry basicity. The basicity arguably derives from an intrinsic kinetic propensity to form stable aromatic bis-(dialkylamino)-cyclopropeniminium cations upon protonation. Not surprisingly, this fascinating link between basicity and aromaticity, compounded with the status of DACs as so-called “superbases” has served as an impetus for continued study into the underlying electronic nature and chemical reactivity of this intriguing class of heterocycles.

In this light, our recently synthesized superbases, DACN (**50**)⁶⁶ and Janus (**45**)⁷⁷, further explored the nature of DACs in the context of freebase strain and intramolecular hydrogen bonding, within the historically relevant proton sponge scaffold. The Dudding group has also reported the first use of a DAC derivative (**40**) as a phase-transfer catalyst (PTC) for benzylation and fluorination reactions (**Figure 34**).³⁵ Operational simplicity, mild reaction conditions, use of inexpensive reagents and solvents, as well as amenity to both large- and small scale synthetic protocols has made phase-transfer protocols quite advantageous from an experimental standpoint. As a result, it is perhaps not surprising that the scope of phase transfer catalysis has continued to evolve at an accelerated pace, resulting in a number of new catalysts and protocols offering complementary and/or distinct modes of reactivity.⁹² Recently a particular emphasis has been placed on bifunctional catalysts stemming from earlier work exploring multisite PTCs

(catalysts with more than one active site),⁹³ these combine both hydrogen bonding and phase-transfer motifs.⁹⁴ Among this class of PTCs, the predominant approach involves combining positively charged quaternary ammonium cations as the phase-transfer functionality and urea or thiourea as the hydrogen bond donor.

As part of our continued interest in phase-transfer reactions and hydrogen bonding, we were particularly interested to investigate the use of protonated DACs as hydrogen bond donors in phase-transfer catalysis. We envisioned the use of **51** (**Figure 34**) as a unique, bifunctional phase-transfer catalyst.

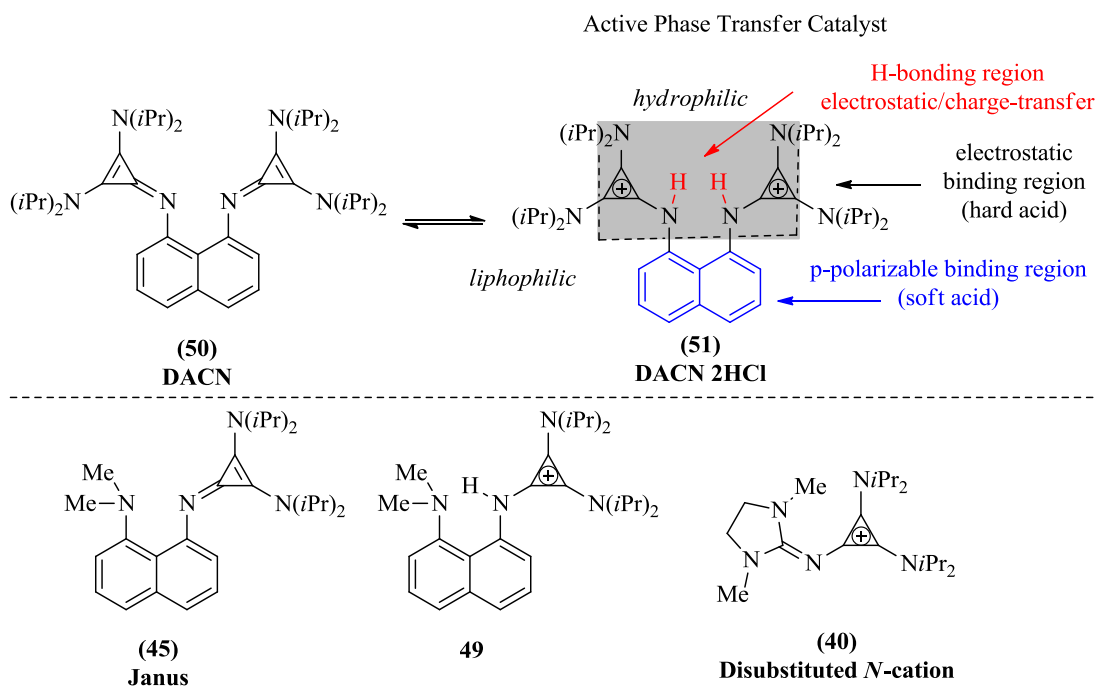


Figure 34: Reported cyclopropenimine compounds by Dudding *et al.*^{35, 66, 77, 97}

The highly diffuse positive charges of DACs make them unique as phase-transfer motifs. This stands in contrast to the localized point charges of widely employed quaternary ammonium (or occasionally phosphonium) cations. With the application of **51** as a PTC, this report demonstrates that protonated DACs can be compatible hydrogen bond donors for phase-transfer chemistry. Thus, DACs have a unique ability to play a bifunctional role, as both the phase-

transfer motif and hydrogen bonding donor. It was initially hypothesized that the functional utility of **51** in phase-transfer catalysis would benefit from a distinct partitioning of lipophilic and hydrophilic surface areas (**Figure 34**), which could be subdivided into a (1) π -polarizable naphthyl ring that would allow for π - π stacking interactions, (2) a pair of highly diffuse cations that would facilitate the transport of anions into a lipophilic organic phase, and (3) a H-bonding region for molecular recognition.

2.2.2 *Experimental Screen for Catalyst Alkylation and Decomposition*

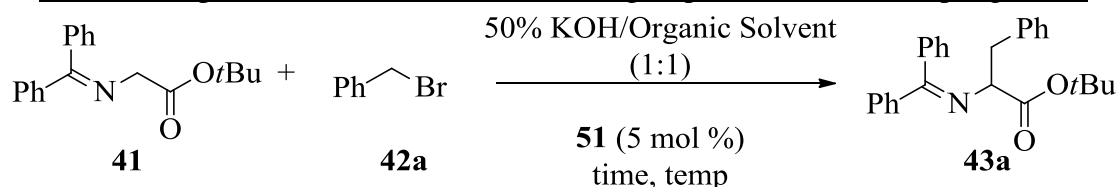
As a corollary, it was foreseen that in situ derived freebase, **50**, might serve a further role acting as an organic base to facilitate the deprotonation of pro-nucleophiles, thus providing another mechanistic dimension to phase-transfer catalysis. At the outset of this study, to explore the potential of the bisprotonated salt of DACN **51** in PTC as a bifunctional and/or multisite phase-transfer catalyst, we chose the well established alkylation of O'Donnell's glycine imines⁹⁵ given the historical significance and the numerous mechanistic investigations using this substrate. Nevertheless, at first it was unclear if **51** would undergo *N*-alkylation, as it would presumably be in equilibrium with **50** under basic conditions, or if the alkylation would be blocked given the sterically encumbered environment of **50**. Investigation of this possibility required a probe; 100 mg of **50** was mixed with excess benzyl bromide in a 1:1 mixture of DCM and 50 % aqueous KOH and stirred at room temperature for 8 hours. To our delight, there was no evidence of catalyst alkylation, and it was easily recovered in near quantitative yield. Although there was no evidence of alkylated catalyst, it was observed that deprotonation under the reaction conditions did indeed occur, as established by dissolution of **51** in a 50 % solution of KOH in D₂O at room temperature. In terms of catalyst stability, it was noted that when a sample of **51**

was left in an aqueous 50 % KOH solution at ambient temperature there was no evident decomposition after 2 weeks, as determined by ^1H NMR.

2.2.3 Optimization of DACN Phase Transfer Reaction Conditions

Given this promising preliminary result, reaction conditions were subsequently screened for the alkylation of benzophenone imine **41** with benzyl bromide **42a** (Table 10). To this end, the polar aprotic solvent acetonitrile (MeCN) was optimal, resulting in complete consumption of the starting material in only 20 minutes at room temperature and a 92 % product yield. The use of slightly less polar dichloromethane (DCM) provided a similar outcome to that of MeCN, with full consumption of the starting material occurring in 45 minutes at room temperature.

Table 10: Optimized reaction conditions using di-protonated DACN sponge **51**.⁹⁶



Entry	Solvent	Temperature	Time	Conversion ^a	Yield ^b
1	MeCN	25 °C	20 min	100%	92%
2	MeCN	0 °C	1 h	100%	91%
3	DCM	25 °C	45 min	100%	92%
4	DCM	0 °C	1.5 h	100%	89%
5	Toluene	25 °C	8 h ^d	51% ^e	36% ^e
6	Toluene	50 °C	8 h ^d	67%	51%

^a Based on ^1H NMR spectroscopy. ^b Isolated yield after column chromatography. ^c In absence of the catalyst, no conversion was observed except 6 % for entry 6 based on ^1H NMR. ^d Noticeable background reaction observed longer than 8 h.

Meanwhile, the use of toluene, on the other hand, resulted in a slight background rate, extended reactions times, and poor overall product yield. At that stage, to investigate the hypothesis that the bisprotonated, dicationic moiety of **51** was critical for catalysis, three

additional compounds all sharing structural similarities with **51** were employed as potential catalysts under the same reaction conditions (**Figure 35**). Namely, phase-transfer alkylation was performed in the presence of 5 mol % of the hydrochloride salts of Janus sponge (**49**),⁷⁷ Alder's proton sponge (**52**),⁵⁶ and t-butyl(bisdiisopropylamino)-cyclopropenimine (**53**).^{33, 88}

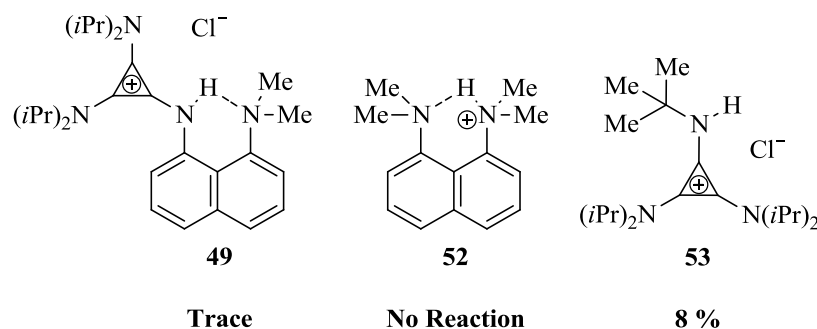


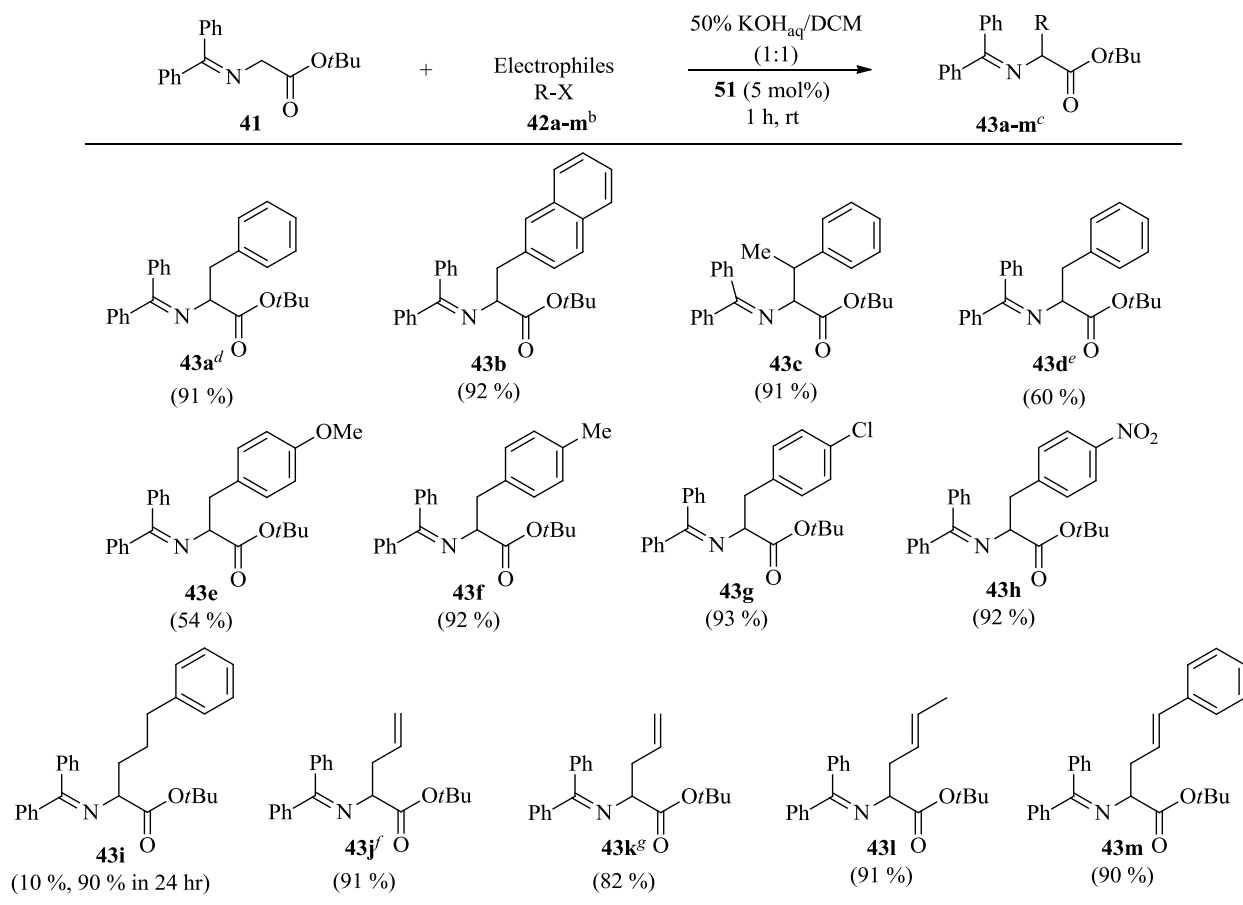
Figure 35: Alternative compounds screened for PTC activity.^{33, 56, 77, 96}

To this end, the use of **49** afforded only trace amounts of the benzylated product, while **52** resulted in no reaction, indicating that the protonated 1,8-diaminonaphthyl ring system was not the only structural feature of **51** leading to PTC catalysis. Conversely, **53** catalyzed the reaction to a small extent, providing 9 % of the desired product along with small amounts of alkylated byproduct. The failure of **49**, **52**, and **53** to impart any appreciable catalytic activity, despite their partial structural similarity to **51**, is notable, as it provides strong evidence that **51** acts uniquely as a phase-transfer catalyst.

2.2.4 Application of DACN in Phase-Transfer Catalysis via Electrophile Screen

Given the dramatic differences in reactivity between these compounds, the ability of **51** as a phase-transfer catalyst was further explored using other electrophiles under the conditions applied for entry 3 in (**Table 10**) with the reaction time extended to 1 h (**Scheme 35**). It was observed that naphthalene bromide (**42b**) was comparable in reactivity to benzyl bromide,

resulting in 92 % isolated yield, while perhaps more interestingly, the more sterically hindered secondary bromide **42c** afforded **43c** in 91 % yield, demonstrating that substitution at the benzylic carbon was tolerated under the reaction conditions.



^a With 1 equiv. ^b With 1.2 equiv. ^c Yields based on isolated product obtained after column chromatography. No product was formed in any reaction in the absence of catalyst **51**. ^d **42a** = benzyl bromide. ^e **42d** = benzyl chloride. ^f **42j** = allyl bromide. ^g **42k** = allyl chloride.

Scheme 35: Electrophile screen for PTC of di-protonated DACN (**51**).⁹⁶

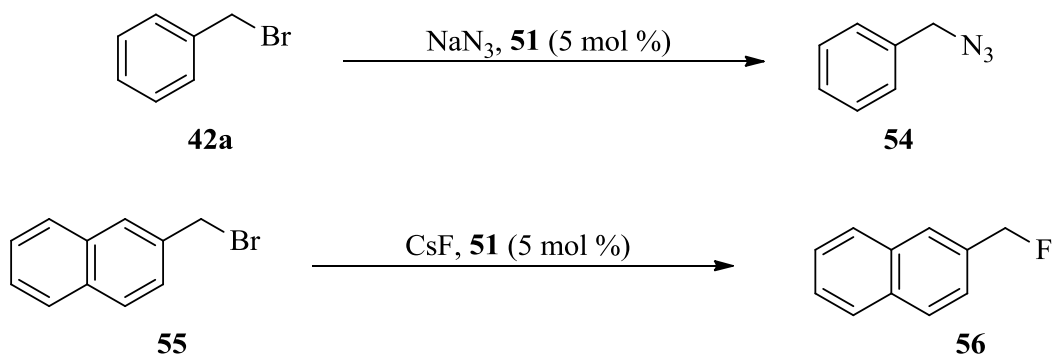
Alternatively, the use of less reactive benzyl chlorides **42d** and 4-methoxybenzyl chloride **42e** led to lower product yields, providing **43d** and **43e** in 60 and 54 % yields, respectively. In contrast, 4-methyl benzyl bromide (**42f**) substrate afforded a yield comparable to that of benzyl bromide, with **43f** isolated in 92 % yield. Furthermore, the use of resonance-donating electron-

withdrawing 4-chloro-substituted and strongly electron-withdrawing 4-nitro-functionalized benzyl bromides **42g** and **42h** provided high product yields. Based on these trends, it would appear that the enhanced leaving group ability of a benzylic bromide relative to that of a chloride effectively supersedes subtle electronic perturbations on reactivity introduced by the inclusion of a *p*-substituent. The results point to a mechanistic scenario involving halide dissociation and C–C bond formation occurring via a transition state involving S_N2 displacement or conceivably even backside nucleophilic addition to a short-lived benzylic cation+X[–] tight ion pair.

Meanwhile, substrate 3-phenyl-1-bromopropane (**42i**) having an aliphatic chain proved to be a far less reactive electrophile, yielding only 10 % of the desired product **43i**, though the reaction does reach completion with longer reaction times (90 % yield after 24 hours). Lastly, allyl bromide (**42j**), crotyl bromide (**42l**), allyl chloride (**42k**), and cinnamyl bromide (**42m**) were all reactive, though allyl chloride gave a slightly lower yield, while the regio-chemical outcome with **42l** and **42m** indicated that a S_N2' displacement of the bromide was not a competing process.

2.2.5 Mechanistic Determination of DACN Phase-Transfer Catalysis

Having demonstrated that **51** was a competent catalyst for interfacial PTC, we next applied it to nucleophilic fluorination and sodium azide substitution reactions, which are PTC processes generally believed to occur by extraction based mechanisms (**Scheme 36**).^{92, 95}



Scheme 36: Extraction type PTC reactions with di-protonated DACN (**51**).^{35, 96}

Emerging from these studies was the instructive finding that in stark contrast to the ability of **51** to facilitate interfacial PTC, it was a much less effective catalyst for extraction PTC, which is interesting given that our recently reported cyclopropeniminium-containing pnictogen *N*-centered cation (**40**) was an effective phase-transfer catalyst for both hydroxide-initiated interfacial and extraction based PTC.³⁵ For instance, under optimized conditions, **51** provided only moderate rate enhancement in the benzylic fluorination of **55** with CsF in MeCN (**Scheme 36**) with respect to the non-catalyzed background reaction. Furthermore, **51** had no effect on catalyzing the bromide displacement of **42a** by azide under PTC conditions (**Appendix B**).

While PTC reactions are renowned for being dynamic processes, wherein product formation is oftentimes complicated by “off-cycle” pre-equilibria, there is little doubt that the alkylation of O’Donnell’s imine in this work proceeds by way of an interfacial hydroxide-initiated mechanism.⁹⁵ Granted this fact, the more relevant question relates to the underlying source of the high catalytic activity of **51**.

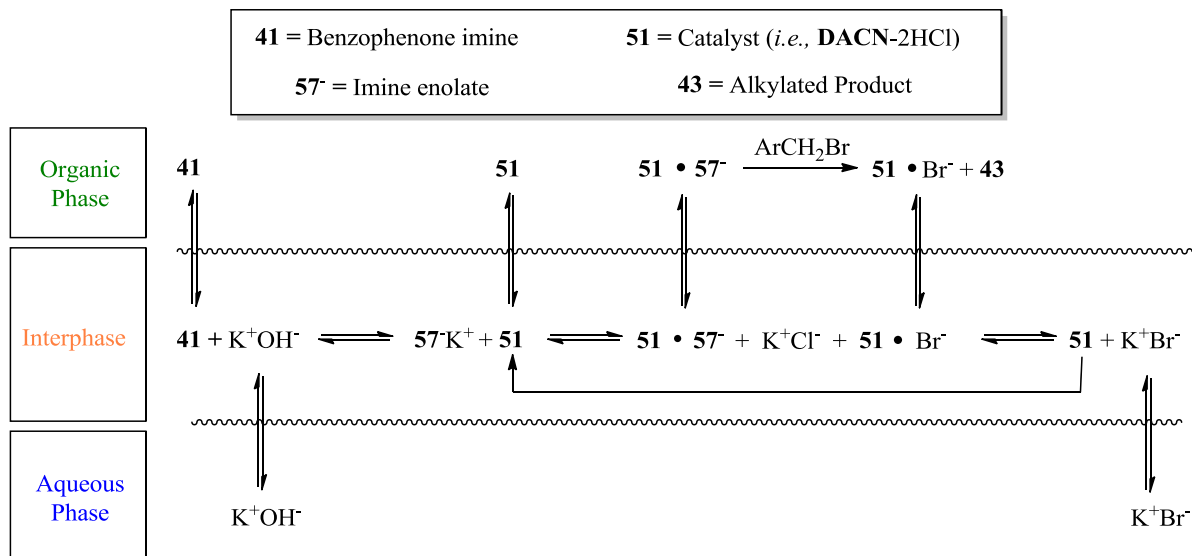


Figure 36: Proposed hydroxide-initiated interfacial PTC mechanism for alkylation of imine **41** to afford product **43**.⁹⁶

In part, it is thought to derive from the tendency of the catalyst to concentrate at the interfacial space, which is known to be an important factor in hydroxide-initiated PTC reactions.⁹⁷ Presumably, the innate organophilicity of **51** also plays a critical role in enhancing the transport rate of anions from the interfacial phase to the organic layer, leading to faster reactions.⁹⁸ Though conjectural, a third aspect of **51**-mediated PTC is the likelihood that the catalyst stabilizes the benzophenone imine enolate (**57⁻**) via a set of heteronuclear positive-charge-assisted hydrogen bonds ((+)CAHB).⁹⁹ Lastly, it is reasoned that **50** undergoes a rapid protonation/deprotonation event at the organic/aqueous interface, given its basicity and the basicity of the aqueous phase.⁹⁸ This would in turn toggle the solubility characteristics of the catalyst between that of a charged hydrophilic **51** dication with H-bonding residues to that of more a lipophilic **50** or **50-H⁺** species, which would be prone to reside in the organic layer. In essence, the dynamics of this system would establish a scenario where the catalyst would be held at the interface by rapid protonation/deprotonation processes. Modeling of the hydrophobic-

hydrophilic surface areas of **51** and the corresponding hydrogen-bound complex **51** · **57⁻** supported this conjecture, as revealed by the hydrophobic-hydrophilic surface area plots depicted below (**Figure 36**).

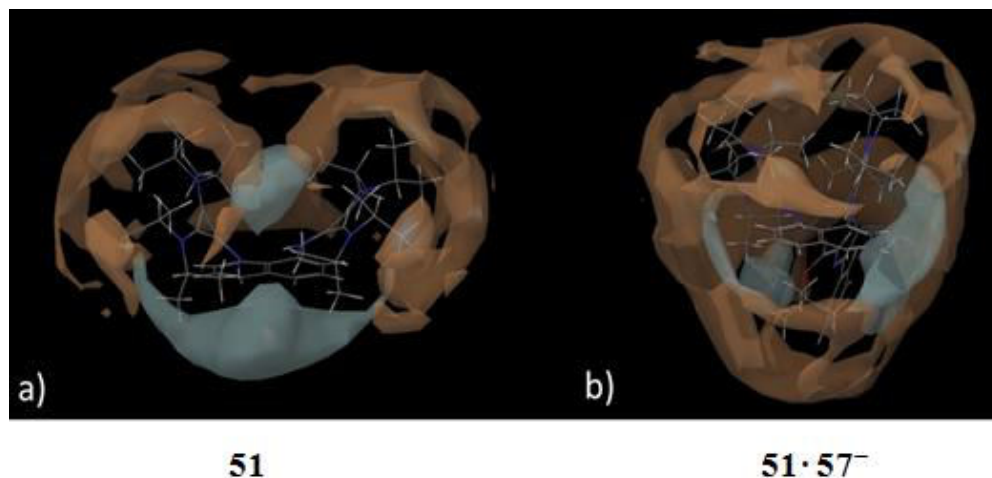


Figure 37: Hydrophobic (orange)/hydrophilic (blue) surfaces of **51** (left) and the **51** · **57⁻** complex (right) generated using Macromodel.⁹⁶

Apparent from these plots was a distinct amphipathic division of hydrophobic-hydrophilic surface volumes in **51** that suggested it would be prone to accumulate at organic-aqueous interfaces (**Figure 37a**), while in **51** · **57⁻**, the hydrophilic surface density was localized at the *re* and *si* faces of the enolate ester carbon and the oxyanion was buried within the interior of this complex (**Figure 37b**). Notably, this encasing of the oxyanion can be likened to that of the role played by hydrophilic-hydrophobic amino acid residues in protein folding and function.¹⁰⁰ Yet more importantly, this discrete arrangement of hydrophilic-hydrophobic surfaces and positioning of H-bond donor sites both stabilize and protect the reactive enolate intermediate, presumably prolonging its lifetime in the organic phase and thereby increasing the probability of reaction with an electrophile.

As for the PTC cycle of these alkylation reactions, it is envisioned that a series of pre-equilibrium steps generate an effective concentration of a reactive benzophenone imine enolate

51 · **57**⁻ complex in the interphase (**Figure 36**). A preliminary model derived from DFT calculations suggests that the computed 34.9 kcal mol⁻¹ binding affinity for this complex was driven by the formation of a bifurcated ((+)CAHB) H-bond/Coulombic interaction, akin to a salt bridge which is a common motif found in enzymes (**Figure 38**).

Migrating into the bulk of the organic phase, **51** · **57**⁻ then engages in C–C bond formation via a transition state assembly such as **TS1** that possesses an activation barrier of 10.7 kcal mol⁻¹ (2.2 kcal mol⁻¹ lower than that of the uncatalyzed transition state; **Appendix B**) and elongated 2.46 Å C–C bond forming distance, which is suggestive of an early transition state leading to alkylated product **43** (**Figure 38**).

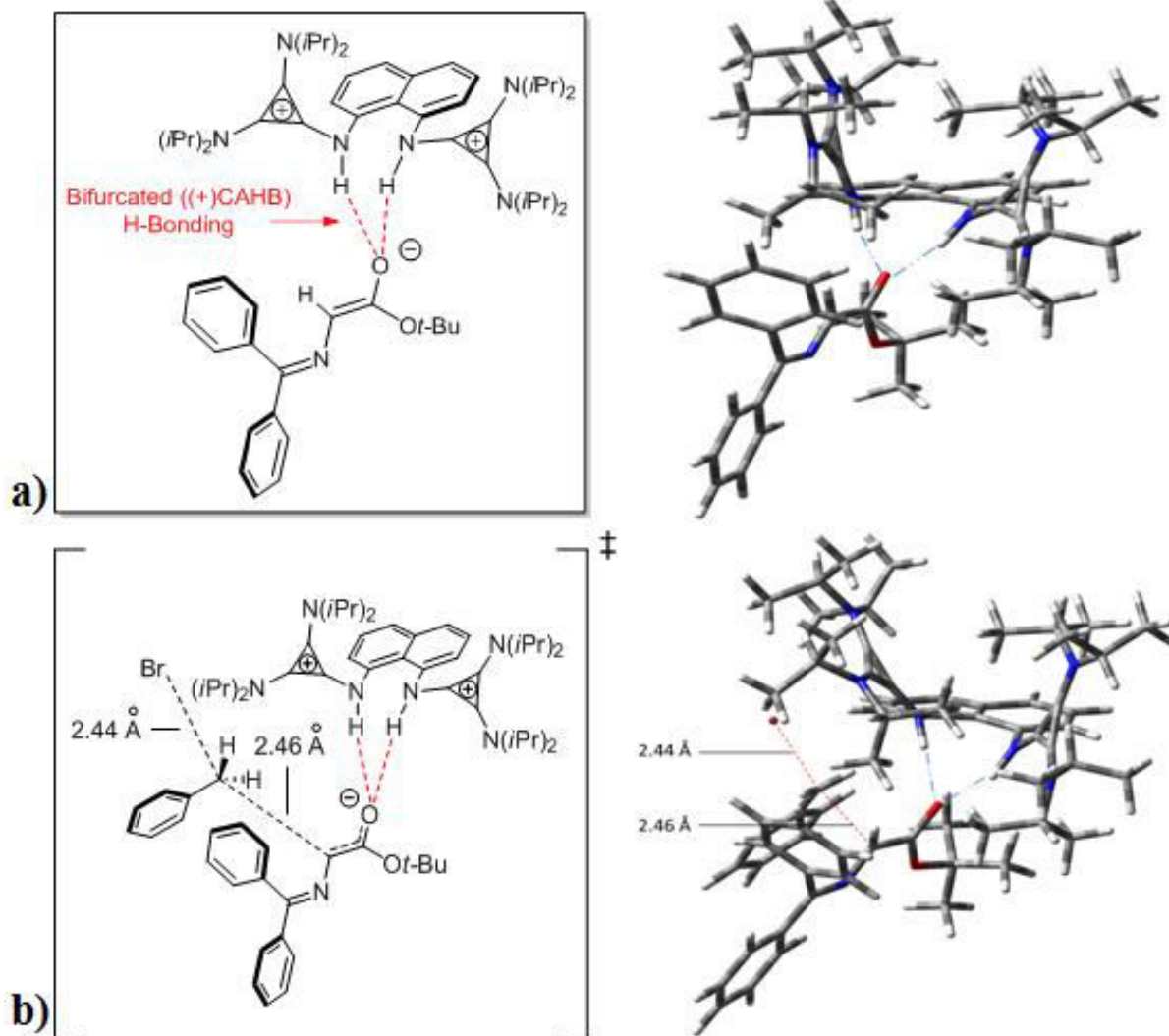


Figure 38: (a) Computed complex $51 \cdot 57^-$ (right). Two-dimensional rendering of favorable binding interaction in $51 \cdot 57^-$ (left). (b) Computed benzylation transition state, **TS1** (right). Two-dimensional rendering of **TS1** (left). Computations performed at the wb97xd/6-31g(d)/def2sv (scrf = dichloromethane) level.⁹⁶

3. Conclusion

In conclusion, the synthesis and theoretical investigation of a non-symmetric, DAC-functionalized proton sponge derivative, coined the “Janus” sponge was developed and subsequently reported. The protonated cyclopropenimine unit displayed weak hydrogen bonding to the adjacent NMe₂ substituent and was found to be replaced by a hydrogen-bonding interaction to a Cl⁻ counterion. Associated with this fact was the rare in-out geometry of the basic nitrogens, which represents the first such instance in the absence of an ortho-substituent as well as in a protonated state. Furthermore, N_{LP} donation into the cyclopropenium cation was found to stabilize its unprecedented geometry. The pK_a of **45** was measured to be 23.8, in good agreement with the computed value of 23.9. Lastly, **49** displayed vibrant luminescence both in solution and in the solid phase, representing the first example of a cyclopropenimine-based fluorescent organic compound.

Also demonstrated was that DACs can be used as hydrogen bond donors in phase-transfer chemistry and we have introduced the first bifunctional DAC-based PTC, **51**. The bis-protonated salt of DACN (i.e., **51**), a shelf-stable salt easily prepared from commercially and/or readily available reagents, was shown to be an effective catalyst for hydroxide-initiated interfacial PTC alkylations, while it was a poor catalyst for PTC processes occurring by extraction-based mechanisms. Evidence was presented that suggests **51** has a tendency to reside at the aqueous/organic interphase and the ability to enclose reactive hydrophilic intermediates in a hydrophobic shell, thus facilitating their transport to the organic phase. Ongoing studies geared toward the development and application of related PTC protocols with chiral DAC-derived catalysts is underway in our lab and will be reported in due course.

4. Experimental Procedures

General computational Methodology: Calculations were carried out at the Kohn-Sham hybrid-DFT B3LYP^{84, 86, 101} level of theory using the Gaussian 09¹⁰² and GaussView v5.0.8 programs. To account for solvent effects, the Integrated Equation Formalism Polarized Continuum Solvation Model (IEFPCM)⁸⁷ was used throughout the computations. All minima were confirmed by the presence of only real vibrational frequencies. QTAIM calculations were computed using AIM2000.⁸³

Materials and methods: Materials were obtained from commercial suppliers and were used without further purification, unless otherwise specified. All reactions were performed under an inert atmosphere. Reactions were monitored by thin layer chromatography (TLC) using TLC silica gel 60 F254. NMR spectra were obtained with a 300 MHz spectrometer (¹H 300 MHz, ¹³C 150.9 MHz, ¹⁹F 292.4 MHz, ¹¹B 96.3 MHz). The chemical shifts are reported as δ values (ppm) relative to tetramethylsilane. FT-IR spectra were obtained with an attenuated total reflectance spectrophotometer from neat samples. HRMS (high-resolution mass spectrometry) spectra were measured using electrospray ionization (ESI) and a time-of-flight (TOF) mass analyzer in positive ionization mode. Absorption spectra were measured using a UV-Vis-NIR spectrophotometer at ambient temperature. Emission spectra were obtained on a Xenon flash lamp fluorescence spectrophotometer at ambient temperature with entrance and exit slit widths set to 5 mm.

4.1 Synthesis of Janus Proton Sponge

4.1.1 Synthesis of *tert*-butyl (8-aminonaphthalen-1-yl)carbamate (**46**)^{39, 77}:

To a flame dried 100 mL round bottom flask backfilled with N_{2(g)} was added 2 g (12.6 mmol, 1 equiv.) of 1,8-diaminonaphthalene followed by the addition of 40 mL of dry THF and 2 mL (27.2 mmol, 2.1 equiv.) of NEt₃, all via syringe. To the resulting mixture 3 g (13.9 mmol, 1.1 equiv.) of di-*tert*-butyl-dicarbonate dissolved in 10 mL of THF was added drop-wise, followed by stirring for 24 hours at room temperature. After 24 hours the THF was removed under reduced pressure using a rotary evaporator (153 mBar). The crude product mixture was dissolved in 20 mL toluene, washed with 10 mL of 1M NaOH, 10 mL of brine, and then 10 mL of distilled H₂O. The organic layer was subsequently dried over MgSO₄, gravity filtered through a funnel and the solvent removed under reduced pressure using a rotary evaporator. Purified compound could be acquired by flash chromatography (20% ethyl acetate in hexanes).

The product **46** was isolated as red crystals in 84% yield. ¹H NMR (300 MHz, CDCl₃): δ = 9.79 (s, 1H), 8.08 (d, J = 7.3 Hz, 1H), 7.49 (t, J = 7.7 Hz, 1H), 7.40 (m, 2H), 7.22 (t, J = 7.7, 1H), 6.78 (d, J = 7.2 Hz, 1H). ¹³C NMR (75 MHz, CDCl₃): δ = 153.3, 140.9, 136.3, 135.5, 126.1, 125.6, 123.6, 122.7, 118.9, 116.9, 116.8, 80.2, 28.5. IR (neat): 3362 cm⁻¹, 3300 cm⁻¹ (N-H stretch, primary amine), 3050 cm⁻¹ (C-H, aromatic stretch), 2977 cm⁻¹ (C-H stretch, alkane), 1687 cm⁻¹ (C=O stretch, amide), 1152 cm⁻¹ (C-O stretch).

4.1.2 Synthesis of *tert*-butyl (8-(dimethylamino)naphthalen-1-yl)carbamate (**47**)^{77, 79}:

To a 100 mL round bottom flask containing 1 g (3.8 mmol, 1 equiv.) of **46**, was added 2.1 g (25.1 mmol, 6.5 equiv.) of Na₂CO₃. The flask was then fitted with a reflux condenser, backfilled with N_{2(g)}, and 50 mL of acetonitrile was added. To the resulting solution 2.6 mL (26.9

mmol, 7.0 equiv.) of freshly distilled Me₂SO₄ was then added drop-wise. The reaction mixture was heated to reflux, and stirred for 12 hours. The mixture was concentrated under reduced pressure, using a rotary evaporator (153 mBar), and diluted with 30 mL of H₂O, extracted 3x with 10 mL of dichloromethane. The combined organic extracts were dried over MgSO₄, gravity filtered and the solvent was removed under reduced pressure. Purified compound could be acquired by flash chromatography (12.5% ethyl acetate in hexanes).

The product **47** was isolated as a clear oil in 70% yield (3.4 mmol, 0.98 g). ¹H NMR (300 MHz, CDCl₃): δ = 12.79 (s, 1H), 8.35-8.32 (dd, J = 7.0, 2.3 Hz, 1H), 7.62 (d, J = 8 Hz, 1H), 7.45-7.27 (m, 4H), 2.81 (s, 6H), 1.58 (s, 9H). ¹³C NMR (75 MHz, CDCl₃): δ = 153.7, 150.3, 137.0, 136.1, 126.4, 125.3, 122.0, 119.3, 117.6, 114.1, 79.2, 45.9, 28.5. IR (neat): 3050 cm⁻¹ (C-H, aromatic stretch), 2973 cm⁻¹, 2932 cm⁻¹, 2873 cm⁻¹, (C-H stretch, alkane), 1709 cm⁻¹ (N-H bend), 1638 cm⁻¹ (C=O stretch, amide) 1135 cm⁻¹ (C-O stretch). HRMS (ESI): m/z calcd for C₁₇H₂₂N₂O₂ (M+H)⁺: 287.1754, found: 287.1748.

4.1.3 Synthesis of *N*¹,*N*¹-dimethylnaphthalene-1,8-diamine (48**)^{77, 81}:**

To a 50 mL round bottom flask containing 250 mg (0.873 mmol, 1 equiv.) of **47**, backfilled with N_{2(g)}, was added 15 mL of dichloromethane. To the resulting mixture, 2.67 mL (34.92 mmol, 40 equiv.) of trifluoroacetic acid was added drop-wise and the reaction was allowed to stir for 12 hours at room temperature. The crude product was diluted with 50 mL of H₂O, quenched with 37 mL of 1M NaOH and extracted 3x with 10 mL of dichloromethane. The combined organic extracts were dried over MgSO₄, gravity filtered through a funnel, and the solvent removed under reduced pressure. Purified compound could be acquired by flash chromatography (11% ethyl acetate in hexanes).

The product **48** was obtained as a brown oil in a 90% yield (0.830 mmol, 154.5 mg). ^1H NMR (300 MHz, CDCl_3): δ = 7.54 (d, J = 8.2 Hz, 1H), 7.34 (t, J = 7.6 Hz, 1H), 7.28 (t, J = 7.6 Hz, 1H), 7.18 (d, J = 7.6 Hz, 2H), 6.64 (dd, J = 7.4, 1.1 Hz, 1H), 6.18 (bs, 2H). ^{13}C NMR (75 MHz, CDCl_3): δ = 152.1, 145.5, 137.0, 126.6, 125.4, 125.4, 118.7, 117.0, 115.1, 109.7, 46.2. IR (neat): 3446 cm^{-1} , 3276 cm^{-1} (N-H stretch, primary amine), 3050 cm^{-1} (C-H, aromatic stretch), 2938 cm^{-1} , 2828 cm^{-1} , 2784 cm^{-1} (C-H stretch, alkane), 1590 cm^{-1} (N-H bend). HRMS (ESI): m/z calcd for $\text{C}_{12}\text{H}_{14}\text{N}_2$ (M+H) $^+$: 187.1230, found: 186.1239.

4.1.4 Synthesis of N-(2,3-bis(diisopropylamino)cycloprop-2-en-1-ylidene)-8-(dimethylamino)naphthalen-1-aminium chloride (Janus•HCl) (49)^{66, 77}:

To a solution of tetrachlorocyclopropene, **14** (0.025 mL, 0.2 mmol), which was prepared according to reported procedures,¹⁹ in dichloromethane (2 mL) was added freshly distilled diisopropylamine (0.11 mL, 0.8 mmol) drop-wise under an inert nitrogen atmosphere. The reaction was stirred for four hours at room temperature, after which **48** was added drop-wise as a solution in dichloromethane (16 mg, 0.1 mmol) and the reaction was stirred for an additional 8 hours. Purified compound could be acquired by flash chromatography (11% methanol in DCM).

The product **49** was obtained as an off-white solid in 90% yield (59 mg, 0.08 mmol). m.p. = 225°C - 230°C. Subsequent X-ray quality single crystals were grown from benzene and ethyl acetate (see below). ^1H NMR (300 MHz, CDCl_3): δ = 13.81 (s, 1H), 7.74 – 7.71 (m, 1H), 7.55 – 7.50 (m, 3H), 7.44 – 7.38 (m, 1H), 6.97 (d, J = 7.0 Hz, 1H), 4.03 – 3.94 (m, 4H), 2.84 (s, 6H) 1.41 (d, J = 6.75 Hz, 24H) 2.75 (s, 6H), 1.14 (d, J = 6.8 Hz, 24H). ^{13}C NMR (75 MHz, CDCl_3): δ = 150.3, 138.2, 136.2, 126.9, 126.7, 125.3, 123.2, 119.9, 119.4, 118.9, 112.3, 110.0, 51.4, 46.4, 22.1. IR (neat): 3050 cm^{-1} (C-H, aromatic stretch), 2965 cm^{-1} , 2788 cm^{-1} (C-H stretch,

alkane), 1709 cm^{-1} (N-H bend), 1524 cm^{-1} (C=C stretch, aromatic), 1489 cm^{-1} (C-N stretch).

HRMS (ESI): m/z calcd for $\text{C}_{27}\text{H}_{40}\text{N}_4$ (M^+): 421.3326, found: 421.3331 (The Cl^- counterion was not observed).

X-ray quality crystals were obtained as follows: **49** was dissolved in vial using slightly more than minimal amount of benzene required for dissolution. The vial was then placed in a beaker filled half an inch deep with ethyl acetate. The beaker was then capped with aluminum foil and placed in a 5 °C fridge, unperturbed for 72 hours.

4.1.5 Synthesis of N^1 -(2,3-bis(diisopropylamino)cycloprop-2-en-1-ylidene)- N^8, N^8 -dimethylnaphthalene-1,8-diamine (Free base of Janus) (45)^{66, 77}:

To a suspension of **49** (35 mg, 0.05 mmol) in toluene (2 mL) under an inert atmosphere, was added dry potassium bis(trimethylsilyl)amide (KHMDs, 0.5M in toluene (0.5 mL, 0.25 mmol), dropwise. The reaction was stirred for two hours. The volatile components were removed under reduced pressure, and the product was extracted with hot hexane.

The resulting product **45** was isolated as yellow crystals in ca. 92% yield (25 mg, 0.04 mmol). m.p. = 94°C - 95°C. $^1\text{H-NMR}$ (300 MHz, CDCl_3): δ = 7.37 (dd, J = 8.1, 1.1 Hz, 1H), 7.30 – 7.19 (m, 3H), 7.03 – 7.00 (m, 1H), 6.88 (dd, J = 7.6, 1.2 Hz, 1H) 3.51 – 3.38 (m, 4H) 2.75 (s, 6H), 1.14 (d, J = 6.8 Hz, 24H). $^{13}\text{C-NMR}$ (75 MHz, CDCl_3): δ = 152.4, 137.7, 125.6, 124.7, 122.5, 120.7, 120.1, 112.8, 112.1, 49.0, 45.5, 22.1. IR (neat): 2965 cm^{-1} , 2925 cm^{-1} (C-H stretch, aromatic), 2818 cm^{-1} , 2765 cm^{-1} (C-H stretch, alkane), 1895 cm^{-1} (N-H bend), 1525 cm^{-1} (C=C stretch, aromatic), 1431 cm^{-1} (C-N stretch). HRMS (ESI): m/z calcd for $\text{C}_{27}\text{H}_{40}\text{N}_4$ (M^+): 420.3326, found: 420.3326.

4.1.6 Reference Information:

Coordinate and thermochemical data for all structures, QTAIM analysis, additional computed MOs for **45** and **49**, NMR spectra for all reported compounds, including the ^1H NMR-based pK_a measurement, and X-ray crystallographic data (CIF file) of compound **49** can be found in **Appendix A**.

4.2 Synthesis of Compounds and Derivatives for PTC DACN Proton Sponge Catalysis

4.2.1 General procedure for phase transfer catalysis

N-(Diphenylmethylene)glycine *tert*-butyl ester **41**, (25 mg, 0.0846 mmol, 1 equiv.), DACN 2HCl (3 mg, 0.00428 mmol, 5 mol %), and electrophile (0.0101 mmol, 1.2 equiv.) was dissolved in 0.5 mL of dichloromethane in a 10 mL vial with a stir bar, followed by the addition of 0.5 mL of 50% aqueous potassium hydroxide. The vial was closed and the reaction was allowed to stir at room temperature for an hour. The reaction was extracted with 3 aliquots of 2 mL dichloromethane; the organic layer was dried with magnesium sulfate, and concentrated in vacuo. Products were isolated using flash column chromatography 9:1 (Hexane: Ethyl Acetate).

4.2.2 Synthesis of *tert*-butyl-2-(diphenylmethyleamino)-3-(phenyl)propanoate (**43a**)⁹⁶

Compound was purified via gravity column chromatography, using a mixture of 97:2:1 (Hexanes : Ethyl Acetate : Triethylamine). The final product was obtained as white crystals in 92% yield (0.0778 mmol, 30 mg). ^1H NMR (300 MHz, CDCl_3): δ = 1.47 (s, 9H), 3.19-3.28 (m, J = 8.9, 4.4Hz, 2H), 4.12-4.16 (dd, J = 9.6, 4.0 Hz, 1H), 6.62-6.64 (d, J = 7.0 Hz, 2H), 7.07-7.10 (m, 2H), 7.19-7.21 (m, 2H), 7.27-7.39 (m, 5H), 7.51-7.53 (t, J = 7.8 Hz, 1H), 7.59-7.62 (d, J = 7.4 Hz, 2H), 7.82-7.85 (d, J = 7.4 Hz, 1H). ^{13}C NMR (75 MHz, CDCl_3): δ = 170.8, 170.2, 139.7,

138.3, 137.6, 132.4, 130.0, 129.8, 128.7, 128.2, 128.0, 127.96, 127.69, 126.1, 81.1, 67.9, 39.6, 28.0.

4.2.3 Synthesis of *tert*-butyl-2-(diphenylmethyleneamino)-3-(naphthalen-2-yl)propanoate (43b)⁹⁶

Compound was purified via gravity column chromatography, using a mixture of 97:2:1 (Hexanes : Ethyl Acetate : Triethylamine). The final product was obtained as yellow oil in 92% yield (0.0778 mmol, 34 mg). ¹H NMR (300 MHz, CDCl₃): δ = 1.48 (s, 9H), 3.35-3.42 (m, 2H), 4.24-4.29 (dd, J = 9.0, 4.4 Hz, 1H), 6.55-6.57 (d, J = 7.2 Hz, 2H), 7.16-7.24 (m, 2H), 7.29-7.35 (m, 3H), 7.41-7.44 (m, 2H), 7.51-7.60 (m, 4H), 7.67-7.70 (d, J = 7.8 Hz, 2H), 7.77-7.85 (m, 2H). ¹³C NMR (75 MHz, CDCl₃): δ = 170.8, 170.4, 139.5, 137.7, 136.3, 135.9, 133.4, 132.4, 132.1, 130.0, 128.7, 128.4, 128.2, 128.0, 127.9, 127.6, 127.5, 127.4, 125.7, 125.2, 81.2, 67.9, 39.7, 28.0.

4.2.4 Synthesis of *tert*-butyl-2-(diphenylmethyleneamino)-3-(phenyl)butanoate (43c)⁹⁶

Compound was purified via gravity column chromatography, using a mixture of 97:2:1 (Hexanes : Ethyl Acetate : Triethylamine). The final product was obtained as yellow oil 91% yield (0.0769 mmol, 31 mg). ¹H NMR (300 MHz, CDCl₃): 1.45 (s, 9H), 3.49-3.61 (m, 1H), 3.99-4.02 (d, J = 8.2 Hz, 1H), 6.75-6.78 (d, J = 6.8 Hz, 2H), 7.14-7.25 (m, 5H), 7.30-7.40 (m, 5H), 7.50-7.53 (d, J = 7.0 Hz, 2H), 7.65-7.68 (d, J = 6.8 Hz, 1H). ¹³C NMR (75 MHz, CDCl₃): δ = 170.7, 170.4, 143.8, 143.4, 136.6, 136.4, 132.4, 130.1, 130.0, 129.97, 128.9, 128.8, 128.6, 128.3, 128.27, 128.23, 128.14, 128.14, 128.0, 127.9, 127.88, 127.82, 127.7, 126.2, 81.0, 80.8, 72.8, 71.9, 43.5, 28.0, 27.8, 18.0, 16.82.

NMR analysis shows a mixture of the two diastereomers, explaining the splitting pattern of proton at 4 ppm, the aromatic signal overlap between 7.14-7.40, as well as the appearance of twice the signals in the carbon spectra.

4.2.5 Synthesis of *tert*-butyl-2-(diphenylmethyleneamino)-3-(phenyl)propanoate (43d)⁹⁶

Compound was purified via gravity column chromatography, using a mixture of 97:2:1 (Hexanes : Ethyl Acetate : Triethylamine). The final product was obtained as white crystals in 60% yield (0.0508 mmol, 19 mg). ¹H NMR (300 MHz, CDCl₃): δ = 1.47 (s, 9H), 3.19-3.28 (m, J = 8.9, 4.4 Hz, 2H), 4.12-4.16 (dd, J = 9.6, 4.0 Hz, 1H), 6.62-6.64 (d, J = 7.0 Hz, 2H), 7.07-7.10 (m, 2H), 7.19-7.21 (m, 2H), 7.27-7.39 (m, 5H), 7.51-7.53 (t, J = 7.8 Hz, 1H), 7.59-7.62 (d, J = 7.4 Hz, 2H), 7.82-7.85 (d, J = 7.4 Hz, 1H). ¹³C NMR (75 MHz, CDCl₃): δ = 170.8, 170.2, 139.7, 138.3, 137.6, 132.4, 130.0, 129.8, 128.7, 128.2, 128.0, 127.96, 127.69, 126.1, 81.1, 67.9, 39.6, 28.0.

4.2.6 Synthesis of *tert*-butyl-2-(diphenylmethyleneamino)-3-(4-methylphenyl)propanoate (43e)⁹⁶

Compound was purified via gravity column chromatography, using a mixture of 97:2:1 (Hexanes : Ethyl Acetate : Triethylamine). The final product was obtained as clear oil in 92% yield (0.0778 mmol, 31 mg). ¹H NMR (300 MHz, CDCl₃): δ = 1.46 (s, 9H), 2.31 (s, 3H), 3.09-3.25 (m, 2H), 4.09-4.13 (dd, J = 9.0, 4.0 Hz, 1H), 6.60-6.71 (d, J = 7.0 Hz, 2H), 6.94-7.03 (dt, J = 8.7, 7.5 Hz, 4H), 7.27-7.39 (m, 6H), 7.58-7.61 (dd, J = 8.0, 1.4 Hz, 2H). ¹³C NMR (75 MHz, CDCl₃): δ = 170.9, 170.1, 139.6, 136.4, 135.5, 135.2, 130.0, 129.7, 128.7, 128.2, 128.1, 128.0, 127.9, 127.7, 81.05, 68.0, 39.1, 28.0, 21.0.

4.2.7 Synthesis of tert-butyl-2-(diphenylmethyleneamino)-3-(4-chlorophenyl)propanoate (43f)⁹⁶

Compound was purified via gravity column chromatography, using a mixture of 97:2:1 (Hexanes : Ethyl Acetate : Triethylamine). The final product was obtained as clear oil in 91% yield (0.0770 mmol, 32 mg). ¹H NMR (300 MHz, CDCl₃): δ = 1.46 (s, 9H), 3.10-3.24 (m, 2H), 4.08-4.13 (dd, J = 8.7, 4.2 Hz, 1H), 6.68-6.70 (d, J = 7.0 Hz, 2H), 6.99-7.02 (d, J = 8.3 Hz, 2H), 7.16-7.19 (d, J = 6.8 Hz, 2H), 7.30-7.40 (m, 6H), 7.57-7.60 (d, J = 6.8 Hz, 2H). ¹³C NMR (75 MHz, CDCl₃): δ = 170.6, 170.5, 139.4, 136.9, 136.2, 132.0, 131.2, 130.2, 128.7, 128.3, 128.2, 128.1, 128.0, 127.6, 81.3, 67.6, 38.9, 28.0.

4.2.8 Synthesis of tert-butyl-2-(diphenylmethyleneamino)-3-(4-nitrophenyl)propanoate (43g)⁹⁶

Compound was purified via gravity column chromatography, using a mixture of 97:2:1 (Hexanes : Ethyl Acetate : Triethylamine). The final product was obtained as white crystals in 93% yield (0.0787 mmol, 34 mg). ¹H NMR (300 MHz, CDCl₃): δ = 1.46 (s, 9H), 3.30-3.33 (m, 2H), 4.17-4.21 (dd, J = 8.0, 2.3 Hz, 1H), 6.72-6.74 (d, J = 6.9 Hz, 2H), 7.25-7.36 (m, 8H), 7.57-7.60 (d, J = 6.9 Hz, 2H), 8.07-8.10 (d, J = 6.9 Hz, 2H). ¹³C NMR (75 MHz, CDCl₃): δ = 170.9, 170.1, 146.6, 146.5, 139.1, 136.0, 130.6, 130.4, 128.7, 128.6, 128.3, 128.1, 127.5, 123.2, 81.7, 67.0, 39.4, 28.0.

4.2.9 Synthesis of tert-butyl-2-(diphenylmethyleneamino)-3-(4-methoxyphenyl)propanoate (43h)⁹⁶

Compound was purified via gravity column chromatography, using a mixture of 97:2:1 (Hexanes : Ethyl Acetate : Triethylamine). The final product was obtained as clear oil in 54%

yield (0.0457 mmol, 19 mg). ^1H NMR (300 MHz, CDCl_3): 1.46 (s, 9 H), 3.12-3.18 (m, 2 H), 3.78 (s, 3 H) 4.07-4.12 (t, $J = 4.0$ Hz, 1H), 6.67-6.69 (d, $J = 6.0$ Hz, 2H), 6.74-6.77 (d, $J = 8.2$ Hz, 2H), 6.98-7.01 (d, $J = 8.2$ Hz, 2H), 7.30-7.39 (m, 6H), 7.58-7.61 (d, $J = 8.2$ Hz, 2H). ^{13}C NMR (75 MHz, CDCl_3): $\delta = 170.9, 170.2, 158.1, 139.6, 136.4, 130.8, 130.4, 130.0, 128.7, 128.2, 128.0, 127.9, 127.7, 113.8, 113.5, 81.0, 68.1, 55.2, 38.7, 28.0$.

4.2.10 Synthesis of tert-butyl-2-(diphenylmethyleamino)-5-(phenyl)pentanoate (43i)⁹⁶

Compound was purified via gravity column chromatography, using a mixture of 97:2:1 (Hexanes : Ethyl Acetate : Triethylamine). The final product was obtained as clear oil in 10 % yield (0.0085 mmol, 3.5 mg). ^1H NMR (300 MHz, CDCl_3): $\delta = 1.46$ (s, 9H), 1.59-1.68 (m, 2H), 1.93-2.01 (dd, $J = 7.8, 6.7$ Hz, 2H), 2.56-2.61 (t, $J = 7.8$ Hz, 2H), 3.95-3.99 (t, $J = 6.4$ Hz, 1H), 7.14-7.19 (m, 5H), 7.32-7.41 (m, 4H), 7.44-7.46 (m, 3H), 7.66-7.68 (d, $J = 6.8$ Hz, 2H). ^{13}C NMR (75 MHz, CDCl_3): $\delta = 171.5, 169.9, 142.2, 139.7, 136.7, 130.1, 128.8, 128.5, 128.4, 128.3, 128.2, 128.0, 127.8, 125.7, 80.8, 65.9, 35.6, 33.3, 28.1, 27.8$.

4.2.11 Synthesis of tert-butyl-2-(diphenylmethyleamino)pent-4-enoate (43j = 43k)⁹⁶

Compound was purified via gravity column chromatography, using a mixture of 97:2:1 (Hexanes : Ethyl Acetate : Triethylamine). The final product was obtained as clear oil in 91% yield (0.0769 mmol, 26 mg). ^1H NMR (300 MHz, CDCl_3): $\delta = 1.46$ (s, 9H), 2.62-2.69 (m, 2H), 4.00-4.05 (dd, $J = 7.7, 2.0$ Hz, 1H), 5.01-5.12 (m, 2H), 5.69-5.79 (m, 1H), 7.17-7.21 (m, 2H), 7.31-7.46 (m, 6H), 7.64-7.67 (d, $J = 6.8$ Hz, 2H). ^{13}C NMR (75 MHz, CDCl_3): $\delta = 170.8, 170.1, 139.7, 136.6, 134.7, 132.4, 130.1, 130.0, 128.8, 128.5, 128.2, 117.2, 81.0, 65.8, 38.1, 28.0$.

4.2.11 Synthesis of *tert*-butyl-2-(diphenylmethyleneamino)hex-4-enoate (43l)⁹⁶

Compound was purified via gravity column chromatography, using a mixture of 97:2:1 (Hexanes : Ethyl Acetate : Triethylamine). The final product was obtained as clear oil in 91% yield (0.0769 mmol, 27 mg). ¹H NMR (300 MHz, CDCl₃): δ = 1.46 (s, 9H), 1.63-1.65 (d, J = 6.1 Hz, 3H), 2.53-2.62 (m, 2H), 3.95- 4.00 (dd, J = 7.6, 2.0 Hz, 1H), 5.31-5.33 (m, 2H), 7.16-7.19 (m, 2H), 7.34-7.46 (m, 6H), 7.64-7.67 (d, J = 6.8 Hz, 2H). ¹³C NMR (75 MHz, CDCl₃): δ = 171.1, 169.8, 139.8, 136.8, 130.1, 128.8, 128.4, 128.3, 128.0, 127.95, 127.93, 127.8, 127.1, 126.1, 80.8, 66.4, 36.9, 28.0, 17.9.

4.2.12 Synthesis of *tert*-butyl-2-(diphenylmethyleneamino)pent-4-enoate (43m)⁹⁶

Compound was purified via gravity column chromatography, using a mixture of 97:2:1 (Hexanes : Ethyl Acetate : Triethylamine). The final product was obtained as clear oil in 82% yield (0.0694 mmol, 24 mg). ¹H NMR (300 MHz, CDCl₃): δ = 1.46 (s, 9H), 2.62-2.69 (m, 2H), 4.00-4.05 (dd, J = 7.7, 2.0 Hz, 1H), 5.01-5.12 (m, 2H), 5.69-5.79 (m, 1H), 7.17-7.21 (m, 2H), 7.31-7.46 (m, 6H), 7.64-7.67 (d, J = 6.8 Hz, 2H). ¹³C NMR (75 MHz, CDCl₃): δ = 170.8, 170.1, 139.7, 136.6, 134.7, 132.4, 130.1, 130.0, 128.8, 128.5, 128.2, 117.2, 81.0, 65.8, 38.1, 28.0.

5. Supporting Information

5.1 Appendix A: Janus Proton Sponge

5.1.1 X-ray Experimental Data

A colorless block-like specimen of C₂₇H₄₁ClN₄, approximate dimensions 0.084 mm x 0.278 mm x 0.343 mm, was used for the X-ray crystallographic analysis. The X-ray intensity data were measured on a Bruker Apex2 with MoK α radiation at -100 °C. Initial unit cell

parameters were obtained from three scans in different orientations. The frames were integrated with the Bruker SAINT software package using a narrow-frame algorithm. The integration of the data using a monoclinic unit cell yielded a total of 31761 reflections to a maximum θ angle of 27.50° (0.77 \AA resolution), of which 7319 were independent (average redundancy 4.340, completeness = 99.7%, $R_{\text{int}} = 3.16 \%$, $R_{\text{sig}} = 3.30 \%$) and 4513 (61.66 %) were greater than $2\sigma(F_2)$. The final cell constants of $a = 33.592(2) \text{ \AA}$, $b = 11.1346(7) \text{ \AA}$, $c = 18.555(1) \text{ \AA}$, $\beta = 113.102(1)^\circ$, volume = $6383.5(7) \text{ \AA}^3$, are based upon the refinement of the XYZ-centroids of 5847 reflections above $20 \sigma(I)$ with $4.773^\circ < 2\theta < 45.92^\circ$. Data were corrected for absorption effects using the numerical method (SADABS). The ratio of minimum to maximum apparent transmission was 0.928. The calculated minimum and maximum transmission coefficients (based on crystal size) are 0.9280 and 1.0000. The structure was solved and refined using the Bruker SHELXTL Software Package, using the space group $C 2/c 1$, with $Z = 8$ for the formula unit, $C_{27}H_{41}ClN_4$. The final anisotropic full-matrix least-squares refinement on F_2 with 293 variables converged at $R_1 = 4.58 \%$, for the observed data and $wR_2 = 14.32 \%$ for all data. The goodness-of-fit was 1.068. The largest peak in the final difference electron density synthesis was 0.193 e-/\AA^3 and the largest hole was -0.310 e-/\AA^3 with an RMS deviation of 0.036 e-/\AA^3 . On the basis of the final model, the calculated density was 0.951 g/cm^3 and $F(000)$, 1984 e-.

[Software: Bruker Apex2 v.2014.11.0. Bruker-AXS, Madison, WI, USA.]

5.1.2 Quantum Yield Calculation

The quantum yield (ϕ) of **49** was measured relative to that of anthracene in ethanol.ⁱⁱ Emission spectra for the quantum yield calculation were acquired using quartz cuvettes in a fluorescence spectrophotometer with a Xenon flash lamp at ambient temperature. Sample and standards were prepared as $1 \times 10^{-5} \text{ M}$ solutions in 95 % ethanol. Entrance and exit slit widths

were set to 5 mm, and the excitation wavelength was 333 nm for both the standard and sample. Quantum yields were calculated using equation S1, according to the 2011 IUPAC technical report on standards for photoluminescence quantum yield measurements in solution.^{i, ii}

$$\phi_f^x = \frac{F^x f_{st} n_x^2}{F^{st} f_x n_{st}^2} \phi_f^{st} \quad \text{Equation S1}$$

Where: ϕ^x and ϕ^{st} are the quantum yields of the sample and the standard, respectively. F^x and F^{st} are the integrated fluorescence intensities of sample and standard spectra. f^x and f^{st} are the absorption factors of the sample and standard at the excitation wavelength (where $f = 1 - 10^{-A}$, and A = absorbance). n^x and n^{st} are the refractive indices of the sample and reference solution, respectively, which were assumed to be the same in this experiment.

- i) Dawson, W. R.; Windsor, M. W. *J. Chem. Phys.* **1968**, 72, 3251-3260.
- ii) Brouwer, A. M. *Pure Appl. Chem.* **2011**, 83, 2213-2228.

5.1.3 Relative pKa Calculations

The pKa calculation of **45** was computed relative to that of 1,8-bis(tetramethylguanidino)naphthalene (TMGN), using the Equation (S2):

Given that $\text{pH} = -\log(Ka)$, and $\Delta G^\circ = -2.303 R \cdot T \cdot \log(Ka)$, $\Delta \text{pKa} = \Delta G^\circ / 2.303 \cdot R \cdot T$

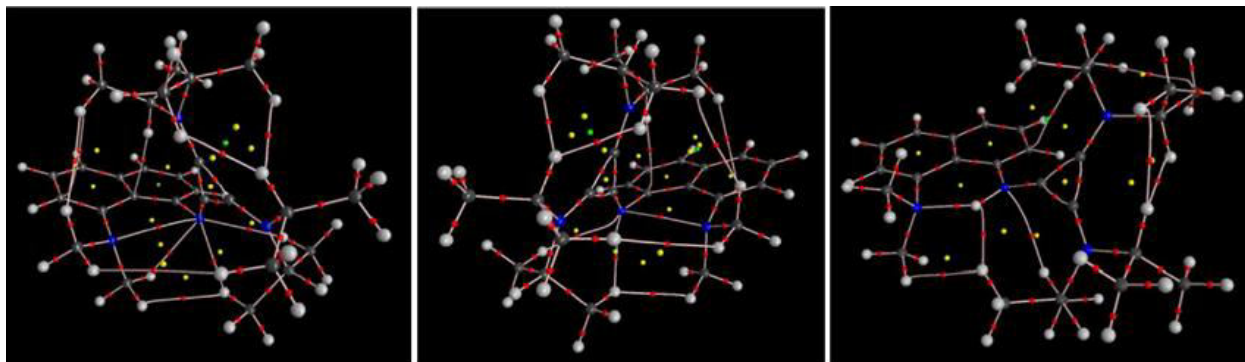
$$\Delta \text{pKa} = [G^\circ(\mathbf{49})_{\text{MeCN}} - G^\circ(\mathbf{45})_{\text{MeCN}} - G^\circ(\text{TMGN})_{\text{MeCN}} + G^\circ(\text{TMGN} \cdot \text{H}^+)_{\text{MeCN}}] / 2.303 \cdot R \cdot T \text{ [Eq. S2]},$$

Since the pKa of TMGN has been measured to be 25.1, and the ΔpKa obtained from equation S2 was found to be ca. -1.18, the predicted pKa using this methodology is 23.9.

5.1.4 Experimental pK_a Determination

Compound **49** (8.6 mg, 0.025 mmol, 1 equiv.) and 1,1,3,3-tetramethylguanidine (TMG) (3.0 μ L, 0.025 mmol, 1 equiv) were dissolved in 0.6 mL MeCN- d_3 . The ^1H NMR chemical shift of the isopropyl groups belonging to **49** in this mixture was compared against those in pure **49** and **45** to estimate the equilibrium ratio and equilibrium constant of the reaction. The equilibrium constant was then used, with the known pK_a of TMG (23.3) to determine the pK_a of **49**. The experiment was performed in two different ways; combining the freebase **45** and the hydrochloride salt of TMG, and combining the hydrochloride salt **49** and the freebase TMG. Each of these two procedures was repeated in triplicate and a representative ^1H NMR spectrum of each is included.

5.1.6 QTAIM Structures

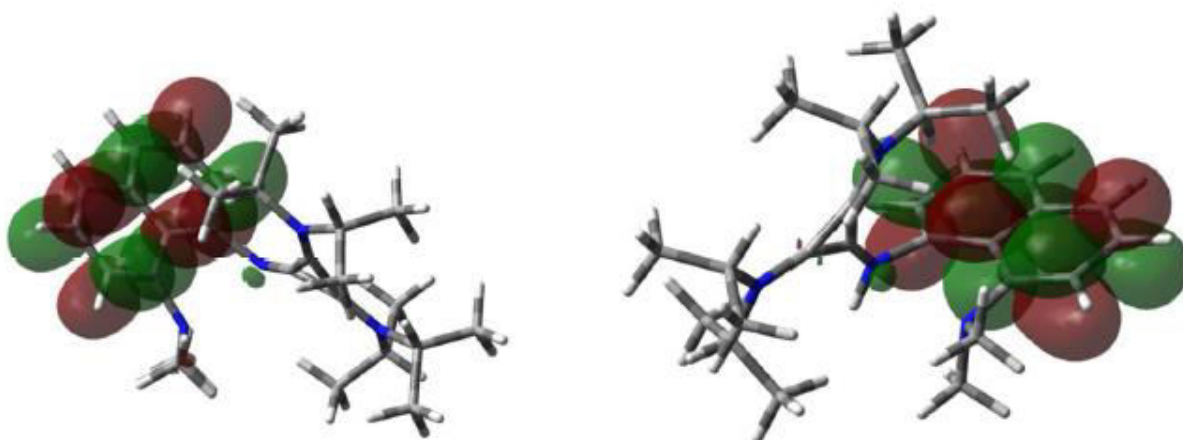


45_{opt}

49_{x-ray}

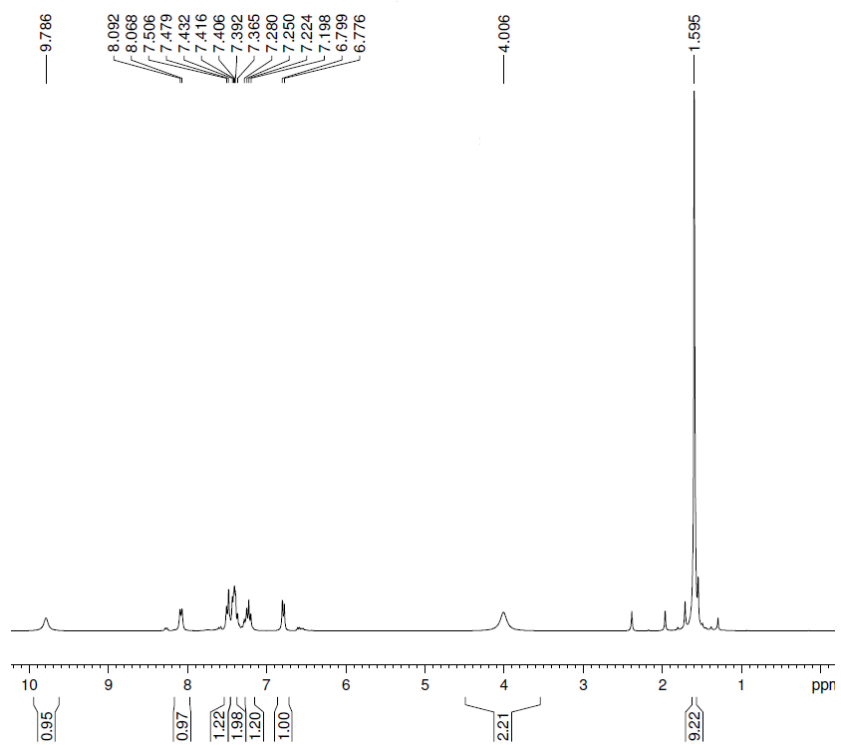
49_{opt}

5.1.7 *B3LYP/6-31G(d,p)* Computed LUMO+1 of 45_{opt} and 49_{xray} (respectively)

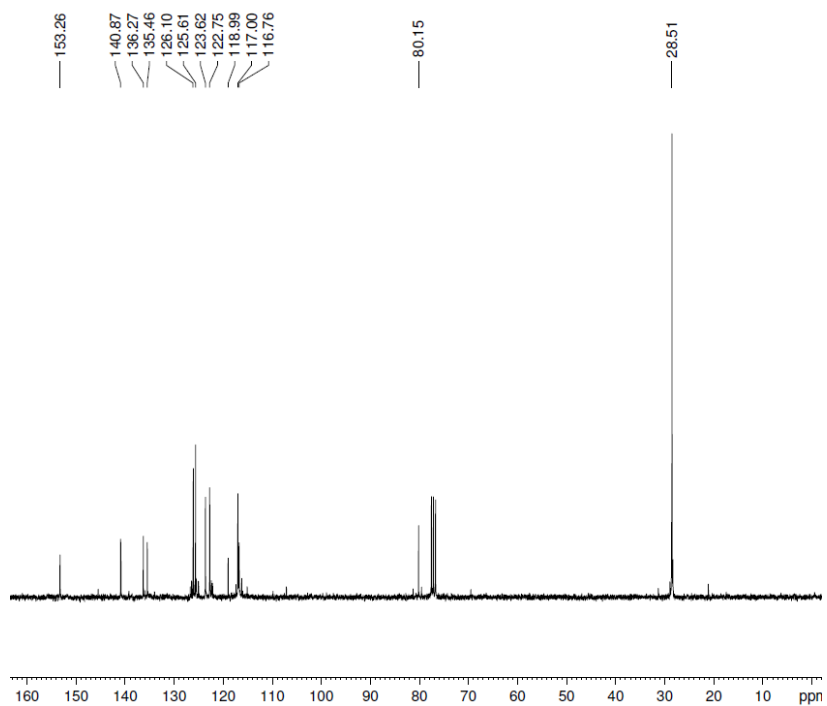


5.1.8 Spectral Data of Janus Related Compounds

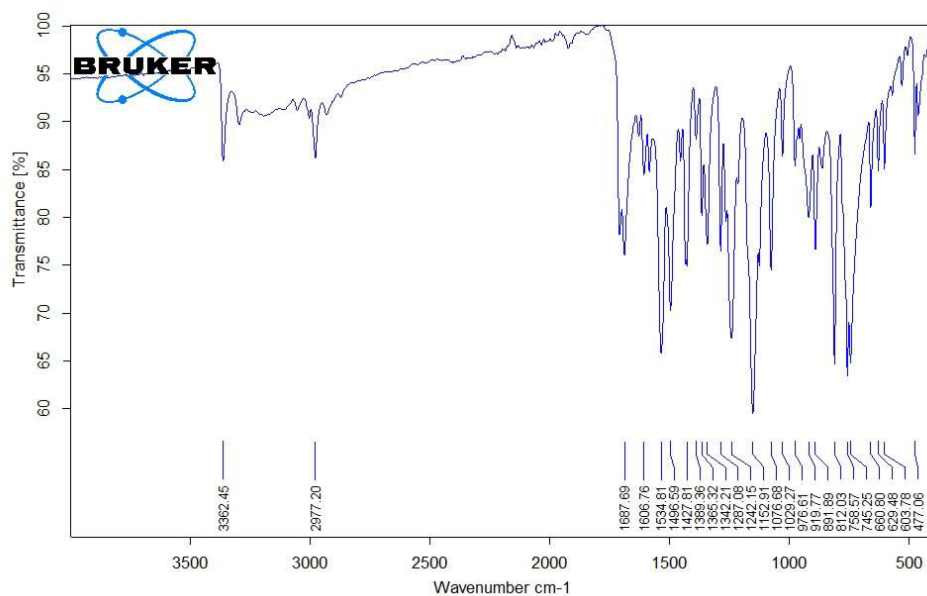
Proton Spectrum (46)



Carbon Spectrum (46)



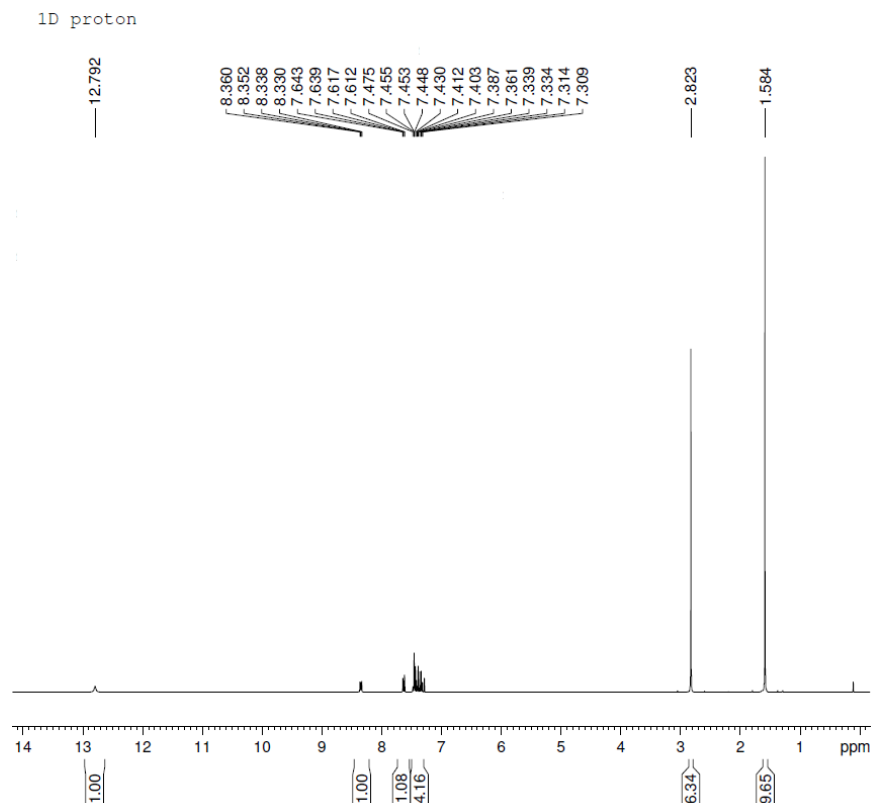
IR Spectrum (46)



C:\Users\Administrator\Desktop\Student Spectra\MonoBoc.0	Sample description	Instrument type and / or accessory	25/06/2015
--	--------------------	------------------------------------	------------

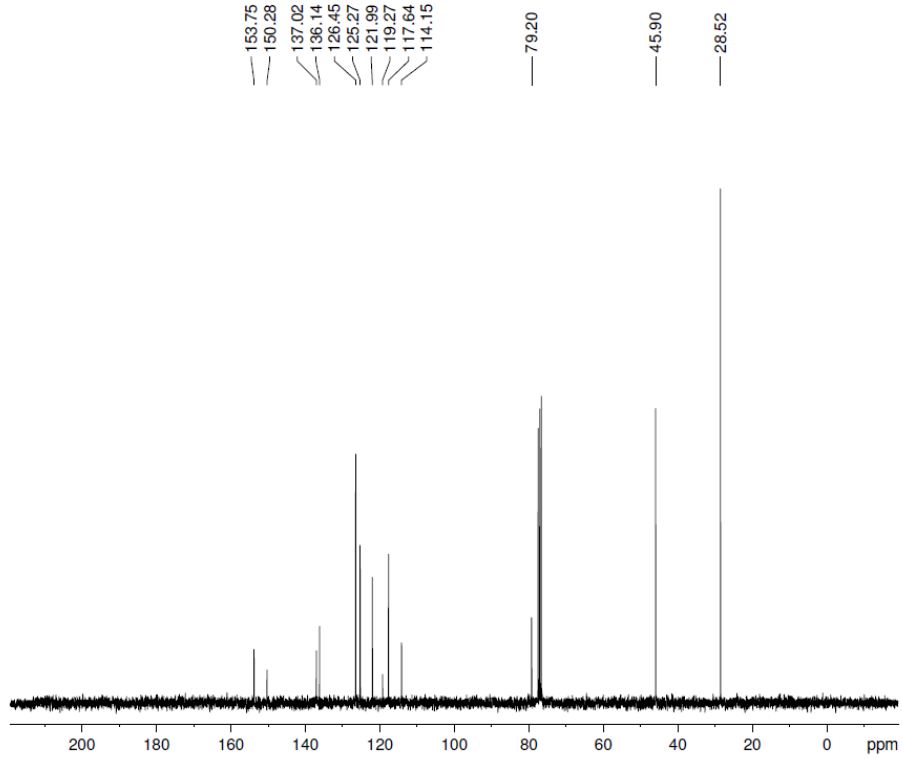
Page 1/1

Proton Spectrum (47)

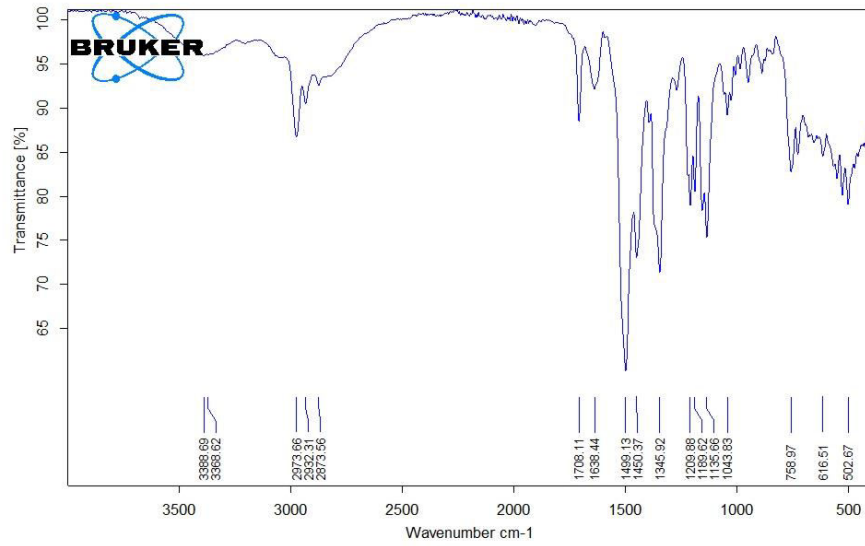


Carbon Spectrum (47)

1D carbon with proton decoupling

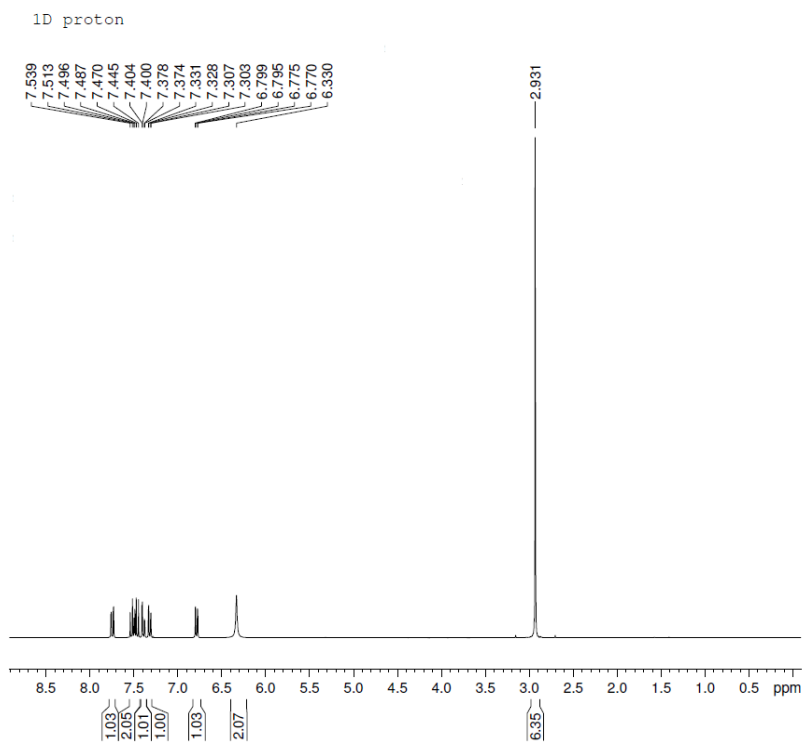


IR Spectrum (47)

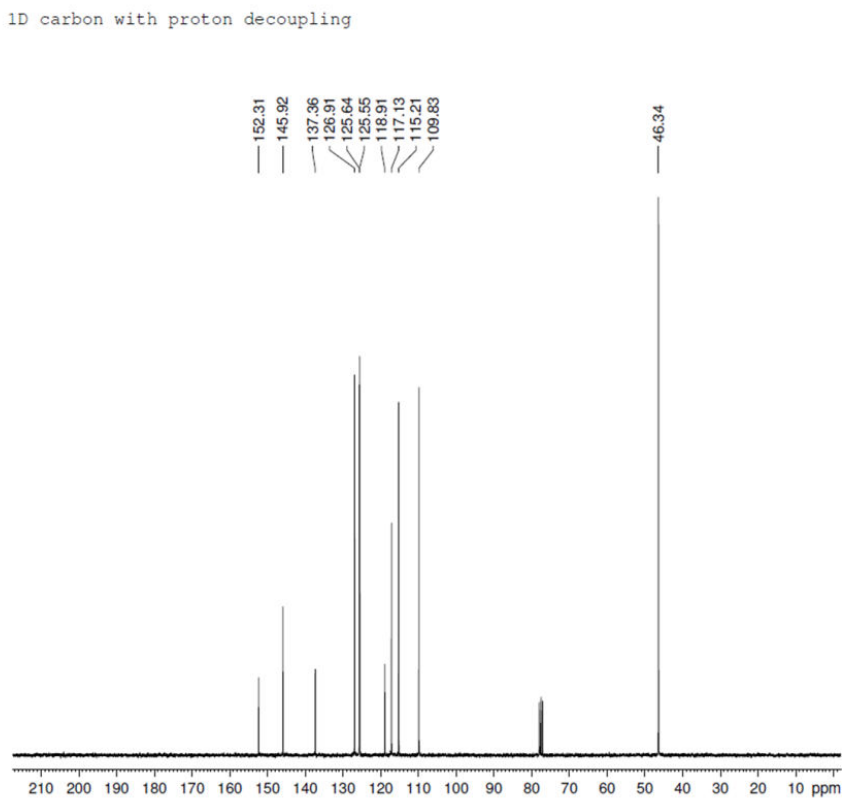


C:\Users\Administrator\Desktop\Spectra\Sample description.1296 Sample description Instrument type and / or accessory 06/06/2014

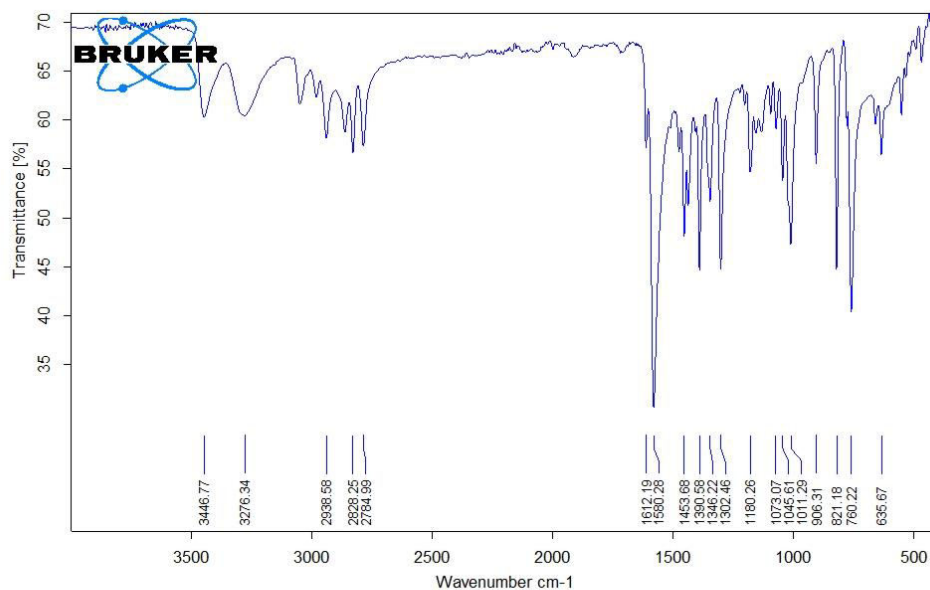
Proton Spectrum (48)



Carbon Spectrum (48)



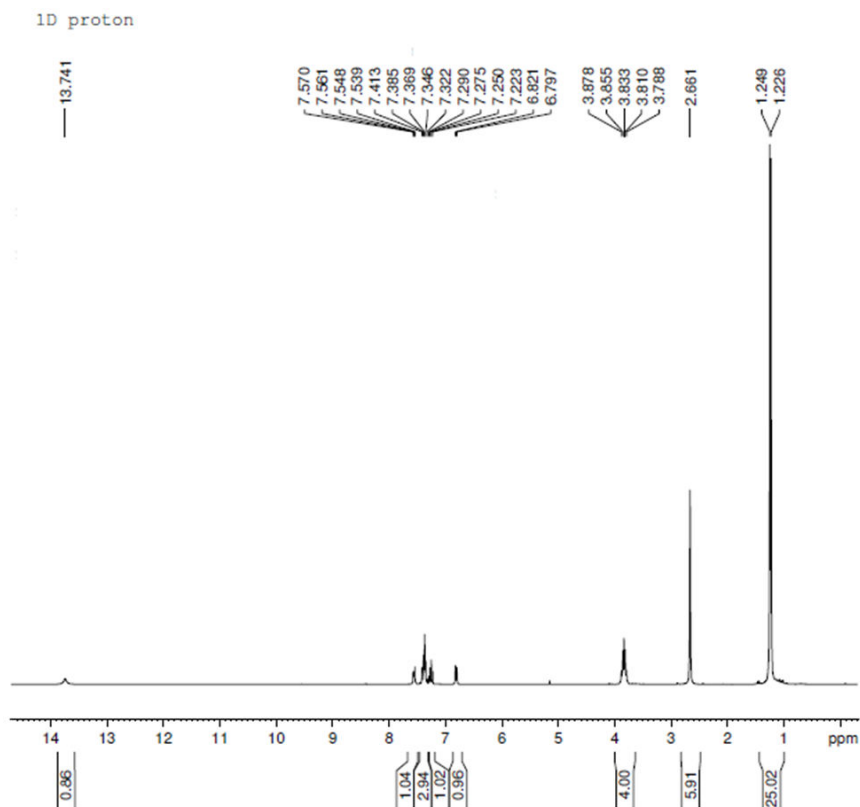
IR Spectrum (48)



C:\Users\Administrator\Desktop\Spectra\LB-Dimethyl.0 LB-Dimethyl Instrument type and / or accessory 16/06/2014

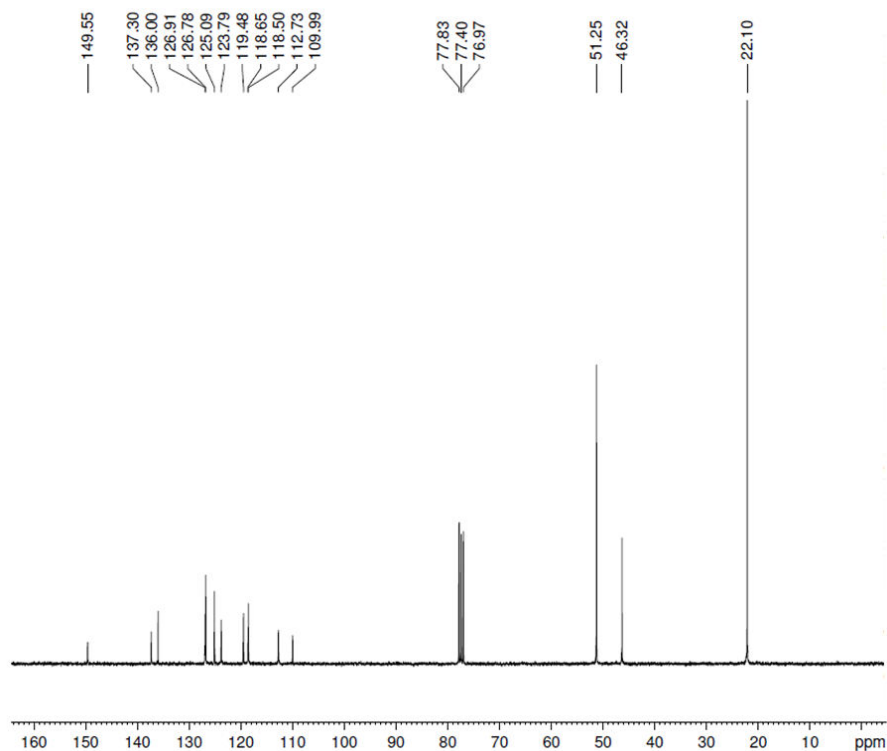
Page 1/1

Proton Spectrum (49)

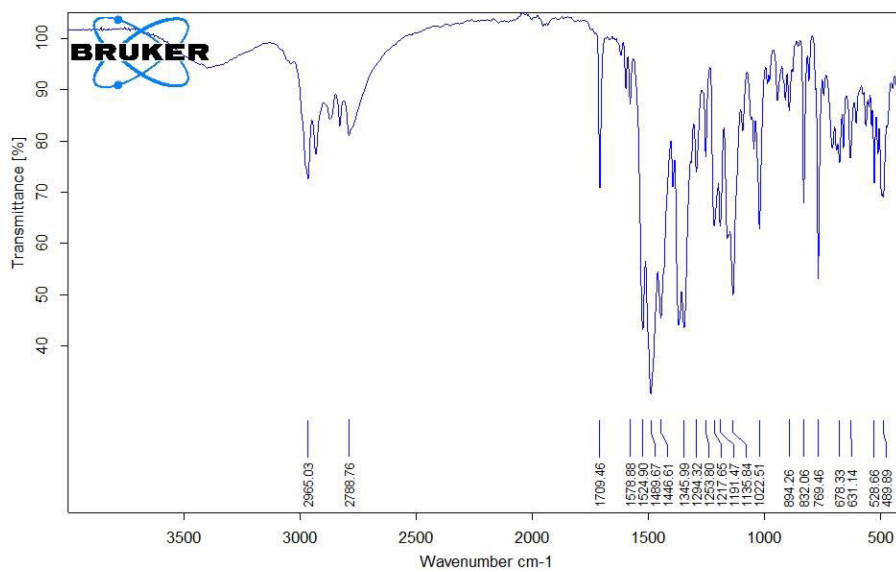


Carbon Spectrum (49)

1D carbon with proton decoupling



IR Spectrum (49)



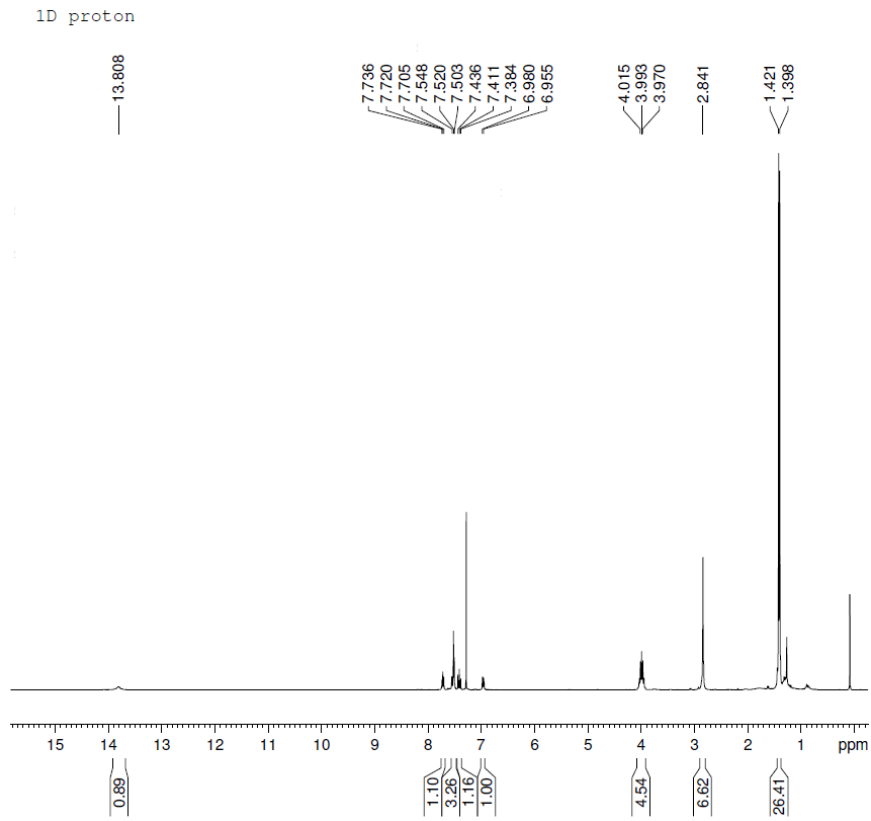
C:\Users\Administrator\Desktop\Student Spectra\Janus HCl.0

Sample description

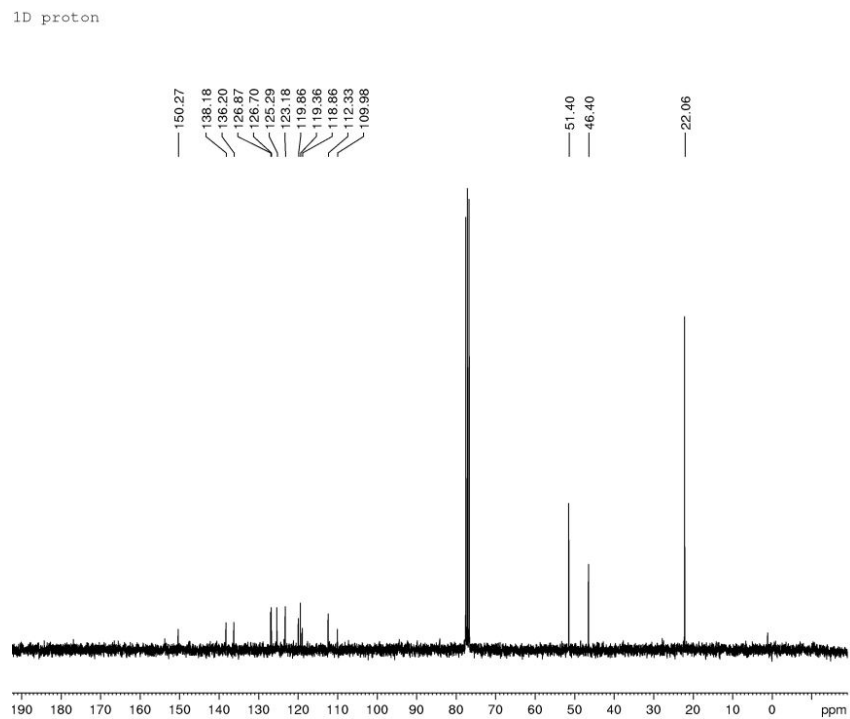
Instrument type and / or accessory

25/06/2015

Proton Spectrum (49-BF₄)

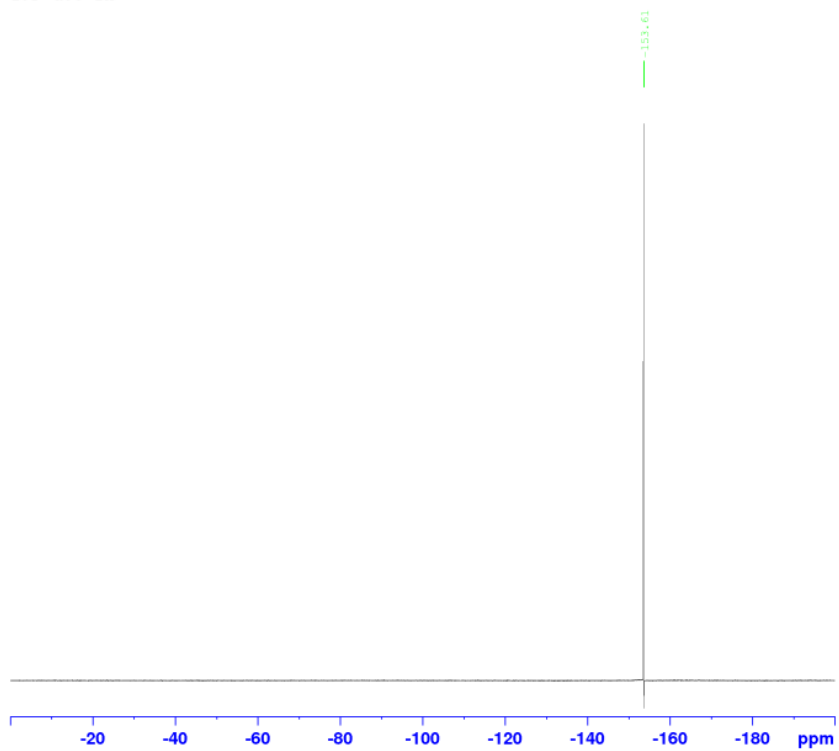


Carbon Spectrum (49-BF₄)



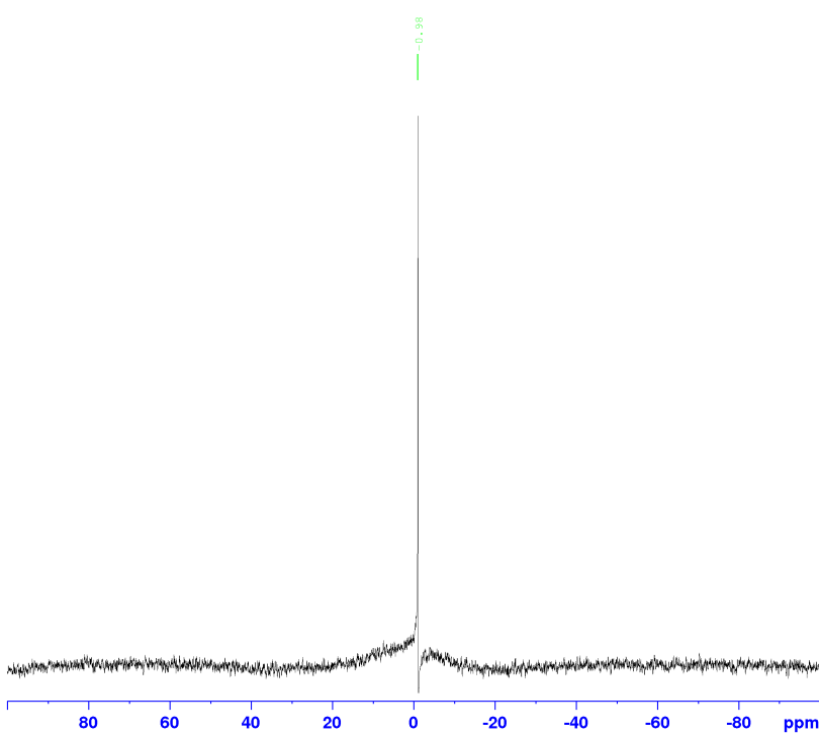
Fluorine Spectrum (**49-BF₄**)

¹⁹F dec 1H

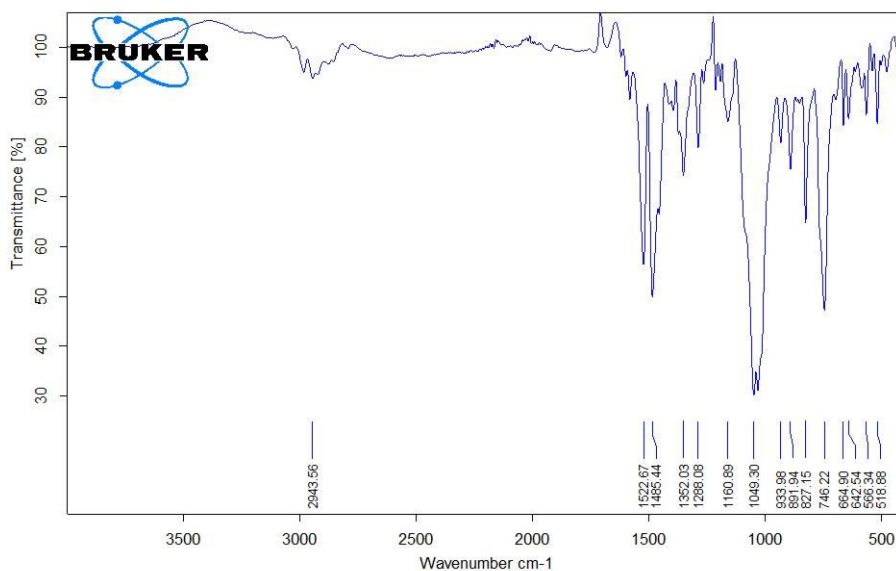


Boron Spectrum (**49-BF₄**)

¹¹B dec 1H



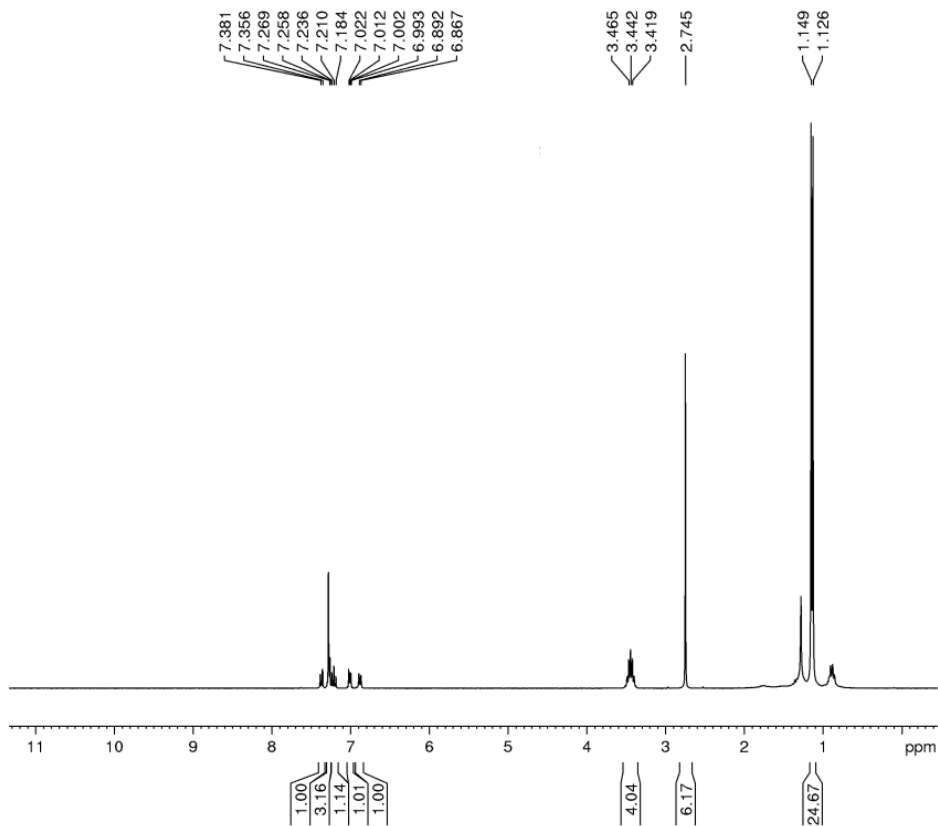
IR Spectrum (49-BF₄)



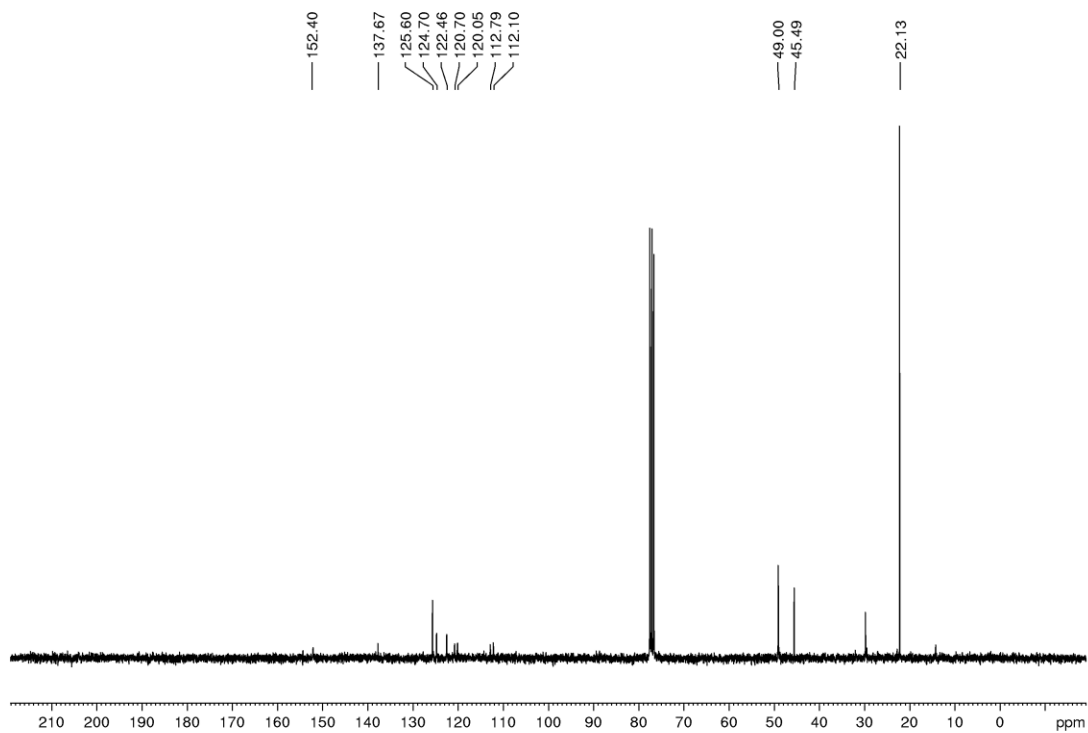
C:\Users\Administrator\Desktop\Student Spectra\Sample description.1300	Sample description	Instrument type and / or accessory	06/06/2014
--	--------------------	------------------------------------	------------

Page 1/1

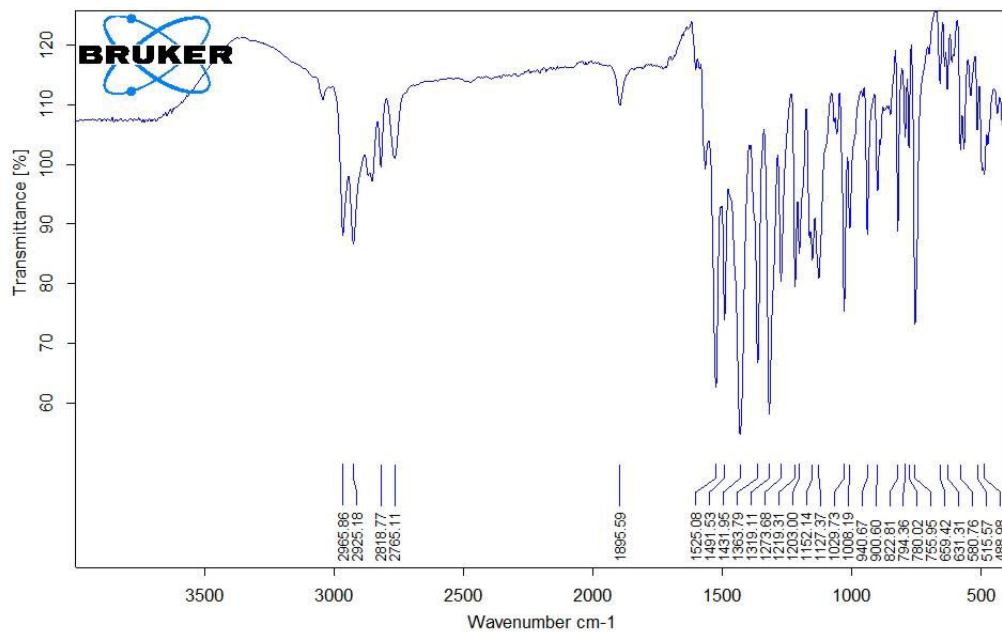
Proton Spectrum (45)



Carbon Spectrum (45)

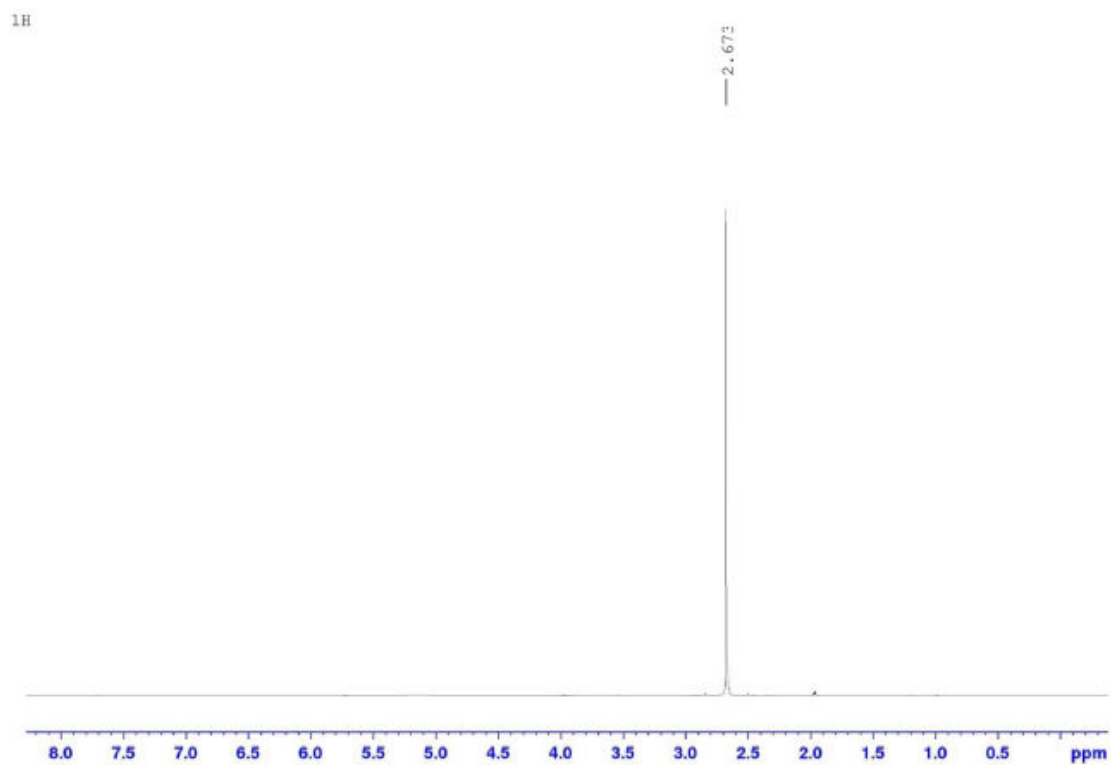


IR Spectrum (45)

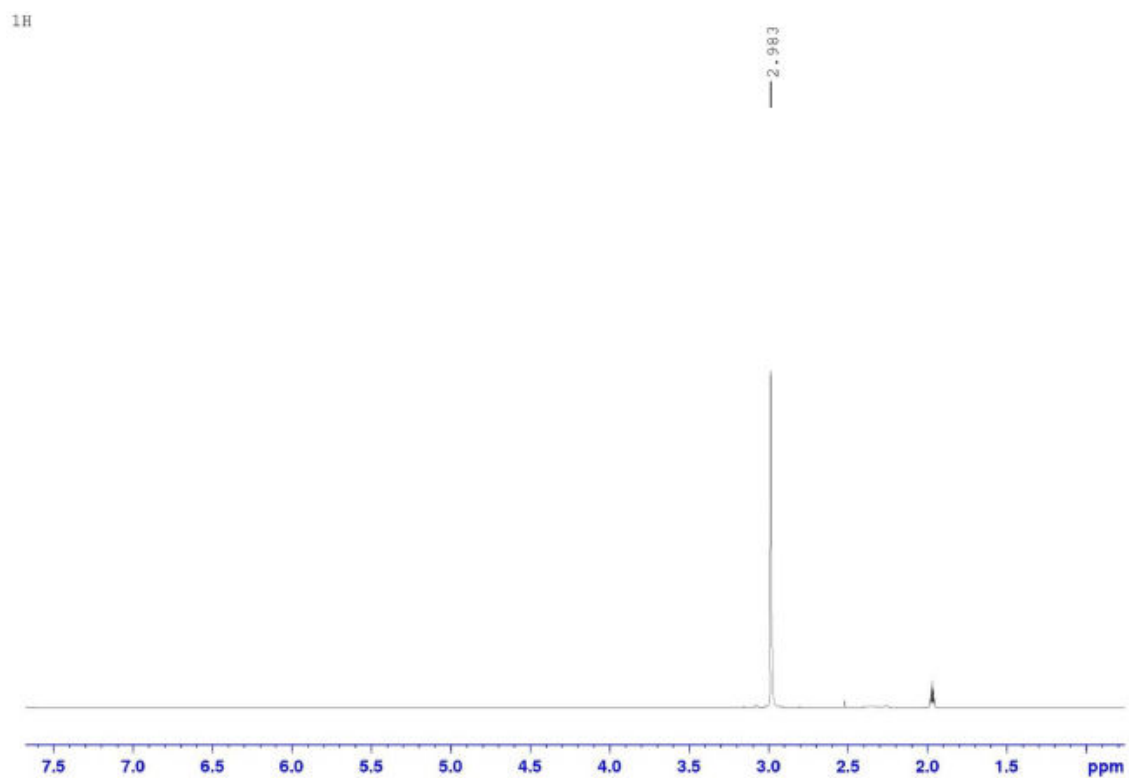


C:\Users\Administrator\Desktop\Student Spectra\Janus freebase.0	Sample description	Instrument type and / or accessory	25/06/2015
---	--------------------	------------------------------------	------------

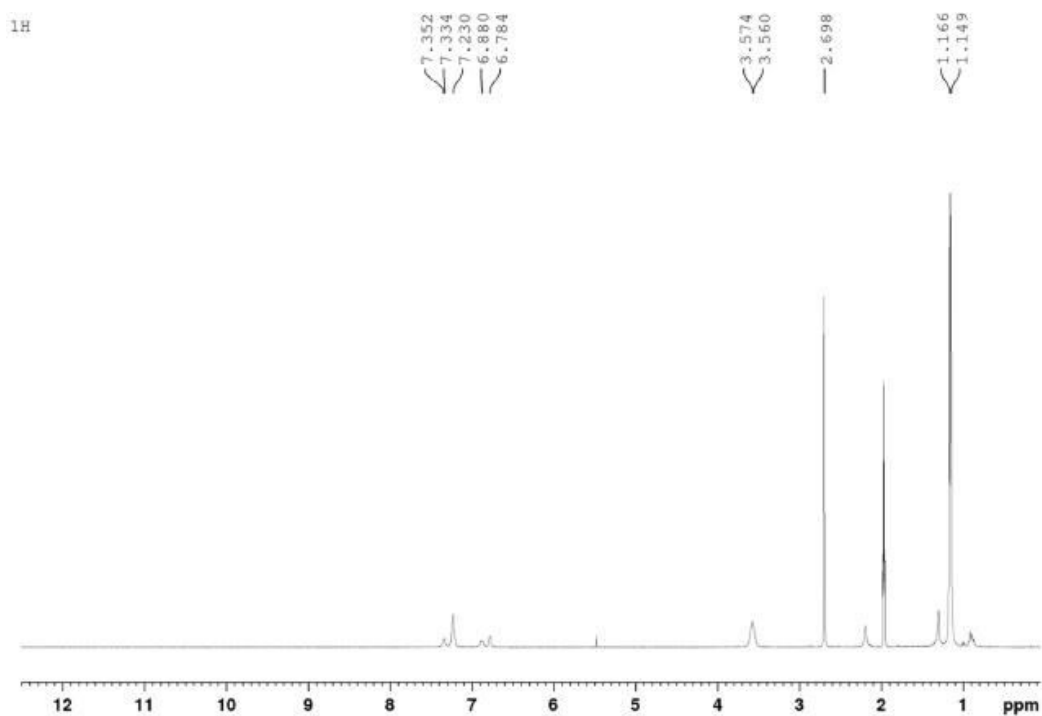
Proton Spectrum (TMG in MeCN-d₃)



Proton Spectrum (TMG-HCl in MeCN-d₃)

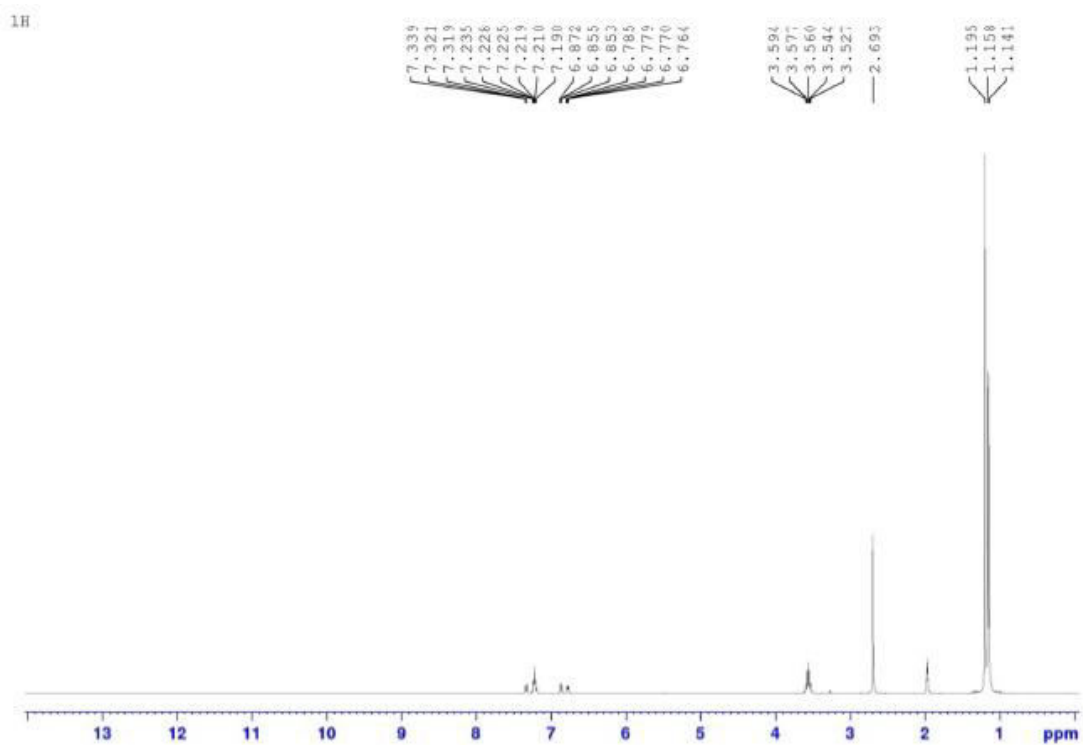


Proton Spectrum (45 in MeCN-d₃)

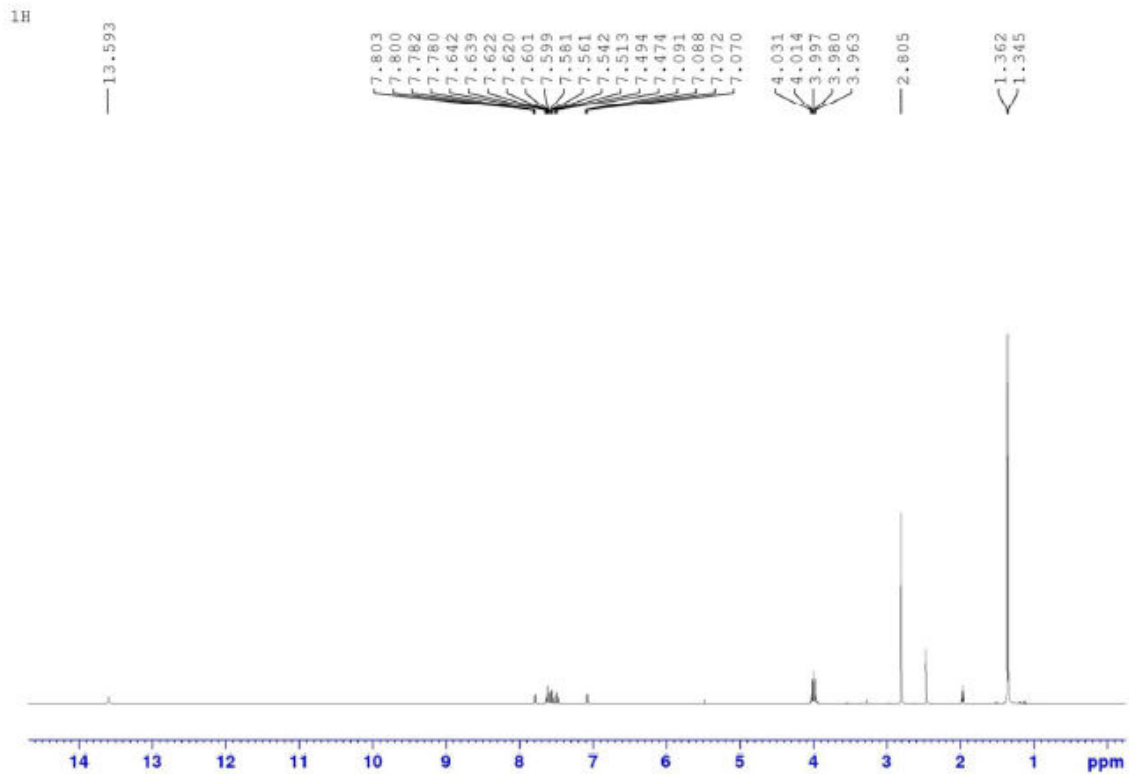


Proton Spectrum (45 in MeCN-d₃)

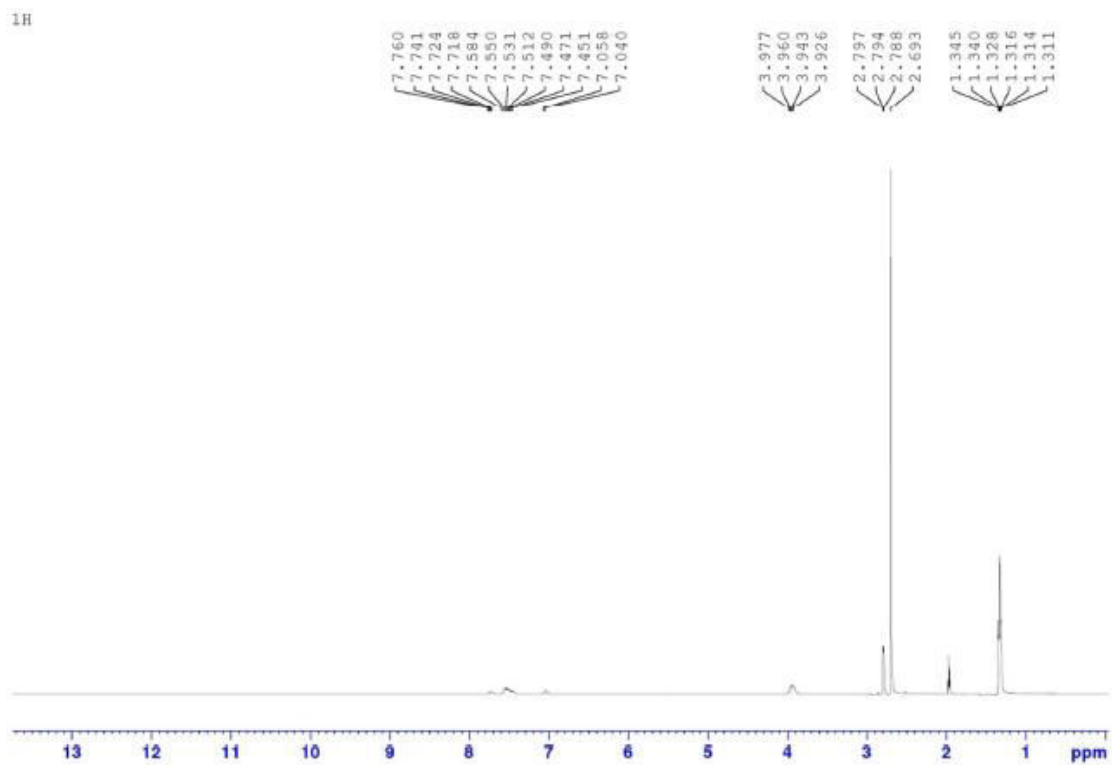
(generated by the addition of excess potassium *tert*-butoxide to a solution of 49 in MeCN-d₃)



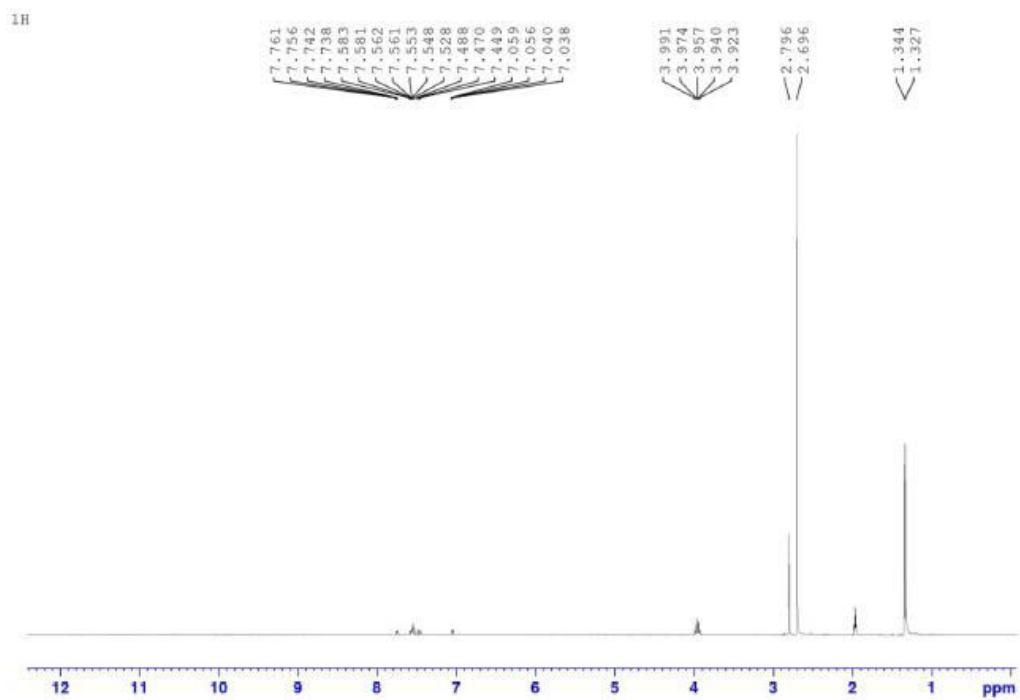
Proton Spectrum (49 in MeCN-d₃)



Proton Spectrum (Mixture of TMG and 49 in MeCN-d₃)

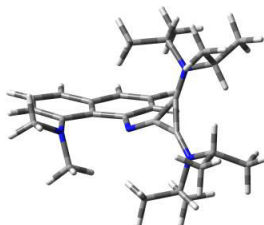


Proton Spectrum (Mixture of TMG-HCl and 45 in MeCN-d₃)



5.1.8 DFT Calculated Geometries and Thermo-chemical Data

Janus (45)



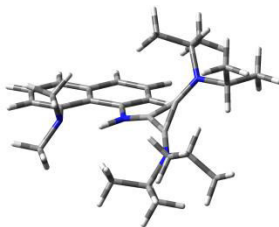
 # opt=calcf freq=norman b3lyp/6-31g(d,p) scrf=(iefpcm,solvent=acetonitrile)

Zero-point correction= 0.149572(Hartree/Particle)
 Thermal correction to Energy= 0.155088
 Thermal correction to Enthalpy= 0.155889
 Thermal correction to Gibbs Free Energy= 0.123748
 Sum of electronic and zero-point Energies= -343.174293
 Sum of electronic and thermal Energies= -343.168777
 Sum of electronic and thermal Enthalpies= -343.167976
 Sum of electronic and thermal Free Energies= -343.200117

0 1

N	0.67903400	-0.78532800	0.59414300	H	0.78994900	2.91255600	0.69141800
C	-0.49420400	-0.25378300	0.38829800	C	0.26036200	2.12904600	-1.97233500
N	-1.66967800	2.04167900	-0.37795100	H	-0.35280000	1.65220300	-2.74291500
C	-1.40261900	0.76794000	-0.00650100	H	0.85448600	1.35642600	-1.47663800
N	-2.87816300	-1.39740600	0.35973400	H	0.95256300	2.81940700	-2.46420400
C	-1.87295800	-0.50713900	0.24470000	C	-2.59849000	-2.71799200	0.97261300
C	1.75619300	-0.00203300	0.99576300	H	-3.56538500	-3.22702300	1.01298000
C	1.58594900	0.87242500	2.07823000	C	-1.64784700	-3.55541800	0.10679100
H	0.60418000	0.91174400	2.54081300	H	-2.04872200	-3.68841600	-0.90217800
C	2.62268300	1.67086900	2.58576600	H	-1.50550200	-4.54572100	0.55207800
H	2.43146400	2.32415500	3.43338300	H	-0.67090400	-3.06906900	0.03516300
C	3.86611000	1.63013500	1.99994000	C	-2.08131900	-2.57304200	2.41000700
H	4.67660400	2.25898200	2.35734000	H	-2.77222400	-1.98102700	3.01744000
C	4.10966900	0.76782000	0.89790300	H	-1.09957800	-2.08967800	2.42436400
C	5.38518600	0.82080000	0.26893200	H	-1.97741100	-3.56038600	2.87126600
H	6.12944700	1.50517800	0.66694300	C	-4.23125800	-1.09354500	-0.15438400
C	5.65639600	0.04494000	-0.82825400	H	-4.14899400	-0.10603200	-0.61236300
H	6.62414900	0.09757700	-1.31968800	C	-4.66030000	-2.06984200	-1.25935200
C	4.68648200	-0.86075100	-1.30177300	H	-3.92705900	-2.08695900	-2.07066800
C	3.43437100	-0.98476600	-0.70855700	H	-5.62419800	-1.75856300	-1.67399800
C	3.07889400	-0.11654000	0.39922900	H	-4.77964200	-3.08957800	-0.87980900
C	-3.08220300	2.48134700	-0.46413500	C	-5.26638700	-1.00850300	0.97593700
H	-3.64302500	1.75269000	0.12707300	H	-4.96357600	-0.27412400	1.72811200
C	-3.29852300	3.84791000	0.19922600	H	-5.39921500	-1.97427000	1.47447400
H	-2.94742700	3.83924100	1.23469900	H	-6.23895800	-0.70863300	0.57325000
H	-4.36612800	4.08853300	0.20034100	N	2.52646900	-1.96353700	-1.19659000
H	-2.78228500	4.65110800	-0.33560500	H	4.94663500	-1.50586400	-2.13212100
C	-3.61858800	2.45249600	-1.90403200	C	2.33691400	-3.10155600	-0.29510800
H	-3.48277200	1.46554800	-2.35676400	H	3.23558100	-3.74328000	-0.25566800
H	-3.11208800	3.18864300	-2.53679300	H	2.09422700	-2.75389200	0.70673900
H	-4.68726800	2.68956800	-1.91372200	H	1.49950200	-3.71029500	-0.64977600
C	-0.61408400	2.89953200	-0.97545300	C	2.71339600	-2.41157300	-2.57008200
H	-1.15854500	3.65940400	-1.54382400	H	2.83041700	-1.55280200	-3.23567600
C	0.22096900	3.62395200	0.08808700	H	3.57987700	-3.08198500	-2.71432800
H	-0.41701000	4.20947600	0.75571900	H	1.82071900	-2.96648600	-2.87713481
H	0.92852300	4.30739700	-0.39376000				

Janus•H⁺ (49_{opt})

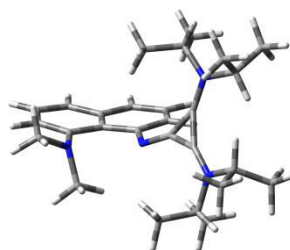


 # opt=calcfc freq=noraman b3lyp/6-31g(d,p) scrf=(iefpcm,solvent=acetonitrile)

Zero-point correction= 0.638390 (Hartree/Particle)
 Thermal correction to Energy= 0.672513
 Thermal correction to Enthalpy= 0.673457
 Thermal correction to Gibbs Free Energy= 0.572796
 Sum of electronic and zero-point Energies= -1271.808994
 Sum of electronic and thermal Energies= -1271.774871
 Sum of electronic and thermal Enthalpies= -1271.773927
 Sum of electronic and thermal Free Energies= -1271.874588

1 1							
N	-0.80857000	-0.40089000	-0.31986300	H	0.13596200	4.76895900	0.66069200
H	-1.18747800	-1.27371200	0.10359100	H	-0.25130400	3.43659200	-0.43363800
C	0.50231200	-0.10692800	-0.22697600	C	0.31722000	2.37309100	2.08317200
N	2.08128800	1.93374900	0.35395500	H	0.84721200	1.71505200	2.77744000
C	1.57039200	0.74423400	0.04535700	H	-0.48849600	1.80649400	1.60813200
N	2.59289000	-1.66007400	-0.41596600	H	-0.14515400	3.17851200	2.66046600
C	1.79091000	-0.61778000	-0.24642500	C	2.03468100	-2.94258900	-0.93714900
C	-1.83164400	0.47621400	-0.72041400	H	2.90949900	-3.56672100	-1.13108600
C	-1.55337800	1.53997400	-1.56138500	C	1.17151700	-3.65055800	0.11334600
H	-0.54019900	1.67410400	-1.92482000	H	1.73258500	-3.82835600	1.03378600
C	-2.56861600	2.42767500	-1.97332800	H	0.83314800	-4.61549600	-0.27527300
H	-2.31459100	3.25715600	-2.62573000	H	0.28253200	-3.06447500	0.36440800
C	-3.86465700	2.23395800	-1.56199800	C	1.30204400	-2.73841000	-2.26720200
H	-4.65404200	2.91144400	-1.87263200	H	1.94736600	-2.24263800	-2.99742800
C	-4.20246600	1.12679000	-0.73668300	H	0.39422300	-2.14089900	-2.14258400
C	-5.55283800	0.92079500	-0.34824100	H	1.00725800	-3.71031500	-2.67304400
H	-6.30205100	1.63039900	-0.68694400	C	4.04617500	-1.56721900	-0.10350400
C	-5.90790100	-0.15361900	0.43064300	H	4.17869900	-0.58143300	0.34378000
H	-6.94188200	-0.30632500	0.72361100	C	4.46654900	-2.60236900	0.94628000
C	-4.92191400	-1.07194100	0.84714800	H	3.86104400	-2.51153200	1.85203100
C	-3.59393400	-0.91771900	0.49559800	H	5.51323800	-2.43474800	1.21585200
C	-3.18463700	0.20564500	-0.30063300	H	4.38444500	-3.62675600	0.57094500
C	3.55953300	2.12189100	0.25481100	C	4.89699200	-1.63894900	-1.37675100
H	3.90362900	1.31025900	-0.38984100	H	4.59962700	-0.86747400	-2.09264500
C	3.92103900	3.43276600	-0.45101100	H	4.81440700	-2.61424500	-1.86641500
H	3.44663300	3.49622000	-1.43364500	H	5.94991800	-1.48555500	-1.12299700
H	5.00502100	3.47167600	-0.59179200	N	-2.61632300	-1.90943100	0.92613200
H	3.63515400	4.31036500	0.13591800	H	-5.21562600	-1.92264600	1.45329700
C	4.24457300	1.99023400	1.62143300	C	-2.97569200	-3.28812700	0.55267300
H	3.98100400	1.04787800	2.11056400	H	-3.84520700	-3.67331500	1.10381200
H	3.97216900	2.81024400	2.29273100	H	-3.19144100	-3.33086800	-0.51687800
H	5.33050500	2.01804000	1.49201000	H	-2.12508600	-3.94199400	0.76429400
C	1.27553200	2.98153700	1.05534600	C	-2.30926600	-1.79406000	2.36400500
H	2.01938700	3.55969100	1.60928700	H	-1.96677200	-0.78000300	2.58408500
C	0.56381000	3.93738200	0.09187800	H	-3.18091800	-2.01413800	2.99727700
H	1.25229000	4.35154700	-0.64771800	H	-1.50972200	-2.49598500	2.61733300

Janus (45)

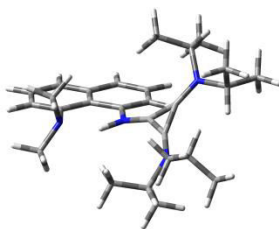


 # opt=calcf freq=noraman b3lyp/6-31g(d,p)

Zero-point correction= 0.624512 (Hartree/Particle)
 Thermal correction to Energy= 0.658769
 Thermal correction to Enthalpy= 0.659713
 Thermal correction to Gibbs Free Energy= 0.557923
 Sum of electronic and zero-point Energies= -1271.318138
 Sum of electronic and thermal Energies= -1271.283881
 Sum of electronic and thermal Enthalpies= -1271.282937
 Sum of electronic and thermal Free Energies= -1271.384727

0 1				H	4.92432500	-2.71968700	-1.05520300
C	-4.32082400	-0.81612500	-1.58884600	H	3.88185700	-1.81849700	-2.17076100
C	-3.13996700	-0.99162800	-0.87971900	H	5.56893400	-1.32626600	-1.92568900
C	-2.98088100	-0.35418700	0.41280000	C	5.36807100	-0.57810400	0.74185000
C	-4.11749600	0.37066200	0.93388700	H	6.26871500	-0.18686500	0.25712800
C	-5.31132600	0.48858800	0.17025400	H	5.05996600	0.12713500	1.51931000
C	-5.40158000	-0.07110200	-1.07668000	H	5.64076800	-1.52056200	1.22801400
H	-4.43389800	-1.29411400	-2.55462800	C	2.78226000	4.03394000	0.35147500
C	-1.75865500	-0.31885300	1.19067800	H	3.80913400	4.41325200	0.32348500
C	-4.05545400	1.01222700	2.19799500	H	2.13806100	4.80263400	-0.08687100
H	-6.14125700	1.04850900	0.59254000	H	2.49246200	3.89978000	1.39709100
H	-6.30885100	0.03040600	-1.66606800	C	3.14730900	2.85278800	-1.87425200
C	-2.89619100	0.98836700	2.93448800	H	2.50936000	3.55301100	-2.42338000
C	-1.76272400	0.33468100	2.42457300	H	4.17214800	3.23617900	-1.92119500
H	-4.93945400	1.52897300	2.56097000	H	3.11570600	1.89029500	-2.39384400
H	-2.84519300	1.47794600	3.90352500	C	-0.58919000	2.02888400	-1.86279700
H	-0.84259300	0.31613100	3.00056000	H	-1.42277400	2.62338200	-2.24970000
N	-0.58178200	-0.98572600	0.82292800	H	0.07137300	1.77793000	-2.69880000
C	0.48688700	-0.33540600	0.50606600	H	-1.00091300	1.09985200	-1.46033400
C	1.87793400	-0.42502900	0.27402200	C	-0.75044300	3.27745200	0.35337400
C	1.25881900	0.78492500	0.06916000	H	-1.17217000	2.42273400	0.88687500
N	2.98459300	-1.20286100	0.33891900	H	-0.20209300	3.89391000	1.07186900
N	1.35686800	2.08933000	-0.29504900	H	-1.58125600	3.87103500	-0.04274600
C	2.87611600	-2.53041700	0.98777600	H	0.56845800	3.72192400	-1.27044400
C	4.24779900	-0.77887900	-0.29010700	H	3.37205700	2.00746000	0.08552300
C	2.69232800	2.70482300	-0.41290200	H	4.03042200	0.19238600	-0.74238100
C	0.16627900	2.82398000	-0.78969100	H	3.88839700	-2.94635400	0.96658400
C	1.94602400	-3.47458700	0.21318500	N	-2.09930300	-1.78615800	-1.43687100
H	2.26500700	-3.57713400	-0.82836300	C	-2.07050300	-1.91092600	-2.88483800
H	1.95062400	-4.46921100	0.67205100	H	-1.09972600	-2.32620100	-3.17746500
H	0.92050700	-3.09523000	0.23256600	H	-2.84812400	-2.57876900	-3.30121900
C	2.44267400	-2.39979600	2.45448100	H	-2.17861600	-0.92795300	-3.35023800
H	2.46534000	-3.37961400	2.94286500	C	-1.92334800	-3.08699300	-0.79121700
H	3.10806700	-1.72663300	3.00356800	H	-0.98791700	-3.53839600	-1.13732000
H	1.41996400	-2.01614600	2.51876600	H	-1.85488000	-2.96699800	0.28783500
C	4.67723100	-1.72002900	-1.42675400	H	-2.75146500	-3.77786700	-1.03352300

Janus•HCl (49)

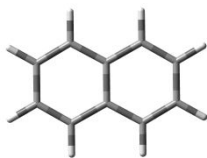


 # opt=calcfreq=noraman b3lyp/6-31g(d,p)

Zero-point correction= 0.638627 (Hartree/Particle)
 Thermal correction to Energy= 0.672981
 Thermal correction to Enthalpy= 0.673925
 Thermal correction to Gibbs Free Energy= 0.571731
 Sum of electronic and zero-point Energies= -1271.752049
 Sum of electronic and thermal Energies= -1271.717696
 Sum of electronic and thermal Enthalpies= -1271.716752
 Sum of electronic and thermal Free Energies= -1271.818946

1	1			C	4.77188000	1.30169000	-1.17078500
C	-4.88154300	1.01431300	0.96248500	H	5.82444600	1.49840800	-0.94703200
C	-3.57640400	0.88983400	0.52763700	H	4.63956000	0.21764300	-1.21916200
C	-3.19331600	-0.21911900	-0.29795400	H	4.55398900	1.70692300	-2.16168800
C	-4.22006100	-1.14541900	-0.69694400	C	4.22054100	1.52904200	1.32955900
C	-5.54631600	-0.97233800	-0.22223500	H	3.61137800	2.07967700	2.05165500
C	-5.87215900	0.07904500	0.59924100	H	4.06189300	0.46143100	1.49489500
H	-5.15674300	1.85894400	1.58648400	H	5.27240700	1.74217000	1.53910600
C	-1.86082700	-0.47276500	-0.78069000	C	3.97995800	-3.21852900	-0.63188200
C	-3.91239100	-2.22260900	-1.57154300	H	3.59002600	-3.02970800	-1.63572900
H	-6.30324600	-1.68765000	-0.52955400	H	5.07179300	-3.25696800	-0.69098100
H	-6.88847800	0.20576100	0.95772000	H	3.63715300	-4.20423800	-0.30456900
C	-2.64165000	-2.38288300	-2.06556400	C	4.13368400	-2.34912200	1.75245500
C	-1.61518300	-1.49740800	-1.67502500	H	5.22548400	-2.29537700	1.71077000
H	-4.70813000	-2.90285000	-1.85820600	H	3.78201500	-1.59572500	2.46280500
H	-2.41803900	-3.18337800	-2.76337800	H	3.87753400	-3.33628400	2.14731500
H	-0.62050100	-1.60113600	-2.09626100	C	0.18786400	-2.51423500	1.89549400
N	-2.59799300	1.91803200	0.87823100	H	-0.31137800	-3.36736600	2.36285700
N	-0.82092800	0.39348100	-0.38053300	H	0.65893400	-1.92314300	2.68630800
C	0.48422900	0.09359500	-0.26324100	H	-0.58565400	-1.90977000	1.41443900
C	1.75391300	0.64663600	-0.23593200	C	0.59508500	-3.88385900	-0.21227200
C	1.57305600	-0.73051300	0.03134300	H	-0.19299800	-3.34332400	-0.73785800
N	2.43237500	1.78101500	-0.40164900	H	1.33799100	-4.21743700	-0.93974500
N	2.08253000	-1.91616100	0.36327400	H	0.14201300	-4.77238400	0.23852200
C	1.65471800	2.96660600	-0.88366200	H	1.92604400	-3.65686800	1.43963200
C	3.88107000	1.95013600	-0.10320300	H	3.96228100	-1.17301200	-0.02552700
C	3.56081900	-2.11579700	0.34708800	H	4.04282800	3.02906500	-0.16331900
C	1.22418600	-3.02528000	0.89012300	H	0.65311500	2.58121800	-1.09227400
H	-1.20237600	1.25738300	0.07012300	C	-2.31522700	1.95888000	2.32381300
C	1.53829000	4.04020400	0.20522300	H	-3.18706300	2.26157200	2.92068600
H	0.88951400	4.84910700	-0.14364900	H	-1.99540300	0.96958900	2.65990200
H	1.11005400	3.62814300	1.12392500	H	-1.50811900	2.67375900	2.51280800
H	2.50683700	4.48677500	0.45007800	C	-2.95751000	3.24700600	0.35074500
C	2.21666800	3.51984300	-2.19771000	H	-3.85632100	3.66875000	0.82210800
H	1.56408100	4.31767700	-2.56378900	H	-2.12629100	3.93687500	0.52798800
H	3.21465100	3.95016900	-2.07144800	H	-3.13333300	3.17594300	-0.72487000
H	2.26592000	2.74334200	-2.96572200				

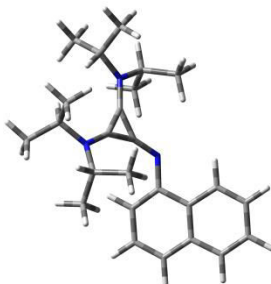
Naphthalene



opt=calcfreq=noraman b3lyp/6-31g(d,p)

Zero-point correction=				0.147645 (Hartree/Particle)			
Thermal correction to Energy=				0.154448			
Thermal correction to Enthalpy=				0.155392			
Thermal correction to Gibbs Free Energy=				0.116449			
Sum of electronic and zero-point Energies=				-385.757742			
Sum of electronic and thermal Energies=				-385.750938			
Sum of electronic and thermal Enthalpies=				-385.749994			
Sum of electronic and thermal Free Energies=				-385.788937			
0 1				H	1.24210000	-2.48938900	0.00002400
C	-1.24468100	1.40245200	-0.00001600	C	2.43304100	-0.70835400	0.00001800
C	-2.43304200	0.70835200	-0.00001000	H	3.37718000	-1.24499500	0.00003100
H	-3.37718200	1.24499200	-0.00001900	C	2.43304100	0.70835200	0.00000500
C	-2.43304100	-0.70835400	0.00000000	C	1.24468200	1.40245100	-0.00000900
H	-3.37718100	-1.24499500	0.00000400	C	0.00000000	0.71680100	-0.00000900
C	-1.24468000	-1.40245100	0.00000400	H	3.37718100	1.24499200	0.00000400
H	-1.24210000	-2.48938900	0.00001000	H	-1.24210200	2.48939400	-0.00002400
C	0.00000000	-0.71679900	0.00000200	H	1.24210400	2.48939300	-0.00002300
C	1.24468000	-1.40245100	0.00001500				

Janus lacking dimethylamino group

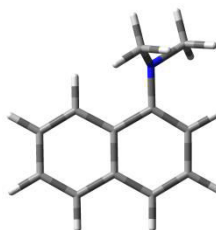


opt=calcfreq=noraman b3lyp/6-31g(d,p)

Zero-point correction=				0.551898 (Hartree/Particle)			
Thermal correction to Energy=				0.581952			
Thermal correction to Enthalpy=				0.582896			
Thermal correction to Gibbs Free Energy=				0.490337			
Sum of electronic and zero-point Energies=				-1137.434806			
Sum of electronic and thermal Energies=				-1137.404753			
Sum of electronic and thermal Enthalpies=				-1137.403809			
Sum of electronic and thermal Free Energies=				-1137.496368			
0 1				C	-1.13502300	0.65944700	0.02517400
N	0.94415100	-0.99007200	0.32039400	N	-2.57638500	-1.56251100	0.16737500
C	-0.21075600	-0.40564100	0.23175000	C	-1.59652000	-0.63621400	0.12010900
N	-1.41728000	1.97694600	-0.14795800	C	2.10036200	-0.29652300	0.66565200

C	2.15832000	0.60833200	1.72344400	H	1.14653000	2.75960500	0.79355100
H	1.25251100	0.80968100	2.28825200	C	0.39858700	2.25264500	-1.85703400
C	3.37118000	1.22494300	2.10200600	H	-0.26218400	1.84199600	-2.62672000
H	3.37018600	1.92191800	2.93644600	H	1.03973600	1.44880200	-1.48699100
C	4.54536500	0.94650700	1.44003100	H	1.04475400	3.00165900	-2.32536600
H	5.47836700	1.41913700	1.73446100	C	-2.20488700	-2.95988900	0.50455500
C	4.54817900	0.01834000	0.36380700	H	-3.14797600	-3.51522300	0.49830300
C	5.73854200	-0.30564600	-0.34254900	C	-1.27198900	-3.57227100	-0.55038200
H	6.66635600	0.17600000	-0.04319900	H	-1.71011700	-3.50719500	-1.55097400
C	5.72776900	-1.20932500	-1.38121400	H	-1.09391600	-4.62886800	-0.32375200
H	6.64875700	-1.44469800	-1.90776400	H	-0.30594600	-3.05780200	-0.55034600
C	4.51862300	-1.83578100	-1.76445400	C	-1.59985800	-3.05553000	1.91171400
C	3.34607900	-1.54270600	-1.10216300	H	-2.26572000	-2.61295000	2.65884300
C	3.32405400	-0.61572300	-0.02884300	H	-0.63313400	-2.54489500	1.94990700
C	-2.82985300	2.40743800	-0.09304300	H	-1.43510800	-4.10492700	2.17731300
H	-3.34698300	1.61235700	0.45255800	C	-3.96853800	-1.22400500	-0.18018700
C	-3.00777200	3.69229600	0.72792200	H	-3.94916000	-0.16317100	-0.44134400
H	-2.58690200	3.57491800	1.73002300	C	-4.46128900	-1.98621100	-1.42021900
H	-4.07306200	3.92488500	0.82665900	H	-3.79451500	-1.81774500	-2.27058400
H	-2.52820300	4.55349000	0.25230400	H	-5.46469100	-1.64628900	-1.69682400
C	-3.46780600	2.52685500	-1.48740700	H	-4.51871300	-3.06421600	-1.23931600
H	-3.35885800	1.59497100	-2.05043200	C	-4.91678700	-1.39534300	1.01612900
H	-3.00714000	3.32948200	-2.07246300	H	-4.57094300	-0.81098600	1.87375400
H	-4.53577700	2.75463100	-1.40321400	H	-4.98974900	-2.44271600	1.32643700
C	-0.40753800	2.90265400	-0.72544900	H	-5.92554500	-1.06001700	0.75345100
H	-0.99429100	3.71329600	-1.17031400	H	4.51782200	-2.55034300	-2.58296400
C	0.50264900	3.51913000	0.34429200	H	2.41147700	-2.01656500	-1.38066000
H	-0.08395400	3.99194600	1.13685100				
H	1.14614200	4.28261800	-0.10640300				

Janus lacking cyclopropenimine substitution



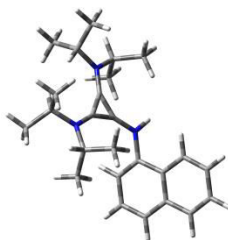
opt=calcfreq=noraman b3lyp/6-31g(d,p)

Zero-point correction= 0.220818 (Hartree/Particle)
Thermal correction to Energy= 0.231666
Thermal correction to Enthalpy= 0.232610
Thermal correction to Gibbs Free Energy= 0.184741
Sum of electronic and zero-point Energies= -519.653547
Sum of electronic and thermal Energies= -519.642699
Sum of electronic and thermal Enthalpies= -519.641755
Sum of electronic and thermal Free Energies= -519.689624

0 1				C	1.11781900	2.16097800	0.15205700
C	0.74627300	-1.54841300	-0.26719800	H	1.92136100	2.88541300	0.25200200
C	2.06445700	-1.94914300	-0.25313800	C	-0.19267700	2.56726200	0.09106700
H	2.31396000	-2.99514700	-0.40647300	H	-0.44071900	3.62354200	0.14485400
C	3.09765100	-1.00332000	-0.05820900	C	-1.23874400	1.62025300	-0.01147900
H	4.13345800	-1.32983400	-0.04180700	C	-0.97546800	0.26268600	-0.07403700
C	2.78989800	0.33034100	0.08551800	C	0.39246000	-0.18519000	-0.08164100
H	3.57968100	1.06693500	0.20918700	N	-2.00760100	-0.71559100	-0.15669500
C	1.44208300	0.77991600	0.06369700	H	-2.26416800	1.97325100	-0.01637800

C	-3.26984900	-0.27908300	-0.73564500	H	-1.26672800	-1.81166400	1.48733700
H	-3.86608600	0.37063800	-0.06978400	H	-2.74206700	-0.89013400	1.84864300
H	-3.08477000	0.25869000	-1.66853500	H	-2.82761900	-2.36597800	0.85499900
H	-3.87770300	-1.16174700	-0.96048200	H	-0.04406400	-2.26629000	-0.45437400
C	-2.22079200	-1.48104400	1.07528800				

Protonated Janus lacking dimethylamino group

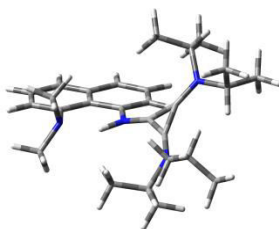


 # opt=calcfc freq=norman b3lyp/6-31g(d,p)

Zero-point correction= 0.565971 (Hartree/Particle)
 Thermal correction to Energy= 0.596303
 Thermal correction to Enthalpy= 0.597248
 Thermal correction to Gibbs Free Energy= 0.504521
 Sum of electronic and zero-point Energies= -1137.855786
 Sum of electronic and thermal Energies= -1137.825453
 Sum of electronic and thermal Enthalpies= -1137.824509
 Sum of electronic and thermal Free Energies= -1137.917236

1 1				C	-0.02554800	2.81846600	-0.56530400
N	0.86501200	-1.13551800	0.26309300	H	-0.48469300	3.73114400	-0.95325000
H	0.82314900	-2.14411300	0.18474400	C	0.85638600	3.20142700	0.62717400
C	-0.31020500	-0.49094400	0.17451700	H	0.27269500	3.67438500	1.42039800
N	-1.19176200	1.97153600	-0.16206400	H	1.62303400	3.91138100	0.30248300
C	-1.07634900	0.65525300	-0.00654700	H	1.36640800	2.32964200	1.04258600
N	-2.75666000	-1.40017000	0.08720800	C	0.76883500	2.18414500	-1.71114600
C	-1.68811200	-0.60738000	0.08899800	H	0.11882500	1.93710400	-2.55547900
C	2.10570600	-0.57329500	0.72114400	H	1.29595500	1.27925400	-1.39694900
C	2.17000700	0.03201800	1.95901300	H	1.52499200	2.89165700	-2.06232900
H	1.27722500	0.09206700	2.57420000	C	-2.59604000	-2.84534600	0.42063600
C	3.39637400	0.54744800	2.43813100	H	-3.61512200	-3.23635600	0.45974500
H	3.43007900	1.02409200	3.41217700	C	-1.84649300	-3.60298200	-0.68244300
C	4.54034400	0.41588100	1.68548600	H	-2.34491200	-3.49617800	-1.64872600
H	5.48800700	0.79338300	2.05814800	H	-1.79681100	-4.66806200	-0.43935300
C	4.51082400	-0.21944800	0.41522300	H	-0.81791000	-3.24393500	-0.79874900
C	5.68443400	-0.36972700	-0.37056800	C	-1.97354900	-3.03937700	1.80776100
H	6.62483300	0.00646000	0.02156500	H	-2.54462900	-2.50816200	2.57368900
C	5.63675900	-0.97913800	-1.60333800	H	-0.93887700	-2.68392100	1.84674000
H	6.54133000	-1.08944300	-2.19265300	H	-1.96524600	-4.10225900	2.06459800
C	4.40673700	-1.45955000	-2.11140800	C	-4.10513900	-0.86638400	-0.25666800
C	3.24782300	-1.33195700	-1.37795900	H	-3.93197700	0.17273200	-0.54516900
C	3.26678100	-0.71938800	-0.09645800	C	-4.70711500	-1.58292700	-1.47148700
C	-2.54765400	2.59272300	-0.09905700	H	-4.03524200	-1.53756700	-2.33294000
H	-3.18760100	1.82825700	0.34963000	H	-5.64766800	-1.09833400	-1.74830400
C	-2.57691400	3.80417000	0.83962100	H	-4.93440200	-2.63239200	-1.26171800
H	-2.21739900	3.54160700	1.83786100	C	-5.03896200	-0.88263900	0.95904900
H	-3.60653000	4.16109600	0.93211500	H	-4.60480400	-0.33566900	1.80101900
H	-1.97807100	4.63717000	0.46074000	H	-5.25765100	-1.90274100	1.28977400
C	-3.08313300	2.92196900	-1.49819400	H	-5.99292400	-0.41372600	0.70126000
H	-3.09276400	2.03657000	-2.14133800	H	4.37788600	-1.92896300	-3.08978500
H	-2.48188200	3.69203100	-1.99098800	H	2.30770700	-1.69097100	-1.78356600
H	-4.10590000	3.30372600	-1.42690000				

49_{opt} Acetonitrile

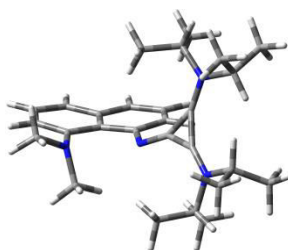


 # opt=calcf freq=noraman b3lyp/6-31g(d,p) scrf=(iefpcm,solvent=acetonitrile)

Zero-point correction= 0.638390 (Hartree/Particle)
 Thermal correction to Energy= 0.672513
 Thermal correction to Enthalpy= 0.673457
 Thermal correction to Gibbs Free Energy= 0.572796
 Sum of electronic and zero-point Energies= -1271.808994
 Sum of electronic and thermal Energies= -1271.774871
 Sum of electronic and thermal Enthalpies= -1271.773927
 Sum of electronic and thermal Free Energies= -1271.874588

l 1

N	-0.80857000	-0.40089000	-0.31986300	C	-4.92191400	-1.07194100	0.84714800
H	-0.14515400	3.17851200	2.66046600	C	-3.59393400	-0.91771900	0.49559800
C	2.03468100	-2.94258900	-0.93714900	C	-3.18463700	0.20564500	-0.30063300
H	2.90949900	-3.56672100	-1.13108600	C	3.55953300	2.12189100	0.25481100
C	1.17151700	-3.65055800	0.11334600	H	3.90362900	1.31025900	-0.38984100
H	1.73258500	-3.82835600	1.03378600	C	3.92103900	3.43276600	-0.45101100
H	0.83314800	-4.61549600	-0.27527300	H	3.44663300	3.49622000	-1.43364500
H	0.28253200	-3.06447500	0.36440800	H	5.00502100	3.47167600	-0.59179200
C	1.30204400	-2.73841000	-2.26720200	H	3.63515400	4.31036500	0.13591800
H	1.94736600	-2.24263800	-2.99742800	C	4.24457300	1.99023400	1.62143300
H	0.39422300	-2.14089900	-2.14258400	H	3.98100400	1.04787800	2.11056400
H	1.00725800	-3.71031500	-2.67304400	H	3.97216900	2.81024400	2.29273100
C	4.04617500	-1.56721900	-0.10350400	C	5.33050500	2.01804000	1.49201000
H	4.17869900	-0.58143300	0.34378000	H	1.27553200	2.98153700	1.05534600
C	4.46654900	-2.60236900	0.94628000	H	2.01938700	3.55969100	1.60928700
H	3.86104400	-2.51153200	1.85203100	C	0.56381000	3.93738200	0.09187800
H	5.51323800	-2.43474800	1.21585200	H	1.25229000	4.35154700	-0.64771800
H	4.38444500	-3.62675600	0.57094500	H	0.13596200	4.76895900	0.66069200
C	4.89699200	-1.63894900	-1.37675100	H	-0.25130400	3.43659200	-0.43363800
H	4.59962700	-0.86747400	-2.09264500	H	-1.18747800	-1.27371200	0.10359100
H	4.81440700	-2.61424500	-1.86641500	C	0.31722000	2.37309100	2.08317200
H	5.94991800	-1.48555500	-1.12299700	C	0.50231200	-0.10692800	-0.22697600
N	2.59289000	-1.66007400	-0.41596600	H	0.84721200	1.71505200	2.77744000
C	1.79091000	-0.61778000	-0.24642500	N	2.08128800	1.93374900	0.35395500
C	-1.83164400	0.47621400	-0.72041400	H	-0.48849600	1.80649400	1.60813200
C	-1.55337800	1.53997400	-1.56138500	C	1.57039200	0.74423400	0.04535700
H	-0.54019900	1.67410400	-1.92482000	N	-2.61632300	-1.90943100	0.92613200
C	-2.56861600	2.42767500	-1.97332800	H	-5.21562600	-1.92264600	1.45329700
H	-2.31459100	3.25715600	-2.62573000	C	-2.97569200	-3.28812700	0.55267300
C	-3.86465700	2.23395800	-1.56199800	H	-3.84520700	-3.67331500	1.10381200
H	-4.65404200	2.91144400	-1.87263200	H	-3.19144100	-3.33086800	-0.51687800
C	-4.20246600	1.12679000	-0.73668300	H	-2.12508600	-3.94199400	0.76429400
C	-5.55283800	0.92079500	-0.34824100	C	-2.30926600	-1.79406000	2.36400500
H	-6.30205100	1.63039900	-0.68694400	H	-1.96677200	-0.78000300	2.58408500
C	-5.90790100	-0.15361900	0.43064300	H	-3.18091800	-2.01413800	2.99727700
H	-6.94188200	-0.30632500	0.72361100	H	-1.50972200	-2.49598500	2.61733300

45_{opt} Acetonitrile

 # opt=calcf freq=noraman b3lyp/6-31g(d,p) scrf=(iefpcm,solvent=acetonitrile)

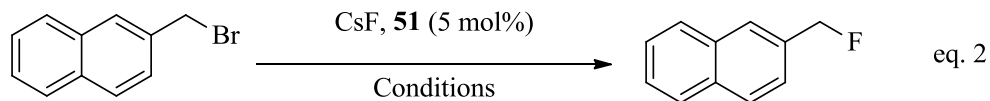
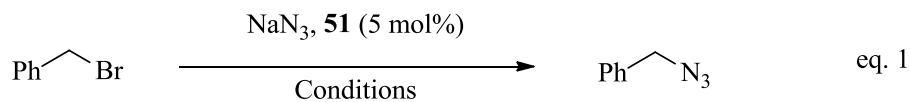
Zero-point correction= 0.149572 (Hartree/Particle)
 Thermal correction to Energy= 0.155088
 Thermal correction to Enthalpy= 0.155889
 Thermal correction to Gibbs Free Energy= 0.123748
 Sum of electronic and zero-point Energies= -343.174293
 Sum of electronic and thermal Energies= -343.168777
 Sum of electronic and thermal Enthalpies= -343.167976
 Sum of electronic and thermal Free Energies= -343.200117

0 1

N	0.67903400	-0.78532800	0.59414300	C	0.26036200	2.12904600	-1.97233500
C	-0.49420400	-0.25378300	0.38829800	H	-0.35280000	1.65220300	-2.74291500
N	-1.66967800	2.04167900	-0.37795100	H	0.85448600	1.35642600	-1.47663800
C	-1.40261900	0.76794000	-0.00650100	H	0.95256300	2.81940700	-2.46420400
N	-2.87816300	-1.39740600	0.35973400	C	-2.59849000	-2.71799200	0.97261300
C	-1.87295800	-0.50713900	0.24470000	H	-3.56538500	-3.22702300	1.01298000
C	1.75619300	-0.00203300	0.99576300	C	-1.64784700	-3.55541800	0.10679100
C	1.58594900	0.87242500	2.07823000	H	-2.04872200	-3.68841600	-0.90217800
H	0.60418000	0.91174400	2.54081300	H	-1.50550200	-4.54572100	0.55207800
C	2.62268300	1.67086900	2.58576600	H	-0.67090400	-3.06906900	0.03516300
H	2.43146400	2.32415500	3.43338300	C	-2.08131900	-2.57304200	2.41000700
C	3.86611000	1.63013500	1.99994000	H	-2.77222400	-1.98102700	3.01744000
H	4.67660400	2.25898200	2.35734000	H	-1.09957800	-2.08967800	2.42436400
C	4.10966900	0.76782000	0.89790300	H	-1.97741100	-3.56038600	2.87126600
C	5.38518600	0.82080000	0.26893200	C	-4.23125800	-1.09354500	-0.15438400
H	6.12944700	1.50517800	0.66694300	H	-4.14899400	-0.10603200	-0.61236300
C	5.65639600	0.04494000	-0.82825400	C	-4.66030000	-2.06984200	-1.25935200
H	6.62414900	0.09757700	-1.31968800	H	-3.92705900	-2.08695900	-2.07066800
C	4.68648200	-0.86075100	-1.30177300	H	-5.62419800	-1.75856300	-1.67399800
C	3.43437100	-0.98476600	-0.70855700	H	-4.77964200	-3.08957800	-0.87980900
C	3.07889400	-0.11654000	0.39922900	C	-5.26638700	-1.00850300	0.97593700
C	-3.08220300	2.48134700	-0.46413500	H	-4.96357600	-0.27412400	1.72811200
H	-3.64302500	1.75269000	0.12707300	H	-5.39921500	-1.97427000	1.47447400
C	-3.29852300	3.84791000	0.19922600	H	-6.23895800	-0.70863300	0.57325000
H	-2.94742700	3.83924100	1.23469900	N	2.52646900	-1.96353700	-1.19659000
H	-4.36612800	4.08853300	0.20034100	H	4.94663500	-1.50586400	-2.13212100
H	-2.78228500	4.65110800	-0.33560500	C	2.33691400	-3.10155600	-0.29510800
C	-3.61858800	2.45249600	-1.90403200	H	3.23558100	-3.74328000	-0.25566800
H	-3.48277200	1.46554800	-2.35676400	H	2.09422700	-2.75389200	0.70673900
H	-3.11208800	3.18864300	-2.53679300	H	1.49950200	-3.71029500	-0.64977600
H	-4.68726800	2.68956800	-1.91372200	C	2.71339600	-2.41157300	-2.57008200
C	-0.61408400	2.89953200	-0.97545300	H	2.83041700	-1.55280200	-3.23567600
H	-1.15854500	3.65940400	-1.54382400	H	3.57987700	-3.08198500	-2.71432800
C	0.22096900	3.62395200	0.08808700	H	1.82071900	-2.96648600	-2.87718300
H	-0.41701000	4.20947600	0.75571900				
H	0.92852300	4.30739700	-0.39376000				
H	0.78994900	2.91255600	0.69141800				

5.2 Appendix B: DACN Proton Sponge Phase Transfer Catalysis

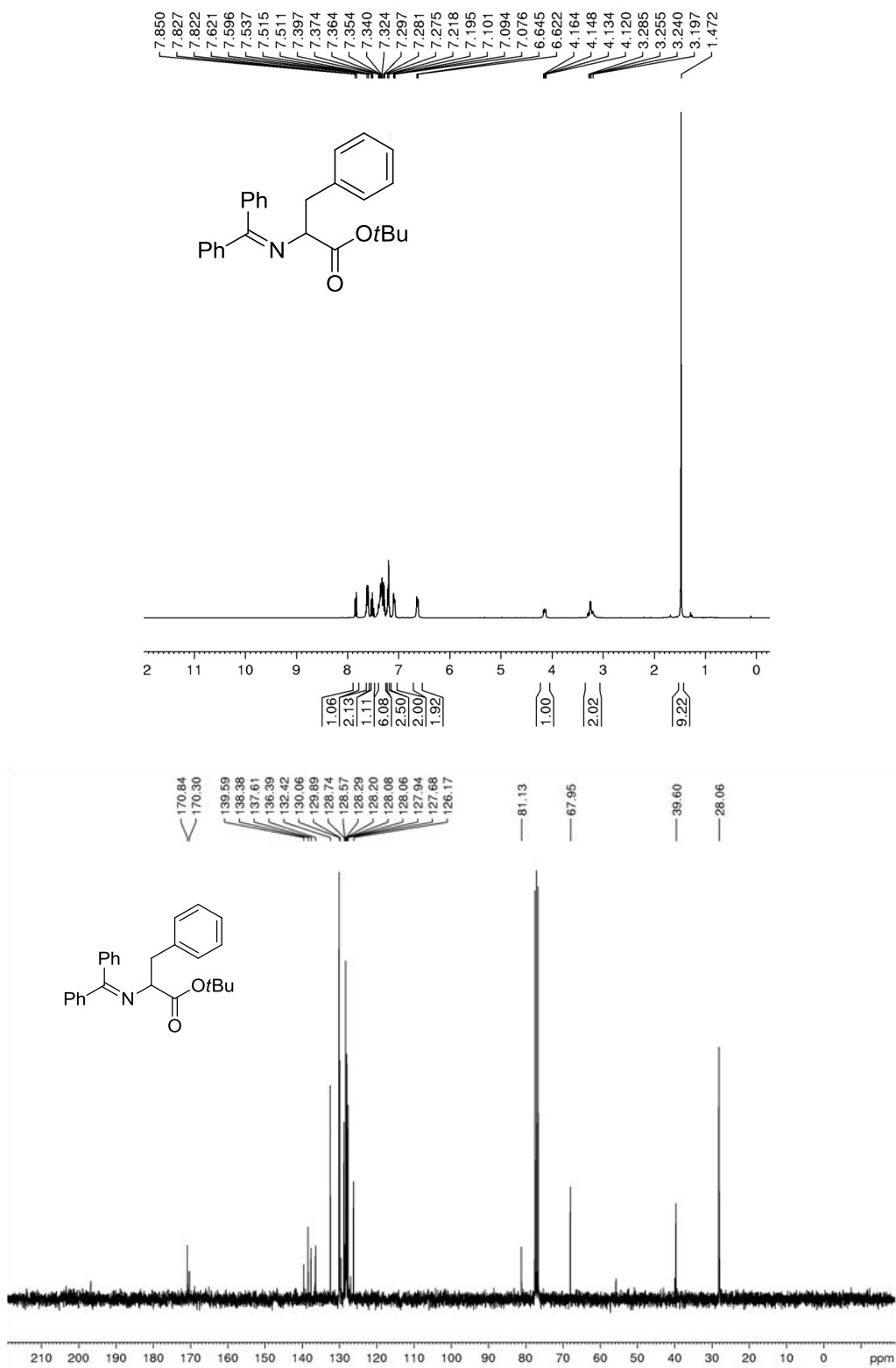
5.2.1 Results for the extraction-type phase transfer reactions



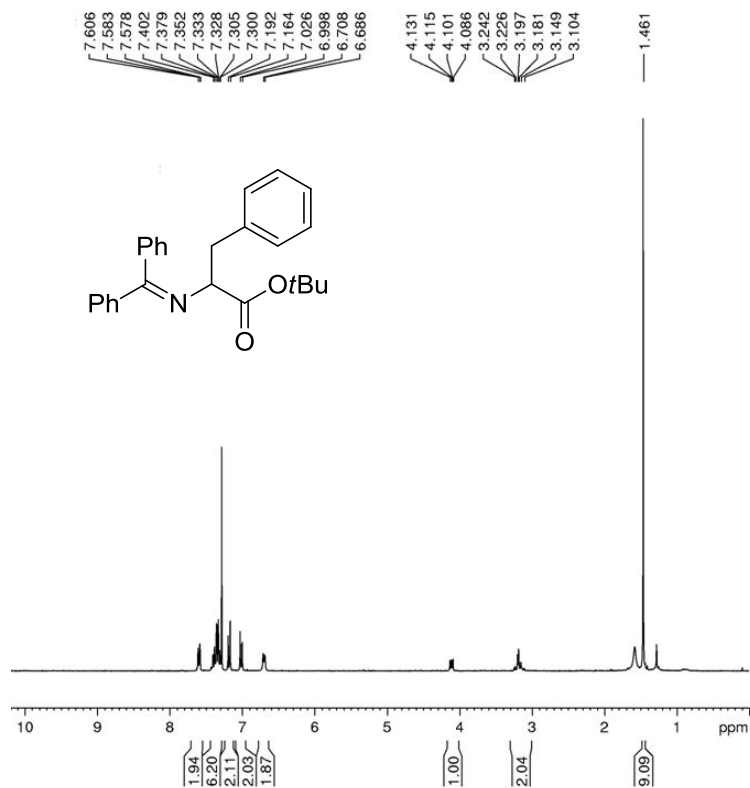
<u>Solvent</u>	<u>Nu</u>	<u>Temp.</u>	<u>Time</u>	<u>Yield</u>	<u>Control</u>
Toluene	CsF	r.t.	24 h	12 %	N. R.
Toluene	CsF	reflux	24 h	28 %	11 %
DCM	CsF	r.t.	24 h	14 %	Trace
MeCN	CsF	r.t.	16 h	3 %	Trace
MeCN	CsF	60 °C	14 h	68 %	32 %
MeCN	CsF	Reflux	5 h	17 %	6 %
MeCN	CsF	Reflux	14 h	86 %	58 %
MeCN	KF	Reflux	24 h	4 %	N. R.
MeCN	NaN ₃	r.t.	24 h	N.R.	N.R.
H ₂ O/DCM	NaN ₃	r.t.	24 h	N.R.	N.R.
H ₂ O/MeC N	NaN ₃	r.t.	24 h	N.R.	N.R.
H ₂ O	NaN ₃	r.t.	24 h	N.R.	N.R.
H ₂ O	NaN ₃	80 °C	24 h	N.R.	N.R.

5.2.2 Proton and Carbon NMR Spectra

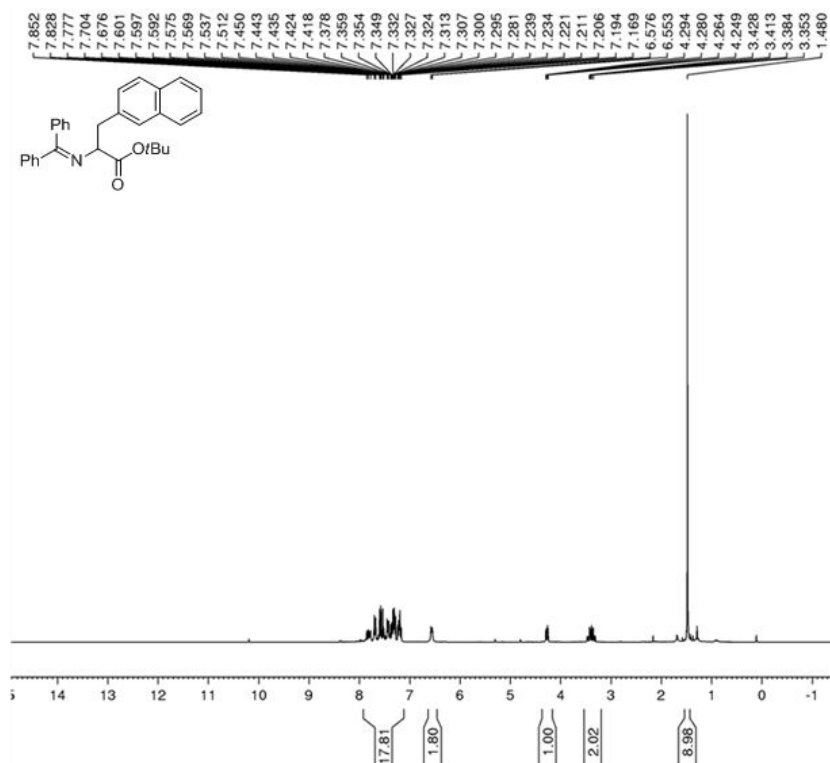
43a Proton and Carbon NMR spectra

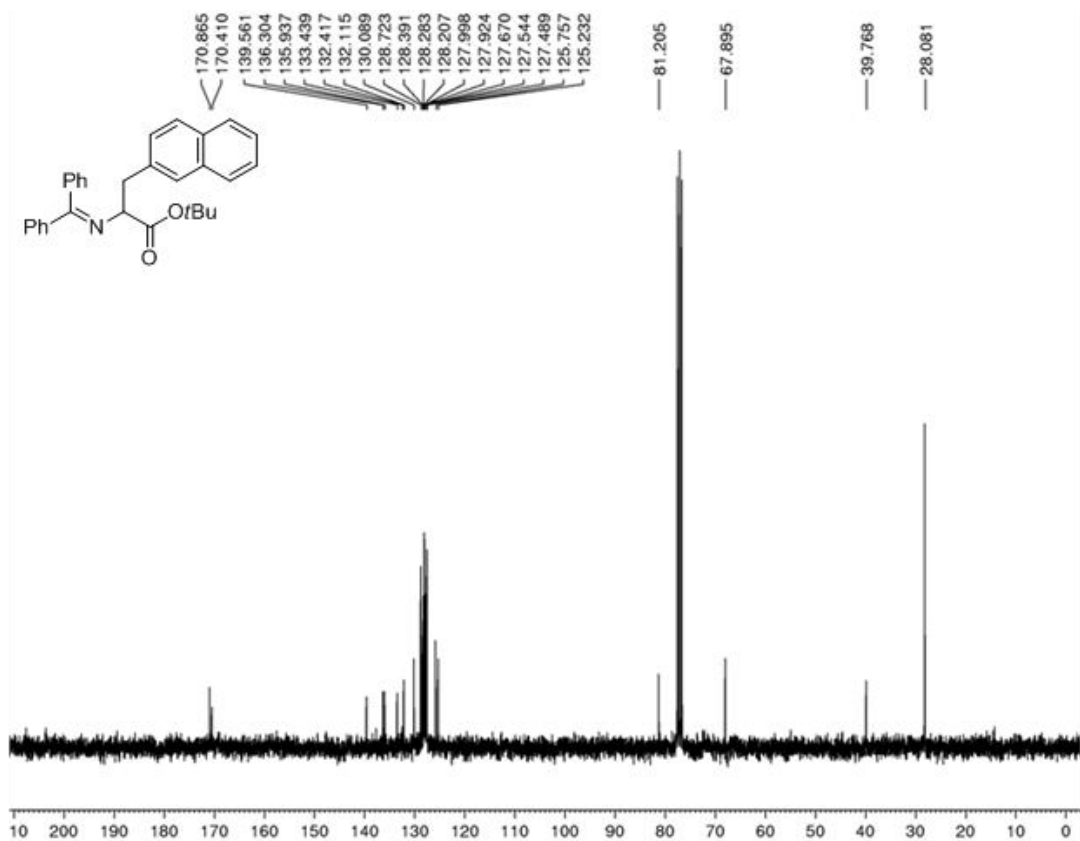


43d Proton NMR spectra

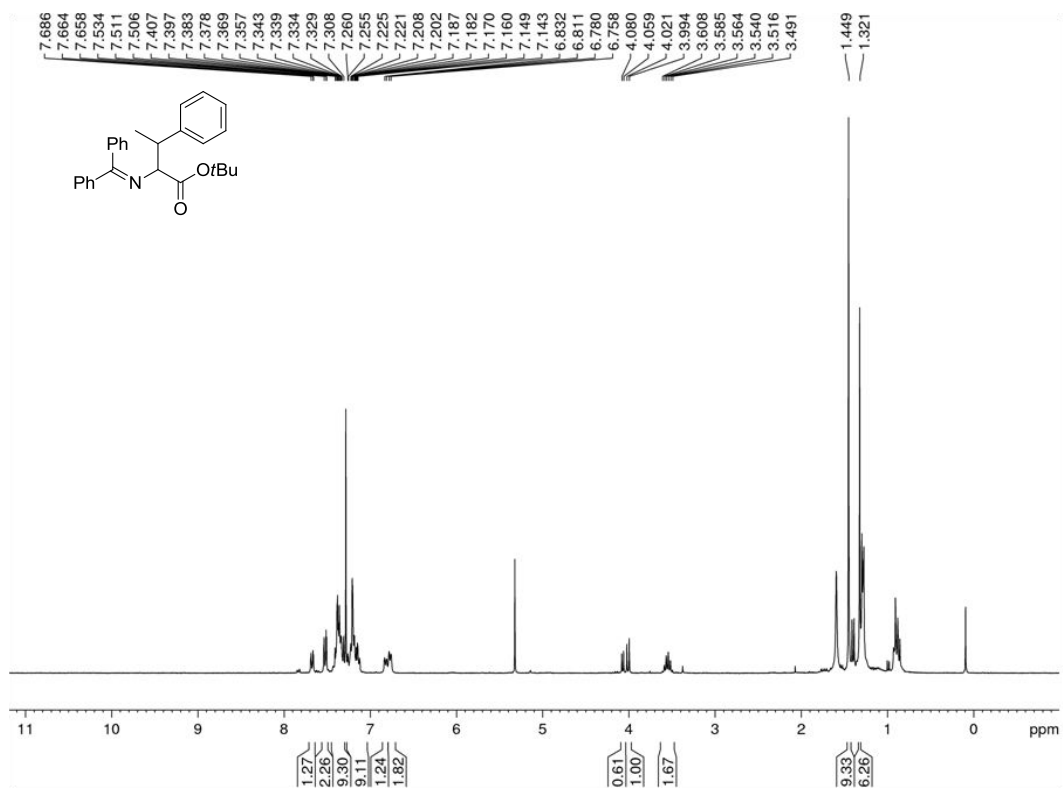


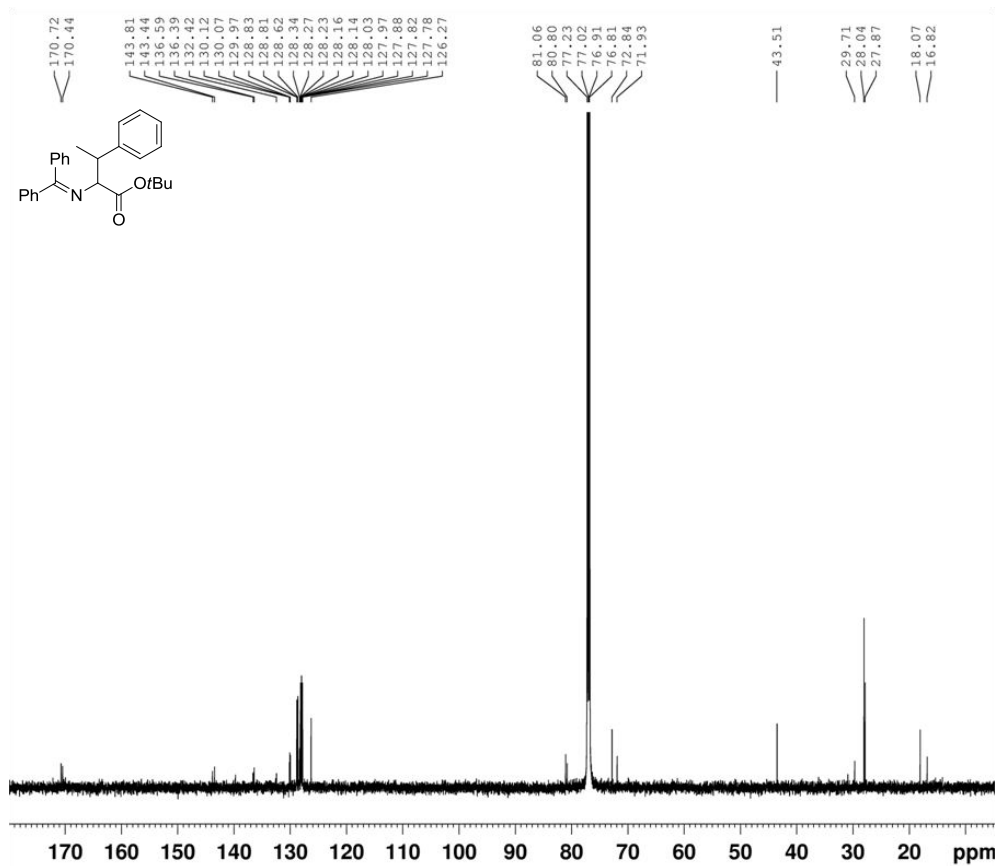
43b Proton and Carbon NMR spectra



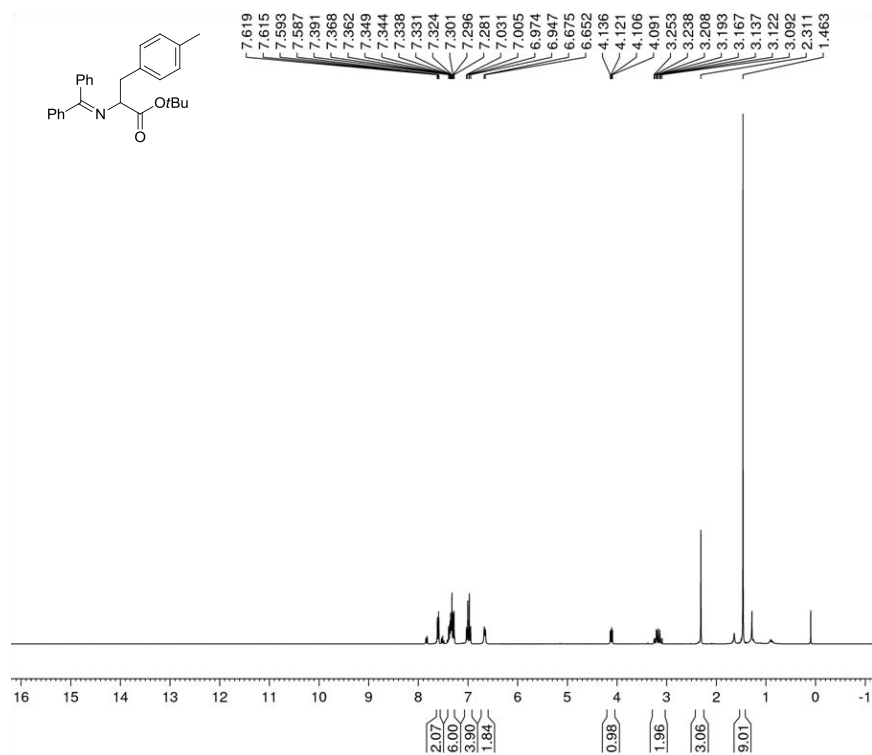


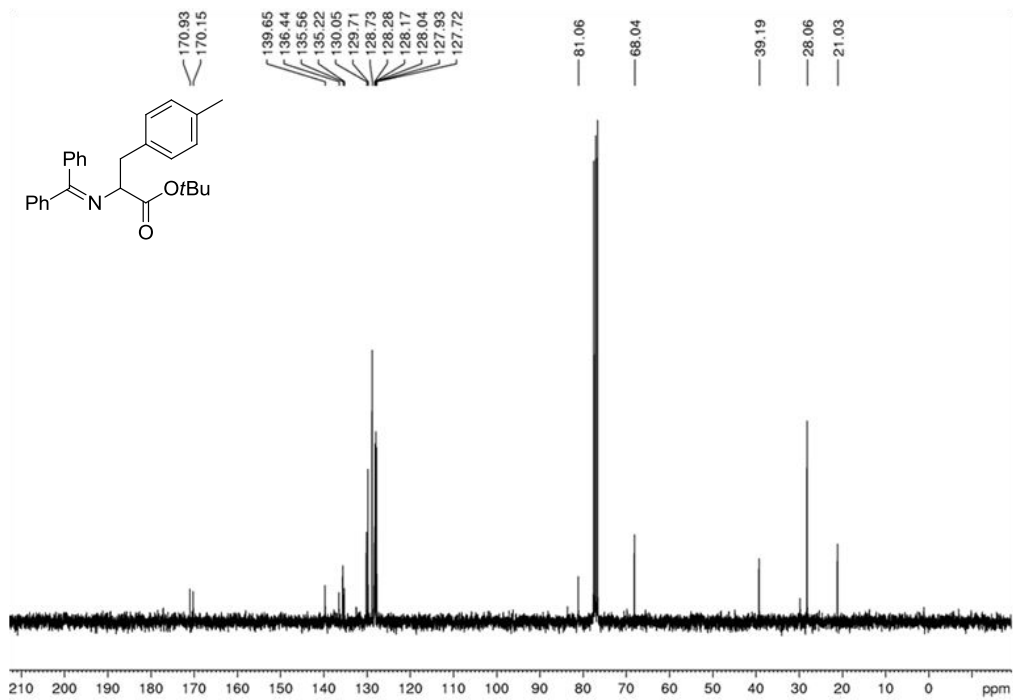
43c Proton and Carbon NMR spectra



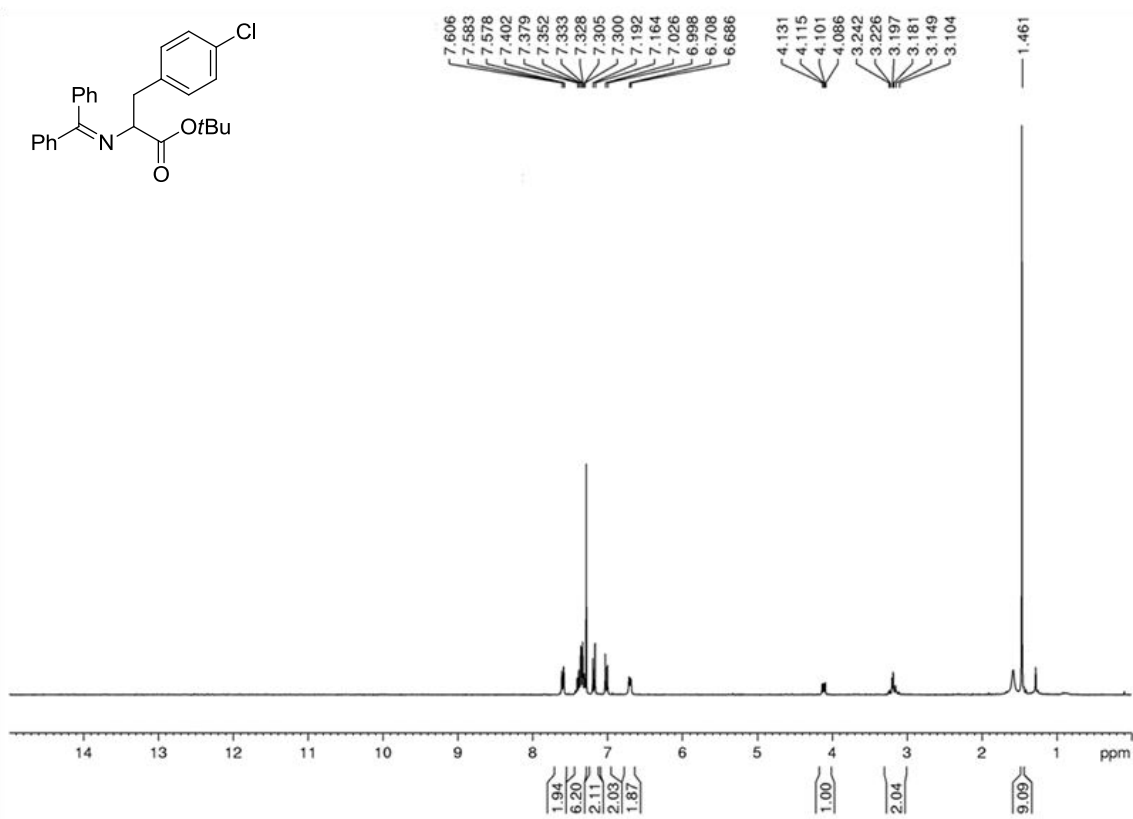


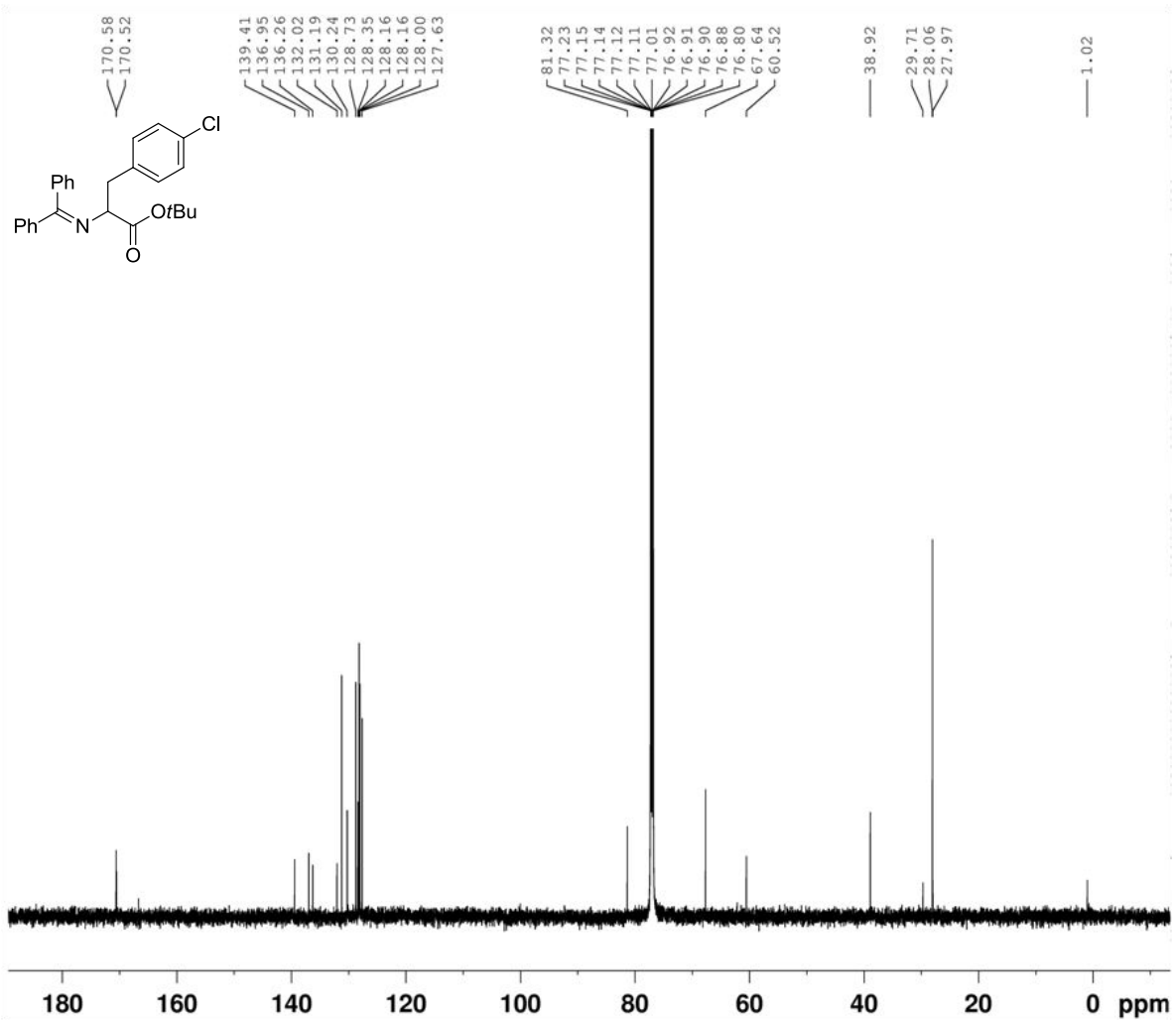
43f Proton and Carbon NMR spectra



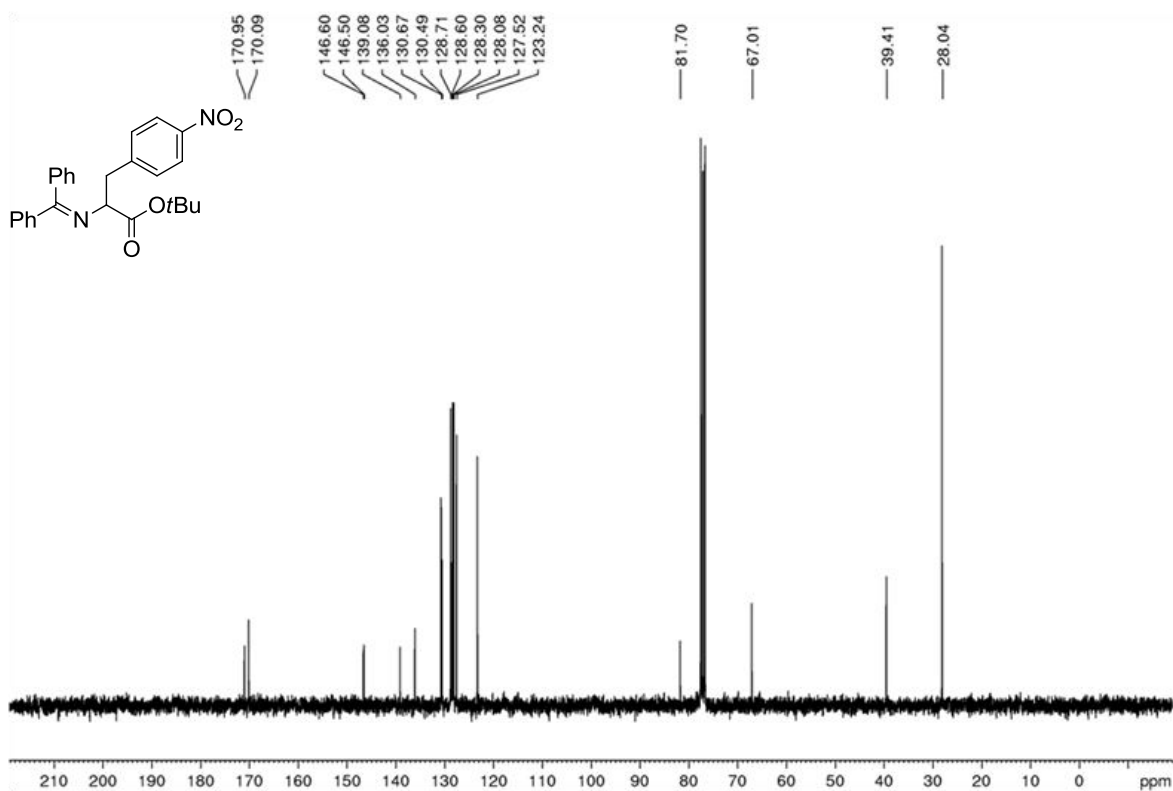
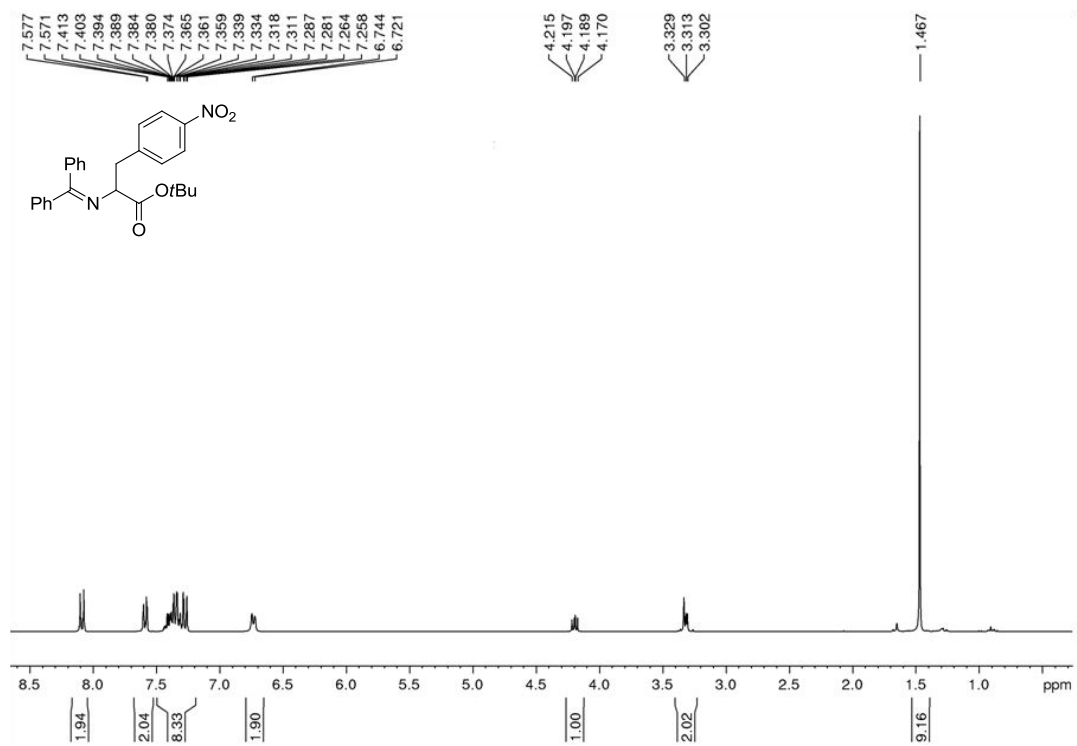


43g Proton and Carbon NMR spectra

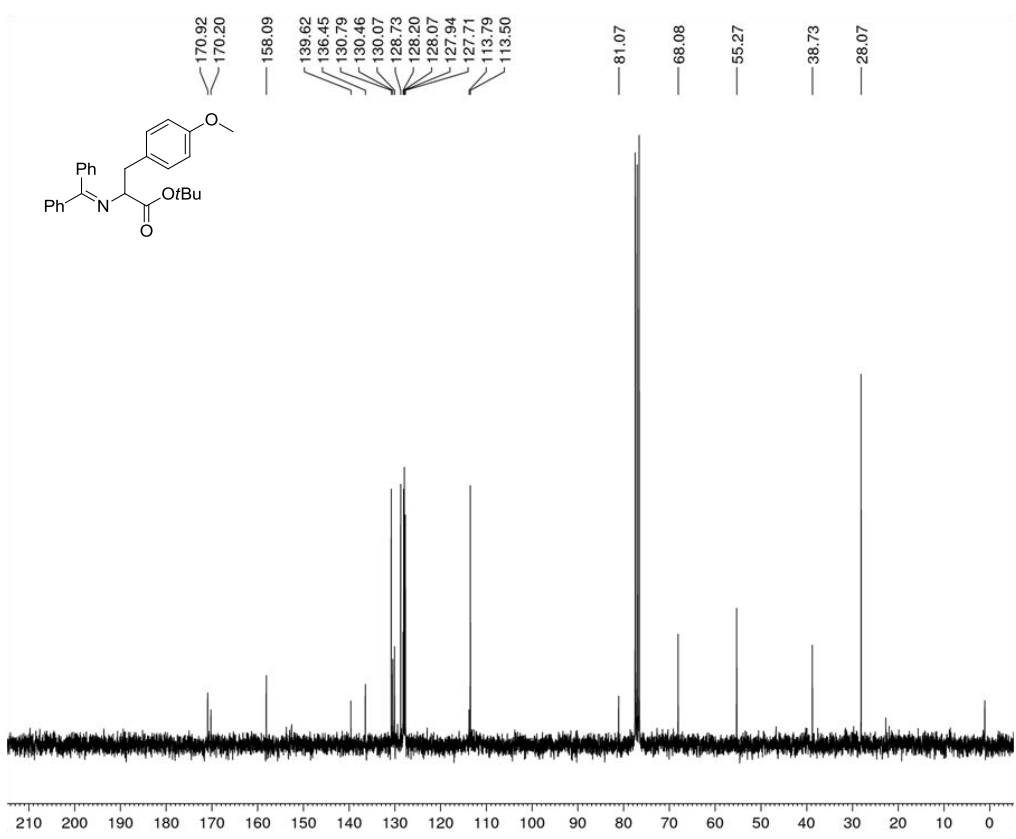
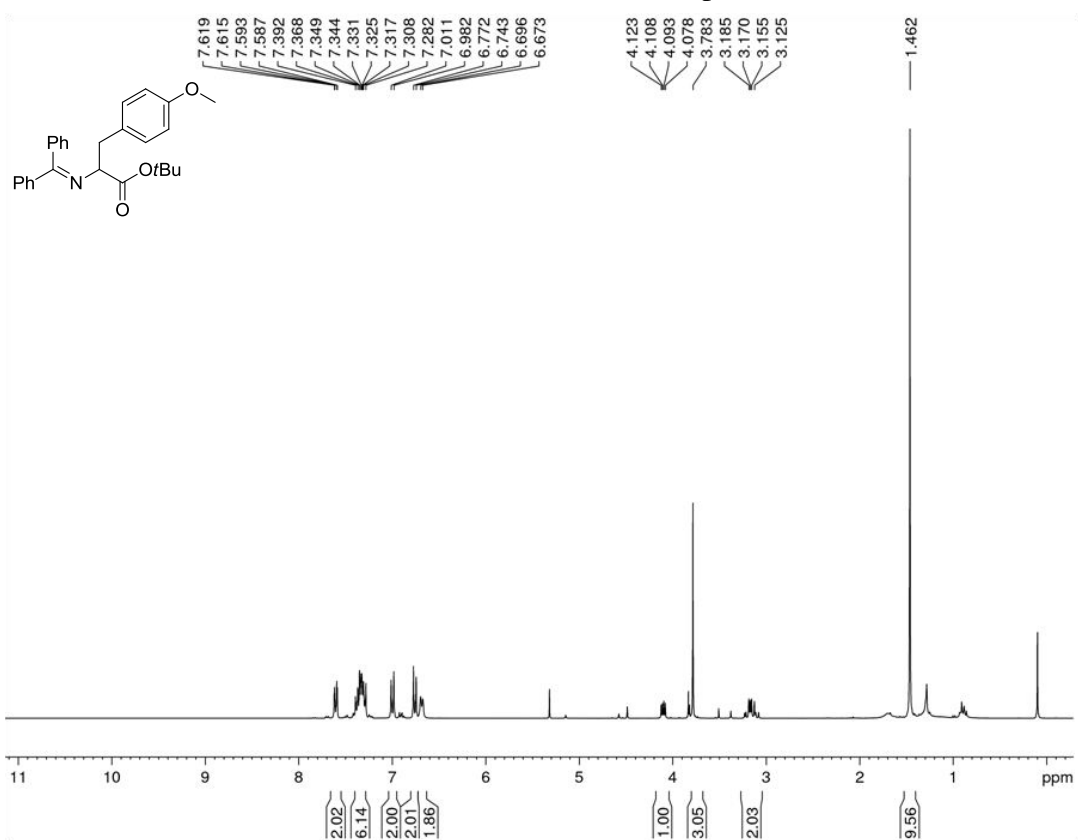




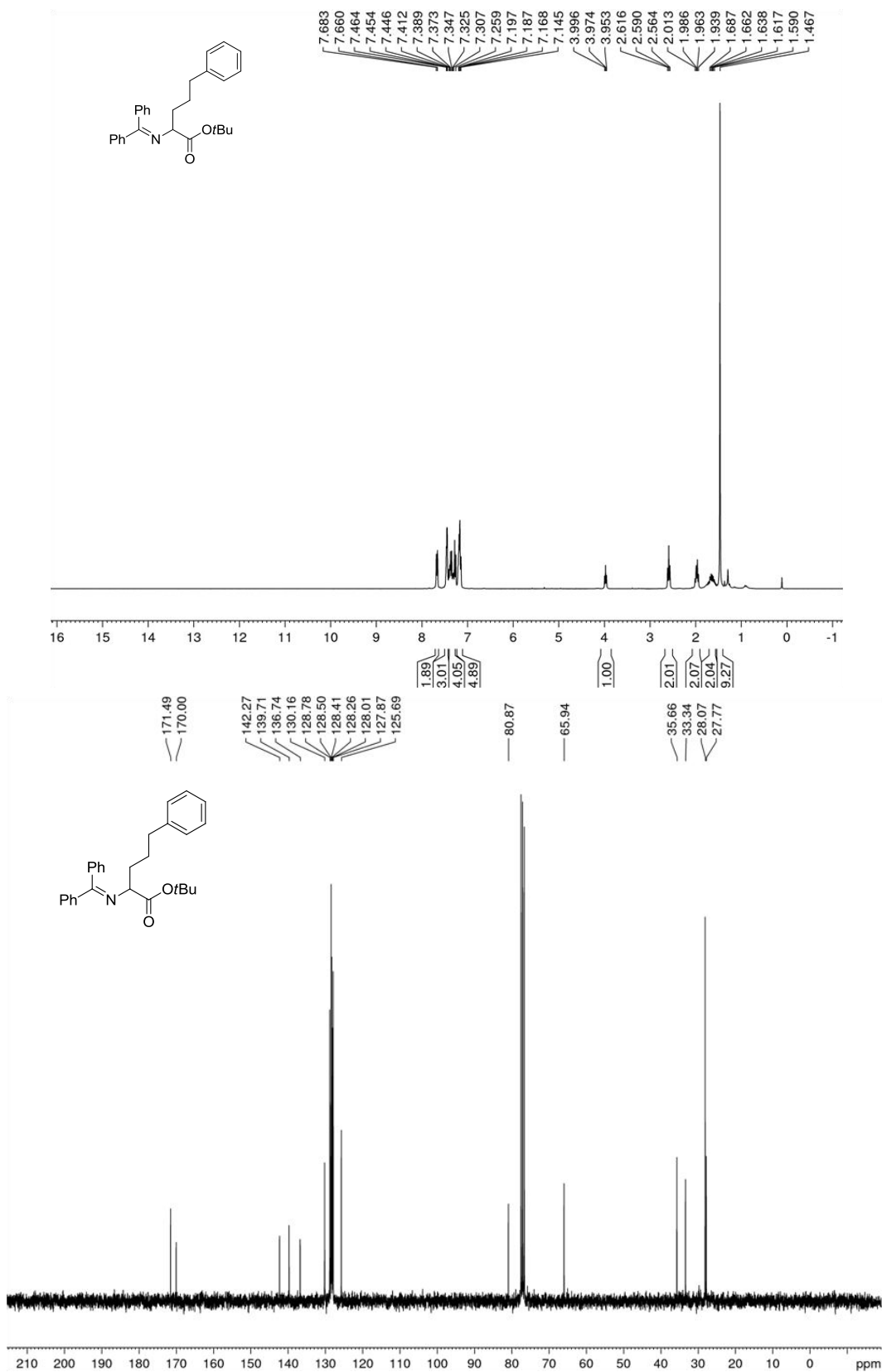
43h Proton and Carbon NMR spectra



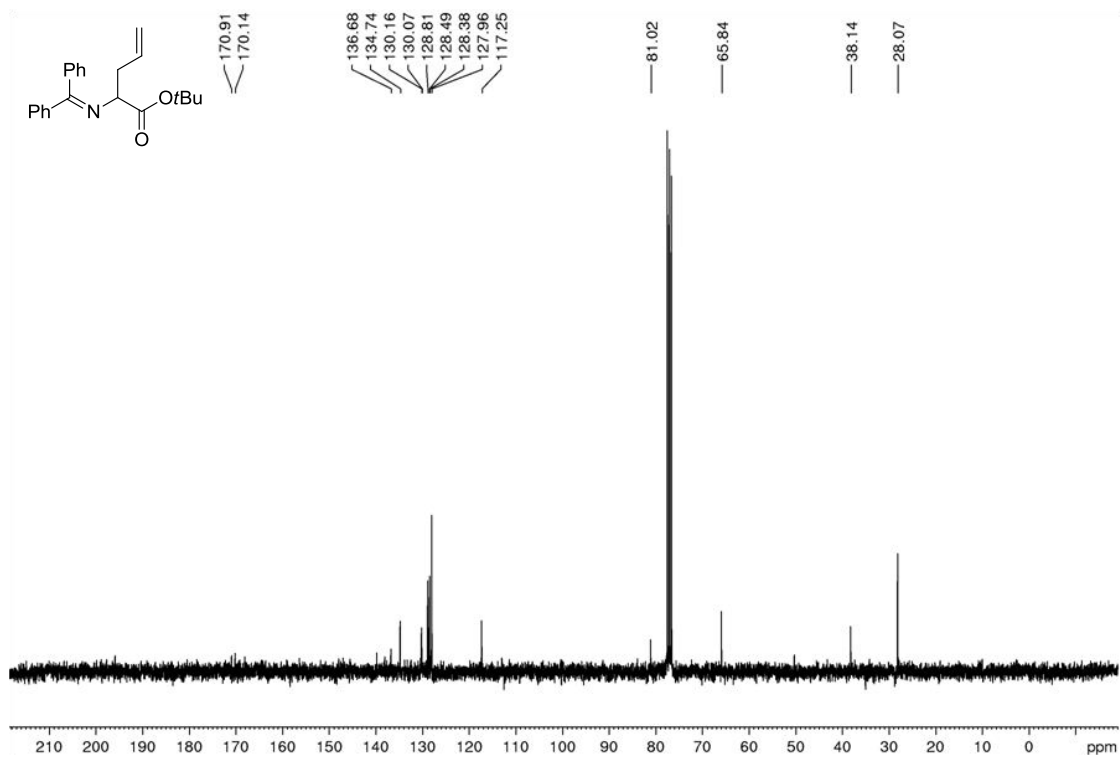
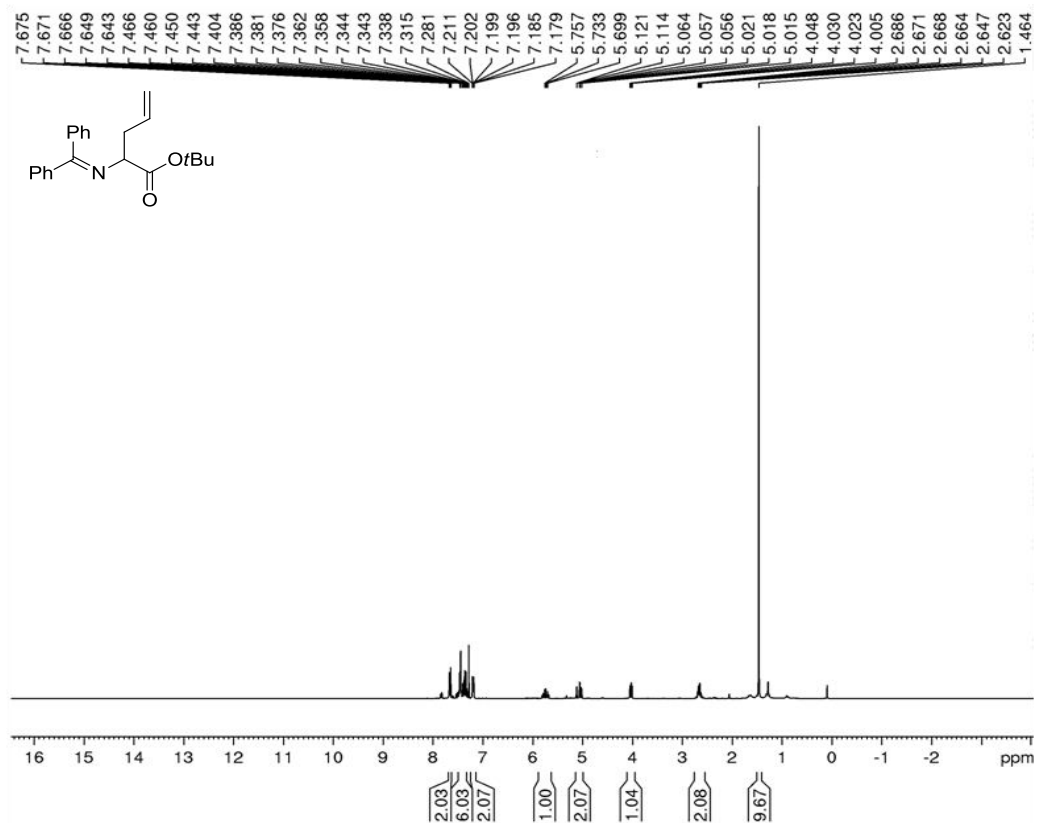
43e Proton and Carbon NMR spectra



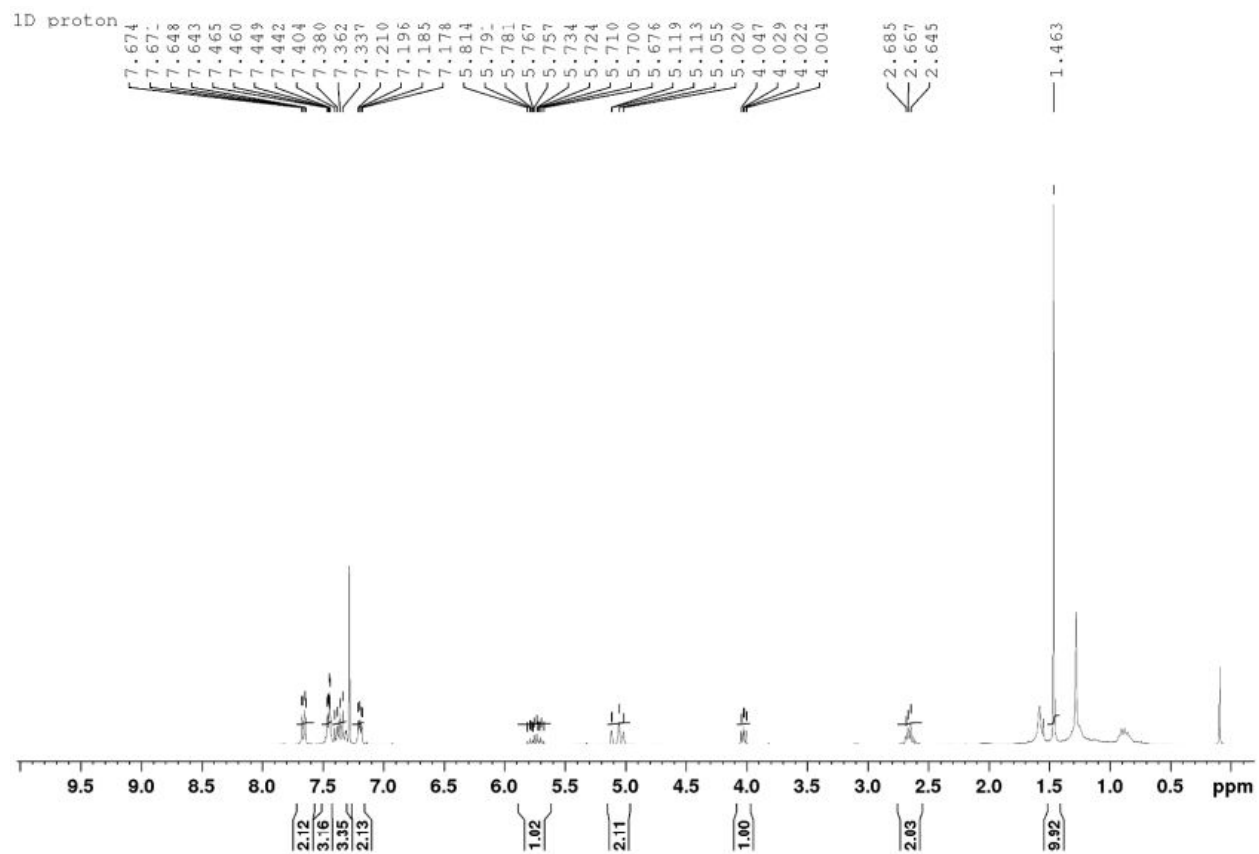
43i Proton and Carbon NMR spectra



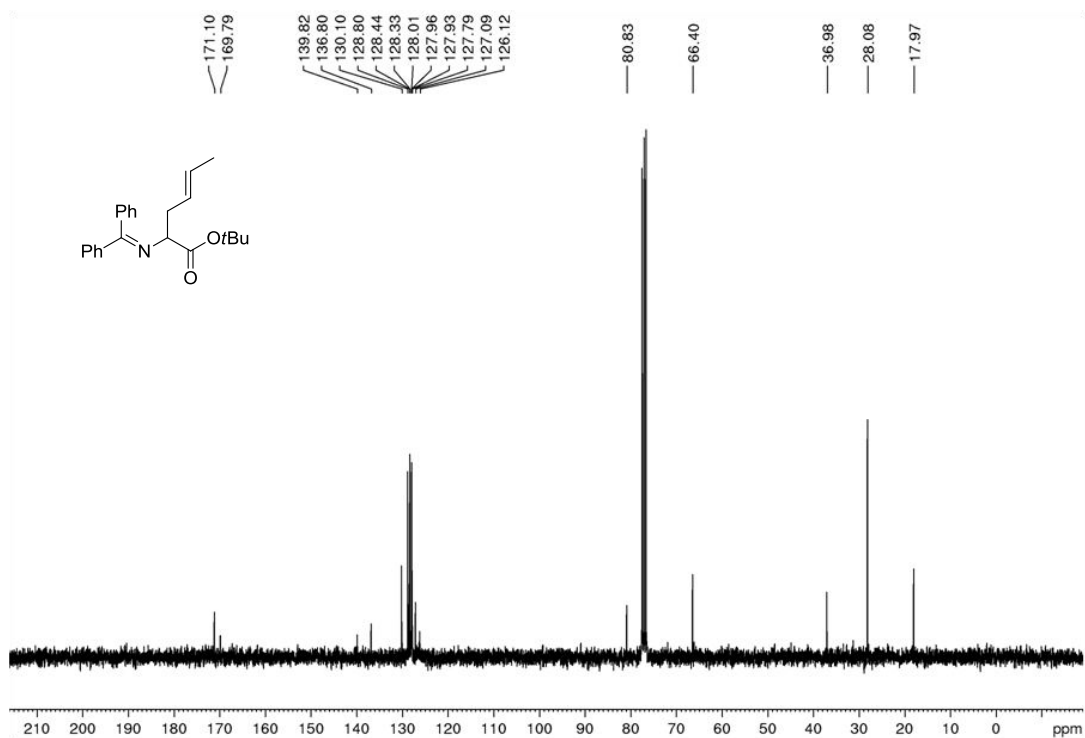
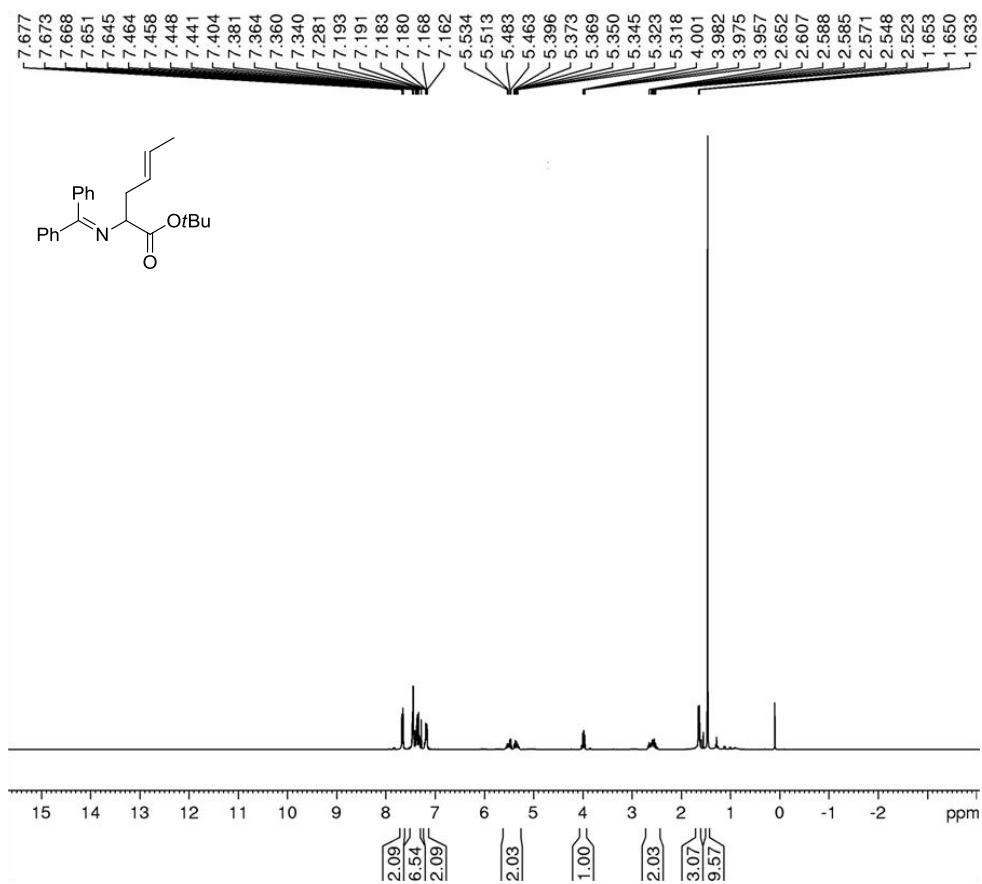
43j Proton and Carbon NMR spectra



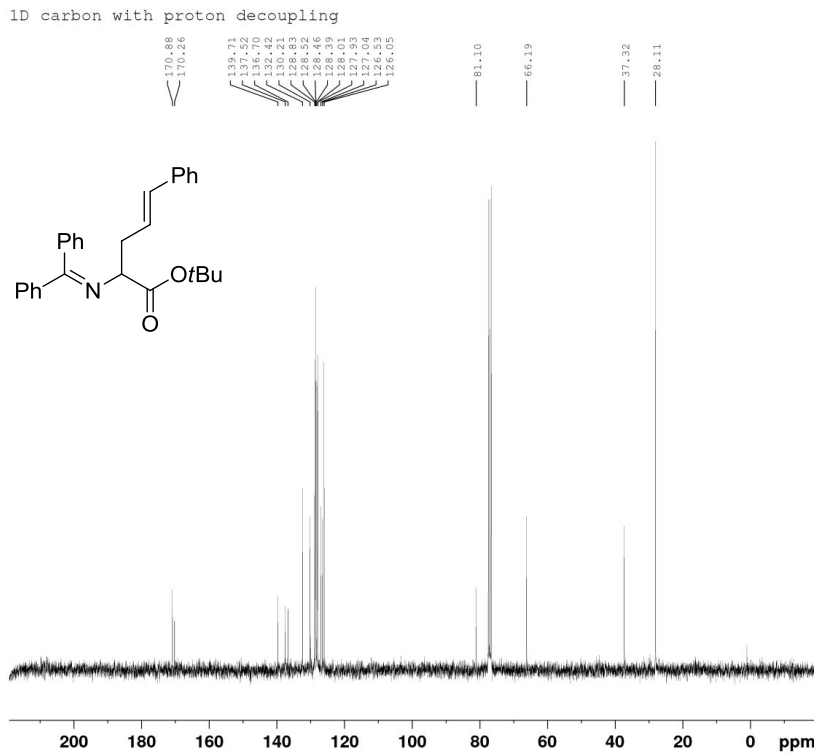
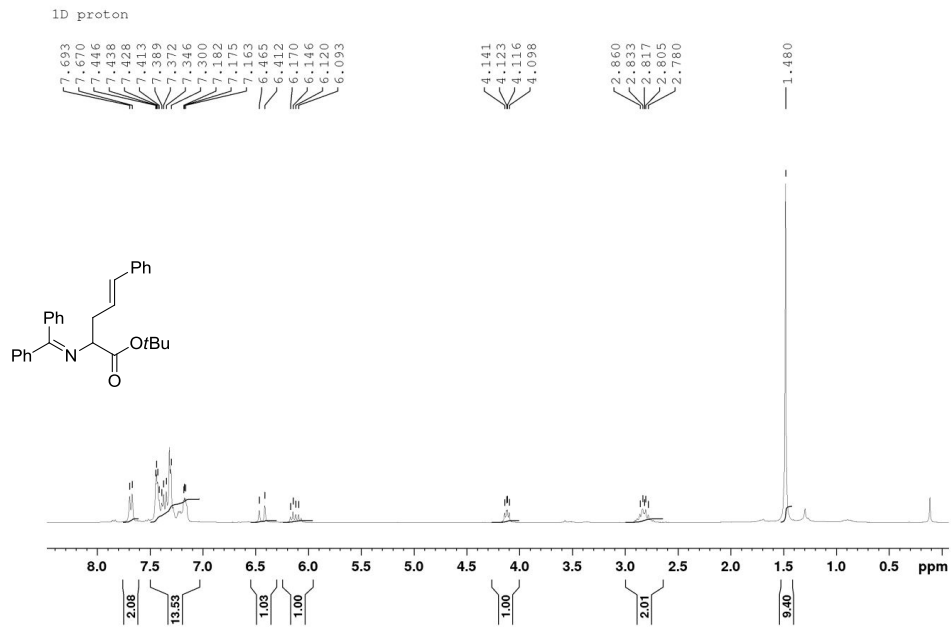
43k Proton and Carbon NMR spectra



431 Proton and Carbon NMR spectra



43m Proton and Carbon NMR spectra



5.2.3 Coordinate and thermochemical data for all computed structures

Enolate, 57

opt=calcfc freq=noraman wb97xd/6-31g(d)/def2sv scrf=(iefpcm,solvent=dichloromethane)

Zero-point correction= 0.349480 (Hartree/Particle)
Thermal correction to Energy= 0.369633
Thermal correction to Enthalpy= 0.370577
Thermal correction to Gibbs Free Energy= 0.299469
Sum of electronic and zero-point Energies= -940.720026
Sum of electronic and thermal Energies= -940.699873
Sum of electronic and thermal Enthalpies= -940.698929
Sum of electronic and thermal Free Energies= -940.770037

-1	1			C	-2.66382500	4.11304100	-0.12688600
O	2.94168700	-2.24927000	0.16640100	H	-4.58396800	3.21400700	-0.49476000
C	2.26387700	-1.21556500	0.08701600	H	-0.61673200	4.67777300	0.24411300
N	0.14797400	-0.05749500	-0.00172400	H	-3.03546700	5.13273700	-0.15831900
C	-1.15740200	0.07493500	-0.00873700	O	2.83683200	0.02801900	0.00906900
C	-2.09818300	-1.08436800	0.01018000	C	4.26786000	0.19479200	0.00538800
C	-3.06904900	-1.22525900	1.01197600	C	0.83786500	-1.19857200	0.06276200
C	-2.02750200	-2.08170000	-0.97261600	H	0.36602100	-2.18060100	0.12148000
C	-3.93759700	-2.31303300	1.02914000	C	4.88553100	-0.31585700	1.30986700
H	-3.14205300	-0.46388600	1.78374500	H	4.76577200	-1.39543500	1.39184200
C	-2.88822900	-3.17472800	-0.95616800	H	5.95127900	-0.06636200	1.34031100
H	-1.28146600	-1.99418400	-1.75692200	H	4.39765000	0.16072600	2.16601400
C	-3.85005000	-3.29494000	0.04479200	C	4.89403800	-0.48022000	-1.21791400
H	-4.68195600	-2.39634200	1.81585700	H	5.96117800	-0.24143800	-1.27217500
H	-2.81257800	-3.93273000	-1.73041500	H	4.76853400	-1.56101300	-1.15980200
H	-4.52547700	-4.14496800	0.05760500	H	4.41414300	-0.11554400	-2.13160700
C	-1.69424500	1.44670200	-0.03901300	C	4.44208200	1.71087600	-0.09062100
C	-3.05351700	1.72834500	-0.27207300	H	3.97814000	2.09309500	-1.00415200
C	-0.83587500	2.55084100	0.14390600	H	3.97399900	2.20339600	0.76663100
C	-3.52741500	3.03689900	-0.31133700	H	5.50499200	1.97074700	-0.10450800
H	-3.75026500	0.91157500	-0.43234100				
C	-1.31021500	3.85338500	0.09831200				
H	0.21539900	2.34747100	0.31784600				

DACN-2H⁺, 51

opt=calcfc freq=noraman wb97xd/6-31g(d)/def2sv scrf=(iefpcm,solvent=dichloromethane)

Zero-point correction= 1.002472 (Hartree/Particle)
Thermal correction to Energy= 1.053442
Thermal correction to Enthalpy= 1.054386
Thermal correction to Gibbs Free Energy= 0.922113
Sum of electronic and zero-point Energies= -1889.402764
Sum of electronic and thermal Energies= -1889.351795
Sum of electronic and thermal Enthalpies= -1889.350851
Sum of electronic and thermal Free Energies= -1889.483124

2	1			C	2.01249900	-0.22835000	-0.84830200
N	1.13027500	0.69788100	-1.25314600	N	4.39692500	-0.45720300	0.26370900
H	0.17370300	0.40199600	-1.40966000	C	3.19580200	-0.65537000	-0.27317900

N	1.75458900	-2.80663400	-0.81154400	H	3.37831700	-4.41378400	-2.24297400
C	2.22853500	-1.58011100	-0.67789400	H	1.93877000	-5.39094300	-1.88325800
N	-1.54176900	1.45842500	-1.33242200	H	3.46727500	-5.74685700	-1.07282600
H	-1.86696900	1.42311800	-2.29359300	C	-0.97612600	1.40629700	2.37791000
C	-2.31684300	0.77123700	-0.45325600	H	-0.62412600	1.74617700	1.40090000
N	-2.12505900	0.51304200	2.09834900	C	0.16642000	0.64297500	3.04120000
C	-2.51785900	0.38845600	0.84743700	H	0.51682900	-0.16966100	2.39578100
N	-4.23318200	-0.94994200	-0.67410900	H	-0.12355300	0.22295600	4.00935900
C	-3.30064000	-0.14991300	-0.19270200	H	0.99724700	1.33132500	3.21775600
C	1.39474900	2.07695800	-1.38030900	C	-1.42098400	2.63483000	3.16615400
C	2.66109000	2.48775900	-1.71627800	H	-2.22165000	3.15900100	2.63604000
H	3.39425600	1.74323900	-2.00907400	H	-0.57700300	3.32094300	3.28109500
C	3.02436100	3.84903700	-1.65016800	H	-1.77762100	2.37178300	4.16751500
H	4.03851300	4.14096000	-1.90169400	C	-2.80354800	-0.18832400	3.20739300
C	2.11287200	4.78002300	-1.23653100	H	-2.32305000	0.18720000	4.11345000
H	2.39083000	5.82406700	-1.13360200	C	-2.54108900	-1.69249000	3.13946500
C	0.77249300	4.40110800	-0.95770800	H	-1.46762900	-1.89224600	3.20668400
C	-0.17091900	5.37308000	-0.53560300	H	-2.90408400	-2.13393700	2.20606000
H	0.16572400	6.39758500	-0.40899800	H	-3.04066700	-2.19941100	3.96969000
C	-1.47635900	5.03736800	-0.29442800	C	-4.27695100	0.20419100	3.28781300
H	-2.19016700	5.78428200	0.03455100	H	-4.83001100	-0.06208700	2.38276700
C	-1.90966100	3.71967300	-0.54012100	H	-4.37365000	1.28370000	3.43445100
H	-2.96187800	3.46811200	-0.44336400	H	-4.75122000	-0.30452700	4.13141300
C	-1.02197600	2.75391500	-0.94756600	C	-5.02664100	-1.83339300	0.20481700
C	0.36812900	3.03924200	-1.09874100	H	-4.59473100	-1.71547000	1.19887400
C	5.21960000	-1.66767600	0.50971900	C	-6.48506300	-1.38466100	0.26442200
H	4.91846300	-2.37744100	-0.26477500	H	-6.55944300	-0.33846000	0.57675900
C	6.70679800	-1.40201100	0.29358100	H	-7.02749700	-2.00115000	0.98672400
H	6.89187000	-0.99874800	-0.70546400	H	-6.98317500	-1.49258000	-0.70450600
H	7.24720700	-2.34809200	0.38827000	C	-4.86591500	-3.29668900	-0.19978300
H	7.11760600	-0.71199100	1.03699100	H	-3.81256100	-3.59258600	-0.18120700
C	4.93225900	-2.26791700	1.88735000	H	-5.26797400	-3.49049000	-1.19935600
H	3.85936300	-2.42995200	2.03780900	C	-5.41373500	-3.92907100	0.50443500
H	5.29079400	-1.61412000	2.68883800	H	-4.54985100	-0.86794900	-2.11974800
H	5.44191100	-3.23071900	1.98899600	H	-5.38912100	-1.55055600	-2.26653800
C	4.74412000	0.78249500	1.00685400	C	-3.38537000	-1.37301900	-2.96855800
H	5.37372000	0.43298400	1.82973500	H	-3.15914700	-2.41679000	-2.73198000
C	5.57342400	1.75880300	0.17641500	H	-2.47520700	-0.78265400	-2.81229200
H	6.46780900	1.28077300	-0.22900000	H	-3.64211100	-1.30943900	-4.02946900
H	5.88945700	2.59357100	0.80975200	C	-5.01634100	0.53357100	-2.50771800
H	4.99607500	2.16730400	-0.65322400	H	-5.85912400	0.84767700	-1.88569800
C	3.51971600	1.43112300	1.64431900	H	-5.33596200	0.53808200	-3.55326300
H	2.96556500	0.69922800	2.23871000	H	-4.21894600	1.27760300	-2.40339000
H	2.84583100	1.87208600	0.90446300				
H	3.84712100	2.23511000	2.30919400				
C	0.39176600	-2.97989500	-1.35718900				
H	0.23826000	-4.05922400	-1.41608200				
C	-0.64780400	-2.40955400	-0.39137100				
H	-0.61405800	-2.92467900	0.57244000				
H	-1.65322500	-2.52126800	-0.80738200				
H	-0.47474100	-1.34416500	-0.20051000				
C	0.28002600	-2.42522800	-2.77549900				
H	1.04864700	-2.86360000	-3.41801900				
H	0.39175700	-1.33627300	-2.81114700				
H	-0.69969000	-2.67329300	-3.19251700				
C	2.49613200	-3.98181500	-0.30885700				
H	3.42979900	-3.58746000	0.09025500				
C	1.75430200	-4.66169300	0.84021200				
H	1.54240400	-3.94683400	1.64113500				
H	2.37649800	-5.46319300	1.24828000				
H	0.81121200	-5.10956400	0.50998700				
C	2.83625300	-4.93717000	-1.45024500				

Catalyst-Enolate Complex, 51•57

 # opt=calcfc freq=noraman wb97xd/6-31g(d)/def2sv scrf=(iefpcm,solvent=dichloromethane)

Zero-point correction= 1.353526 (Hartree/Particle)
 Thermal correction to Energy= 1.426216
 Thermal correction to Enthalpy= 1.427160
 Thermal correction to Gibbs Free Energy= 1.245099
 Sum of electronic and zero-point Energies= -2830.200290
 Sum of electronic and thermal Energies= -2830.127599
 Sum of electronic and thermal Enthalpies= -2830.126655
 Sum of electronic and thermal Free Energies= -2830.308717

I 1

N	1.16499700	0.78084300	-1.64954000	C	3.86662800	-0.99846400	-0.05677200
H	0.17954500	1.02594500	-1.45856900	H	3.15297100	-1.71634500	0.36147000
C	1.41365900	-0.44431100	-2.12514200	H	3.35025600	-0.04899700	-0.22869100
N	3.46837000	-2.07025800	-2.25757100	H	4.64604400	-0.81726000	0.68617500
C	2.26871100	-1.51039100	-2.32715500	C	-1.31591000	-1.56550700	-3.60575800
N	-0.08977400	-2.28728000	-3.19474200	H	-1.87005100	-2.27544700	-4.22493100
C	0.92138600	-1.60868800	-2.68287900	C	-2.16358400	-1.19389100	-2.39679600
N	0.88284200	1.59525400	1.02981000	H	-2.44569500	-2.08617200	-1.83155600
H	-0.03520000	1.36524300	0.61437200	H	-3.07664800	-0.67996800	-2.71062700
C	1.52942000	0.74620700	1.82138800	H	-1.62282400	-0.51830000	-1.72925500
N	3.88805600	0.76330900	2.92350400	C	-0.97625300	-0.35541900	-4.47380000
C	2.65589000	0.42035900	2.55027000	H	-0.32752900	-0.64043000	-5.30778600
N	0.97132100	-1.61187300	2.74799800	H	-0.48140300	0.43203600	-3.89479100
C	1.58399900	-0.46559500	2.47996400	H	-1.89818400	0.07031500	-4.88007300
C	2.09586800	1.84673800	-1.73395400	C	0.02215700	-3.74240900	-3.41179200
C	2.85546800	1.95997200	-2.87641700	H	0.94986500	-4.03922300	-2.91850900
H	2.74474100	1.21230900	-3.65657500	C	-1.11410600	-4.49258100	-2.71777700
C	3.72999200	3.04578600	-3.07306100	H	-1.14861600	-4.24564400	-1.65210100
H	4.31925400	3.09838400	-3.98239600	H	-0.94986600	-5.56933500	-2.81935400
C	3.78335200	4.04877800	-2.14457900	H	-2.08766800	-4.26317400	-3.16254700
H	4.41526900	4.91752200	-2.30212800	C	0.13375000	-4.07285900	-4.89886900
C	3.00897500	3.97790500	-0.95757700	H	0.97200300	-3.53592600	-5.35398100
C	3.07310200	5.03691100	-0.01256900	H	-0.77989600	-3.80436400	-5.43927000
H	3.69804800	5.89502700	-0.24176300	H	0.29603800	-5.14661500	-5.03098900
C	2.36089200	4.98700200	1.15385300	C	4.44095000	2.04210800	2.42586400
H	2.40186200	5.80374800	1.86636800	H	3.78950500	2.34053900	1.60338600
C	1.59922400	3.83856000	1.45111600	C	5.84244300	1.85930300	1.84752400
H	1.08242600	3.75367900	2.40143700	H	5.84319100	1.10384000	1.05668600
C	1.53391700	2.78236000	0.57621700	H	6.57339900	1.56949400	2.60939600
C	2.18334100	2.83902100	-0.70127200	H	6.17587900	2.80653500	1.41336200
C	3.64299200	-3.42570500	-2.82211000	C	4.38044400	3.12811400	3.49790000
H	2.86430200	-3.52275200	-3.58315400	H	3.35839000	3.24520200	3.87110400
C	4.98425900	-3.57157800	-3.53588500	H	4.70294100	4.08389900	3.07420000
H	5.10096800	-2.80582400	-4.30766600	H	5.03545200	2.89633300	4.34495700
H	5.02872000	-4.55362000	-4.01515800	C	4.60093000	0.02990000	3.98715300
H	5.82864900	-3.50491500	-2.84257700	H	5.44443500	0.67106100	4.25477700
C	3.42998100	-4.49525900	-1.74892700	C	5.18329300	-1.28531500	3.46814500
H	2.46693300	-4.36029600	-1.24379300	H	5.93224600	-1.08932600	2.69487200
H	4.21841800	-4.46030300	-0.98973000	H	4.41731900	-1.93347700	3.03223000
H	3.44602900	-5.49058800	-2.20264800	H	5.66758700	-1.83144900	4.28312200
C	4.49512100	-1.53106400	-1.33858300	C	3.74392600	-0.10856900	5.24548400
H	5.11392100	-2.39130600	-1.06943100	H	2.83370900	-0.68972800	5.07372000
C	5.38285200	-0.48987600	-2.01564500	H	3.44594900	0.87931500	5.60910900
H	5.84296300	-0.88892400	-2.92315900	H	4.31558400	-0.60971700	6.03166300
H	6.18101200	-0.18451200	-1.33116500	C	1.64104000	-2.68713800	3.49621400
H	4.80355800	0.39969100	-2.27965600	H	2.61563800	-2.28493100	3.77279000

C	0.89250500	-3.01825400	4.78668500	H	-4.25351700	-2.02998100	-0.44531700
H	0.74286200	-2.11635100	5.38786400	C	-4.00922200	-3.44676200	2.63386900
H	1.47396100	-3.73484800	5.37421300	H	-4.75628300	-2.56385800	4.44981600
H	-0.08629500	-3.46704000	4.58870600	H	-3.39054100	-4.06834900	0.66413400
C	1.87612200	-3.91353800	2.61445200	H	-3.63303600	-4.33947600	3.12490200
H	2.45671800	-3.64875800	1.72455700	C	-6.90688400	0.40595200	0.65674600
H	0.93260400	-4.36477500	2.28979700	C	-7.85876200	-0.52815800	1.09265200
H	2.43142500	-4.67047900	3.17632300	C	-7.37537800	1.63906100	0.17062400
C	-0.39721300	-1.81453800	2.22737500	C	-9.22106100	-0.24112700	1.04838700
H	-0.69991100	-2.80187300	2.58471000	H	-7.53287000	-1.49429000	1.46613900
C	-0.41898600	-1.84637600	0.70001500	C	-8.73324700	1.92241400	0.12406200
H	0.29456500	-2.58212300	0.31201800	H	-6.64634400	2.36562500	-0.17230600
H	-0.18417900	-0.86689900	0.27136400	C	-9.66877800	0.98461400	0.56493100
H	-1.42230400	-2.11477200	0.35856300	H	-9.93551300	-0.98481000	1.39101000
C	-1.36135000	-0.79128300	2.82003700	H	-9.06762700	2.88375600	-0.25730300
H	-1.29841800	-0.79690600	3.91242000	H	-10.73116200	1.20768400	0.52947600
H	-2.38657500	-1.03226900	2.53160900	O	-3.06725200	2.67533400	-1.31944200
H	-1.14800300	0.22236700	2.46370800	C	-2.32906400	3.77838800	-1.89534600
O	-1.19990700	1.56662400	-0.62314800	C	-1.57233900	4.55069500	-0.81402300
C	-2.47008400	1.68613700	-0.61466800	H	-0.78808900	3.93574200	-0.37110400
C	-3.29968300	0.80753600	0.07126600	H	-1.11160200	5.44332000	-1.25073000
H	-2.79476100	-0.02328200	0.55787400	H	-2.26246200	4.86985700	-0.02595700
N	-4.65124200	0.94779500	0.09521900	C	-1.39803700	3.30733600	-3.01621700
C	-5.45450700	0.11366900	0.67944100	H	-1.92958300	2.61559200	-3.67782700
C	-4.97988300	-1.13271900	1.36344900	H	-1.07195200	4.16840900	-3.60972700
C	-5.11775300	-1.30337900	2.74551200	H	-0.51308300	2.80846900	-2.62084100
C	-4.35866800	-2.14938400	0.62900600	C	-3.43901900	4.64998300	-2.48415000
C	-4.63996900	-2.45042700	3.37594100	H	-3.99151800	4.09952600	-3.25235200
H	-5.60480100	-0.52717100	3.32987100	H	-4.14238700	4.95167300	-1.70210200
C	-3.87219000	-3.29345600	1.25483900	H	-3.01342300	5.55013000	-2.93867100

Uncatalyzed Benzylation Transition State, TS1_u

opt=(calcf,ts,noeigen) freq=norman wb97xd/6-31g(d)/def2sv scrf=(iefpcm,solvent=dichloromethane)

Zero-point correction= 0.471798 (Hartree/Particle)
Thermal correction to Energy= 0.500100
Thermal correction to Enthalpy= 0.501044
Thermal correction to Gibbs Free Energy= 0.410493
Sum of electronic and zero-point Energies= -3783.206422
Sum of electronic and thermal Energies= -3783.178120
Sum of electronic and thermal Enthalpies= -3783.177175
Sum of electronic and thermal Free Energies= -3783.267726

-1 1							
O	2.42731500	0.77655000	2.43649100	H	-4.93018600	2.65368400	2.67605100
C	1.80738900	-0.05169100	1.76334800	C	-2.05211800	-2.11172100	-0.19854400
C	0.39182200	0.03596300	1.51213900	C	-3.42330200	-2.38748900	-0.30181900
H	-0.12886800	0.75342900	2.14586700	C	-1.16373400	-2.91118400	-0.93938200
N	-0.25475100	-0.95865700	0.85512600	C	-3.89066500	-3.41419100	-1.11954300
C	-1.53460000	-1.01700900	0.65559400	H	-4.13417400	-1.79366500	0.26498400
C	-2.49975900	-0.01854700	1.21519800	C	-1.63085900	-3.93458600	-1.75162500
C	-3.24732400	0.81056500	0.37030200	H	-0.10237700	-2.69890200	-0.86718300
C	-2.65214800	0.13184900	2.59834500	C	-2.99986100	-4.19310500	-1.85139800
C	-4.11469100	1.76761300	0.88980700	H	-4.95892500	-3.60386200	-1.18239300
H	-3.14957300	0.69829900	-0.70650600	H	-0.92361800	-4.53324100	-2.31995400
C	-3.52040100	1.08567100	3.12162700	H	-3.36377600	-4.99009200	-2.49354500
H	-2.07917000	-0.50621200	3.26571400	O	2.40339000	-1.10083300	1.14512900
C	-4.25360600	1.90812200	2.26881200	C	3.78144900	-1.45865300	1.38935800
H	-4.68183500	2.40438400	0.21717300	C	0.03060100	0.28761900	-2.03712900
H	-3.62607700	1.18718000	4.19796400	C	0.49544300	-0.55316400	-3.04062400

C	1.86498800	-0.68282400	-3.26447400	C	4.74420200	-0.37861200	0.89301800
C	2.76686700	0.04088200	-2.48405000	H	4.58614300	0.55729200	1.42975300
C	2.30204200	0.87498500	-1.47571400	H	5.77720700	-0.71034400	1.04662000
C	0.92946500	0.99467300	-1.23048400	H	4.59720000	-0.20594000	-0.17710200
H	-1.03571900	0.39168700	-1.86384100	C	3.95038700	-2.72789400	0.55444800
H	-0.21183700	-1.11379700	-3.64443100	H	4.97261100	-3.11050800	0.64265600
H	2.22896800	-1.34089100	-4.04814100	H	3.25504500	-3.50351200	0.89098700
H	3.83486400	-0.05088900	-2.66102700	H	3.74430000	-2.51332800	-0.49912400
H	3.00005800	1.43231000	-0.85755400	C	3.99743600	-1.76484300	2.87292300
C	0.44208300	1.82735700	-0.13529200	H	3.26371100	-2.50285400	3.21465700
H	1.13439800	2.25618200	0.57335600	H	4.99935300	-2.18113100	3.02378800
H	-0.60648800	1.81219700	0.11626600	H	3.89434400	-0.85985400	3.47370000
Br	0.13301200	3.95481400	-1.20418900				

Uncatalyzed Benzyltion Transition State, **TS1_u** - IRC precomplex

opt=calcfreq=norman wb97xd/6-31g(d)/def2sv scrf=(iefpcm,solvent=dichloromethane)

Zero-point correction= 0.471712 (Hartree/Particle)
Thermal correction to Energy= 0.500773
Thermal correction to Enthalpy= 0.501717
Thermal correction to Gibbs Free Energy= 0.407639
Sum of electronic and zero-point Energies= -3783.224171
Sum of electronic and thermal Energies= -3783.195110
Sum of electronic and thermal Enthalpies= -3783.194166
Sum of electronic and thermal Free Energies= -3783.288244

-1 1

O	-2.09305500	-0.04994300	-3.16590900	C	-3.82334800	-1.25203900	-1.31149900
C	-1.61404900	-0.69374100	-2.22324400	C	-1.08031300	0.50730100	1.51042800
C	-0.21920500	-0.76533900	-1.92810500	C	-1.97400800	0.06156000	2.47970600
H	0.43413700	-0.21301600	-2.60765200	C	-3.03703800	0.86963300	2.87678700
N	0.22865700	-1.39155000	-0.83574800	C	-3.20240000	2.12992200	2.30253000
C	1.46244600	-1.40053600	-0.39723500	C	-2.30960800	2.57456400	1.33305300
C	2.56508800	-0.68041200	-1.10578400	C	-1.24642300	1.76345900	0.92617700
C	3.06570800	0.52683300	-0.60412300	H	-0.26816300	-0.13209800	1.18164000
C	3.08592700	-1.16035600	-2.31324600	H	-1.83572400	-0.92129700	2.92150400
C	4.05398600	1.23418100	-1.28405800	H	-3.73699500	0.51985900	3.63008200
H	2.65841200	0.92489500	0.32187000	H	-4.02990500	2.76376700	2.60750900
C	4.07722400	-0.45971400	-2.99561800	H	-2.43955600	3.55514200	0.88158700
H	2.70085300	-2.09180800	-2.72051100	C	-0.30214100	2.22107200	-0.13720900
C	4.56666900	0.74006700	-2.48156400	H	-0.78658200	2.82868600	-0.89990300
H	4.41857600	2.17451700	-0.87920800	H	0.23331800	1.39411500	-0.60251400
H	4.47037000	-0.85133700	-3.93004000	Br	1.10216400	3.40665300	0.61554700
H	5.33862100	1.28825400	-3.01442600	C	-4.20262800	0.20776900	-1.05334000
C	1.73385700	-2.07903100	0.87776400	H	-3.91741600	0.83683900	-1.89762200
C	3.03041600	-2.17762500	1.41569100	H	-5.28443100	0.28864000	-0.89711700
C	0.68411800	-2.65988800	1.62169700	H	-3.69583700	0.57074500	-0.15332900
C	3.26275300	-2.80941300	2.63466900	C	-4.22722200	-2.10474300	-0.10729700
H	3.86796600	-1.74965800	0.87205100	H	-5.31272400	-2.07319700	0.03590900
C	0.92035400	-3.28894500	2.83513800	H	-3.92570200	-3.14669600	-0.25647100
H	-0.32194600	-2.59675400	1.21830600	H	-3.74336800	-1.72809500	0.80006300
C	2.21319700	-3.37020000	3.35805200	C	-4.47547200	-1.79566500	-2.58504500
H	4.27782500	-2.86454500	3.02089400	H	-4.16308800	-2.83244100	-2.75214000
H	0.08591400	-3.72290900	3.38133600	H	-5.56693500	-1.77802500	-2.48511100
H	2.39584600	-3.86112500	4.30963500	H	-4.18222700	-1.19638400	-3.44774000
O	-2.39380700	-1.41385100	-1.35890000				

Uncatalyzed Benzylaton Transition State **TS1_u** - IRC product

 # opt=calcfc freq=noraman wb97xd/6-31g(d)/def2sv scrf=(iefpcm,solvent=dichloromethane)

Zero-point correction= 0.475926 (Hartree/Particle)
 Thermal correction to Energy= 0.503449
 Thermal correction to Enthalpy= 0.504393
 Thermal correction to Gibbs Free Energy= 0.415128
 Sum of electronic and zero-point Energies= -3783.296141
 Sum of electronic and thermal Energies= -3783.268618
 Sum of electronic and thermal Enthalpies= -3783.267674
 Sum of electronic and thermal Free Energies= -3783.356939

-1 1

O	2.97421600	1.00903300	-1.74094700	C	3.47569200	1.97986700	0.86318800
C	2.14922800	0.86831500	-0.85998400	C	0.91508500	-3.14986800	-0.30995000
C	0.80464500	0.19018800	-1.11216500	C	1.52800100	-4.09708900	0.50569000
H	0.28501800	0.86473400	-1.80898500	C	2.91544400	-4.11576700	0.64168800
N	0.06400300	-0.04719100	0.10364600	C	3.68548100	-3.18590800	-0.05248100
C	-0.98401200	0.63010400	0.36065400	C	3.07040300	-2.24100500	-0.87150600
C	-1.45519800	1.80252500	-0.44771400	C	1.67911100	-2.20628800	-1.00409000
C	-2.52531600	1.67087100	-1.33537500	H	-0.16746400	-3.13111600	-0.42030500
C	-0.81205500	3.03519400	-0.31180400	H	0.91967700	-4.82275600	1.03876100
C	-2.94452700	2.76972000	-2.08075200	H	3.39309700	-4.85358600	1.28029400
H	-2.99411000	0.69579600	-1.45197400	H	4.76825200	-3.19708000	0.03997100
C	-1.24158800	4.13386000	-1.05133600	H	3.67586200	-1.51942300	-1.41379500
H	0.02566900	3.12693700	0.37460700	C	1.00144600	-1.15398900	-1.84886900
C	-2.30918000	4.00207000	-1.93682100	H	1.57683200	-0.95388400	-2.75827100
H	-3.76922200	2.66229700	-2.77935100	H	0.00248200	-1.49722500	-2.13609500
H	-0.74118600	5.09108600	-0.93796000	Br	-2.84660200	-2.15846200	-1.50238900
H	-2.64291100	4.85745800	-2.51699800	C	4.67862900	1.04682300	0.73759400
C	-1.78667900	0.25559500	1.55854400	H	4.93800000	0.87420800	-0.30777300
C	-2.71760200	1.13797100	2.11296500	H	5.53854300	1.49606600	1.24473900
C	-1.61428400	-1.00542700	2.14148100	H	4.46019700	0.08443200	1.21143200
C	-3.45322500	0.77486200	3.23882700	C	3.15293900	2.24671400	2.33041800
H	-2.86785200	2.11586100	1.66592900	H	3.99129500	2.76231100	2.80860600
C	-2.34922100	-1.36771600	3.26219800	H	2.26032100	2.87378100	2.41984600
H	-0.90140900	-1.69011500	1.69482700	H	2.97218100	1.30656300	2.85967400
C	-3.27062800	-0.47787300	3.81613100	C	3.67020400	3.29240500	0.10725400
H	-4.17101200	1.47212600	3.66096300	H	2.76436300	3.90435000	0.17274700
H	-2.21139100	-2.35070400	3.70317900	H	4.49533700	3.85116200	0.56046500
H	-3.84741100	-0.76501600	4.69072100	H	3.90127800	3.11270400	-0.94361200
O	2.26976600	1.30204300	0.38891900				

51 catalyzed benzylaton, **TS1**

 # opt=(calcfc,ts,noeigen) freq=noraman wb97xd/6-31g(d)/def2sv scrf=(iefpcm,solvent=dichloromethane)

Zero-point correction= 1.474045 (Hartree/Particle)
 Thermal correction to Energy= 1.555729
 Thermal correction to Enthalpy= 1.556673
 Thermal correction to Gibbs Free Energy= 1.354817
 Sum of electronic and zero-point Energies= -5672.698146
 Sum of electronic and thermal Energies= -5672.616462
 Sum of electronic and thermal Enthalpies= -5672.615518
 Sum of electronic and thermal Free Energies= -5672.817374

11

N	-2.09483400	-1.30141500	1.83910800	C	-3.30776000	-4.84688700	-1.42746500
H	-1.08983300	-1.49831700	1.78672800	H	-4.04922300	-4.13270900	-1.79483200
C	-2.91382400	-1.97845400	1.03575100	C	-2.44326400	-5.24483500	-2.62251900
N	-5.31342600	-1.70121600	0.01915400	H	-1.92748900	-4.37928400	-3.04737300
C	-4.09850000	-2.12415800	0.34058100	H	-3.08753200	-5.67110800	-3.39665700
N	-2.53593100	-4.11345100	-0.40369800	H	-1.69772500	-6.00192600	-2.36218400
C	-3.06272700	-3.04488500	0.17340200	C	-4.02828000	-6.04248800	-0.80590400
N	-1.06552900	0.93429900	0.55118600	H	-4.66871800	-5.72477000	0.02341400
H	-0.54515100	0.06011400	0.47895800	H	-3.31041900	-6.77605200	-0.42325500
C	-1.31809500	1.63630000	-0.55967300	H	-4.65183300	-6.53976300	-1.55486700
N	-2.24040400	4.01780200	-1.07576400	C	-2.42705400	4.60715000	0.26453200
C	-1.76682800	2.78465600	-1.18120200	H	-2.29484400	3.77985500	0.96239200
N	-1.14238900	1.06895400	-3.09317900	C	-3.84895000	5.13297100	0.45220900
C	-1.34472700	1.69259400	-1.93326600	H	-4.58366500	4.36184200	0.20230800
C	-2.49827100	-0.37597700	2.83870000	H	-4.05194200	6.01885700	-0.15809500
C	-3.33815900	-0.81091200	3.83612400	H	-3.98953800	5.41709900	1.49943800
H	-3.73629900	-1.81986400	3.78388800	C	-1.35918200	5.65981600	0.55558000
C	-3.63769500	0.01072600	4.94073500	H	-0.36202800	5.25868100	0.34735600
H	-4.31445400	-0.34910800	5.70821700	H	-1.41059300	5.95923900	1.60717700
C	-3.01426800	1.22307800	5.07049700	H	-1.50676400	6.55723100	-0.05557700
H	-3.17991600	1.83704300	5.95070300	C	-2.42025600	4.85855700	-2.27460500
C	-2.12927200	1.69835500	4.06847500	H	-2.86958900	5.78360400	-1.90645300
C	-1.44686000	2.93259500	4.24250700	C	-3.43409800	4.22785100	-3.22992400
H	-1.60891700	3.48919700	5.16071100	H	-4.40624000	4.13749900	-2.73589200
C	-0.58543700	3.39653600	3.28698100	H	-3.13605700	3.22823200	-3.55825100
H	-0.03736300	4.32118400	3.43328700	H	-3.55247000	4.85232700	-4.11991300
C	-0.43634700	2.68847100	2.07502400	C	-1.07442600	5.23101500	-2.90317900
H	0.20811000	3.07298800	1.28694600	H	-0.44333600	4.35712700	-3.08202000
C	-1.12085400	1.51924700	1.85108300	H	-0.51118600	5.88643800	-2.23357100
C	-1.91974300	0.93013500	2.88419000	H	-1.23066000	5.75320900	-3.85189600
C	-6.16932800	-2.56916700	-0.81641100	C	-0.88765800	1.82855200	-4.33131200
H	-5.74905500	-3.57294800	-0.71237600	C	-1.17710200	2.85408200	-4.10703900
C	-7.59876600	-2.63142300	-0.28262800	C	0.60399800	1.83188600	-4.66966800
H	-7.60979000	-2.94537700	0.76474000	H	1.17870500	2.20235800	-3.81420900
H	-8.16666900	-3.36015500	-0.86800400	H	0.78828300	2.48309200	-5.52977500
H	-8.11377400	-1.66925500	-0.36658700	H	0.96121500	0.82768700	-4.92523400
C	-6.10486300	-2.15496400	-2.28599900	C	-1.76473500	1.34374400	-5.48323200
H	-5.07048400	-2.15252400	-2.64535800	H	-2.81996700	1.33187800	-5.19279500
H	-6.52070700	-1.15281600	-2.43597600	H	-1.48728900	0.33991600	-5.82093000
H	-6.68307700	-2.85251800	-2.89918300	H	-1.64724900	2.02020200	-6.33501400
C	-5.72193600	-0.30299800	0.28469200	C	-0.85363200	-0.37590500	-3.06251800
H	-6.56045800	-0.12534800	-0.39323100	H	-0.71293000	-0.66612400	-4.10581300
C	-6.21666700	-0.12190300	1.71733900	C	-2.05515200	-1.13838600	-2.51070700
H	-7.02345000	-0.82385800	1.94479500	H	-2.95882900	-0.91490900	-3.08584600
H	-6.59463700	0.89596900	1.85478500	H	-2.23582700	-0.86971700	-1.46388100
H	-5.40563600	-0.28010400	2.43368200	H	-1.86910100	-2.21530500	-2.54623100
C	-4.62295500	0.69166800	-0.08665200	C	0.42469700	-0.69906900	-2.30376100
H	-4.28096800	0.53151200	-1.11422500	H	1.27022500	-0.11490500	-2.67380100
H	-3.76303100	0.61980700	0.58628400	H	0.67108500	-1.75712700	-2.41718000
H	-5.01524700	1.71000800	-0.00865900	H	0.30988100	-0.50395600	-1.23548700
C	-1.26264200	-4.66295900	0.11826400	O	0.59382900	-1.08769000	1.51980600
H	-1.18333200	-5.66212400	-0.31609300	C	1.84501000	-1.22429500	1.56259100
C	-0.07333500	-3.83077000	-0.35773200	C	2.64064500	-1.22299200	0.38965100
H	-0.02773600	-3.80916800	-1.45074900	H	2.09153500	-1.38838000	-0.53160100
H	0.86092300	-4.26153000	0.01590100	N	3.99423400	-1.40293000	0.45141200
H	-0.12649700	-2.80108400	0.01196900	C	4.72067300	-1.54947400	-0.60663500
C	-1.30105500	-4.82695400	1.63651700	C	4.13721600	-1.65659800	-1.98574300
H	-2.17532400	-5.40900000	1.94352600	C	4.22940100	-0.60183300	-2.89914600
H	-1.32702600	-3.86193700	2.15172000	C	3.46594800	-2.82176400	-2.37233900
H	-0.40009300	-5.35005000	1.96887300	C	3.65667000	-0.70475500	-4.16542400

H	4.76201300	0.30412300	-2.62200600	C	3.16552300	1.88801300	2.19591500
C	2.90124500	-2.93118600	-3.63980500	C	3.47774400	1.60480400	0.86050600
H	3.38721400	-3.64514500	-1.66747500	H	5.05658300	1.47240400	-0.59769200
C	2.99160800	-1.87019200	-4.53901800	H	6.84659600	2.04704400	1.00876400
H	3.73359000	0.12542700	-4.86139800	H	6.28055800	2.52869200	3.37775500
H	2.38827000	-3.84531600	-3.92474700	H	3.91813000	2.43021000	4.13248900
H	2.54884200	-1.95307300	-5.52716400	H	2.13035000	1.83469200	2.51959800
C	6.19228000	-1.62577900	-0.44926600	C	2.43537800	1.18575400	-0.05957100
C	7.02874600	-1.95982900	-1.52201500	H	1.43317600	1.01938000	0.29687700
C	6.78105400	-1.35959200	0.79746700	H	2.69585800	0.83316800	-1.04489100
C	8.41012900	-2.02817500	-1.35485100	Br	1.66243400	3.27541800	-1.06296200
H	6.59787300	-2.17124700	-2.49606100	C	1.19474100	-0.11493600	4.39902500
C	8.15699700	-1.42893800	0.96214700	H	0.45915400	0.17465500	3.64893600
H	6.13329400	-1.09031600	1.62477700	H	0.68385200	-0.23248800	5.36051900
C	8.98149200	-1.76408500	-0.11401200	H	1.93517000	0.68351100	4.50058700
H	9.04007100	-2.29197800	-2.19979700	C	0.89330600	-2.60390600	4.05666300
H	8.59350900	-1.21764700	1.93444500	H	0.67435200	-2.85277700	5.10006100
H	10.05834000	-1.81746200	0.01669400	H	-0.04815600	-2.36734200	3.55963200
O	2.51521300	-1.32356400	2.71710300	H	1.33503000	-3.48430600	3.57904000
C	1.87274200	-1.42847100	4.01630500	C	3.05556500	-1.70177900	4.94357500
C	4.81040200	1.67973900	0.43875800	H	3.52614600	-2.65889700	4.69867900
C	5.81411900	2.00749300	1.34136300	H	3.80383500	-0.90994500	4.84061000
C	5.49581900	2.27417400	2.67179700	H	2.71838700	-1.73335700	5.98437100
C	4.16736500	2.21894800	3.09666500				

51 catalyzed TS1 – IRC precomplex

opt=calcfc freq=noraman wb97xd/6-31g(d)/def2sv scrf=(iefpcm,solvent=dichloromethane)

Zero-point correction= 1.475825 (Hartree/Particle)
Thermal correction to Energy= 1.557387
Thermal correction to Enthalpy= 1.558331
Thermal correction to Gibbs Free Energy= 1.356719
Sum of electronic and zero-point Energies= -5672.715369
Sum of electronic and thermal Energies= -5672.632807
Sum of electronic and thermal Enthalpies= -5672.632863
Sum of electronic and thermal Free Energies= -5672.834475

I 1							
N	-2.22911400	-1.55766200	1.43945200	H	-2.86002600	0.60532800	6.22894200
H	-1.26805200	-1.89526100	1.28415000	C	-1.77870200	0.73667800	4.36329100
C	-3.17067100	-1.91610200	0.56848500	C	-0.90469200	1.75590400	4.82881300
N	-5.51948000	-1.05138900	-0.21077000	H	-1.00254200	2.09187600	5.85684700
C	-4.38283600	-1.72236600	-0.06407200	C	0.04777300	2.29351600	4.00760300
N	-3.20161700	-3.71976100	-1.31039000	H	0.73049500	3.05514400	4.36835800
C	-3.52079400	-2.73452800	-0.48789600	C	0.11636000	1.88212300	2.66083200
N	-0.69819900	0.65235600	0.76619500	H	0.81811300	2.35540500	1.98114000
H	-0.26231400	-0.24165700	0.49136700	C	-0.73169900	0.92157700	2.16731400
C	-1.01307000	1.59202800	-0.12262800	C	-1.66101200	0.25165400	3.02554400
N	-1.92222400	4.02381500	0.08865100	C	-6.52724600	-1.56761900	-1.16034700
C	-1.48096600	2.86654600	-0.38700300	H	-6.31963300	-2.63756400	-1.24956100
N	-1.05289700	1.71521500	-2.72742600	C	-7.94129700	-1.43863100	-0.59835100
C	-1.14345300	2.00951600	-1.42919900	H	-8.01757200	-1.92712500	0.37691900
C	-2.47107000	-0.86827300	2.65569000	H	-8.64320800	-1.92272700	-1.28340300
C	-3.41264300	-1.36947800	3.52410200	H	-8.25195000	-0.39441700	-0.49284800
H	-3.99192300	-2.23870500	3.22657400	C	-6.37570100	-0.91443700	-2.53445500
C	-3.59489700	-0.80677800	4.80317000	H	-5.36238600	-1.05455800	-2.92637700
H	-4.35260500	-1.21429300	5.46385000	H	-6.57572200	0.16126500	-2.48607800
C	-2.77068600	0.20168100	5.22489100	H	-7.08330600	-1.35593700	-3.24251100

C	-5.63595000	0.33660300	0.29320900	C	-2.10809400	-0.50262900	-2.73770000
H	-6.43765100	0.78302400	-0.30005900	H	-3.00758500	-0.07573900	-3.19190700
C	-6.04806700	0.37616400	1.76173900	H	-2.23926300	-0.51508900	-1.64984700
H	-6.98325800	-0.16753200	1.92100000	H	-2.00085100	-1.53892200	-3.06820000
H	-6.19294200	1.41410400	2.07837900	C	0.40005200	-0.30456600	-2.53179700
H	-5.27457700	-0.06572300	2.39578500	H	1.28388800	0.29670900	-2.76252900
C	-4.36795300	1.14374300	0.02028600	H	0.55886900	-1.30469100	-2.94349700
H	-4.06852700	1.06232200	-1.02957600	H	0.32261600	-0.41644200	-1.44843200
H	-3.53616400	0.81506300	0.65213400	O	0.41372600	-1.79722900	0.99204200
H	-4.55062700	2.19937500	0.23956400	C	1.64548200	-2.12870800	0.98432700
C	-2.01319000	-4.55566200	-1.01798900	C	2.50079200	-1.85231600	-0.07775800
H	-2.12014500	-5.43382600	-1.65906200	H	2.04580000	-1.42278500	-0.96459900
C	-0.72491400	-3.82879000	-1.39873600	N	3.84773200	-2.00917500	0.02584500
H	-0.73190400	-3.55807200	-2.45904500	C	4.68494500	-1.69384000	-0.91118500
H	0.13718300	-4.47823400	-1.21715500	C	4.26175700	-1.21233000	-2.26550600
H	-0.57732900	-2.92407000	-0.79963200	C	4.58569300	0.07650900	-2.70600600
C	-2.01313200	-5.04301900	0.42946000	C	3.51591200	-2.03491600	-3.11706300
H	-2.96136700	-5.53058600	0.67579600	C	4.15343900	0.54176600	-3.94585400
H	-1.84452800	-4.22533800	1.13657400	H	5.18573800	0.71602300	-2.06367500
H	-1.20465800	-5.76633100	0.56873900	C	3.09711000	-1.58132300	-4.36486100
C	-4.12496900	-4.09108900	-2.40118800	H	3.25921400	-3.03882100	-2.78979200
H	-4.78478000	-3.22976200	-2.52662100	C	3.40598900	-0.28759100	-4.78014400
C	-3.39478200	-4.28986600	-3.72761600	H	4.40471000	1.55021800	-4.26231200
H	-2.81752900	-3.40142600	-3.99795100	H	2.52084900	-2.23702100	-5.01160000
H	-4.13321900	-4.46934200	-4.51433100	H	3.07226600	0.07119900	-5.74960100
H	-2.72036000	-5.15131600	-3.70613500	C	6.13251200	-1.77282900	-0.60590000
C	-4.96649800	-5.30442200	-2.00790100	C	7.11020800	-1.71211600	-1.60951300
H	-5.50297400	-5.11788700	-1.07190500	C	6.56467900	-1.90622300	0.72427500
H	-4.34032800	-6.19296000	-1.87350100	C	8.46594100	-1.78075700	-1.29701400
H	-5.69901500	-5.52423900	-2.79013100	H	6.80955300	-1.61413000	-2.64862100
C	-2.01305200	4.21654300	1.55145900	C	7.91554700	-1.97758800	1.03437700
H	-1.84599900	3.22921600	1.98210300	H	5.81321400	-1.94235000	1.50535200
C	-3.40989200	4.66288600	1.98030000	C	8.87836100	-1.91331000	0.02582800
H	-4.17403400	3.97553800	1.60607500	H	9.20266300	-1.73423800	-2.09449300
H	-3.65073200	5.67479900	1.63975600	H	8.22235700	-2.07637600	2.07248400
H	-3.46012400	4.66496900	3.07330800	H	9.93566800	-1.96535400	0.26929500
C	-0.91688500	5.15419500	2.05252000	O	2.19171700	-2.80584900	2.02279900
H	0.06366800	4.81581800	1.70352800	C	1.57269200	-2.93527800	3.32059300
H	-0.91261100	5.17108800	3.14660100	C	4.97220400	2.04780200	0.45812400
H	-1.07673500	6.17925500	1.69999700	C	6.01365800	1.91473900	1.36837200
C	-2.19721400	5.15422200	-0.81767500	C	5.80827500	1.23301000	2.56723200
H	-2.61641700	5.93482200	-0.17914600	C	4.55961200	0.68659300	2.84934000
C	-3.27751400	4.78297600	-1.83376300	C	3.51933300	0.81409600	1.93386200
H	-4.21452900	4.55524600	-1.31678900	C	3.72029200	1.48982800	0.73079100
H	-3.00737900	3.90677200	-2.43009400	H	5.12469300	2.59051700	-0.47180500
H	-3.45374700	5.61581200	-2.52039500	H	6.98625900	2.34166400	1.14445500
C	-0.90673600	5.71746100	-1.41854900	H	6.62215100	1.12581000	3.27782500
H	-0.32832500	4.95710600	-1.94962200	H	4.39772300	0.15306500	3.78134000
H	-0.26442700	6.11924600	-0.62951100	H	2.55167200	0.36743400	2.14155600
H	-1.13788000	6.52431000	-2.12003300	C	2.61326400	1.58800800	-0.26411800
C	-0.83561500	2.77539400	-3.72853800	H	1.76847500	0.95499800	-0.00164100
H	-1.08803300	3.70714000	-3.22371200	H	2.93468600	1.37128400	-1.28143300
C	0.63956200	2.84458500	-4.12782200	Br	1.88891100	3.43582200	-0.37189700
H	1.25851500	3.00045700	-3.23830600	C	1.36163000	-1.56346000	3.95837300
H	0.80289300	3.67638700	-4.82008100	H	0.71042300	-0.94645200	3.33890200
H	0.96696500	1.92367800	-4.62318200	H	0.89687900	-1.67434600	4.94388100
C	-1.77779100	2.63507200	-4.92166800	H	2.32051200	-1.05143000	4.08719700
H	-2.81654300	2.54557400	-4.58888900	C	0.26920600	-3.73703000	3.25770900
H	-1.53564600	1.76647600	-5.54220700	H	0.02381800	-4.11648900	4.25539900
H	-1.69199100	3.52309600	-5.55463500	H	-0.56760000	-3.12964000	2.91231200
C	-0.86788700	0.30403000	-3.11299000	H	0.38628000	-4.59123500	2.58357900
H	-0.77585400	0.31022400	-4.20089100	C	2.62073200	-3.72457000	4.10625400

H	2.76735300	-4.71374500	3.66089500	H	2.30163800	-3.85272500	5.14540700
H	3.57813900	-3.19493900	4.09460000				

51 catalyzed TS1 – IRC product

opt=calcfrc freq=noraman wb97xd/6-31g(d)/def2sv scrf=(iefpcm,solvent=dichloromethane)

Zero-point correction= 1.480009 (Hartree/Particle)
Thermal correction to Energy= 1.561225
Thermal correction to Enthalpy= 1.562169
Thermal correction to Gibbs Free Energy= 1.360549
Sum of electronic and zero-point Energies= -5672.775055
Sum of electronic and thermal Energies= -5672.693839
Sum of electronic and thermal Enthalpies= -5672.692895
Sum of electronic and thermal Free Energies= -5672.894514

1 1							
N	-1.19889700	1.03192800	-2.16053000	H	-5.92495000	2.36630800	-0.62240300
H	-0.22650600	0.84543400	-1.92323500	C	-5.43245000	1.52212600	-2.52539300
C	-1.73514800	2.17360500	-1.72834200	H	-5.86067500	2.34368100	-3.10603800
N	-4.10787100	3.14257400	-1.17734900	H	-6.17834600	0.72458700	-2.45118400
C	-2.80721100	2.95424500	-1.34008600	H	-4.56769900	1.12559500	-3.06521000
N	-0.62628600	4.35557200	-0.85395700	C	-4.46698400	0.85532800	-0.27536000
C	-1.50171400	3.43176400	-1.21488500	H	-4.14371500	1.22431400	0.70382600
N	-1.22908900	-0.98260600	-0.27086900	H	-3.61667700	0.36975100	-0.76513300
H	-0.31904500	-0.53794500	-0.19164400	H	-5.23387000	0.09161600	-0.11771900
C	-1.97574000	-1.09131800	0.82953300	C	0.77400100	4.22860500	-1.31819900
N	-4.13773100	-2.38754200	1.46068100	H	1.22787900	5.20594200	-1.13866600
C	-3.07023500	-1.59560800	1.49121300	C	1.53039600	3.18791100	-0.49554000
N	-1.84123300	0.05603900	3.15066000	H	1.59982400	3.49031800	0.55307100
C	-2.21856300	-0.69895800	2.12271800	H	2.54568700	3.06536700	-0.88612100
C	-1.83437800	0.08132900	-3.00386200	H	1.04219400	2.20904800	-0.53306000
C	-2.34291400	0.50770200	-4.20781900	C	0.84309400	3.96438100	-2.82156900
H	-2.31453700	1.56733100	-4.44530600	H	0.27549800	4.71919900	-3.37390700
C	-2.84408300	-0.41523800	-5.14792700	H	0.45241600	2.97598700	-3.08346800
H	-3.25298500	-0.05429800	-6.08554900	H	1.88515900	4.00424200	-3.15129800
C	-2.74557700	-1.75805400	-4.89825000	C	-1.08331100	5.58054000	-0.16846100
H	-3.06909400	-2.48228200	-5.63990100	H	-2.07759400	5.34188400	0.21744700
C	-2.21660100	-2.23461500	-3.67054900	C	-0.20601100	5.91295400	1.03658100
C	-2.08930800	-3.62990700	-3.43505200	H	-0.16201500	5.07165600	1.73372000
H	-2.38130900	-4.31712100	-4.22375100	H	-0.63522200	6.77067700	1.56194100
C	-1.60234400	-4.10016900	-2.24563100	H	0.81429700	6.18246100	0.74617600
H	-1.48650700	-5.16539800	-2.07558300	C	-1.19907300	6.74259400	-1.15364600
C	-1.28694600	-3.19498800	-1.21058200	H	-1.86767600	6.48424200	-1.98140900
H	-0.97841100	-3.54589500	-0.22745100	H	-0.22164200	7.00509700	-1.57225100
C	-1.42242400	-1.84212300	-1.39572300	H	-1.59800800	7.62717000	-0.64863100
C	-1.81633000	-1.30652500	-2.66245700	C	-4.31920200	-3.26450800	0.28697400
C	-4.58308300	4.48201100	-0.77119100	H	-3.68503200	-2.83201000	-0.48872600
H	-3.77791400	5.16899200	-1.04561200	C	-5.75423700	-3.22643700	-0.23324700
C	-5.81537300	4.90276300	-1.56887900	H	-6.08269900	-2.19631300	-0.40124400
H	-5.62482500	4.83302400	-2.64337200	H	-6.46015700	-3.71145500	0.44853800
H	-6.05868400	5.94164600	-1.32841500	H	-5.80090800	-3.76197800	-1.18632500
H	-6.69258000	4.29453600	-1.32695400	C	-3.82692400	-4.68231800	0.57465500
C	-4.80207900	4.55189300	0.73979300	H	-2.82603100	-4.65134400	1.01890000
H	-3.89217100	4.26762900	1.27943000	H	-3.78890000	-5.25919400	-0.35516900
H	-5.60906700	3.88228900	1.05565000	H	-4.50073200	-5.20152900	1.26586700
H	-5.07480100	5.56991200	1.03333800	C	-4.92435300	-2.60970300	2.68658000
C	-5.03340500	1.98741300	-1.12787100	H	-5.73940500	-3.27255400	2.38770900

C	-5.56900900	-1.29948300	3.14355800	C	2.21133000	-4.01725000	-0.49109600
H	-6.25144300	-0.93126900	2.37135200	C	3.19407400	-3.03923800	-0.32054800
H	-4.83123600	-0.51464600	3.33436200	H	5.13813000	-2.37222200	-0.95331600
H	-6.13715800	-1.45777000	4.06471200	H	5.45937000	-4.20985300	-2.57701500
C	-4.10898700	-3.34270400	3.75931300	H	3.68124200	-5.91599400	-2.89917300
H	-3.10662000	-2.92178500	3.87650500	H	1.60549200	-5.79650200	-1.53378000
H	-3.96817900	-4.39019900	3.47989100	H	1.32085400	-3.98392100	0.13263800
H	-4.62545600	-3.30926500	4.72347000	C	2.95695500	-1.91959100	0.67245100
C	-2.31067700	-0.23458000	4.51673100	H	1.94285300	-2.01219800	1.07767200
H	-3.11609900	-0.95817500	4.39695000	H	3.63874400	-2.01170100	1.52556400
C	-1.21236200	-0.90330300	5.34338600	Br	-0.30870900	-3.48590500	2.39574500
H	-0.82455500	-1.77580800	4.80685200	C	1.73422400	-1.93401500	-3.63663100
H	-1.61947700	-1.22479000	6.30734800	H	0.83789400	-1.75534700	-3.04125200
H	-0.38457300	-0.21327100	5.54293100	H	1.42763200	-2.12379400	-4.67014300
C	-2.89845800	1.00809700	5.18115400	H	2.24168700	-2.82383000	-3.25337300
H	-3.68333200	1.44793700	4.55760300	C	2.02005100	0.54724900	-4.12149400
H	-2.13744100	1.77267700	5.36964600	H	1.87217200	0.46998800	-5.20284700
H	-3.33521900	0.73428200	6.14623800	H	1.04522300	0.71359400	-3.66183900
C	-0.71228700	0.98171300	2.94821200	H	2.66160600	1.41135200	-3.92271800
H	-0.56895100	1.48086600	3.90959900	C	3.94996800	-1.03577000	-4.39876000
C	-1.07906600	2.04557000	1.91563000	H	4.64221100	-0.18947900	-4.35333600
H	-1.99946000	2.56831400	2.19490100	H	4.44337900	-1.91887900	-3.98329600
H	-1.22583800	1.59423600	0.92792400	H	3.70420400	-1.22980100	-5.44679900
H	-0.27044200	2.77603700	1.82918700				
C	0.58650900	0.26534700	2.59085600				
H	0.83655700	-0.50658500	3.32102500				
H	1.40078900	0.99424600	2.54492600				
H	0.51245400	-0.22674900	1.61838300				
O	1.22684200	-0.12566600	-1.24319800				
C	2.43429500	-0.34760400	-1.20768200				
C	3.15442800	-0.47395200	0.12550400				
H	2.63121000	0.20457000	0.80693600				
N	4.55710600	-0.16106500	-0.00842900				
C	5.13379000	0.58715800	0.85118200				
C	4.44873400	1.20521500	2.03741900				
C	4.26887600	0.48256000	3.21881700				
C	3.98982300	2.52244400	1.96236900				
C	3.63425800	1.07084500	4.31010100				
H	4.63387500	-0.53805500	3.28873700				
C	3.34035900	3.10392000	3.04788900				
H	4.14401000	3.09153800	1.05041300				
C	3.16442200	2.37940200	4.22525500				
H	3.50139800	0.50275700	5.22535700				
H	2.97972500	4.12590300	2.97547900				
H	2.66573500	2.83432300	5.07551900				
C	6.58281800	0.88266900	0.66176100				
C	7.32349200	1.53721700	1.65063400				
C	7.22278200	0.49625900	-0.52345900				
C	8.67929700	1.79425000	1.46202800				
H	6.84454300	1.84240200	2.57549600				
C	8.57296700	0.75636200	-0.71131900				
H	6.64177100	-0.00566200	-1.29016900				
C	9.30665200	1.40574600	0.28267700				
H	9.24382200	2.29831400	2.24049200				
H	9.05737100	0.45424800	-1.63496700				
H	10.36341900	1.60688700	0.13501700				
O	3.19502800	-0.53667000	-2.25096400				
C	2.67587100	-0.73435700	-3.61758900				
C	4.36956300	-3.12893800	-1.07529200				
C	4.54245400	-4.15736200	-1.99626500				
C	3.54637600	-5.11724800	-2.17544100				
C	2.38355200	-5.04773800	-1.41374300				

References

1. Hofmann, A. W.; *Proc. R. Soc. Lond.* **1856**, 8, 1-3.
2. Kekulé, F. A.; *Bulletin de la Societe Chimique de Paris* **3**: 98–110.
3. Hückel, E.; *Z. Physik*, **1931**, 70, 204–86.
4. Yates, K.; *Hückel Molecular Orbital Theory*, **1978**, Academic Press Inc. (London) Ltd., Chapter II & III, 27-120.
5. George, D. V.; *Principles of Quantum Chemistry*, **1972**, Pergamon Press Inc., Chapter 12: Hückel Molecular-orbital Theory, 210-225.
6. Roberts, J. D.; Streitwieser, A. Jr.; Regan, C. M.; *J. Am. Chem. Soc.* **1952**, 74, 4579-4582.
7. Craig, D. P.; *J. Chem. Soc.* **1951**, 3175-3183.
8. Breslow, R.; *J. Am. Chem. Soc.* **1957**, 79, 5318-5319.
9. Breslow, R.; Yuan, C.; *J. Am. Chem. Soc.* **1958**, 80, 5991-5994.
10. Krebs, A. W.; *Angew. Chem. Int. Ed.* **1965**, 4, 10-22.
11. Farnum, D. G.; Burr, M.; *J. Am. Chem. Soc.* **1960**, 82, 2651.
12. Breslow, R.; Hover, H.; Chang, H. W.; *J. Am. Chem. Soc.* **1962**, 84, 3168-3174.
13. Kende, A. S.; *J. Am. Chem. Soc.* **1963**, 85, 1882-1884.
14. Wiberg, K. B.; Bartley, W. J.; Lossing, F. P.; *J. Am. Chem. Soc.* **1962**, 84, 3980-3981.
15. (a) Glass, G. P.; Kistiakowsky, G. B.; *J. Chem. Physics.* **1964**, 40, 1448-1449;
(b) Kistiakowsky, G. B.; Michael, J. V.; *J. Chem. Physics.* **1964**, 40, 1447-1448.
16. (a) Tobey, S. W.; West, R.; *J. Am. Chem. Soc.* **1964**, 86, 1459;
(b) Tobey, S. W.; West, R.; *J. Am. Chem. Soc.* **1964**, 86, 4215-4216.
17. Breslow, R.; Groves, J. T.; *J. Am. Chem. Soc.* **1970**, 92, 984-987.
18. Schneider, W. G.; Spiesecke, H.; *Tett. Lett.* **1961**, 14, 468-472.
19. Tobey, S. W.; West, R.; *Tett. Lett.* **1963**, 4, 1179-1182.
20. Tobey, S. W.; West, R.; *J. Am. Chem. Soc.* **1965**, 88, 2478-2481.

21. Tobey, S. W.; West, R.; *J. Am. Chem. Soc.* **1965**, *88*, 2481-2488.
22. Soulen, R. L.; Sepiol, J.; *J. Org. Chem.* **1975**, *40*, 3791-3793.
23. D'yakonov, I. D.; Kostikov, R. R.; *Rus. Chem. Rev.* **1967**, *36*, 557-563.
24. Manatt, S. L.; Roberts, J. D.; *J. Org. Chem.* **1959**, *24*, 1336-1342.
25. Breslow, R.; Chang, H. W.; *J. Am. Chem. Soc.* **1961**, *83*, 2367-2375.
26. Breslow, R.; Lockhart, J.; Chang, H. W.; *J. Am. Chem. Soc.* **1961**, *83*, 2375-2382.
27. (a) Yoshida, Z.; Tawara, J.; *J. Am. Chem. Soc.* **1971**, *93*, 2573-2574;
(b) Yoshida, Z.; Ogoshi, H.; Hirota, S.; *Tett. Lett.* **1973**, *14*, 869-872.
28. Weiss, R.; Hertel, M.; *J. Chem. Soc., Chem Commun.* **1980**, 223-224.
29. Weiss, R.; Priesner, C.; *Angew. Chem. Int. Ed.* **1978**, *17*, 445.
30. Weiss, R.; Priesner, C.; Wolfe, H.; *Angew. Chem. Int. Ed.* **1978**, *17*, 446.
31. Weiss, R.; Miess, G.-E.; Haller, A.; Reinhardt, W.; *Angew. Chem. Int. Ed.* **1986**, *25*, 103-104.
32. Huiying, L.; Kangtai, R.; Douglas C. N.; *J. Org. Chem.* **2001**, *66*, 8556-8562.
33. Bandar, J.; Lambert, T.; *J. Am. Chem. Soc.* **2012**, *134*, 5552-5555.
34. Ishikawa, T.; *Superbases for Organic Synthesis: Guanidines, Amidines, and Phosphazenes and Related Organocatalysts*, **2009**, New York: John Wiley and Sons.
35. Mirabdolbaghi, R.; Dudding, T.; *Org. Lett.* **2014**, *16*, 2790-2793.
36. Cox, D. P.; Terpinski, J.; Lawrynowicz, W.; *J. Org. Chem.* **1984**, *49*, 3216-3221.
37. a) Mirabdolbaghi, R.; Dudding, T.; *Org. Lett.* **2015**, *17*, 1930-1933.
b) Mirabdolbaghi, R.; Dudding, T.; *J. Org. Chem.* **2016**, *81*, 2675-2679.
38. a) Kovacevic, B.; Maksic, Z.; *J. Phys. Chem. A.* **1999**, *103*, 6678-6684;
b) Z. Gattin, B. Kovacevic, Z. Maksic, *Eur. J. Org. Chem.* **2005**, *2005*, 3206-3213.
39. Sauer, M.; Yeung, C.; Chong, J. H.; Patrick, B. O.; MacLachlan M. J.; *J. Org. Chem.* **2006**, *71*, 775-778.

40. McNaught, A. D.; Wilkinson, A.; *Compendium of Chemical Terminology*, 2nd ed. **1997**, (The "Gold Book"), IUPAC, Blackwell Scientific Publications, Oxford, UK.
41. Lide, D. R.; *CRC Handbook of Chemistry and Physics, Student Edition*, 84th ed. **2004**, CRC Press.
42. Loudon, M. G.; *Organic Chemistry*, 4th ed. **2005**, New York: Oxford University Press, 317-318.
43. March, J.; Smith, M.; *Advanced Organic Chemistry*, 6th ed. **2007**, New York: John Wiley and Sons, Chapter 8: Acids and Bases.
44. Haflinger, G.; Kuske, F. K. H.; *The Chemistry of Amidines and Imidates*. **1991**, 2, 1–100.
45. Ishikawa, T.; *Superbases for Organic Synthesis: Guanidines, Amidines, and Phosphazenes and Related Organocatalysts*, **2009**, New York: John Wiley and Sons.
46. Raczynska, E. D.; Cyranski, M. K.; Gutowski, M.; Rak, J.; Gal, J.; Maria, P.; Darowska, M.; Dumczmal, K.; *J. Phys. Org. Chem.* **2003**, 16, 91–106.
47. Schwesinger, R.; Misssfeldt, M.; Peters, K.; von Schnering, A. G.; *Angew. Chem. Int. Ed.* **1987**, 26, 1165–1167.
48. Kurzer, F.; Pitchfork, E. D.; *Fortschr. Chem. Forsch.* **1968**, 10, 375472.
49. Chamorro, E.; Escobar, C. A.; Sienra, R.; Perez, P. J.; *J. Phys. Chem.* **2005**, 109, 10068–10076.
50. Alder, R. W.; *Chem. Rev.* **1989**, 89, 1215–1223.
51. Schwesinger, R.; *Chimia.* **1985**, 39, 269–272.
52. a) Schwesinger, R.; Schlemper, H.; *Angew. Chem. Int. Ed.* **1987**, 26, 1167–1169;
b) Schwesinger, R.; Hasenfratz, C.; Schlemper, H.; Walz, L.; Peters, E.; Peters, K.; Georg von Schnering, H.; *Angew. Chem. Int. Ed.* **1993**, 32, 1361–1363.
53. a) Schwesinger, R.; Schlemper, H.; Hasenfratz, C.; et al., *Liebigs Annalen.* **1996**, 1055–1081;
b) Koppel, I. A.; Schwesinger, R.; Breuer T.; Burk, P.; Herodes, K.; Leito, I.; Mishima, M.; *J. Phys. Chem. A.* **2001**, 105, 9575–9586.

54. a) Allen, C. W.; *Coord. Chem. Rev.*, **1994**, *130*, 137–173;
b) Allen, C. W.; *Organophosph. Chem.* **1996**, *27*, 308–351;
c) Kondo, Y.; Ueno, M.; Tanaka, Y.; *J. Syn. Org. Chem.* **2005**, *63*, 453–463.
55. a) Kisanga, P. B.; Verkade, J. G.; Schwesinger, R.; *J. Org. Chem.* **2000**, *65*, 5431–5432;
b) Verkade, J. G.; Kisanga, P. B.; *Tetrahedron.* **2003**, *59*, 7819–7858;
c) Verkade, J. G.; Kisanga, P. B.; *Aldrichimica Acta.* **2004**, *37*, 3–14.
56. a) Alder, R. W.; Bowman, P. S.; Steele, W. R.; Winterman, D. R.; *Chem. Comm.* **1968**, 723–724;
b) Alder, R. W.; Bryce, M. R.; Goode, N. C.; *J. Chem. Soc. Perkin Trans I.* **1981**, *11*, 2840–2847.
57. Raab, V.; Kipke, J.; Gschwind, R. M.; Sundermyer, J.; *Chem. - Eur. J.* **2002**, *8*, 1682–1693.
58. Raab, V.; Gauchenova, E.; Merkoulov, A.; Harms, K.; Sundermeyer, J.; Kovacevic, B.; Maksic, Z. B.; *J. Am. Chem. Soc.* **2005**, *127*, 15738–15743.
59. Kovacevic, B.; Maskic, Z. B.; *Chem. – Eur. J.* **2002**, *8*, 1694–1702.
60. Caubère, P.; *Chem. Rev.* **1993**, *93*, 2317–2334.
61. Schlosser, M.; *Mod. Syn. Methods.* **1992**, *6*, 227–271.
62. Raczynska, E. D.; Decouzon, M.; Gal, J.; Maria, P.; Wozniak, K.; Krug, R.; Cairns, S.; *Trends Org. Chem.* **1998**, *7*, 95–103.
63. Lau, Y. K.; Saluya, P. S.; Kebarle, P.; Alder, R. W.; *J. Am. Chem. Soc.* **1978**, *100*, 7328–7333.
64. Platts, J. A.; Howard, S. T.; *J. Org. Chem.* **1994**, *59*, 4647–4651.
65. Guo, H.; Salahub, D. R.; *J. Mol. Struct. (Theochem).* **2001**, *547*, 113–118.
66. Belding, L.; Dudding, T.; *Chem. - Eur. J.* **2013**, *20*, 1032–1037
67. Mallinson, P. R.; Wozniak, K.; Smith, G. T.; McCormack, K. L.; *J. Am. Chem. Soc.* **1997**, *119*, 11502–11509.
68. Howard, S. T.; *J. Am. Chem. Soc.* **2000**, *122*, 8238–8244.
69. Llamas-Saiz, A. L.; Foces-Foces, C.; Elguero, J.; *J. Mol. Struct.* **1994**, *328*, 297–323.

70. Korzhenevskaya, N. G.; Schroeder, G.; Brzezinski, B.; Rybachenko, V. I.; *Russ. J. Org. Chem.* **2001**, *37*, 1603–1610.
71. Pozharskii, A. F.; Ozeryanskii, V. A.; Starykova, Z. A.; *J. Chem. Soc., Perkin Trans. 2.* **2002**, 318–322.
72. Korzhenevskaya, N. G.; Rybachenko, V. I.; Schroeder, G.; *Tetrahedron Lett.* **2002**, *43*, 6043–6045.
73. Kim, I. S.; Zee, O. P.; Jung, Y. H.; *Org. Lett.* **2006**, *8*, 4101–4104.
74. Diem, M. J.; Burow, D.F.; Fry, J.L.; *J. Org. Chem.* **1977**, *42*, 1801–1802.
75. a) Hansen, D. B.; Wan, X.; Carroll, P. J.; Joullie, M. M.; *J. Org. Chem.* **2005**, *70*, 3120–3126;
b) Hansen, D. B.; Joullie, M. M.; *Tetrahedron: Asymmetry*, **2005**, *16*, 3963–3969.
76. Keyes, R. F.; Carter, J. J.; Zhang, X.; Ma, Z.; *Org. Lett.* **2005**, *7*, 847–849.
77. Belding, L.; Stoyanov, P.; Dudding, T.; *J. Org. Chem.* **2016**, *81*, 6–13.
78. Greene, T. W.; Wuts, P. G. M.; *Greene's Protective Groups in Organic Chemistry*, 4th ed. **2007**, New Jersey: John Wiley and Sons.
79. Modified synthesis taken from: Aranyos, A.; Old, D. W.; Kiyomori, A.; Wolfe, J. P.; Sadighi, J. P.; Buchwald, S. L.; *J. Am. Chem. Soc.* **1999**, *121*, 4369–4378.
80. Solomons, T. W.; Fryhle, C. B.; *Organic Chemistry*, 10th ed. **2011**, New York: John Wiley and Sons.
81. Shendage, D. M.; Frohlich, R.; Haufe, G.; *Organic Lett.* **2004**, *6*, 3675–3678.
82. Starks, C. M.; *J. Am. Chem. Soc.* **1971**, *93*, 195–199.
83. (a) Szemik-Hojniak, A.; Rettig, W.; Deperasińska, I.; *Chem. Phys. Lett.* **2001**, *343*, 404–412;
(b) Szemik-Hojniak, A.; Balkowski, G.; Wurlpel, G. W. H.; Herbich, J.; van der Waals, J. H.; Buma, W. J.; *J. Phys. Chem. A* **2004**, *108*, 10623–10631;
(c) Balkowski, G.; Szemik-Hojniak, A.; van Stokkum, I. H. M.; Zhang, H.; Buma, W. J.; *J. Phys. Chem. A* **2005**, *109*, 3535–3541.

84. (a) Raab, V.; Kipke, J.; Gschwind, R. M.; Sundermeyer, J.; *Chem.-Eur. J.* **2002**, *8*, 1682–1693;
 (b) Raab, V.; Gauchenova, E.; Merkoulov, A.; Harms, K.; Sundermeyer, J.; Kovačević, B.; Maksic, Z. B.; *J. Am. Chem. Soc.* **2005**, *127*, 15738–15743;
 (c) Belding, L.; Dudding, T.; *Chem. - Eur. J.* **2014**, *20*, 1032–1037.
85. (a) Weiss, R.; Brenner, T.; Hampel, F.; Wolski, A.; *Angew. Chem.* **1995**, *107*, 481–483;
 (b) Weiss, R.; Brenner, T.; Hampel, F.; Wolski, A. *Angew. Chem., Int. Ed.* **1995**, *34*, 439–441;
 (c) Weiss, R.; Rechinger, M.; Hampel, F.; Wolski, A.; *Angew. Chem., Int. Ed.* **1995**, *34*, 441–443.
86. (a) Szemik-Hojniak, A.; Zwier, J. M.; Buma, W. J.; Bursi, R.; van der Waals, J. H.; *J. Am. Chem. Soc.* **1998**, *120*, 4840–4844;
 (b) Szemik-Hojniak, A.; Rettig, W.; Deperasińska, I.; *Chem. Phys. Lett.* **2001**, *343*, 404–412.
87. (a) Schleyer, P. v. R.; Maerker, C.; Dransfeld, A.; Jiao, H.; Hommes, N. J. R. v. E.; *J. Am. Chem. Soc.* **1996**, *118*, 6317–6318;
 (b) Chen, Z. F.; Wannere, C. S.; Corminboeuf, C.; Puchta, R.; Schleyer, P. v. R.; *Chem. Rev.* **2005**, *105*, 3842–3888;
 (c) Schleyer, P. v. R.; Jiao, H.; Hommes, N. J. R. v. E.; Malkin, V. G.; Malkina, O. L.; *J. Am. Chem. Soc.* **1997**, *119*, 12669–12670;
 (d) von RaguéSchleyer, P.; Manoharan, M.; Wang, Z.-X.; Kiran, B.; Jiao, H.; Puchta, R.; van Eikema Hommes, N. J. R.; *Org. Lett.* **2001**, *3*, 2465–2468;
 (e) Fallah-Bagher-Shaidaei, H.; Wannere, C. S.; Corminboeuf, C.; Puchta, R.; Schleyer, P. v. R.; *Org. Lett.* **2006**, *8*, 863–866.
88. (a) Bandar, J. S.; Lambert, T. H.; *J. Am. Chem. Soc.* **2013**, *135*, 11799–11802;
 (b) Wilde, M. M. D.; Gravel, M.; *Angew. Chem., Int. Ed.* **2013**, *52*, 12651–12654.
89. Bandar, J. S.; Tanaset, A.; Lambert, T. A.; *Chem. - Eur. J.* **2015**, *21*, 7365–7368.
90. (a) Curnow, O. J.; MacFarlane, D. R.; Walst, K.; *Chem. Commun.* **2011**, *47*, 10248–10250;
 (b) Curnow, O. J.; Holmes, M. T.; Ratten, L. C.; Walst, K. J.; Yunis, R.; *RSC Adv.* **2012**, *2*, 10794–10797.
91. (a) Bruns, H.; Patil, M.; Carreras, J.; Vazquez, A.; Thiel, W.; Goddard, R.; Alcarazo, M.; *Angew. Chem., Int. Ed.* **2010**, *49*, 3680–3683;
 (b) Kozma, Á.; Gopakumar, G.; Farès, C.; Thiel, W.; Alcarazo, M.; *Chem.-Eur. J.* **2013**, *19*, 3542–3546.
92. (a) Hashimoto, T.; Maruoka, K.; *Chem. Rev.* **2007**, *107*, 5656–5682;

- (b) Denmark, S. E.; Gould, N. D.; Wolf, L. M.; *J. Org. Chem.* **2011**, *76*, 4260–4336;
- (c) Yang, X.; Phipps, R. J.; Toste, F. D.; *J. Am. Chem. Soc.* **2014**, *136*, 5225–5228;
- (d) Woźniak, Ł.; Murphy, J. J.; Melchiorre, P.; *J. Am. Chem. Soc.* **2015**, *137*, 5678–5681.
93. (a) Jayachandran, P.; Wang, M.-L.; *Synth. Commun.* **1999**, *29*, 4101–4112;
(b) Balakrishnan, T.; Jayachandran, J. P.; *Synth. Commun.* **1995**, *25*, 3821;
(c) Balakrishnan, T.; Jayachandran, J. P.; *J. Chem. Soc., Perkin Trans. 2* **1995**, 2081.
94. (a) Bernal, P.; Fernandez, R.; Lassaletta, J. M.; *Chem. - Eur. J.* **2010**, *16*, 7714–7718;
(b) Johnson, K. M.; Rattley, M. S.; Sladojevich, F.; Barber, D. M.; Nuñez, M. G.; Goldys, A. M.; Dixon, D. J.; *Org. Lett.* **2012**, *14*, 2492–2495;
(c) Novacek, J.; Waser, M.; *Eur. J. Org. Chem.* **2013**, *2013*, 637–648;
(d) Wang, B.; Liu, Y.; Sun, C.; Wei, Z.; Cao, J.; Liang, D.; Lin, Y.; Duan, H.; *Org. Lett.* **2014**, *16*, 6432–6435;
(e) Shirakawa, S.; Koga, K.; Tokuda, T.; Yamamoto, K.; Maruoka, K. *Angew. Chem., Int. Ed.* **2014**, *53*, 6220–6223;
(f) Parvez, Md. M.; Haraguchi, N.; Itsuno, S.; *Macromolecules* **2014**, *47*, 1922–1928;
(g) Li, M.; Woods, P. A.; Smith, M. D.; *Chem. Sci.* **2013**, *4*, 2907–2911.
95. O'Donnell, M. J.; Eckrich, T. M.; *Tetrahedron Lett.* **1978**, *19*, 4625–4628.
96. Belding, L.; Stoyanov, P.; Dudding, T.; *J. Org. Chem.* **2016**, *81*, 553–558.
97. Makosza, M.; Lasek, W.; *J. Phys. Org. Chem.* **1993**, *6*, 412–420.
98. Herriott, A.; Picker, D.; *J. Am. Chem. Soc.* **1975**, *97*, 2345–2349.
99. Belding, L.; Taimoory, S. M.; Dudding, T.; *ACS Catal.* **2015**, *5*, 343–349.
100. Meirovitch, H.; Scheraga, H. A.; *Macromolecules* **1980**, *13*, 1406–1414.
101. (a) Pozharskii, A. F.; Ryabtsova, O. V.; Ozeryanskii, V. A.; Degtyarev, A. V.; Kazheva, O. N.; Alexandrov, G. G.; Dyachenko, O. A.; *J. Org. Chem.* **2003**, *68*, 10109–10122.
(b) Pozharskii, A. F.; Degtyarev, A. V.; Ryabtsova, O. V.; Ozeryanskii, V. A.; Kletskii, M. W.; Starikova, Z. A.; Sobczyk, L.; Filarowski, A. *J. Org. Chem.* **2007**, *72*, 3006–3019.

102. (a) Weiss, R.; Schloter, K.; *Tetrahedron Lett.* **1975**, *16*, 3491–3494.
(b) Azhar Hashmi, S. M.; Prasanna, S.; Radhakrishnan, T. P.; *Synth. Met.* **1992**, *48*, 39–47.

References

1. Hofmann, A. W.; *Proc. R. Soc. Lond.* **1856**, 8, 1-3.
2. Kekulé, F. A.; *Bulletin de la Societe Chimique de Paris* **3**: 98–110.
3. Hückel, E.; *Z. Physik*, **1931**, 70, 204–86.
4. Yates, K.; *Hückel Molecular Orbital Theory*, **1978**, Academic Press Inc. (London) Ltd., Chapter II & III, 27-120.
5. George, D. V.; *Principles of Quantum Chemistry*, **1972**, Pergamon Press Inc., Chapter 12: Hückel Molecular-orbital Theory, 210-225.
6. Roberts, J. D.; Streitwieser, A. Jr.; Regan, C. M.; *J. Am. Chem. Soc.* **1952**, 74, 4579-4582.
7. Craig, D. P.; *J. Chem. Soc.* **1951**, 3175-3183.
8. Breslow, R.; *J. Am. Chem. Soc.* **1957**, 79, 5318-5319.
9. Breslow, R.; Yuan, C.; *J. Am. Chem. Soc.* **1958**, 80, 5991-5994.
10. Krebs, A. W.; *Angew. Chem. Int. Ed.* **1965**, 4, 10-22.
11. Farnum, D. G.; Burr, M.; *J. Am. Chem. Soc.* **1960**, 82, 2651.
12. Breslow, R.; Hover, H.; Chang, H. W.; *J. Am. Chem. Soc.* **1962**, 84, 3168-3174.
13. Kende, A. S.; *J. Am. Chem. Soc.* **1963**, 85, 1882-1884.
14. Wiberg, K. B.; Bartley, W. J.; Lossing, F. P.; *J. Am. Chem. Soc.* **1962**, 84, 3980-3981.
15. (a) Glass, G. P.; Kistiakowsky, G. B.; *J. Chem. Physics.* **1964**, 40, 1448-1449;
(b) Kistiakowsky, G. B.; Michael, J. V.; *J. Chem. Physics.* **1964**, 40, 1447-1448.
16. (a) Tobey, S. W.; West, R.; *J. Am. Chem. Soc.* **1964**, 86, 1459;
(b) Tobey, S. W.; West, R.; *J. Am. Chem. Soc.* **1964**, 86, 4215-4216.
17. Breslow, R.; Groves, J. T.; *J. Am. Chem. Soc.* **1970**, 92, 984-987.
18. Schneider, W. G.; Spiesecke, H.; *Tett. Lett.* **1961**, 14, 468-472.
19. Tobey, S. W.; West, R.; *Tett. Lett.* **1963**, 4, 1179-1182.
20. Tobey, S. W.; West, R.; *J. Am. Chem. Soc.* **1965**, 88, 2478-2481.

21. Tobey, S. W.; West, R.; *J. Am. Chem. Soc.* **1965**, *88*, 2481-2488.
22. Soulen, R. L.; Sepiol, J.; *J. Org. Chem.* **1975**, *40*, 3791-3793.
23. D'yakonov, I. D.; Kostikov, R. R.; *Rus. Chem. Rev.* **1967**, *36*, 557-563.
24. Manatt, S. L.; Roberts, J. D.; *J. Org. Chem.* **1959**, *24*, 1336-1342.
25. Breslow, R.; Chang, H. W.; *J. Am. Chem. Soc.* **1961**, *83*, 2367-2375.
26. Breslow, R.; Lockhart, J.; Chang, H. W.; *J. Am. Chem. Soc.* **1961**, *83*, 2375-2382.
27. (a) Yoshida, Z.; Tawara, J.; *J. Am. Chem. Soc.* **1971**, *93*, 2573-2574;
(b) Yoshida, Z.; Ogoshi, H.; Hirota, S.; *Tett. Lett.* **1973**, *14*, 869-872.
28. Weiss, R.; Hertel, M.; *J. Chem. Soc., Chem Commun.* **1980**, 223-224.
29. Weiss, R.; Priesner, C.; *Angew. Chem. Int. Ed.* **1978**, *17*, 445.
30. Weiss, R.; Priesner, C.; Wolfe, H.; *Angew. Chem. Int. Ed.* **1978**, *17*, 446.
31. Weiss, R.; Miess, G.-E.; Haller, A.; Reinhardt, W.; *Angew. Chem. Int. Ed.* **1986**, *25*, 103-104.
32. Huiying, L.; Kangtai, R.; Douglas C. N.; *J. Org. Chem.* **2001**, *66*, 8556-8562.
33. Bandar, J.; Lambert, T.; *J. Am. Chem. Soc.* **2012**, *134*, 5552-5555.
34. Ishikawa, T.; *Superbases for Organic Synthesis: Guanidines, Amidines, and Phosphazenes and Related Organocatalysts*, **2009**, New York: John Wiley and Sons.
35. Mirabdolbaghi, R.; Dudding, T.; *Org. Lett.* **2014**, *16*, 2790-2793.
36. Cox, D. P.; Terpinski, J.; Lawrynowicz, W.; *J. Org. Chem.* **1984**, *49*, 3216-3221.
37. a) Mirabdolbaghi, R.; Dudding, T.; *Org. Lett.* **2015**, *17*, 1930-1933.
b) Mirabdolbaghi, R.; Dudding, T.; *J. Org. Chem.* **2016**, *81*, 2675-2679.
38. a) Kovacevic, B.; Maksic, Z.; *J. Phys. Chem. A.* **1999**, *103*, 6678-6684;
b) Z. Gattin, B. Kovacevic, Z. Maksic, *Eur. J. Org. Chem.* **2005**, *2005*, 3206-3213.
39. Sauer, M.; Yeung, C.; Chong, J. H.; Patrick, B. O.; MacLachlan M. J.; *J. Org. Chem.* **2006**, *71*, 775-778.

40. McNaught, A. D.; Wilkinson, A.; *Compendium of Chemical Terminology*, 2nd ed. **1997**, (The "Gold Book"), IUPAC, Blackwell Scientific Publications, Oxford, UK.
41. Lide, D. R.; *CRC Handbook of Chemistry and Physics, Student Edition*, 84th ed. **2004**, CRC Press.
42. Loudon, M. G.; *Organic Chemistry*, 4th ed. **2005**, New York: Oxford University Press, 317-318.
43. March, J.; Smith, M.; *Advanced Organic Chemistry*, 6th ed. **2007**, New York: John Wiley and Sons, Chapter 8: Acids and Bases.
44. Haflinger, G.; Kuske, F. K. H.; *The Chemistry of Amidines and Imidates*. **1991**, 2, 1–100.
45. Ishikawa, T.; *Superbases for Organic Synthesis: Guanidines, Amidines, and Phosphazenes and Related Organocatalysts*, **2009**, New York: John Wiley and Sons.
46. Raczynska, E. D.; Cyranski, M. K.; Gutowski, M.; Rak, J.; Gal, J.; Maria, P.; Darowska, M.; Dumczmal, K.; *J. Phys. Org. Chem.* **2003**, 16, 91–106.
47. Schwesinger, R.; Misssfeldt, M.; Peters, K.; von Schnering, A. G.; *Angew. Chem. Int. Ed.* **1987**, 26, 1165–1167.
48. Kurzer, F.; Pitchfork, E. D.; *Fortschr. Chem. Forsch.* **1968**, 10, 375472.
49. Chamorro, E.; Escobar, C. A.; Sienna, R.; Perez, P. J.; *J. Phys. Chem.* **2005**, 109, 10068–10076.
50. Alder, R. W.; *Chem. Rev.* **1989**, 89, 1215–1223.
51. Schwesinger, R.; *Chimia*. **1985**, 39, 269–272.
52. a) Schwesinger, R.; Schlemper, H.; *Angew. Chem. Int. Ed.* **1987**, 26, 1167–1169;
b) Schwesinger, R.; Hasenfratz, C.; Schlemper, H.; Walz, L.; Peters, E.; Peters, K.; Georg von Schnering, H.; *Angew. Chem. Int. Ed.* **1993**, 32, 1361–1363.
53. a) Schwesinger, R.; Schlemper, H.; Hasenfratz, C.; et al., *Liebigs Annalen*. **1996**, 1055–1081;
b) Koppel, I. A.; Schwesinger, R.; Breuer T.; Burk, P.; Herodes, K.; Leito, I.; Mishima, M.; *J. Phys. Chem. A*. **2001**, 105, 9575–9586.

54. a) Allen, C. W.; *Coord. Chem. Rev.*, **1994**, *130*, 137–173;
b) Allen, C. W.; *Organophosph. Chem.* **1996**, *27*, 308–351;
c) Kondo, Y.; Ueno, M.; Tanaka, Y.; *J. Syn. Org. Chem.* **2005**, *63*, 453–463.
55. a) Kisanga, P. B.; Verkade, J. G.; Schwesinger, R.; *J. Org. Chem.* **2000**, *65*, 5431–5432;
b) Verkade, J. G.; Kisanga, P. B.; *Tetrahedron.* **2003**, *59*, 7819–7858;
c) Verkade, J. G.; Kisanga, P. B.; *Aldrichimica Acta.* **2004**, *37*, 3–14.
56. a) Alder, R. W.; Bowman, P. S.; Steele, W. R.; Winterman, D. R.; *Chem. Comm.* **1968**, 723–724;
b) Alder, R. W.; Bryce, M. R.; Goode, N. C.; *J. Chem. Soc. Perkin Trans 1.* **1981**, *11*, 2840–2847.
57. Raab, V.; Kipke, J.; Gschwind, R. M.; Sundermyer, J.; *Chem. - Eur. J.* **2002**, *8*, 1682–1693.
58. Raab, V.; Gauchenova, E.; Merkoulov, A.; Harms, K.; Sundermeyer, J.; Kovacevic, B.; Maksic, Z. B.; *J. Am. Chem. Soc.* **2005**, *127*, 15738–15743.
59. Kovacevic, B.; Maskic, Z. B.; *Chem. – Eur. J.* **2002**, *8*, 1694–1702.
60. Caubère, P.; *Chem. Rev.* **1993**, *93*, 2317–2334.
61. Schlosser, M.; *Mod. Syn. Methods.* **1992**, *6*, 227–271.
62. Raczynska, E. D.; Decouzon, M.; Gal, J.; Maria, P.; Wozniak, K.; Krug, R.; Cairns, S.; *Trends Org. Chem.* **1998**, *7*, 95–103.
63. Lau, Y. K.; Saluya, P. S.; Kebarle, P.; Alder, R. W.; *J. Am. Chem. Soc.* **1978**, *100*, 7328–7333.
64. Platts, J. A.; Howard, S. T.; *J. Org. Chem.* **1994**, *59*, 4647–4651.
65. Guo, H.; Salahub, D. R.; *J. Mol. Struct. (Theochem).* **2001**, *547*, 113–118.
66. Belding, L.; Dudding, T.; *Chem. - Eur. J.* **2013**, *20*, 1032–1037
67. Mallinson, P. R.; Wozniak, K.; Smith, G. T.; McCormack, K. L.; *J. Am. Chem. Soc.* **1997**, *119*, 11502–11509.
68. Howard, S. T.; *J. Am. Chem. Soc.* **2000**, *122*, 8238–8244.
69. Llamas-Saiz, A. L.; Foces-Foces, C.; Elguero, J.; *J. Mol. Struct.* **1994**, *328*, 297–323.

70. Korzhenevskaya, N. G.; Schroeder, G.; Brzezinski, B.; Rybachenko, V. I.; *Russ. J. Org. Chem.* **2001**, *37*, 1603–1610.
71. Pozharskii, A. F.; Ozeryanskii, V. A.; Starykova, Z. A.; *J. Chem. Soc., Perkin Trans. 2.* **2002**, 318–322.
72. Korzhenevska, N. G.; Rybachenko, V. I.; Schroeder, G.; *Tetrahedron Lett.* **2002**, *43*, 6043–6045.
73. Kim, I. S.; Zee, O. P.; Jung, Y. H.; *Org. Lett.* **2006**, *8*, 4101–4104.
74. Diem, M. J.; Burow, D.F.; Fry, J.L.; *J. Org. Chem.* **1977**, *42*, 1801–1802.
75. a) Hansen, D. B.; Wan, X.; Carroll, P. J.; Joullie, M. M.; *J. Org. Chem.* **2005**, *70*, 3120–3126;
b) Hansen, D. B.; Joullie, M. M.; *Tetrahedron: Asymmetry*, **2005**, *16*, 3963–3969.
76. Keyes, R. F.; Carter, J. J.; Zhang, X.; Ma, Z.; *Org. Lett.* **2005**, *7*, 847–849.
77. Belding, L.; Stoyanov, P.; Dudding, T.; *J. Org. Chem.* **2016**, *81*, 6–13.
78. Greene, T. W.; Wuts, P. G. M.; *Greene's Protective Groups in Organic Chemistry*, 4th ed. **2007**, New Jersey: John Wiley and Sons.
79. Modified synthesis taken from: Aranyos, A.; Old, D. W.; Kiyomori, A.; Wolfe, J. P.; Sadighi, J. P.; Buchwald, S. L.; *J. Am. Chem. Soc.* **1999**, *121*, 4369–4378.
80. Solomons, T. W.; Fryhle, C. B.; *Organic Chemistry*, 10th ed. **2011**, New York: John Wiley and Sons.
81. Shendage, D. M.; Frohlich, R.; Haufe, G.; *Organic Lett.* **2004**, *6*, 3675–3678.
82. Starks, C. M.; *J. Am. Chem. Soc.* **1971**, *93*, 195–199.
83. (a) Szemik-Hojniak, A.; Rettig, W.; Deperasińska, I.; *Chem. Phys. Lett.* **2001**, *343*, 404–412;
(b) Szemik-Hojniak, A.; Balkowski, G.; Worpel, G. W. H.; Herbich, J.; van der Waals, J. H.; Buma, W. J.; *J. Phys. Chem. A* **2004**, *108*, 10623–10631;
(c) Balkowski, G.; Szemik-Hojniak, A.; van Stokkum, I. H. M.; Zhang, H.; Buma, W. J.; *J. Phys. Chem. A* **2005**, *109*, 3535–3541.

84. (a) Raab, V.; Kipke, J.; Gschwind, R. M.; Sundermeyer, J.; *Chem.-Eur. J.* **2002**, *8*, 1682–1693;
(b) Raab, V.; Gauchenova, E.; Merkoulov, A.; Harms, K.; Sundermeyer, J.; Kovačević, B.; Maksic, Z. B.; *J. Am. Chem. Soc.* **2005**, *127*, 15738–15743;
(c) Belding, L.; Dudding, T.; *Chem. - Eur. J.* **2014**, *20*, 1032–1037.
85. (a) Weiss, R.; Brenner, T.; Hampel, F.; Wolski, A.; *Angew. Chem.* **1995**, *107*, 481–483;
(b) Weiss, R.; Brenner, T.; Hampel, F.; Wolski, A. *Angew. Chem., Int. Ed.* **1995**, *34*, 439–441;
(c) Weiss, R.; Rechinger, M.; Hampel, F.; Wolski, A.; *Angew. Chem., Int. Ed.* **1995**, *34*, 441–443.
86. (a) Szemik-Hojniak, A.; Zwier, J. M.; Buma, W. J.; Bursi, R.; van der Waals, J. H.; *J. Am. Chem. Soc.* **1998**, *120*, 4840–4844;
(b) Szemik-Hojniak, A.; Rettig, W.; Deperasińska, I.; *Chem. Phys. Lett.* **2001**, *343*, 404–412.
87. (a) Schleyer, P. v. R.; Maerker, C.; Dransfeld, A.; Jiao, H.; Hommes, N. J. R. v. E.; *J. Am. Chem. Soc.* **1996**, *118*, 6317–6318;
(b) Chen, Z. F.; Wannere, C. S.; Corminboeuf, C.; Puchta, R.; Schleyer, P. v. R.; *Chem. Rev.* **2005**, *105*, 3842–3888;
(c) Schleyer, P. v. R.; Jiao, H.; Hommes, N. J. R. v. E.; Malkin, V. G.; Malkina, O. L.; *J. Am. Chem. Soc.* **1997**, *119*, 12669–12670;
(d) von RaguéSchleyer, P.; Manoharan, M.; Wang, Z.-X.; Kiran, B.; Jiao, H.; Puchta, R.; van Eikema Hommes, N. J. R.; *Org. Lett.* **2001**, *3*, 2465–2468;
(e) Fallah-Bagher-Shaidaei, H.; Wannere, C. S.; Corminboeuf, C.; Puchta, R.; Schleyer, P. v. R.; *Org. Lett.* **2006**, *8*, 863–866.
88. (a) Bandar, J. S.; Lambert, T. H.; *J. Am. Chem. Soc.* **2013**, *135*, 11799–11802;
(b) Wilde, M. M. D.; Gravel, M.; *Angew. Chem., Int. Ed.* **2013**, *52*, 12651–12654.
89. Bandar, J. S.; Tanaset, A.; Lambert, T. A.; *Chem. - Eur. J.* **2015**, *21*, 7365–7368.
90. (a) Curnow, O. J.; MacFarlane, D. R.; Walst, K.; *Chem. Commun.* **2011**, *47*, 10248–10250;
(b) Curnow, O. J.; Holmes, M. T.; Ratten, L. C.; Walst, K. J.; Yunis, R.; *RSC Adv.* **2012**, *2*, 10794–10797.
91. (a) Bruns, H.; Patil, M.; Carreras, J.; Vazquez, A.; Thiel, W.; Goddard, R.; Alcarazo, M.; *Angew. Chem., Int. Ed.* **2010**, *49*, 3680–3683;
(b) Kozma, Á.; Gopakumar, G.; Farès, C.; Thiel, W.; Alcarazo, M.; *Chem.-Eur. J.* **2013**, *19*, 3542–3546.
92. (a) Hashimoto, T.; Maruoka, K.; *Chem. Rev.* **2007**, *107*, 5656–5682;

- (b) Denmark, S. E.; Gould, N. D.; Wolf, L. M.; *J. Org. Chem.* **2011**, *76*, 4260–4336;
- (c) Yang, X.; Phipps, R. J.; Toste, F. D.; *J. Am. Chem. Soc.* **2014**, *136*, 5225–5228;
- (d) Woźniak, Ł.; Murphy, J. J.; Melchiorre, P.; *J. Am. Chem. Soc.* **2015**, *137*, 5678–5681.
93. (a) Jayachandran, P.; Wang, M.-L.; *Synth. Commun.* **1999**, *29*, 4101–4112;
(b) Balakrishnan, T.; Jayachandran, J. P.; *Synth. Commun.* **1995**, *25*, 3821;
(c) Balakrishnan, T.; Jayachandran, J. P.; *J. Chem. Soc., Perkin Trans. 2* **1995**, 2081.
94. (a) Bernal, P.; Fernandez, R.; Lassaletta, J. M.; *Chem. - Eur. J.* **2010**, *16*, 7714–7718;
(b) Johnson, K. M.; Rattley, M. S.; Sladojevich, F.; Barber, D. M.; Nuñez, M. G.; Goldys, A. M.; Dixon, D. J.; *Org. Lett.* **2012**, *14*, 2492–2495;
(c) Novacek, J.; Waser, M.; *Eur. J. Org. Chem.* **2013**, *2013*, 637–648;
(d) Wang, B.; Liu, Y.; Sun, C.; Wei, Z.; Cao, J.; Liang, D.; Lin, Y.; Duan, H.; *Org. Lett.* **2014**, *16*, 6432–6435;
(e) Shirakawa, S.; Koga, K.; Tokuda, T.; Yamamoto, K.; Maruoka, K. *Angew. Chem., Int. Ed.* **2014**, *53*, 6220–6223;
(f) Parvez, Md. M.; Haraguchi, N.; Itsuno, S.; *Macromolecules* **2014**, *47*, 1922–1928;
(g) Li, M.; Woods, P. A.; Smith, M. D.; *Chem. Sci.* **2013**, *4*, 2907–2911.
95. O'Donnell, M. J.; Eckrich, T. M.; *Tetrahedron Lett.* **1978**, *19*, 4625–4628.
96. Belding, L.; Stoyanov, P.; Dudding, T.; *J. Org. Chem.* **2016**, *81*, 553–558.
97. Makosza, M.; Lasek, W.; *J. Phys. Org. Chem.* **1993**, *6*, 412–420.
98. Herriott, A.; Picker, D.; *J. Am. Chem. Soc.* **1975**, *97*, 2345–2349.
99. Belding, L.; Taimoory, S. M.; Dudding, T.; *ACS Catal.* **2015**, *5*, 343–349.
100. Meirovitch, H.; Scheraga, H. A.; *Macromolecules* **1980**, *13*, 1406–1414.
101. (a) Pozharskii, A. F.; Ryabtsova, O. V.; Ozeryanskii, V. A.; Degtyarev, A. V.; Kazheva, O. N.; Alexandrov, G. G.; Dyachenko, O. A.; *J. Org. Chem.* **2003**, *68*, 10109–10122.
(b) Pozharskii, A. F.; Degtyarev, A. V.; Ryabtsova, O. V.; Ozeryanskii, V. A.; Kletskii, M. W.; Starikova, Z. A.; Sobczyk, L.; Filarowski, A. *J. Org. Chem.* **2007**, *72*, 3006–3019.

102. (a) Weiss, R.; Schloter, K.; *Tetrahedron Lett.* **1975**, *16*, 3491–3494.
(b) Azhar Hashmi, S. M.; Prasanna, S.; Radhakrishnan, T. P.; *Synth. Met.* **1992**, *48*, 39–47.